

Figure 5-25. Predicted 24-hr average NH_3 concentration (ppb) on June 24, 1987 for baseline case.

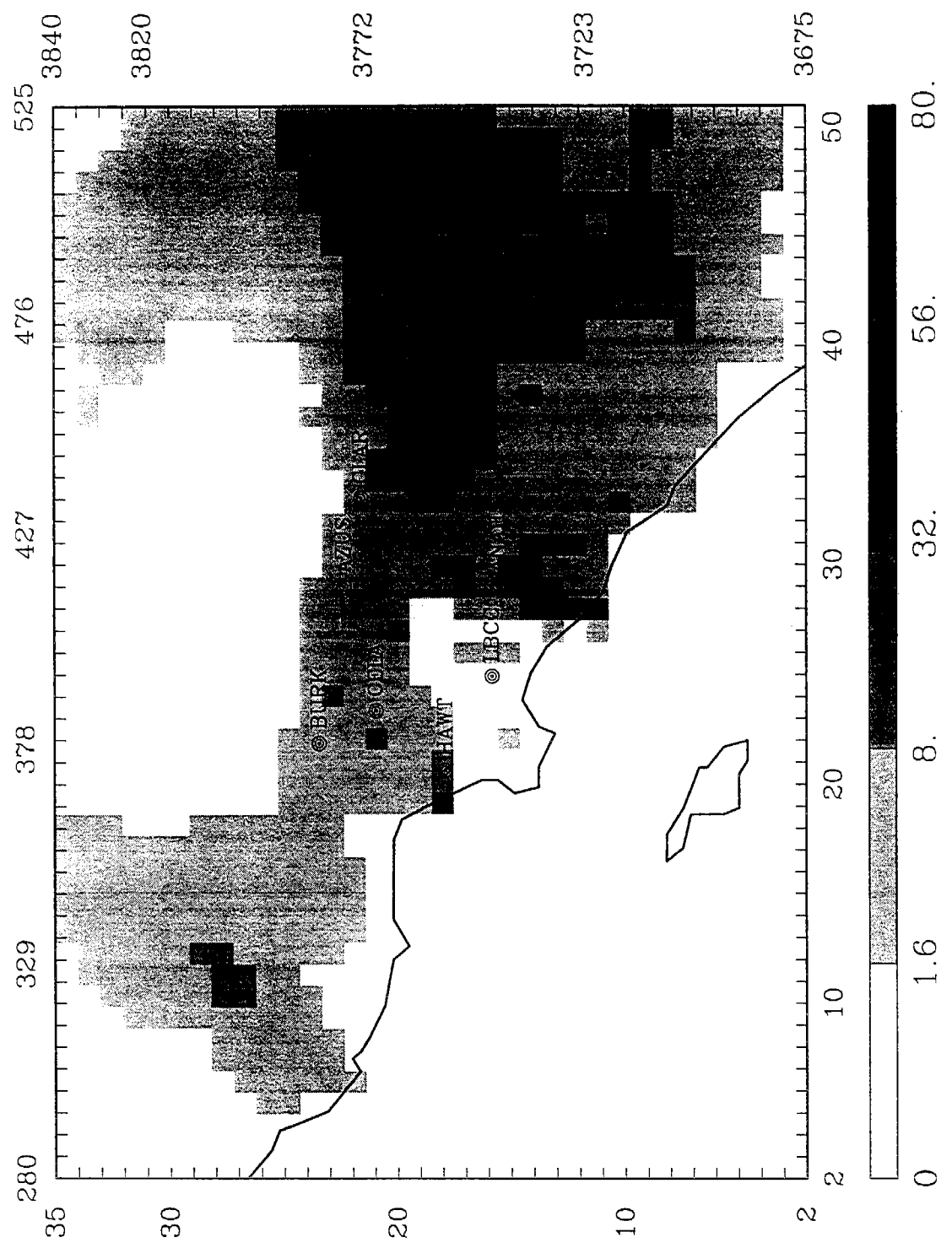


Figure 5-26. Predicted 24-hr average NH₃ concentration (ppb) on June 25, 1987 for baseline case.

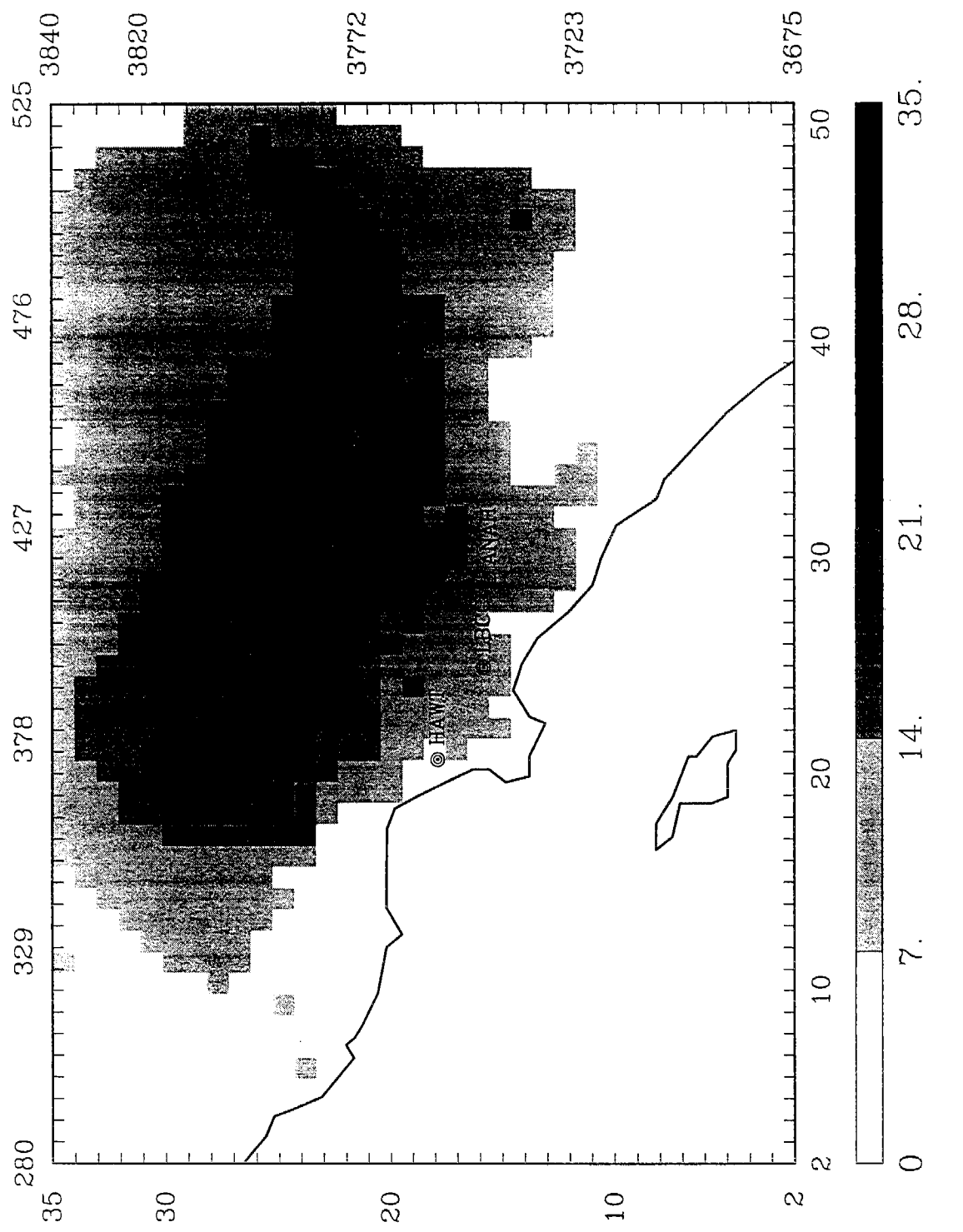


Figure 5-27. Predicted 24-hr average PM_{10} OM concentration ($\mu\text{g}/\text{m}^3$) on June 24, 1987 for baseline case.

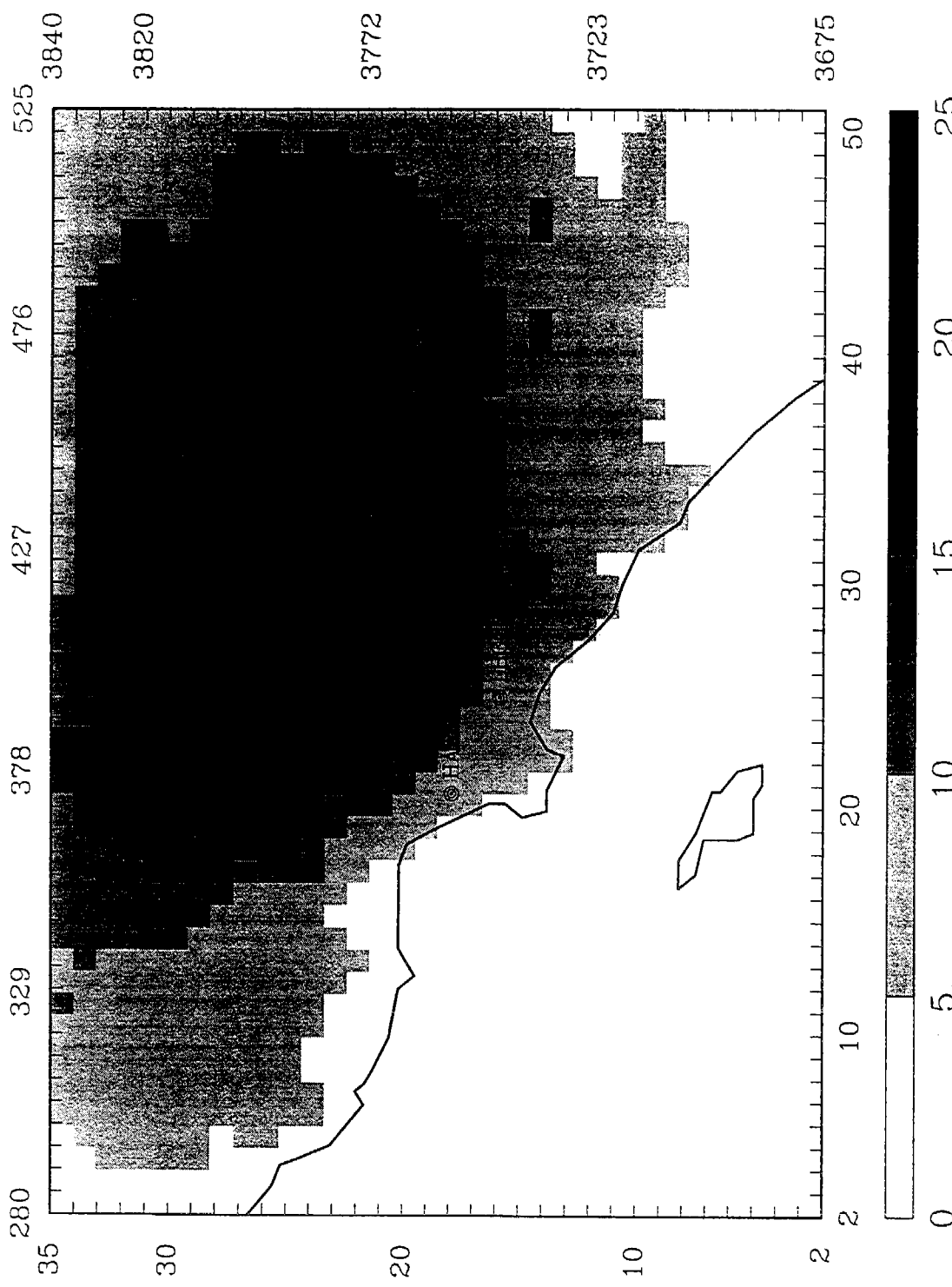


Figure 5-28. Predicted 24-hr average PM_{10} OM concentration ($\mu\text{g}/\text{m}^3$) on June 25, 1987 for baseline case.

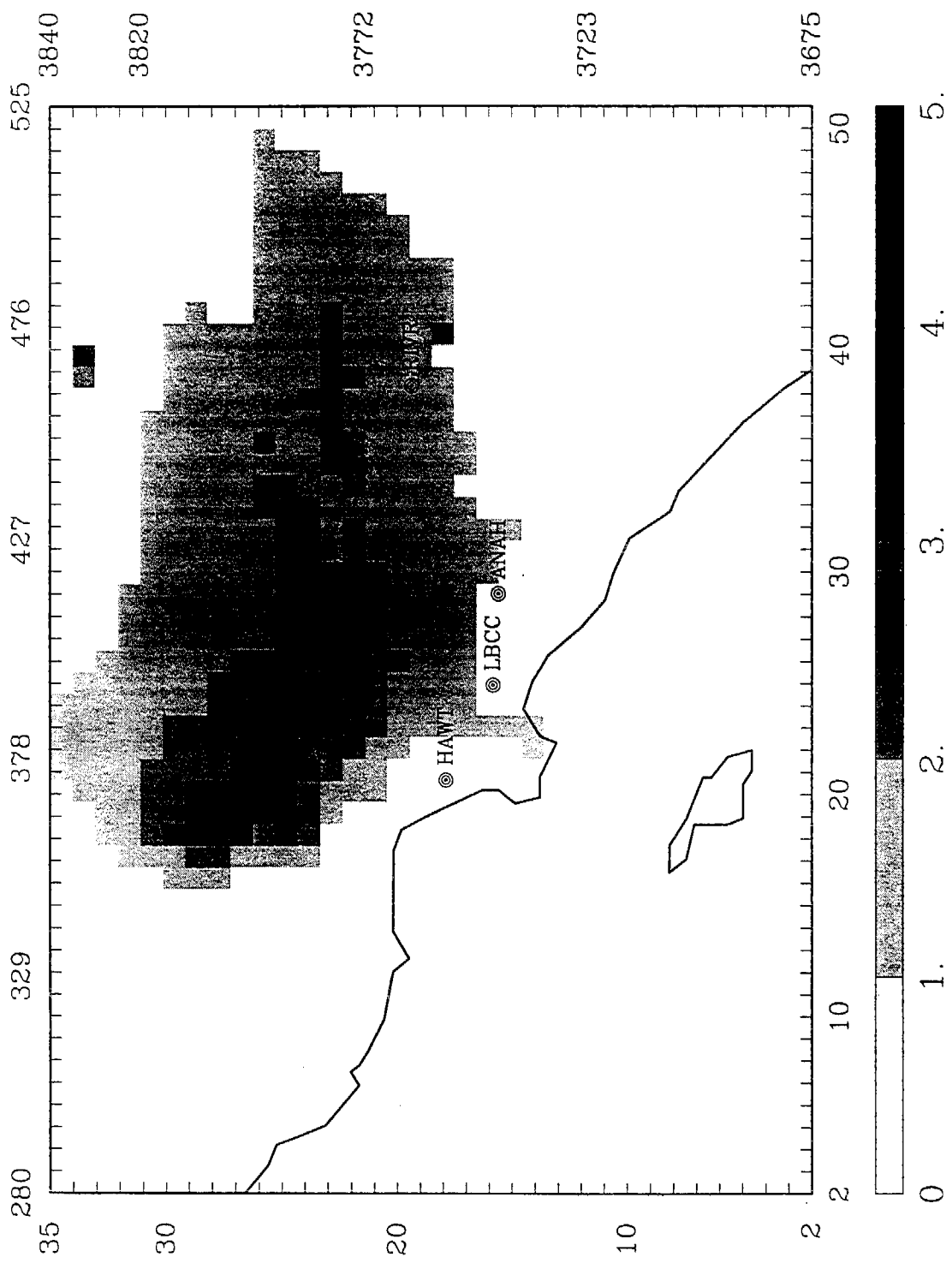


Figure 5-29. Predicted 24-hr average PM_{10} EC concentration ($\mu\text{g}/\text{m}^3$) on June 24, 1987 for baseline case.

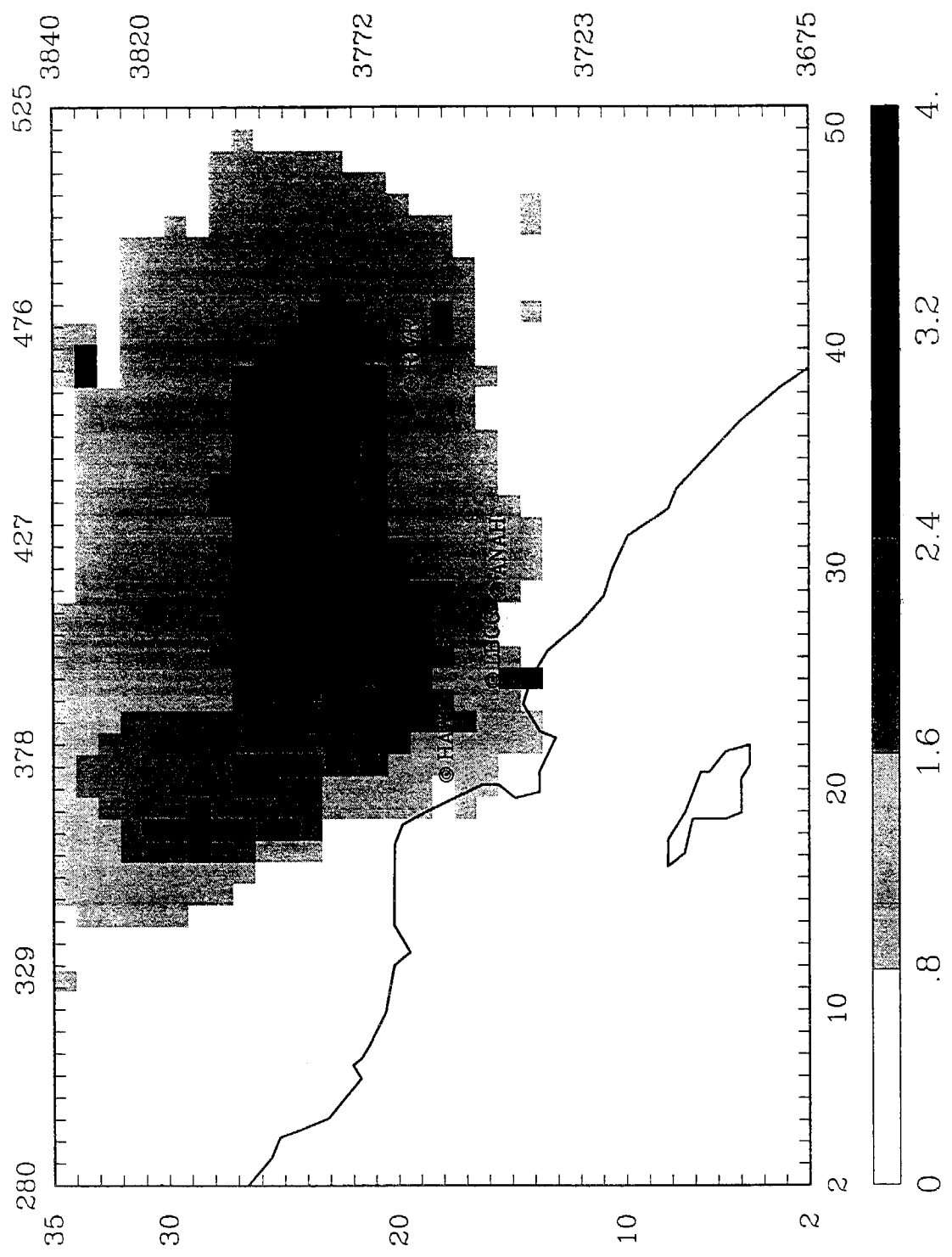


Figure 5-30. Predicted 24-hr average PM_{10} EC concentration ($\mu\text{g}/\text{m}^3$) on June 25, 1987 for baseline case.

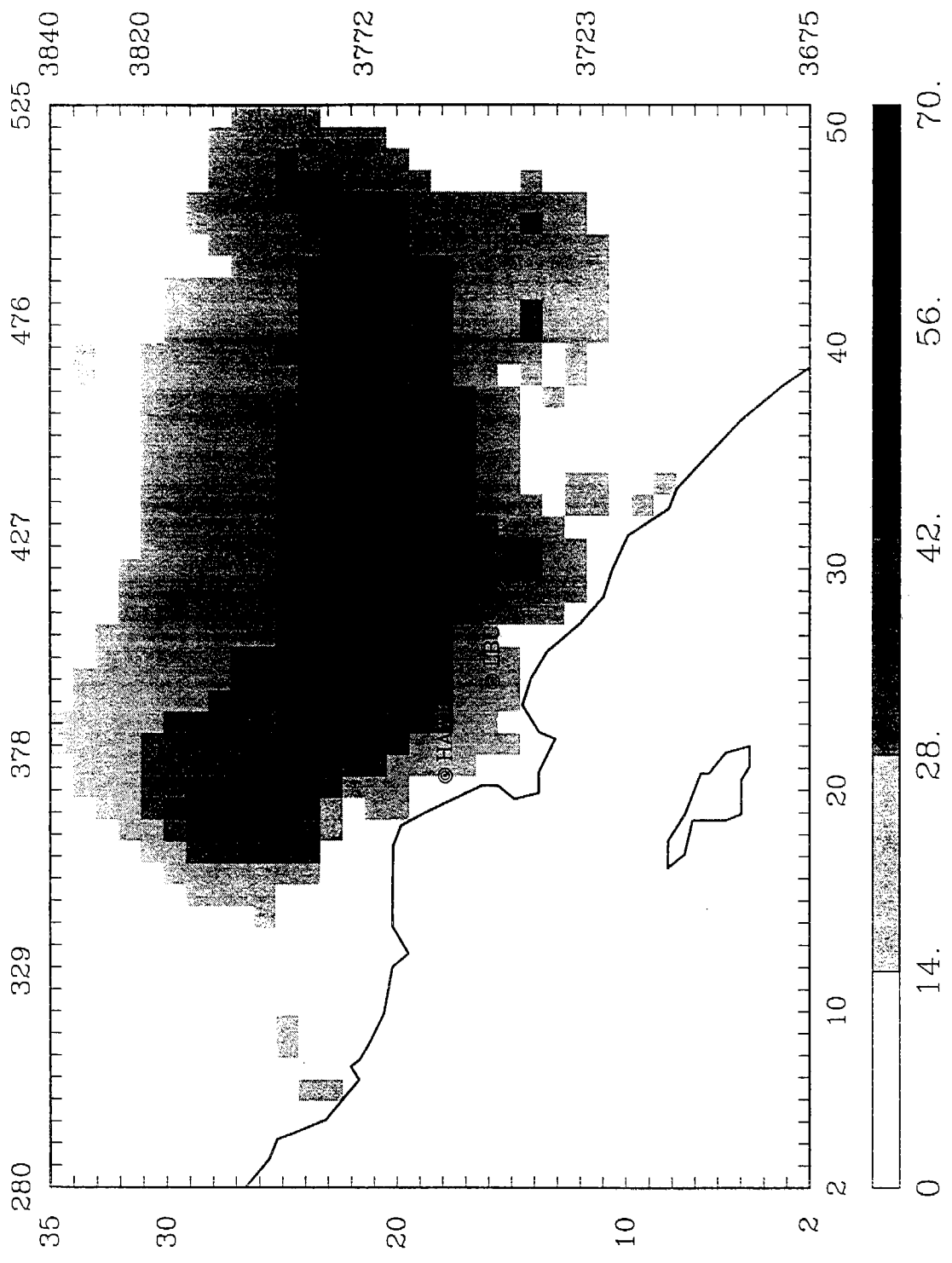


Figure 5-31. Predicted 24-hr average crustal PM₁₀ concentration ($\mu\text{g}/\text{m}^3$) on June 24, 1987 for baseline case.

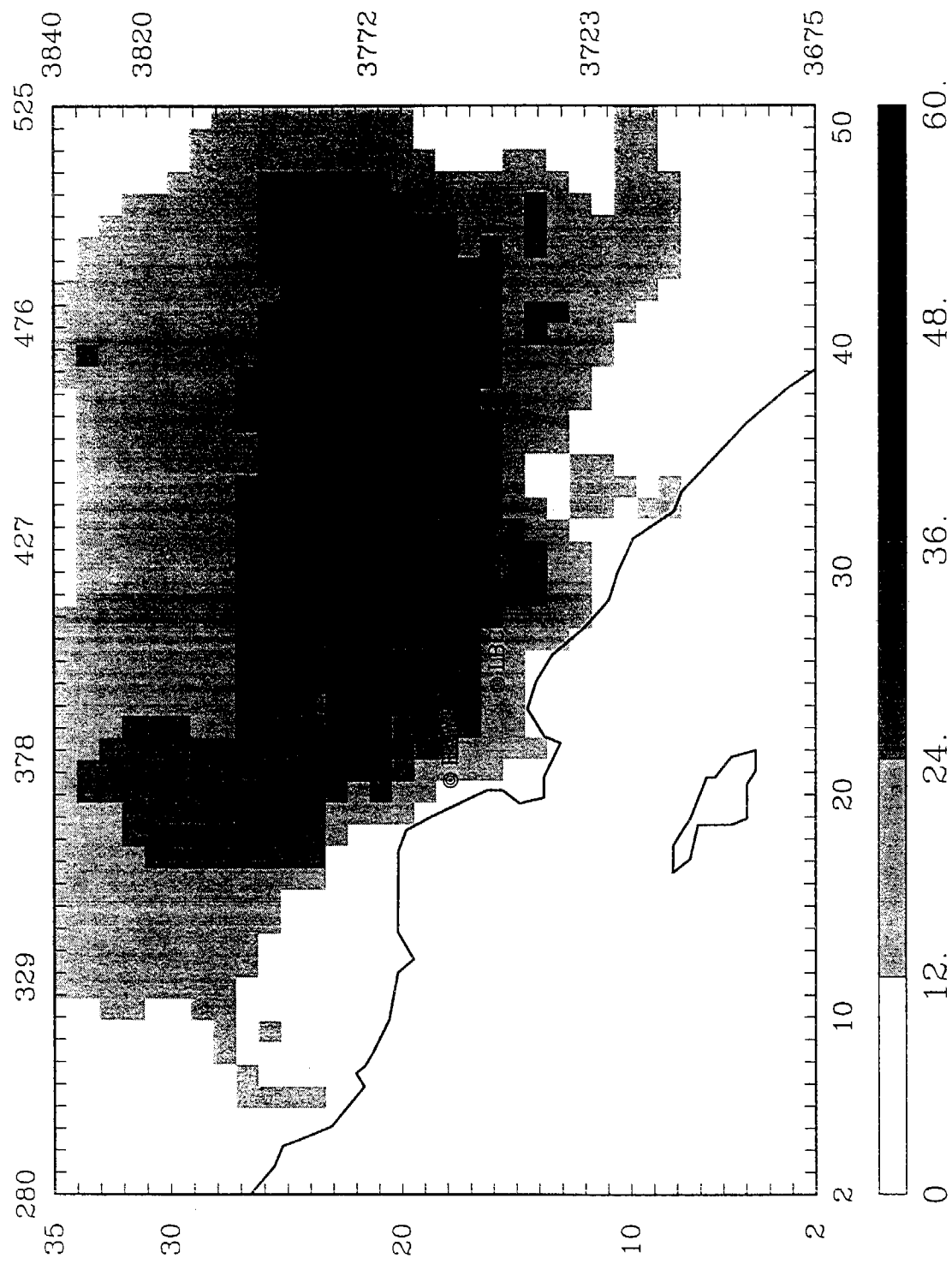


Figure 5-32. Predicted 24-hr average crustal PM₁₀ concentration ($\mu\text{g}/\text{m}^3$) on June 25, 1987 for baseline case.

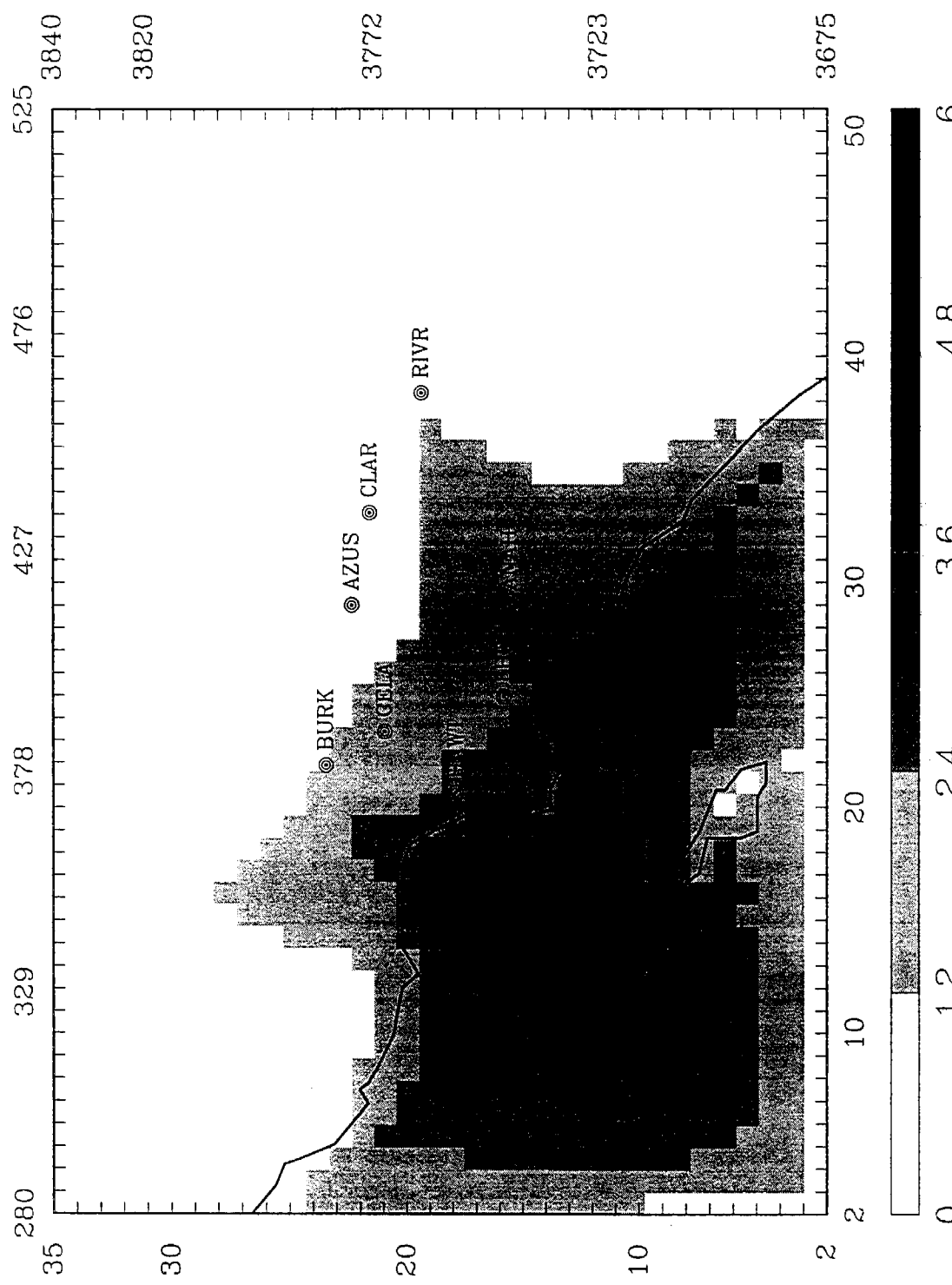


Figure 5-33. Predicted 24-hr average PM_{10} Na concentration ($\mu\text{g}/\text{m}^3$) on June 24, 1987 for baseline case.

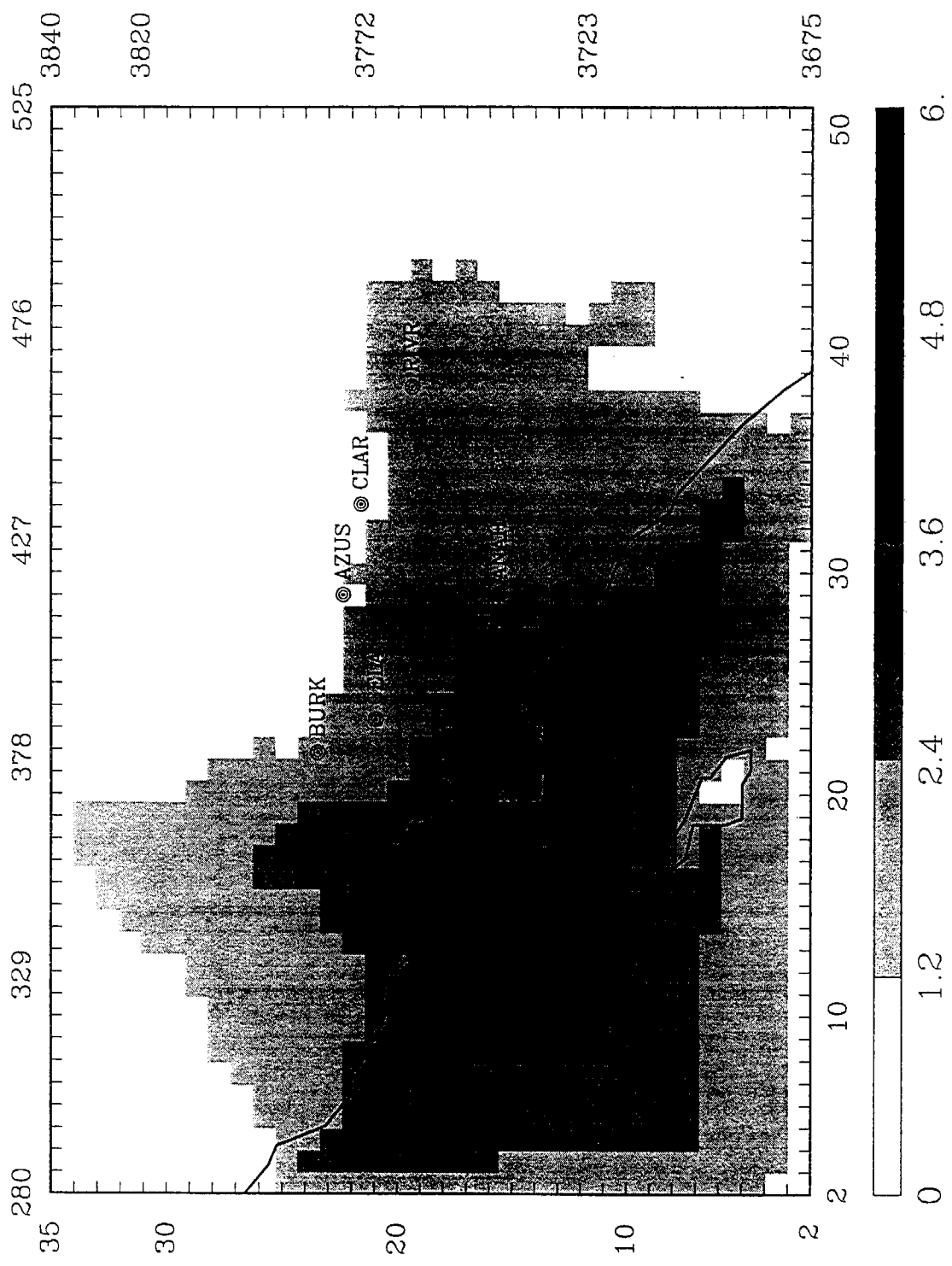


Figure 5-34. Predicted 24-hr average PM_{10} Na concentration ($\mu\text{g}/\text{m}^3$) on June 25, 1987 for baseline case.

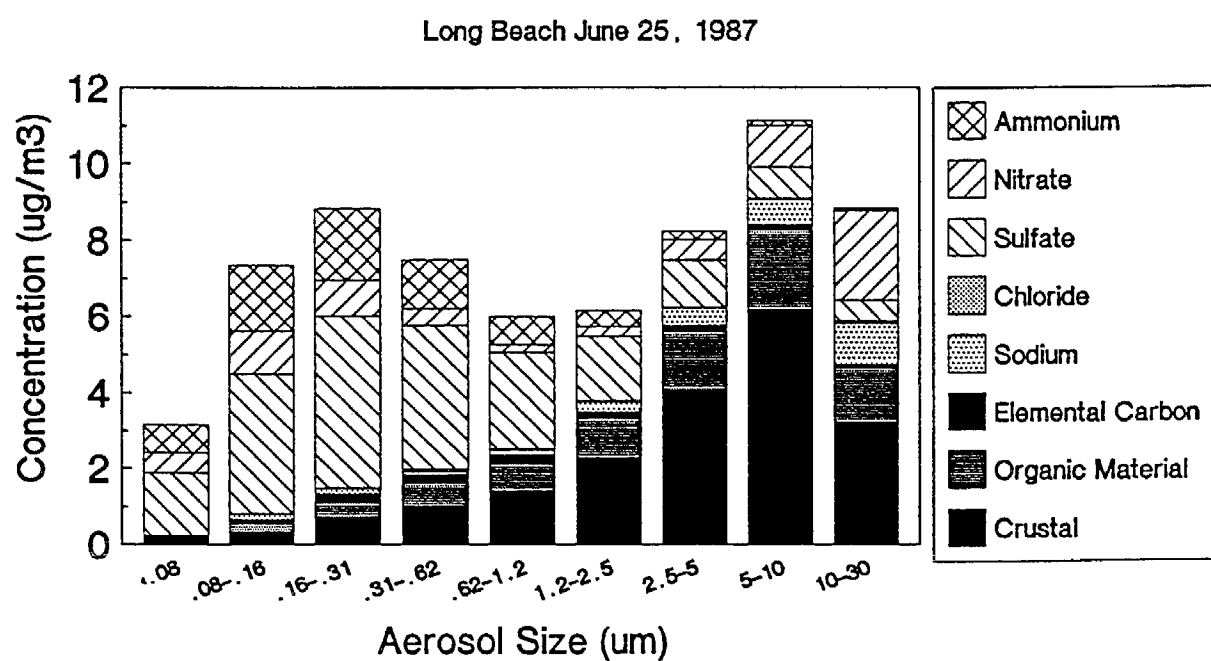
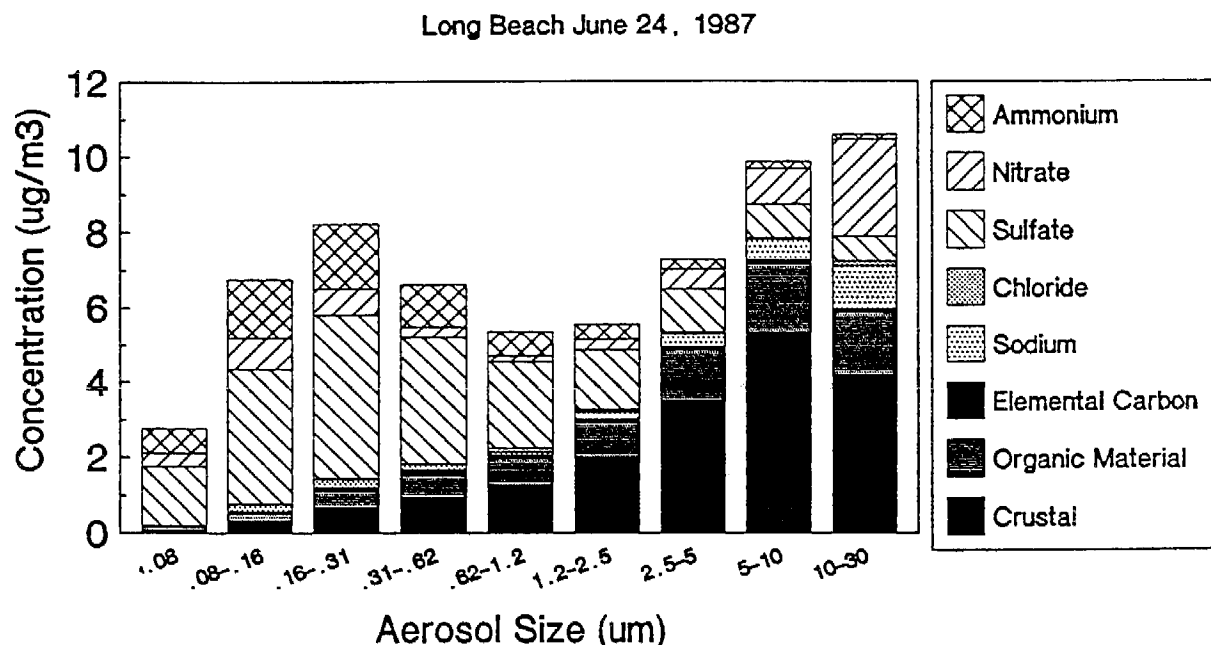
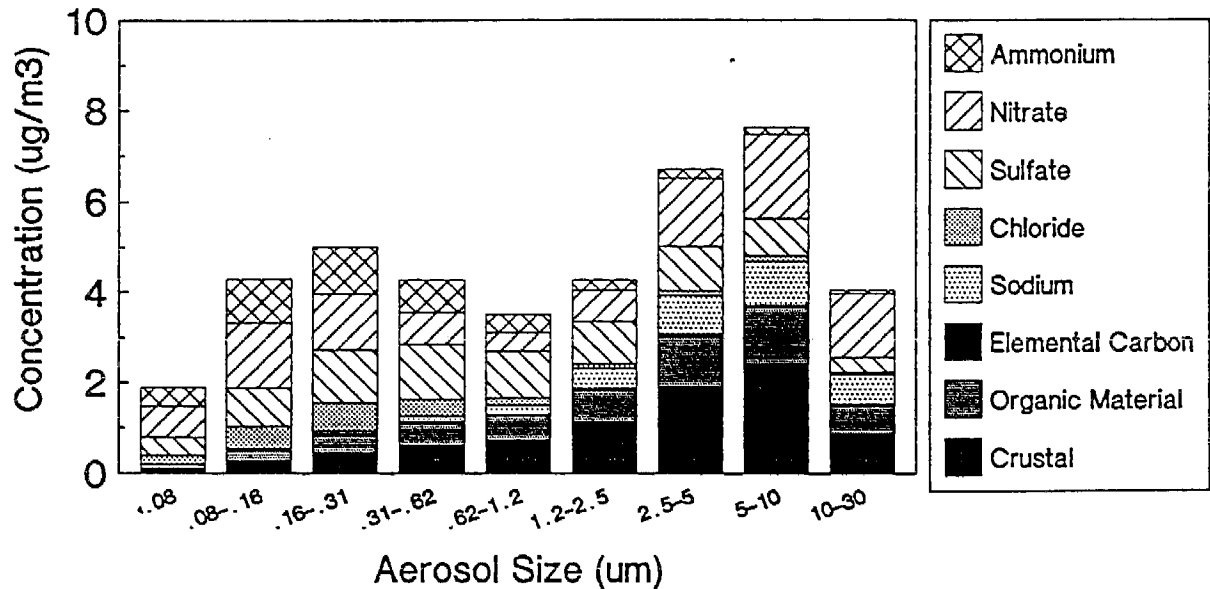


Figure 5-35. Predicted aerosol size distribution at Long Beach on June 24-25, 1987.

Hawthorne June 24, 1987



Hawthorne June 25, 1987

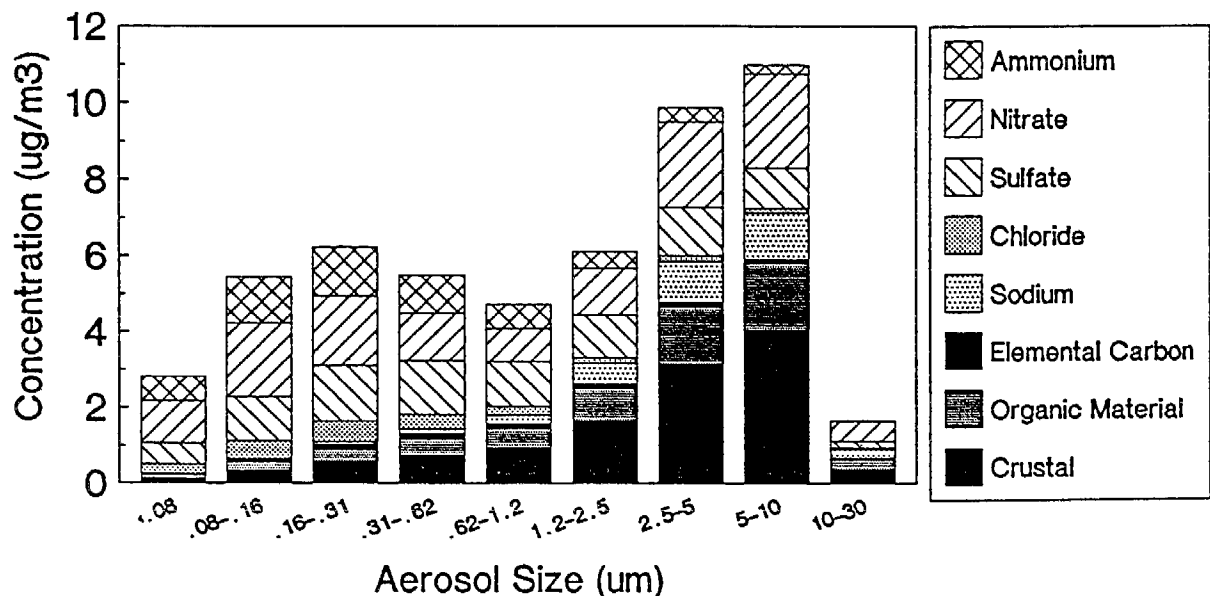


Figure 5-36. Predicted aerosol size distribution at Hawthorne on June 24-25, 1987.

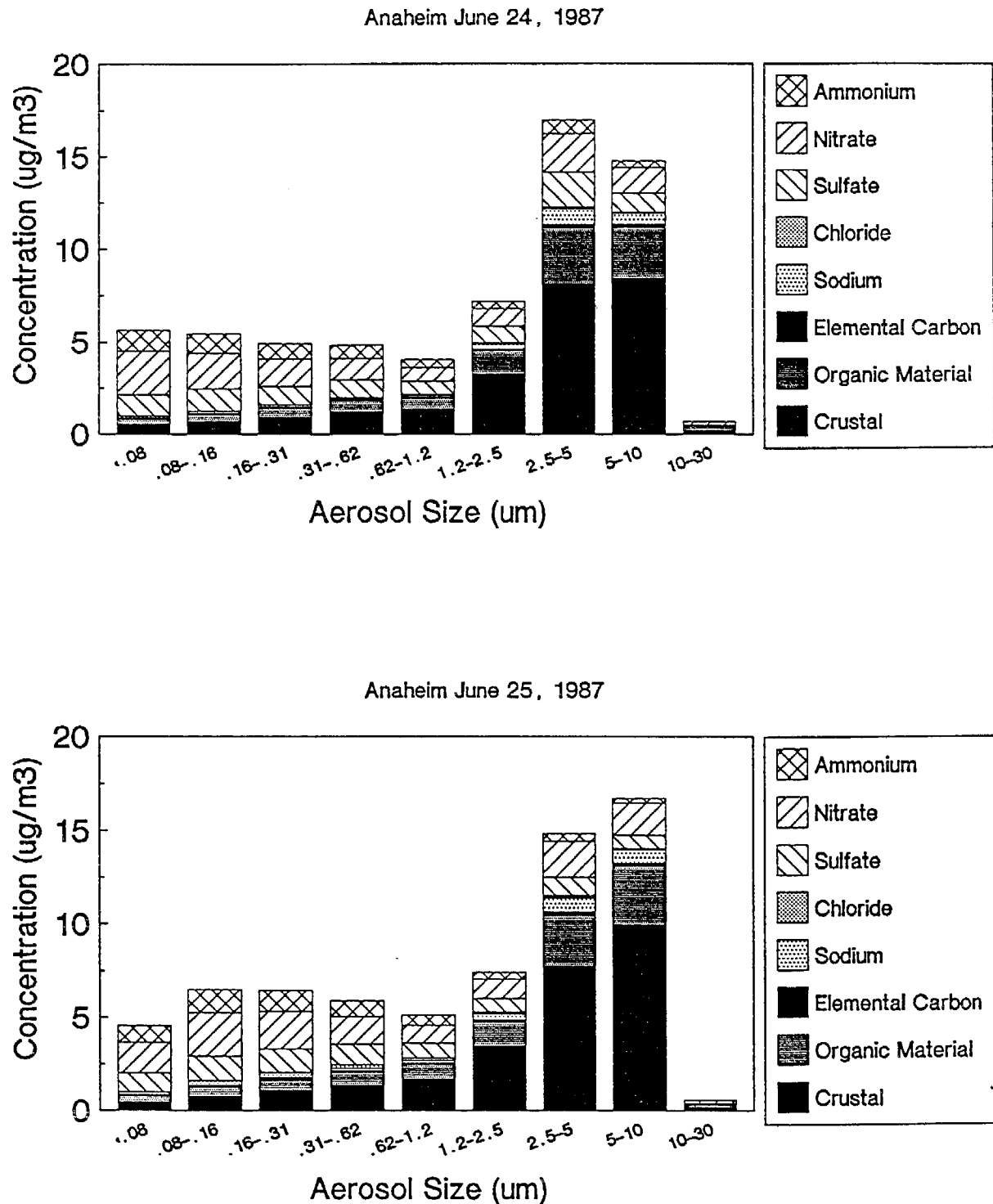
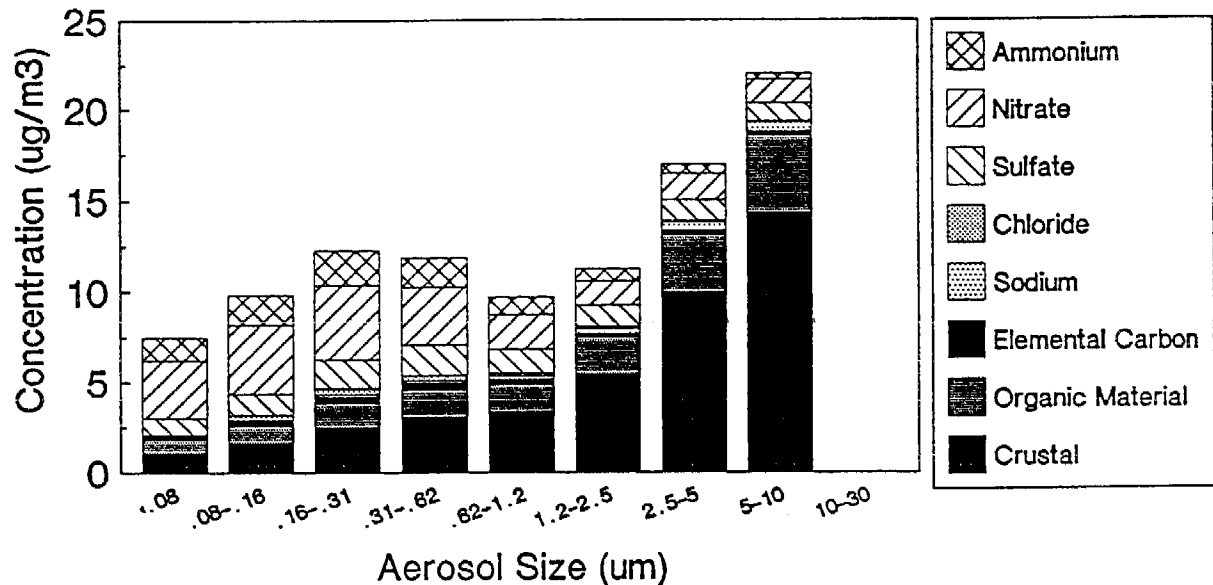


Figure 5-37. Predicted aerosol size distribution at Anaheim on June 24-25, 1987.

Los Angeles June 24, 1987



Los Angeles June 25, 1987

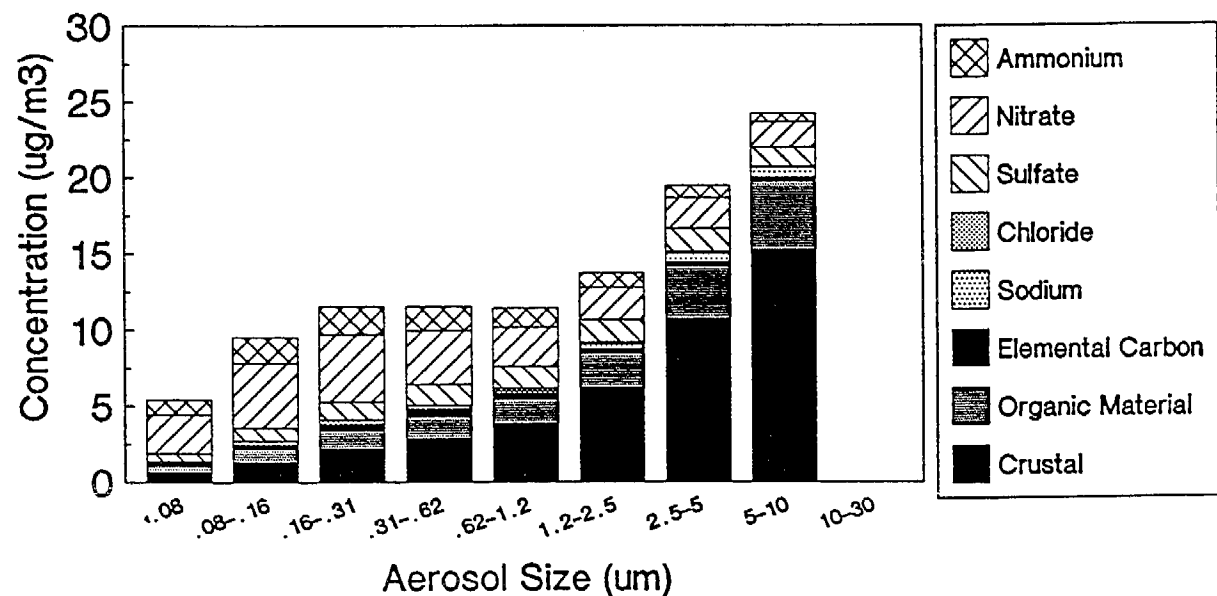
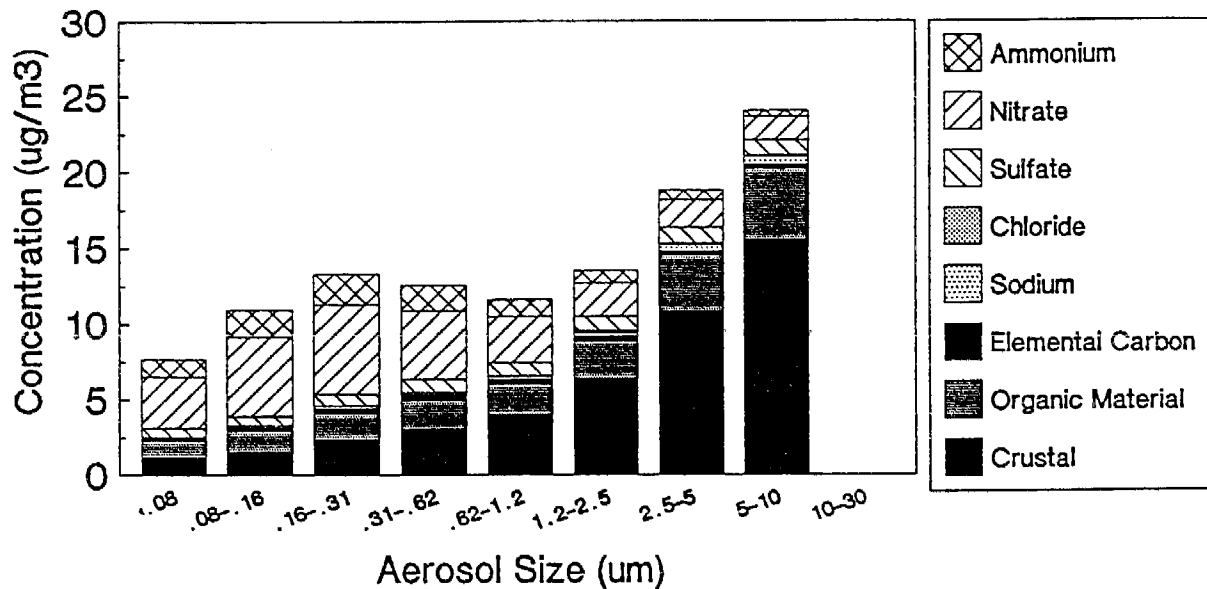


Figure 5-38. Predicted aerosol size distribution at Los Angeles on June 24-25, 1987.

Burbank June 24, 1987



Burbank June 25, 1987

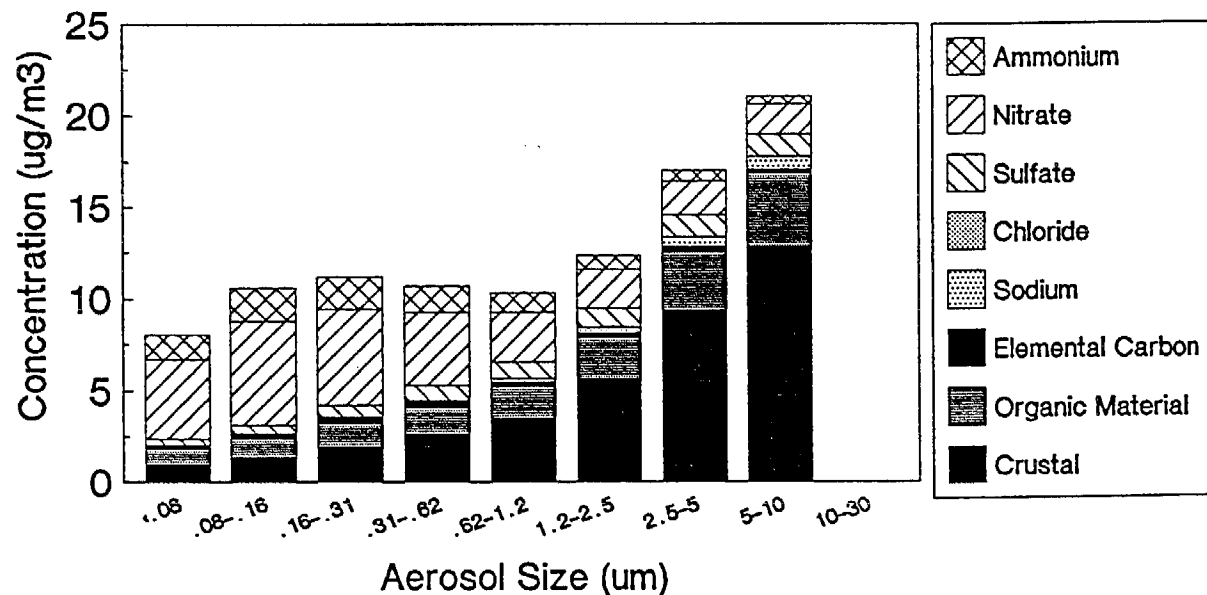
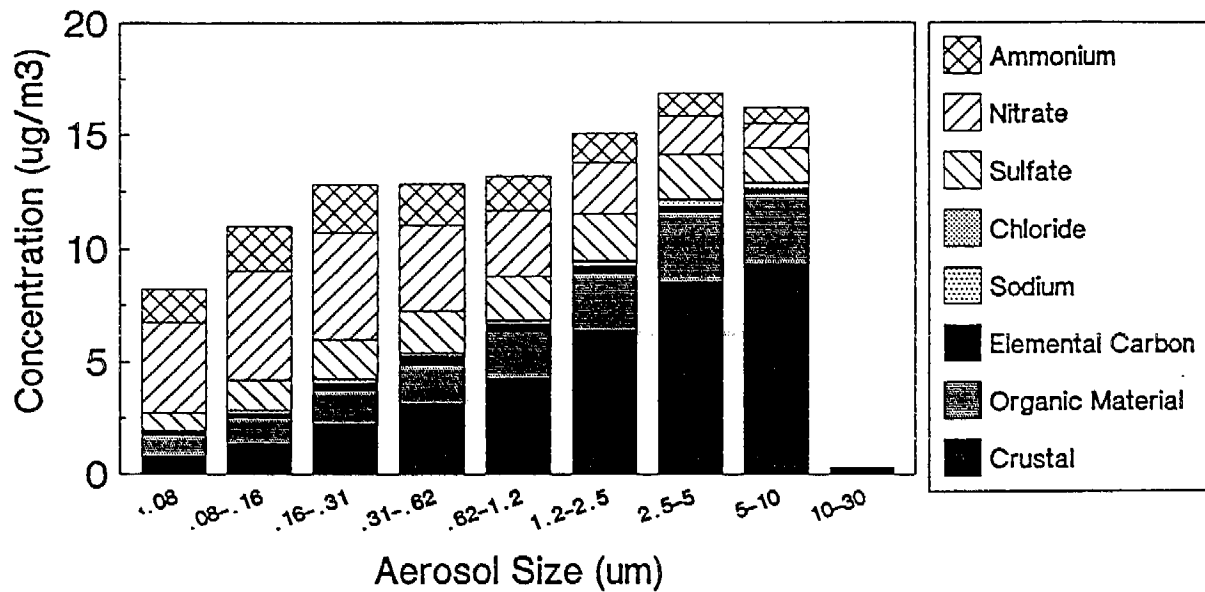


Figure 5-39. Predicted aerosol size distribution at Burbank on June 24-25, 1987.

Azusa June 24, 1987



Azusa June 25, 1987

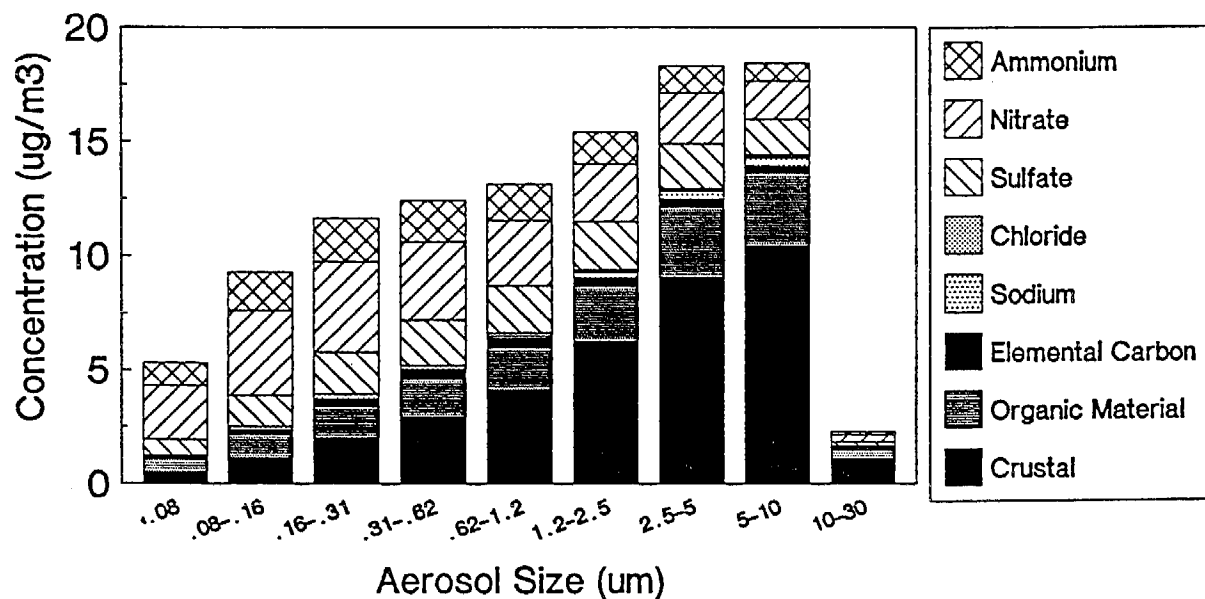
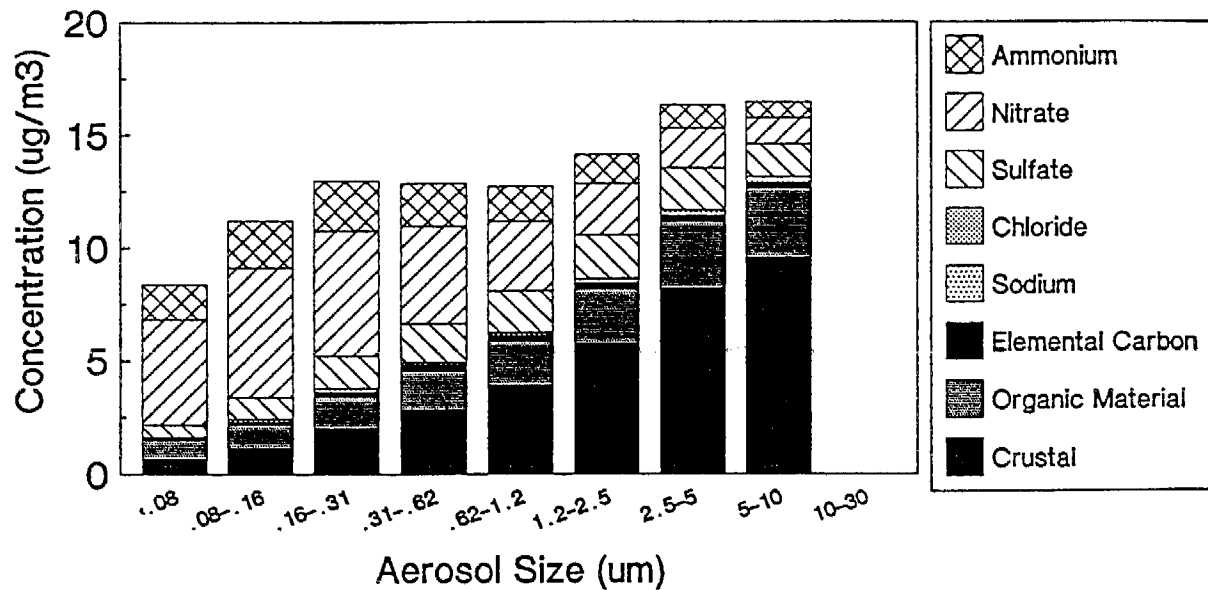


Figure 5-40. Predicted aerosol size distribution at Azusa on June 24-25, 1987.

Claremont June 24, 1987



Claremont June 25, 1987

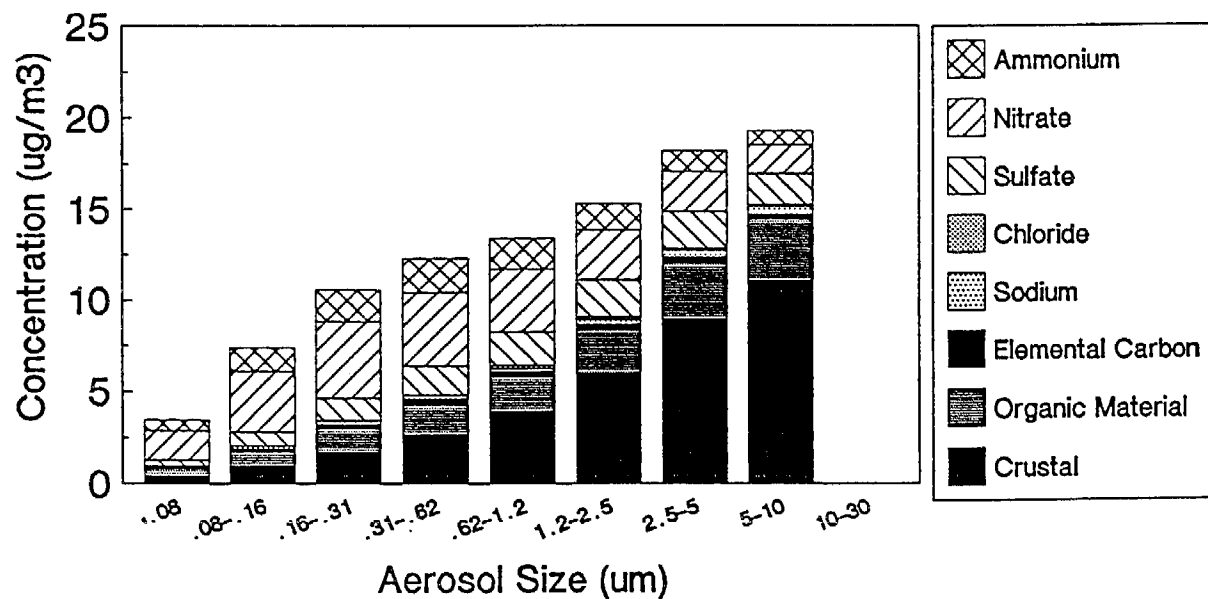
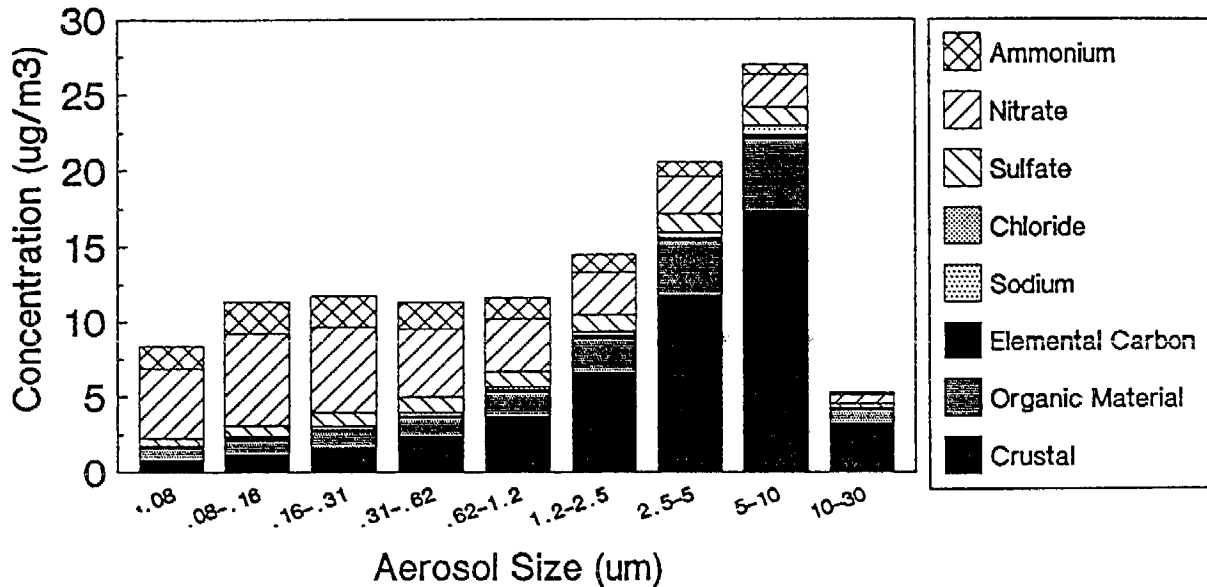


Figure 5-41. Predicted aerosol size distribution at Claremont on June 24-25, 1987.

Riverside June 24, 1987



Riverside June 25, 1987

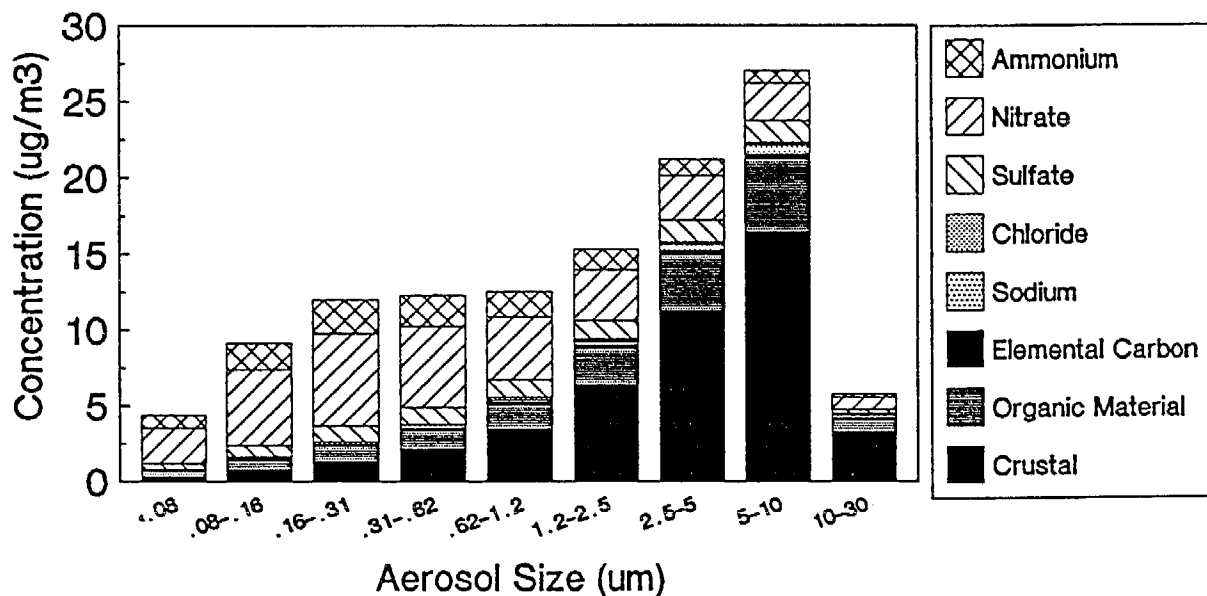


Figure 5-42. Predicted aerosol size distribution at Riverside on June 24-25, 1987.

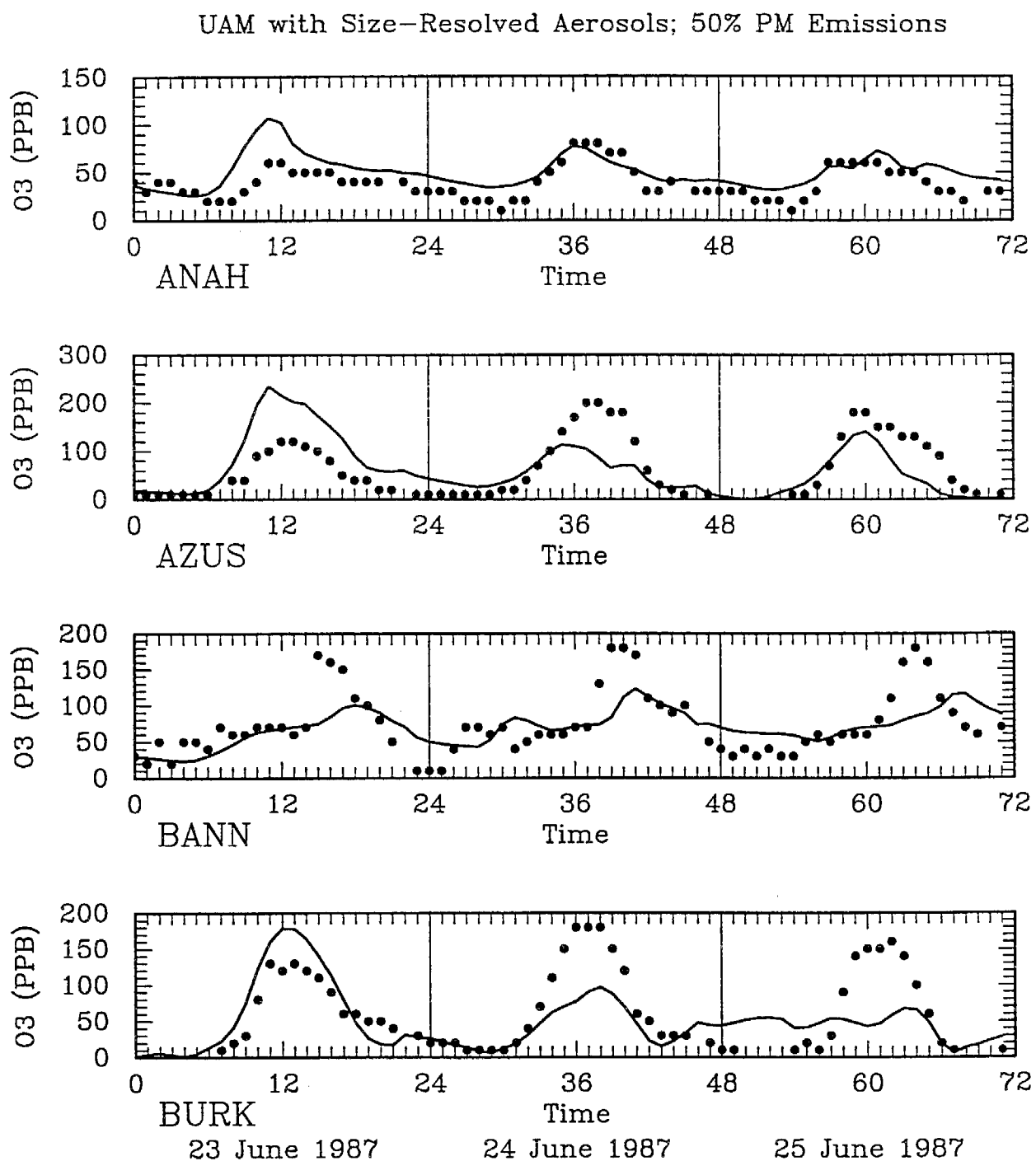


Figure 5-43. Predicted and observed 1-hr ozone concentrations on June 23-25, 1987.

Page 1 of 10

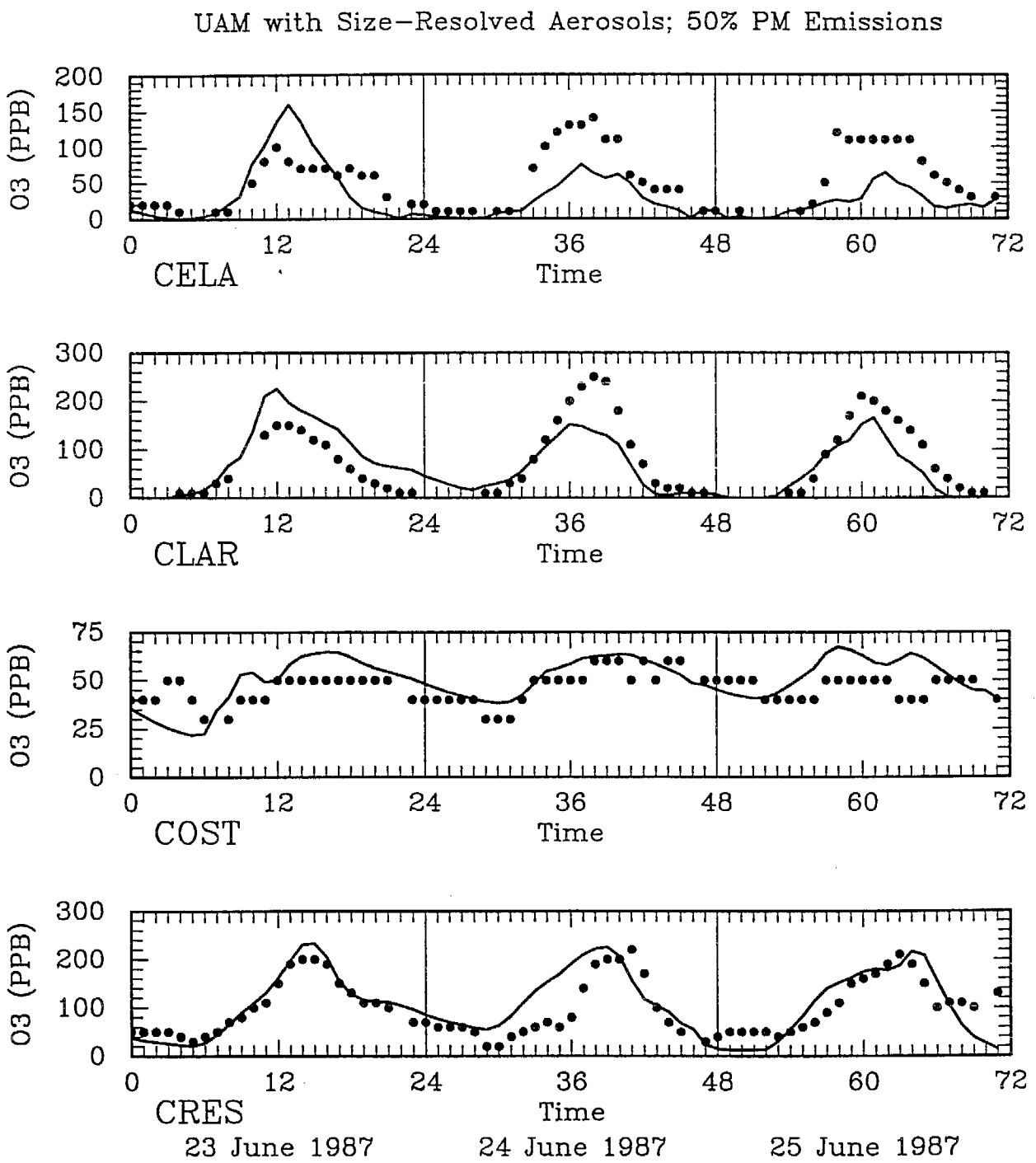


Figure 5-43. Predicted and observed 1-hr ozone concentrations on June 23-25, 1987.

Page 2 of 10

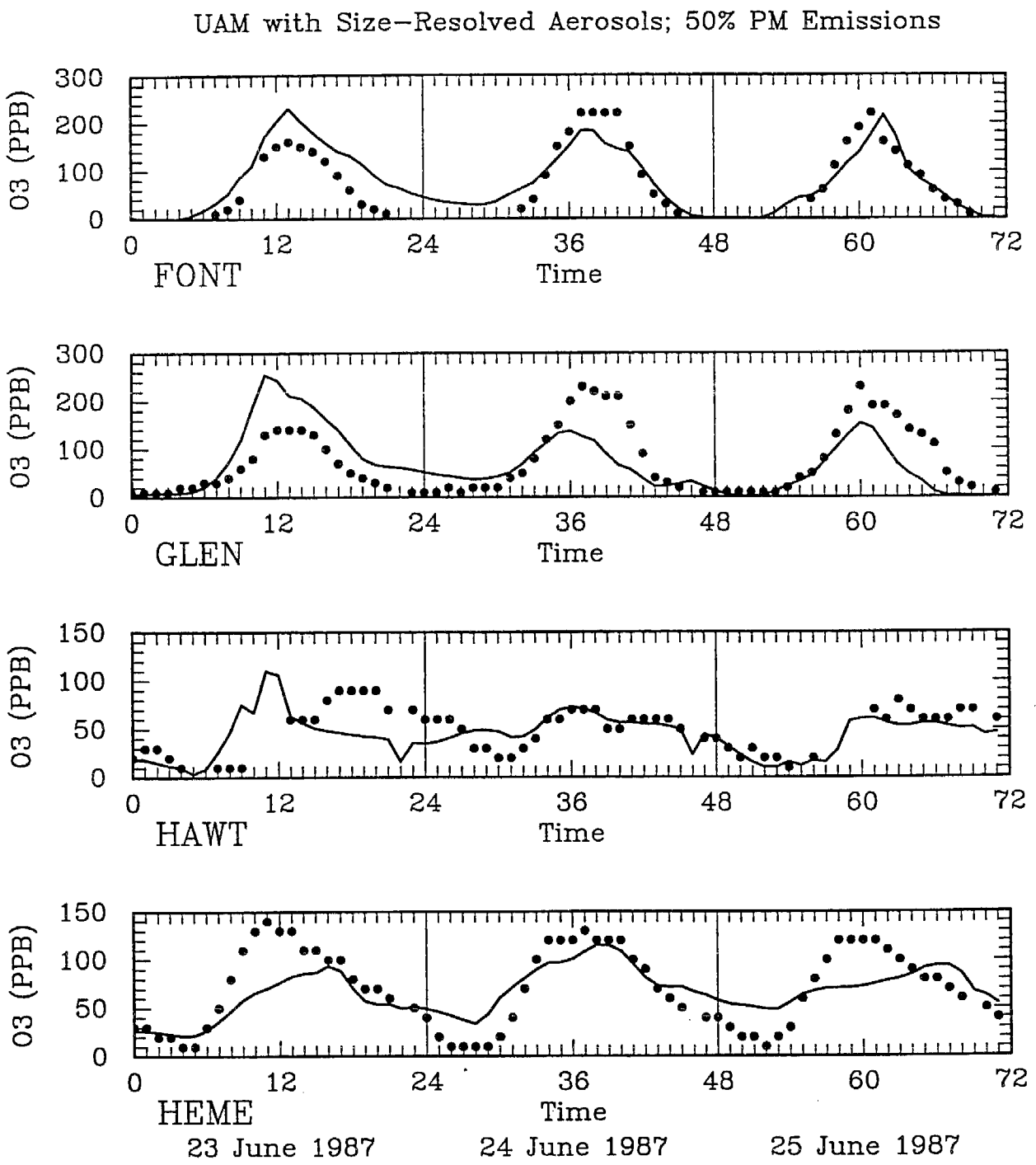


Figure 5-43. Predicted and observed 1-hr ozone concentrations on June 23-25, 1987.

Page 3 of 10

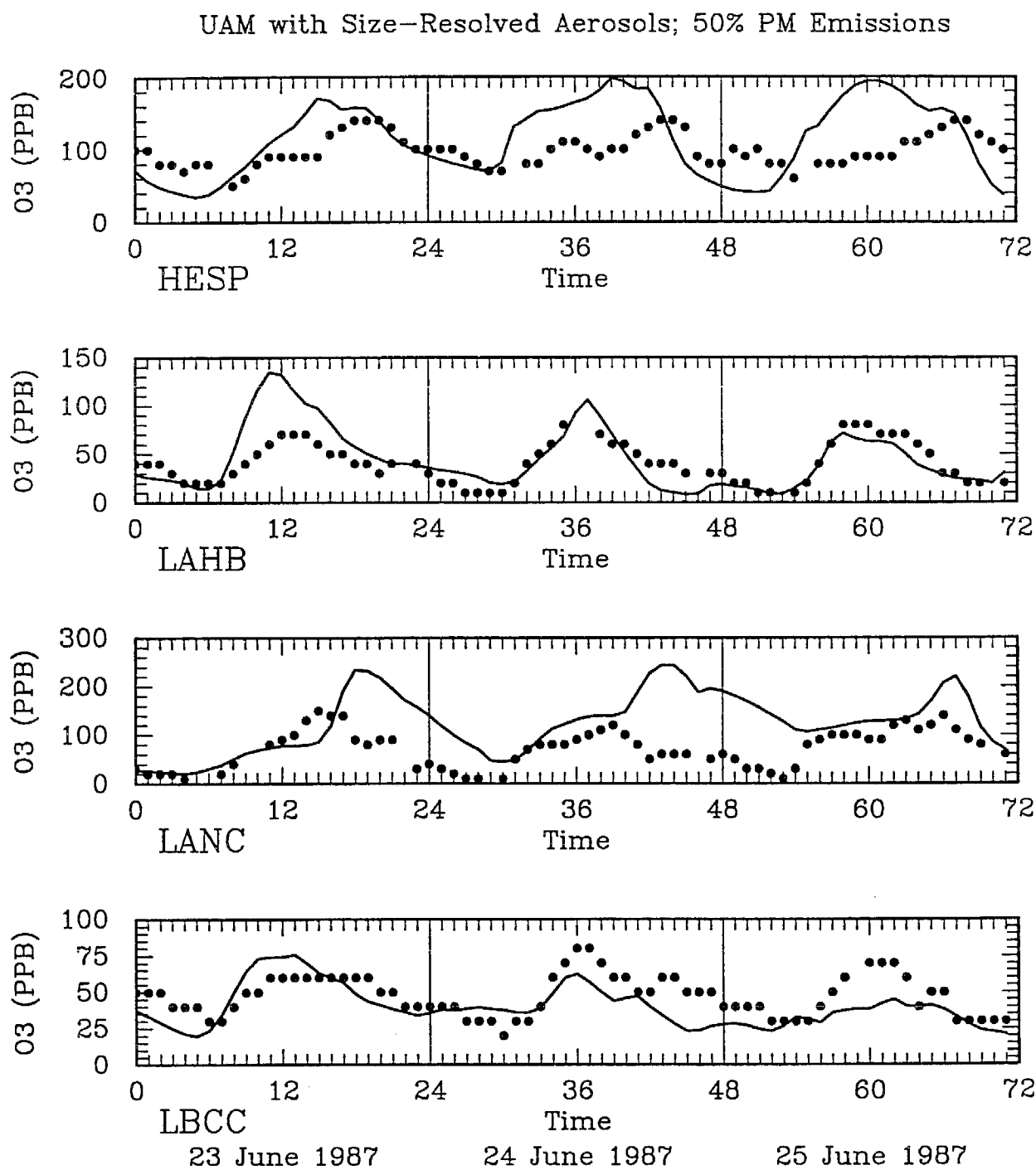


Figure 5-43. Predicted and observed 1-hr ozone concentrations on June 23-25, 1987.

Page 4 of 10

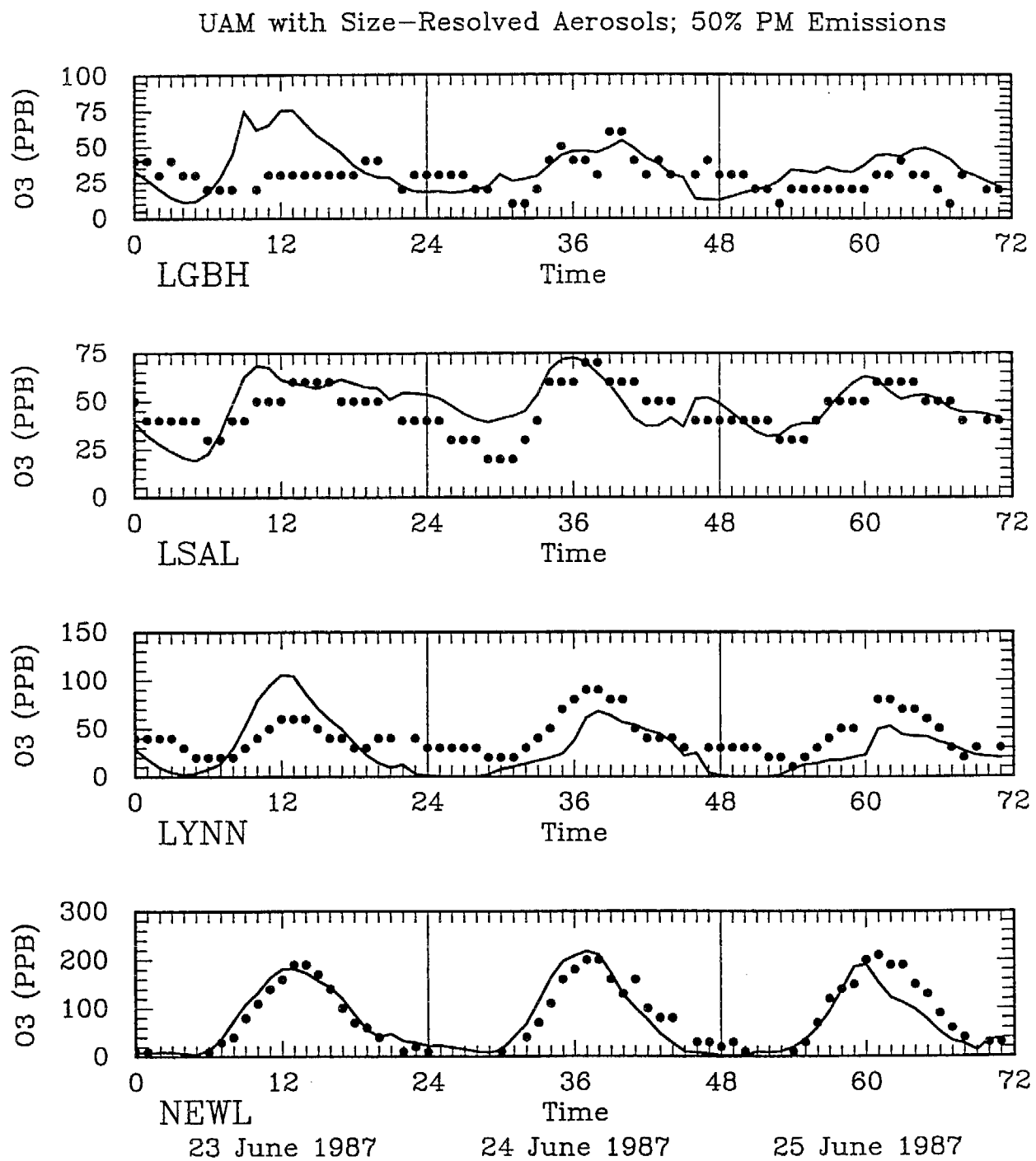


Figure 5-43. Predicted and observed 1-hr ozone concentrations on June 23-25, 1987.

Page 5 of 10

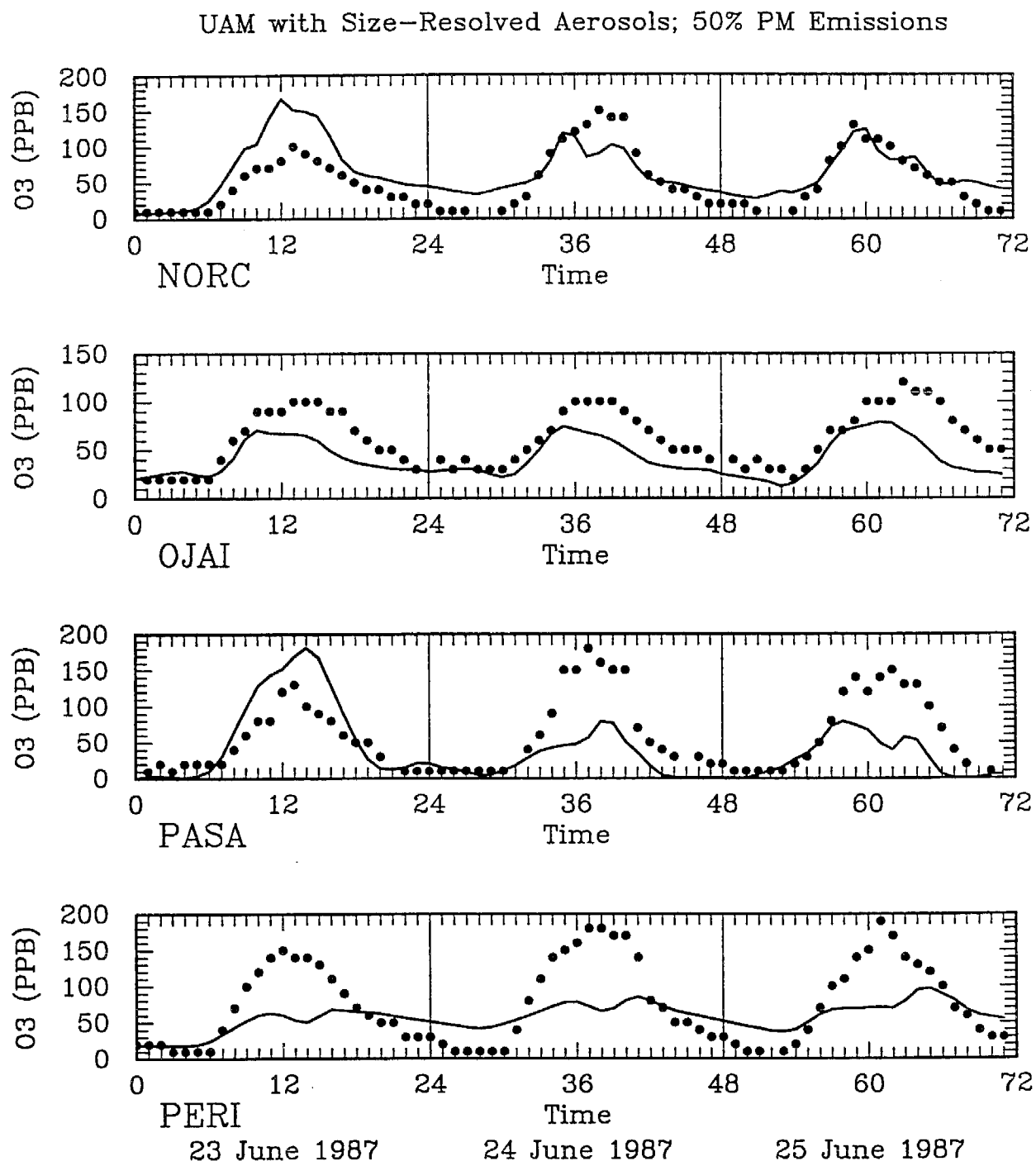


Figure 5-43. Predicted and observed 1-hr ozone concentrations on June 23-25, 1987.

Page 6 of 10

UAM with Size-Resolved Aerosols; 50% PM Emissions

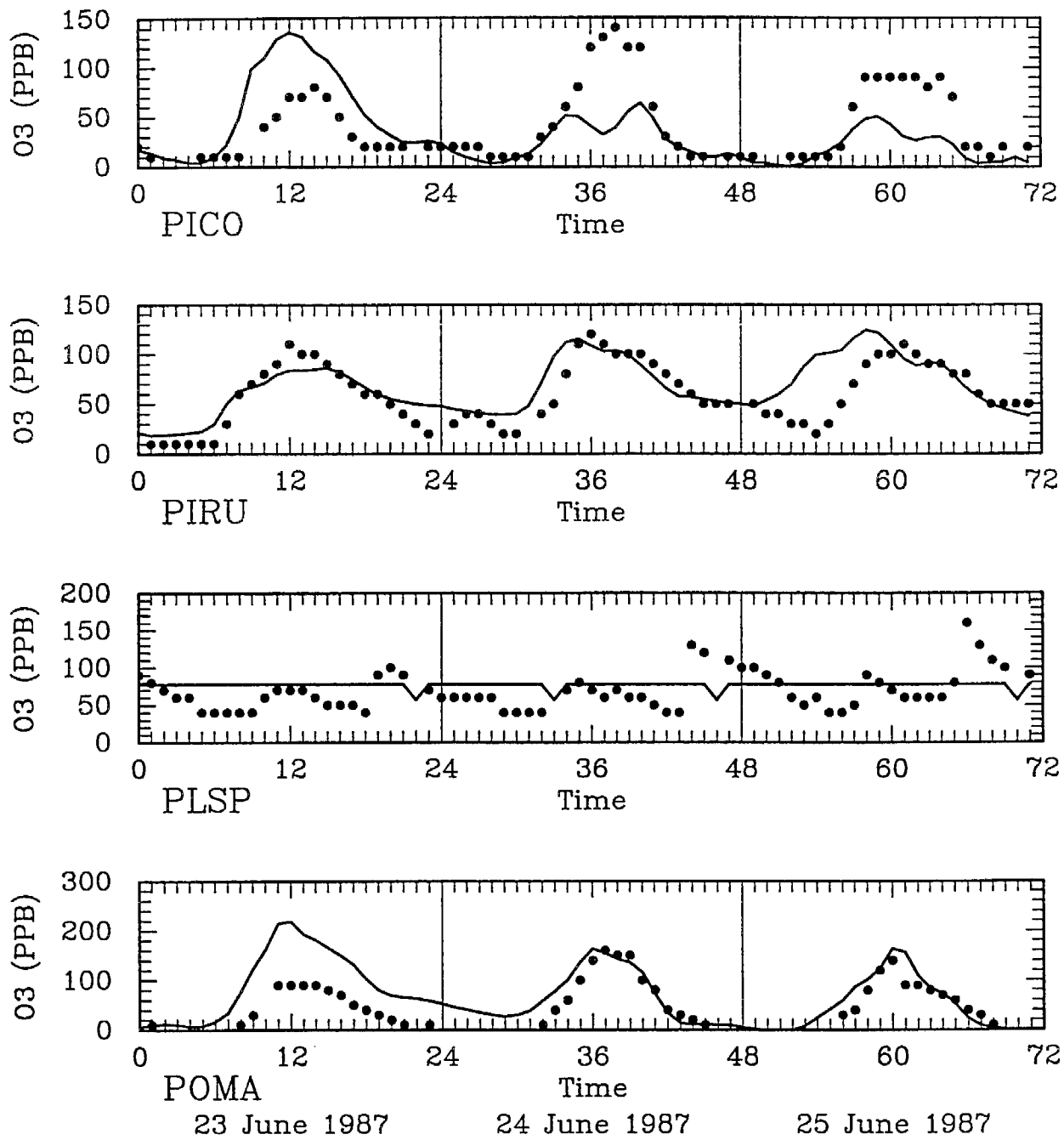


Figure 5-43. Predicted and observed 1-hr ozone concentrations on June 23-25, 1987.

Page 7 of 10

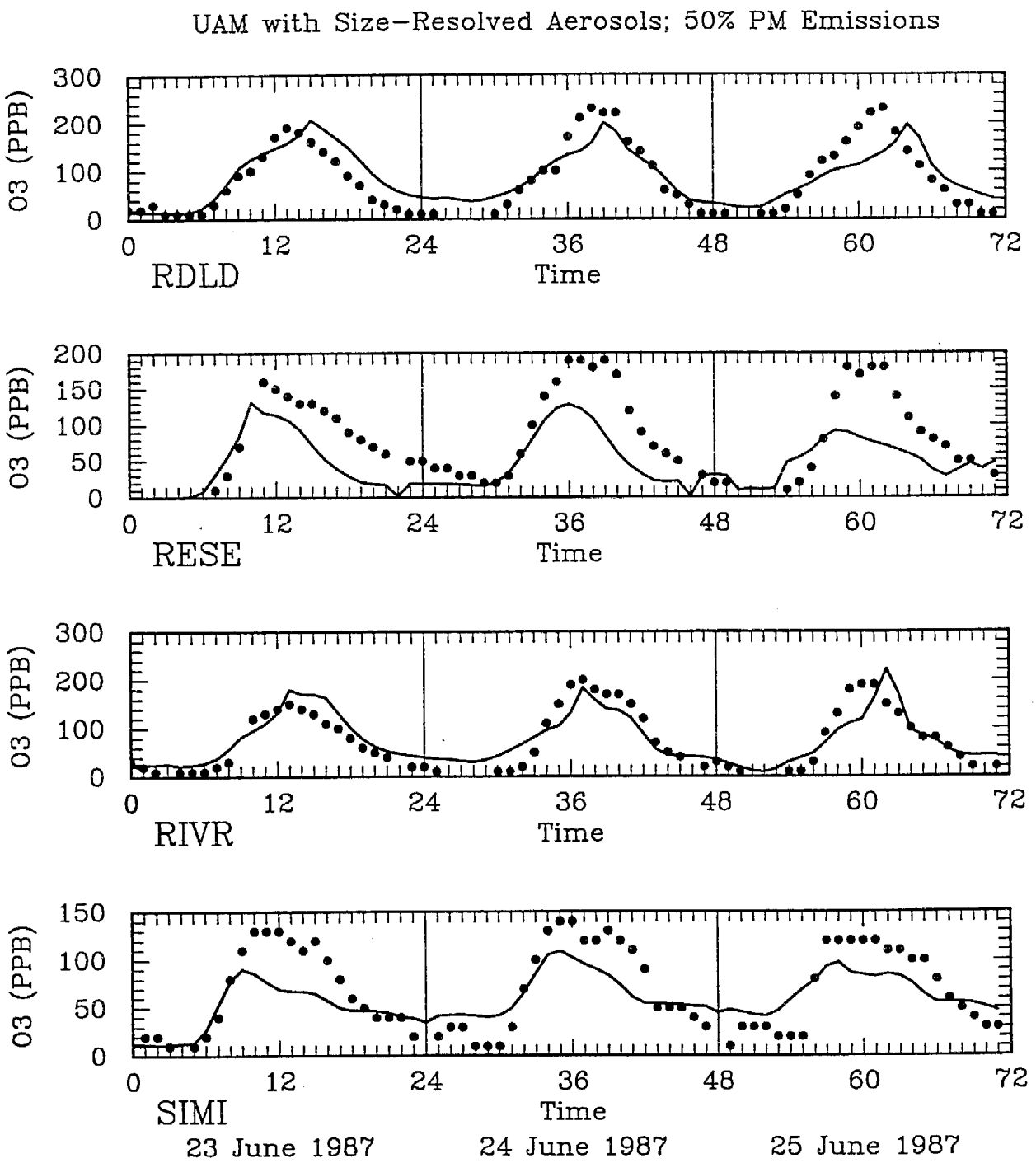


Figure 5-43. Predicted and observed 1-hr ozone concentrations on June 23-25, 1987.

Page 8 of 10

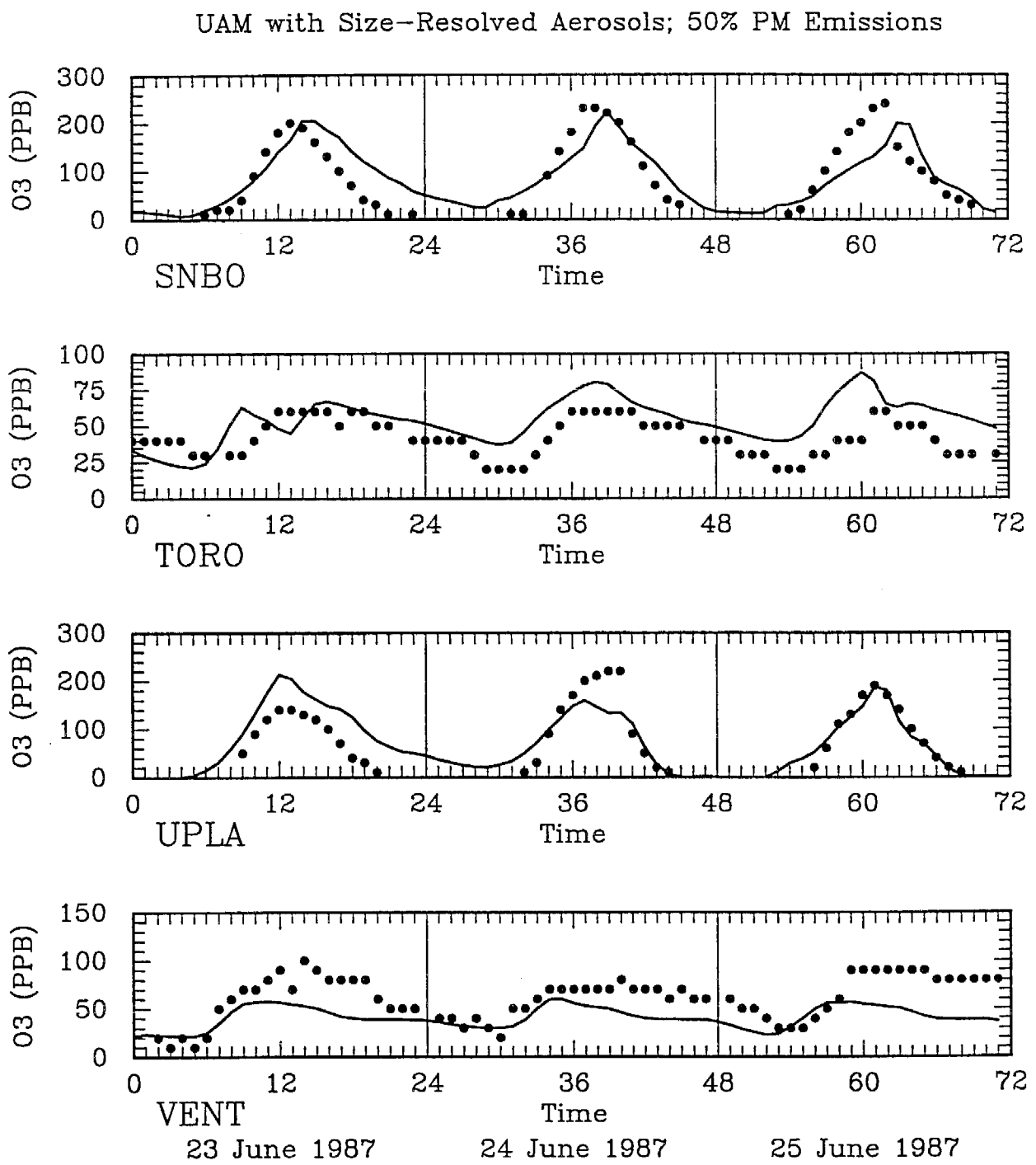


Figure 5-43. Predicted and observed 1-hr ozone concentrations on June 23-25, 1987.

Page 9 of 10

UAM with Size-Resolved Aerosols; 50% PM Emissions

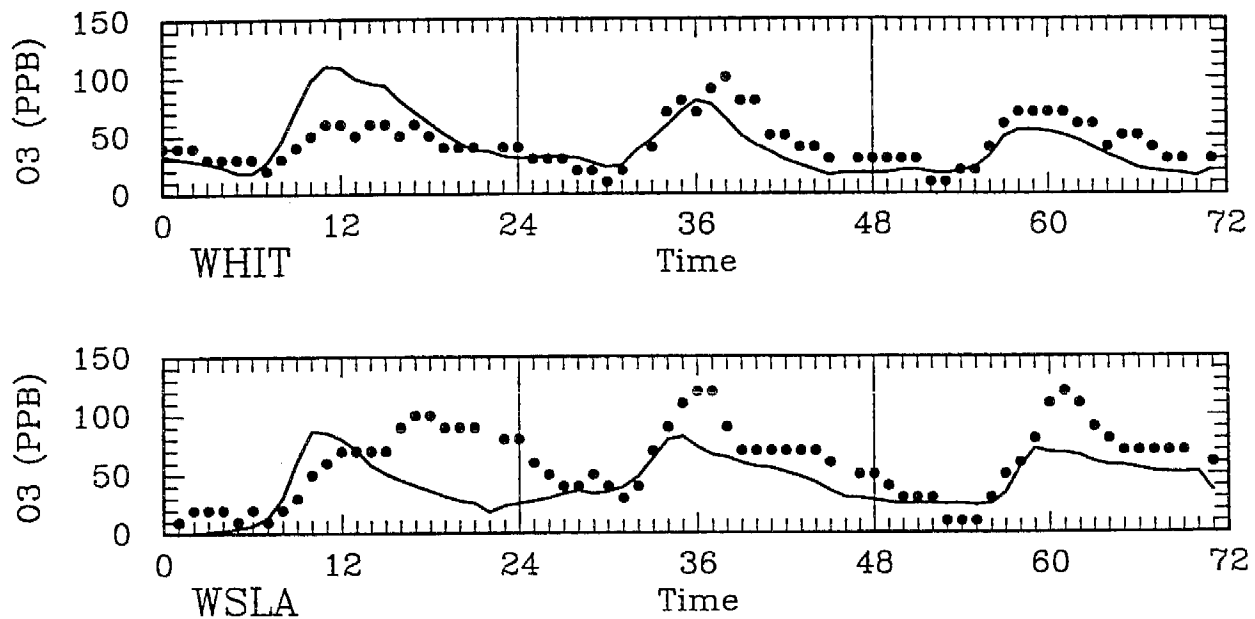


Figure 5-43. Predicted and observed 1-hr ozone concentrations on June 23-25, 1987.

Page 10 of 10

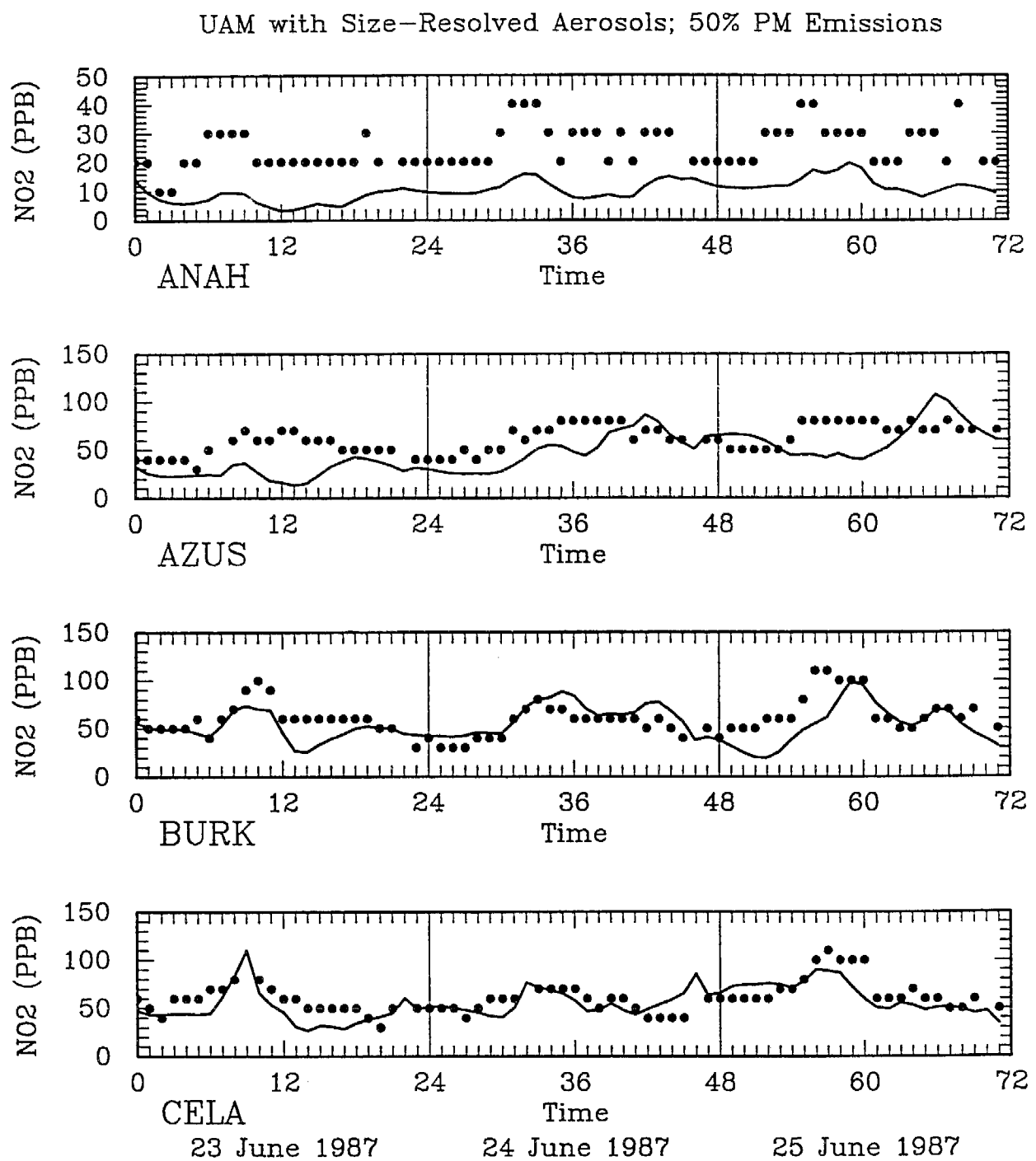


Figure 5-44. Predicted and observed 1-hr nitrogen dioxide concentrations on June 23-25, 1987.

Page 1 of 5

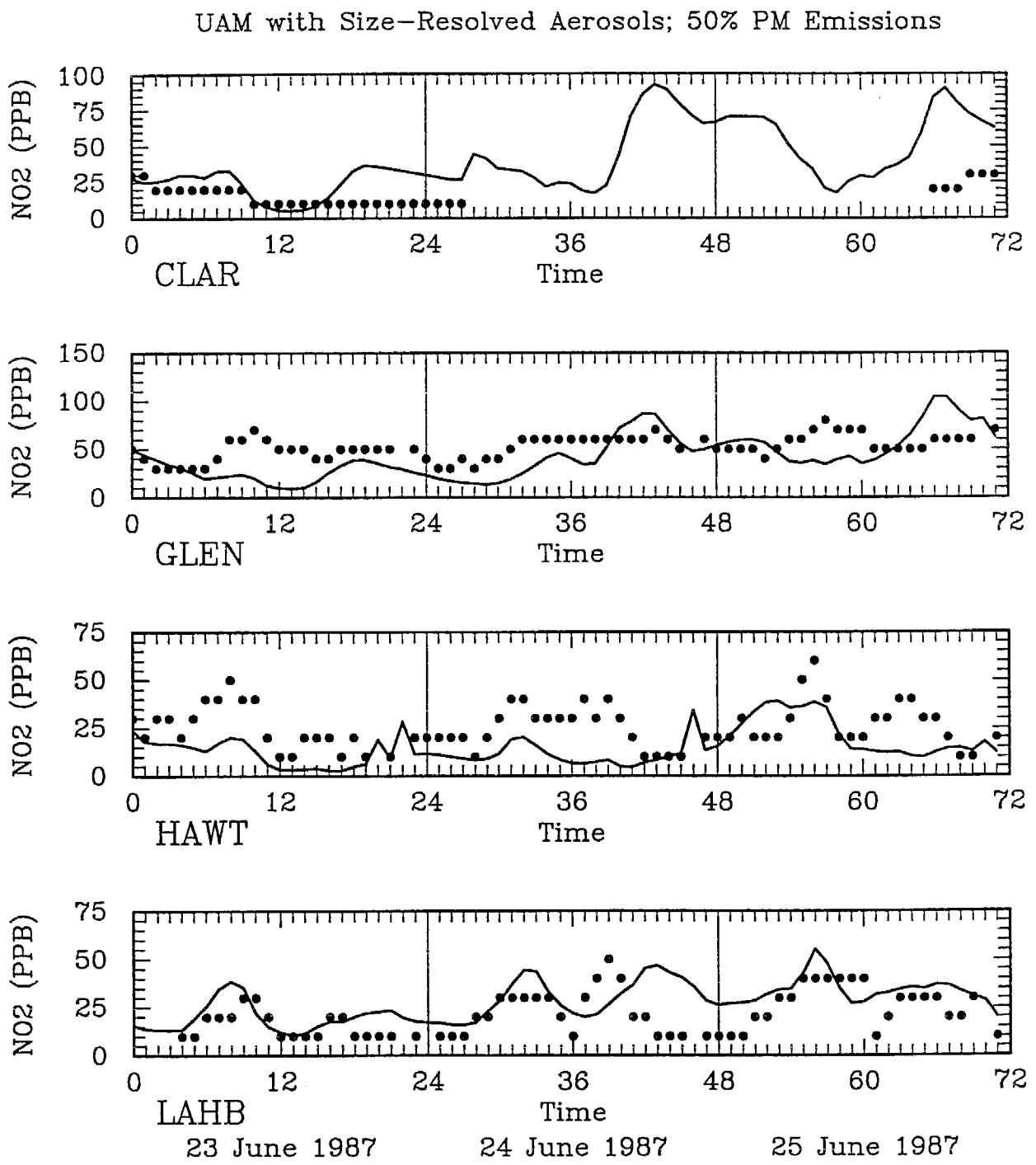


Figure 5-44. Predicted and observed 1-hr nitrogen dioxide concentrations on June 23-25, 1987.

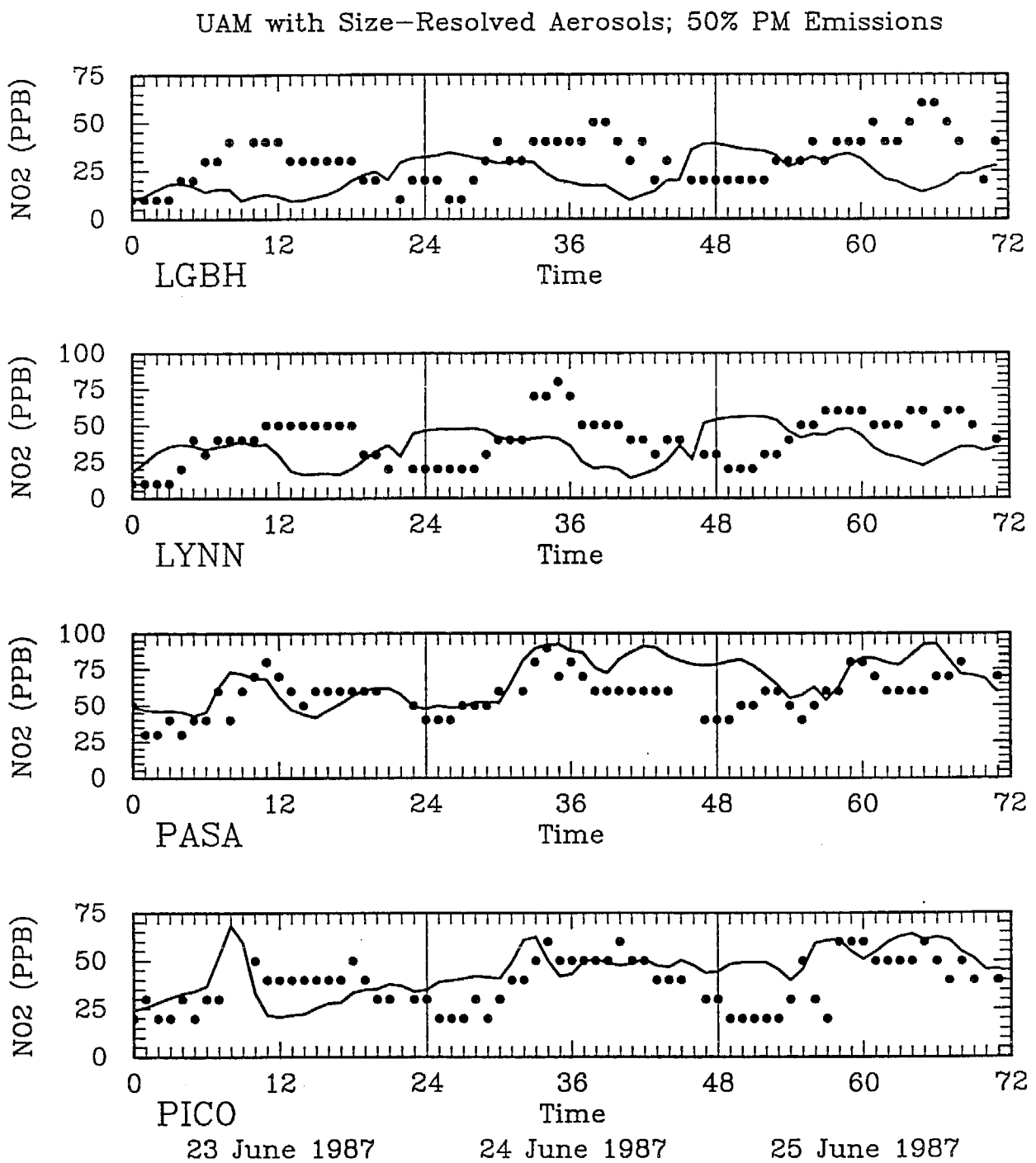


Figure 5-44. Predicted and observed 1-hr nitrogen dioxide concentrations on June 23-25, 1987.

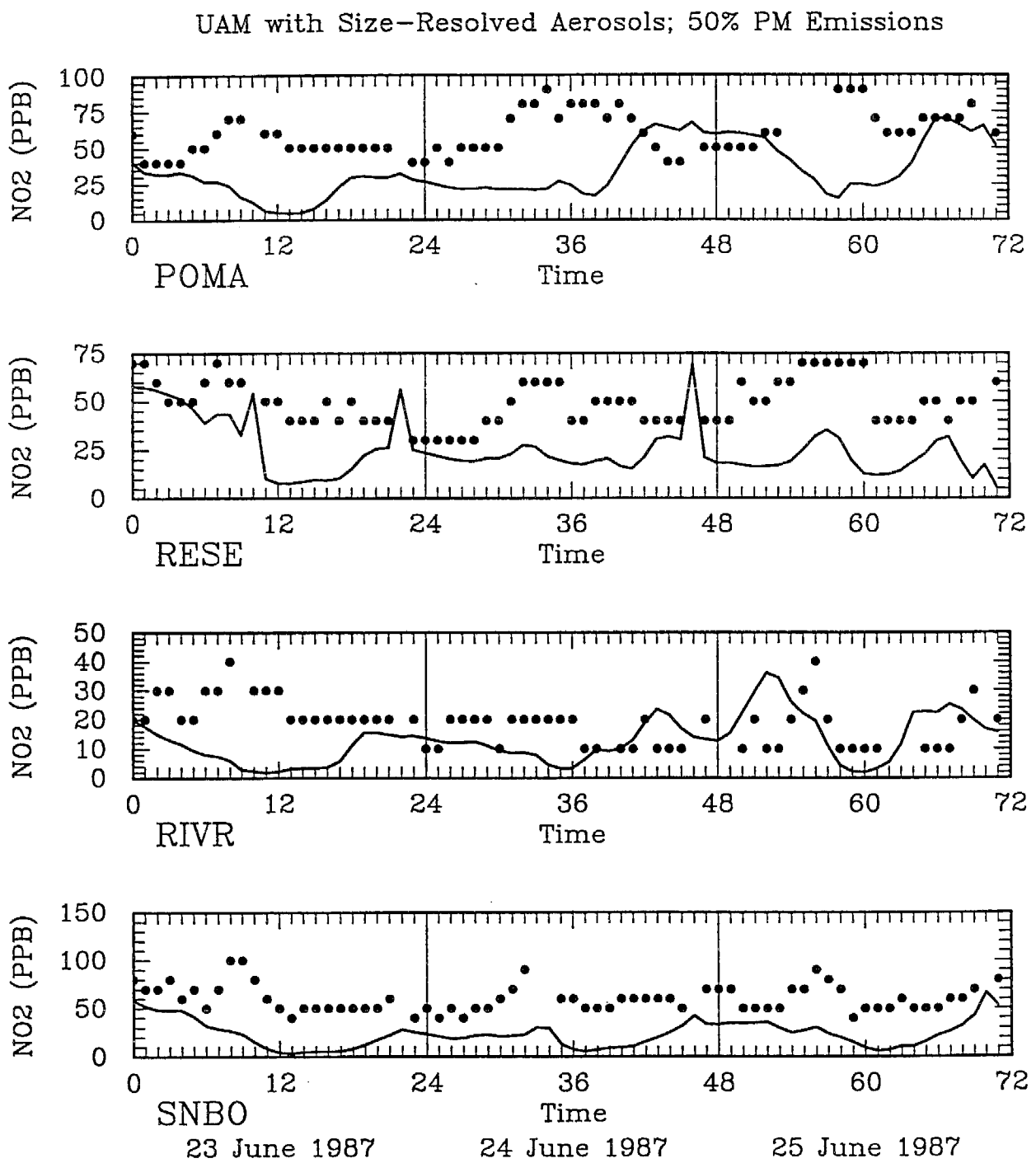


Figure 5-44. Predicted and observed 1-hr nitrogen dioxide concentrations on June 23-25, 1987.

Page 4 of 5

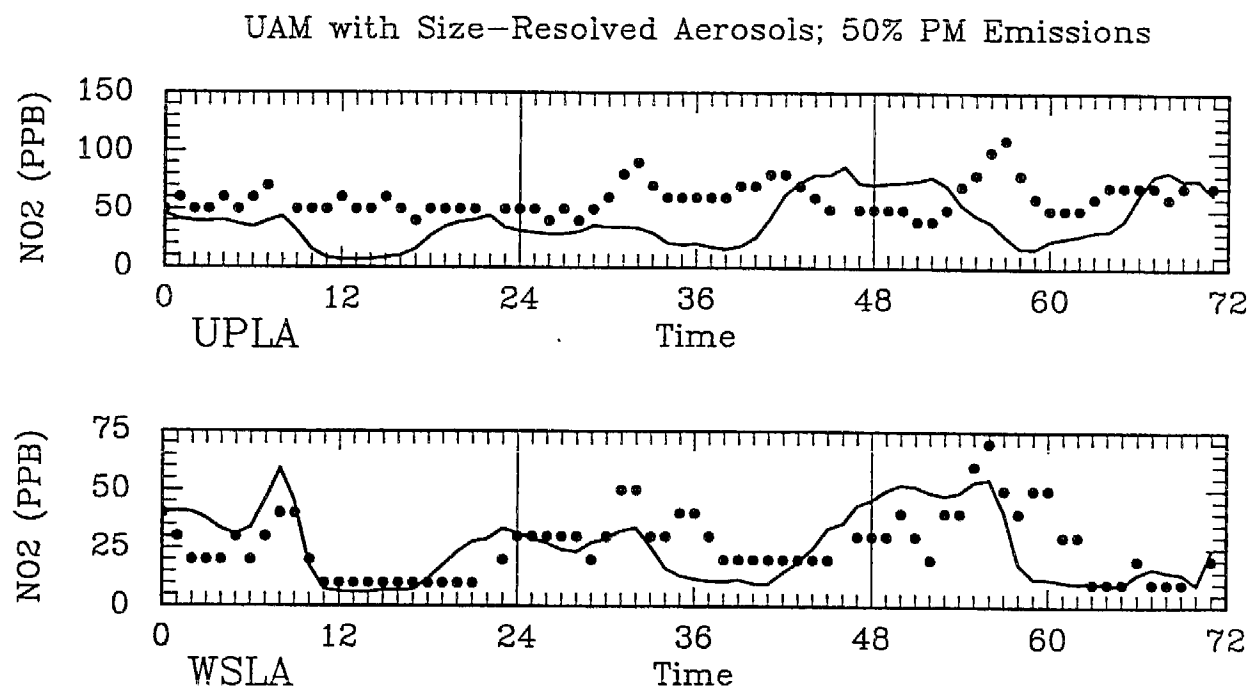
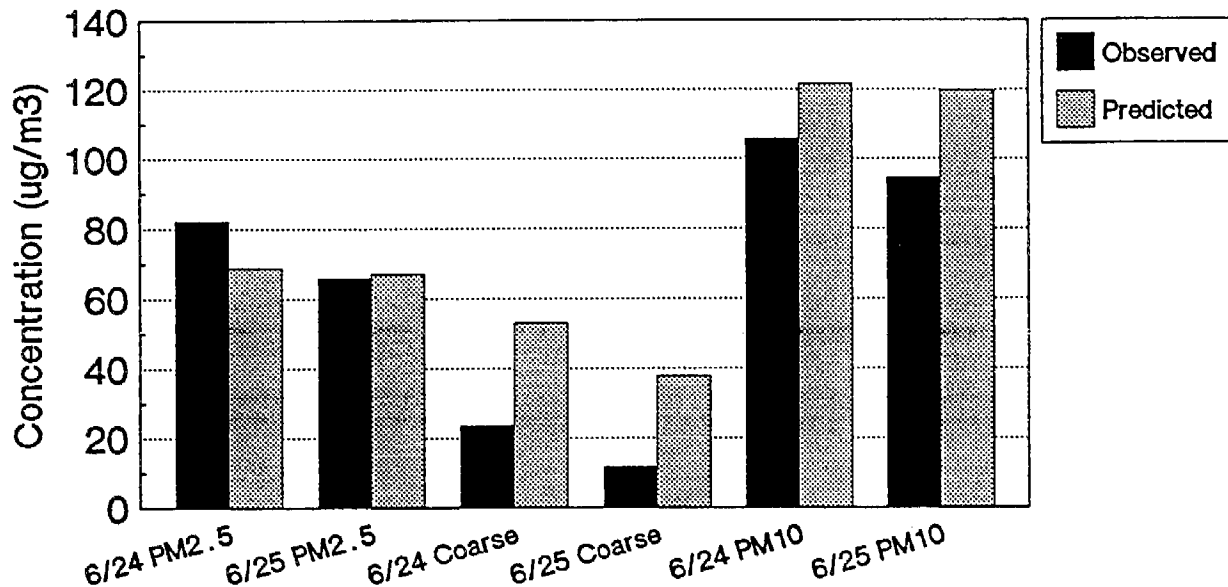


Figure 5-44. Predicted and observed 1-hr nitrogen dioxide concentrations on June 23-25, 1987.

Page 5 of 5

Maximum PM Mass
 24-hr Average at the Highest SCAQS Station
 June 24-25, 1987



Average PM Mass
 24-hr Average - Mean at the SCAQS Stations
 June 24-25, 1987

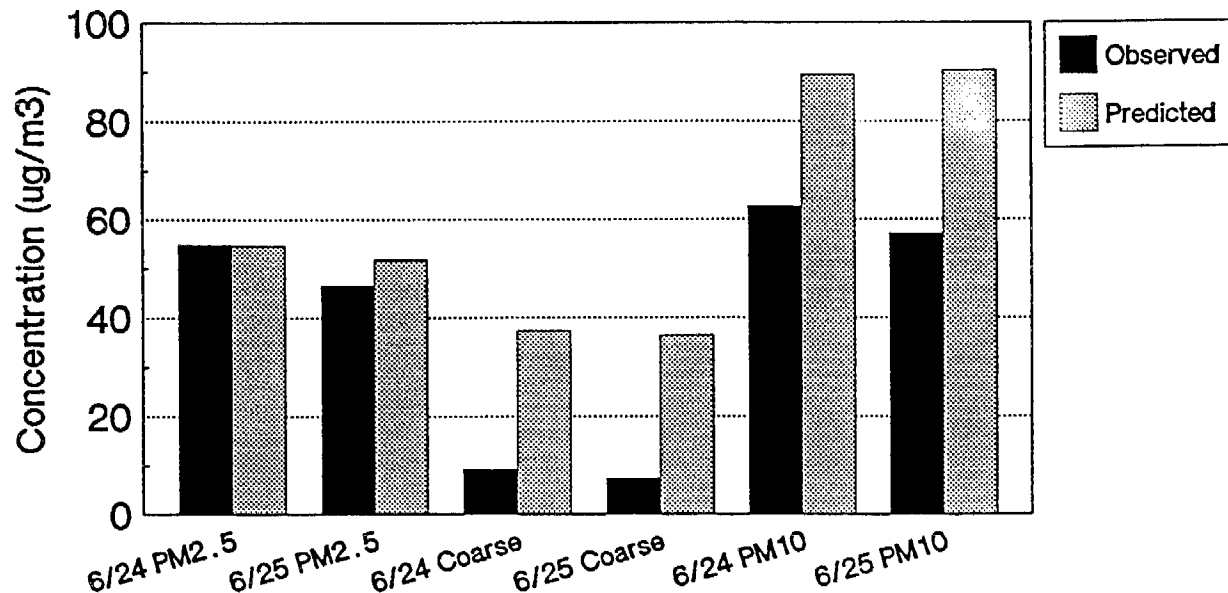
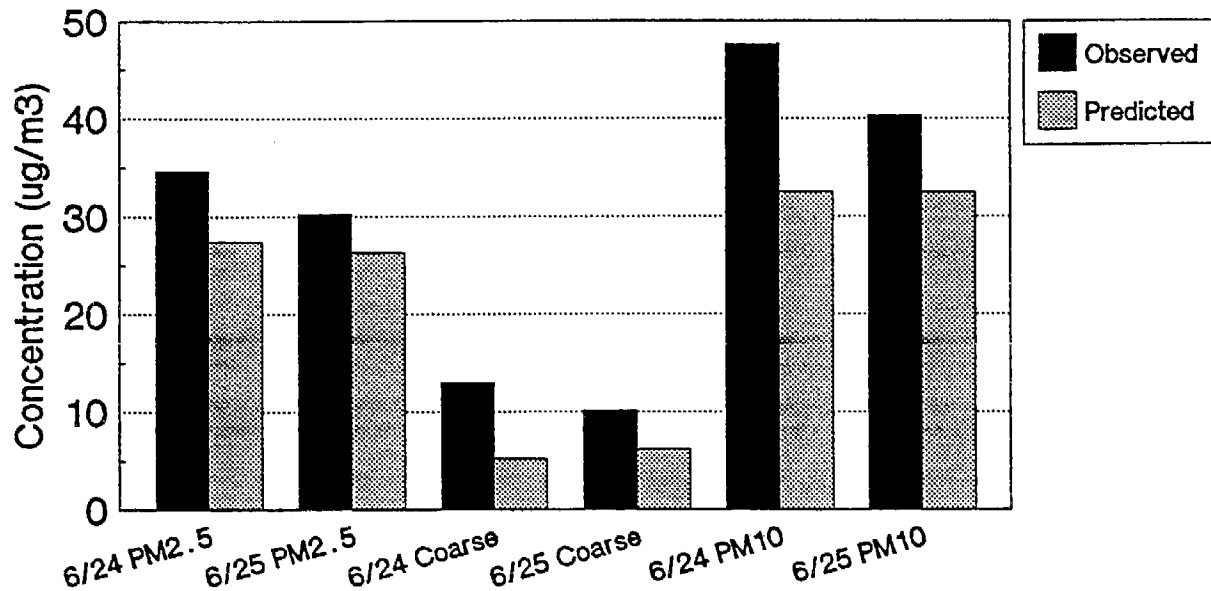


Figure 5-45. Predicted and observed mean and maximum 24-hr average PM mass on June 24-25, 1987.

Maximum Nitrate
 24-hr Average at the Highest SCAQS Station
 June 24-25, 1987



Average Nitrate
 24-hr Average - Mean at the SCAQS Stations
 June 24-25, 1987

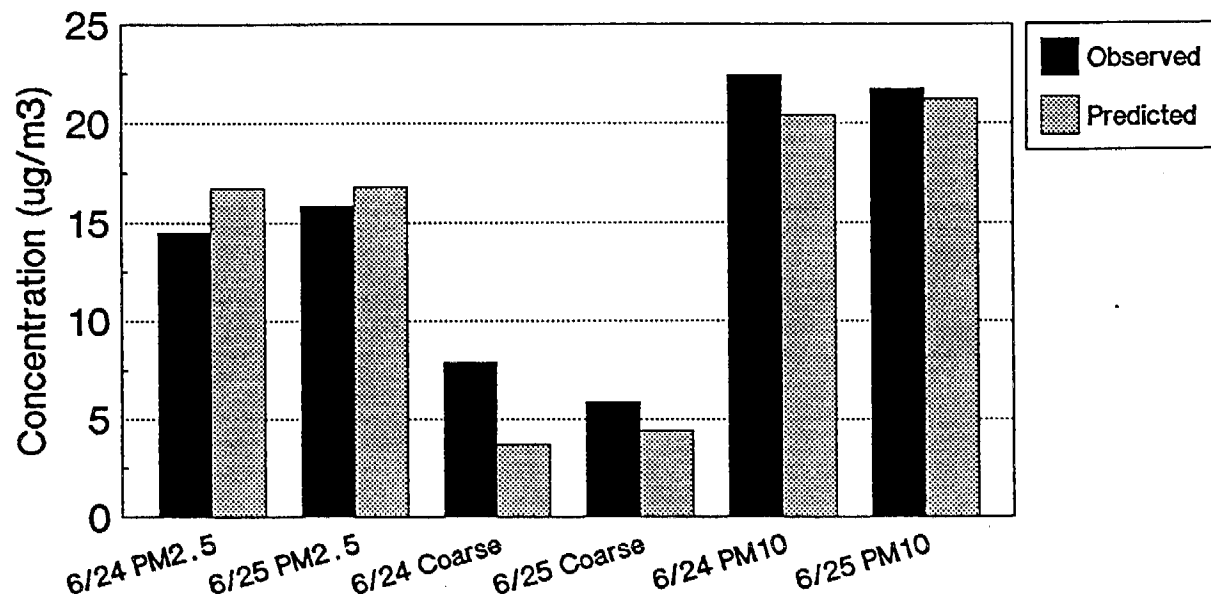
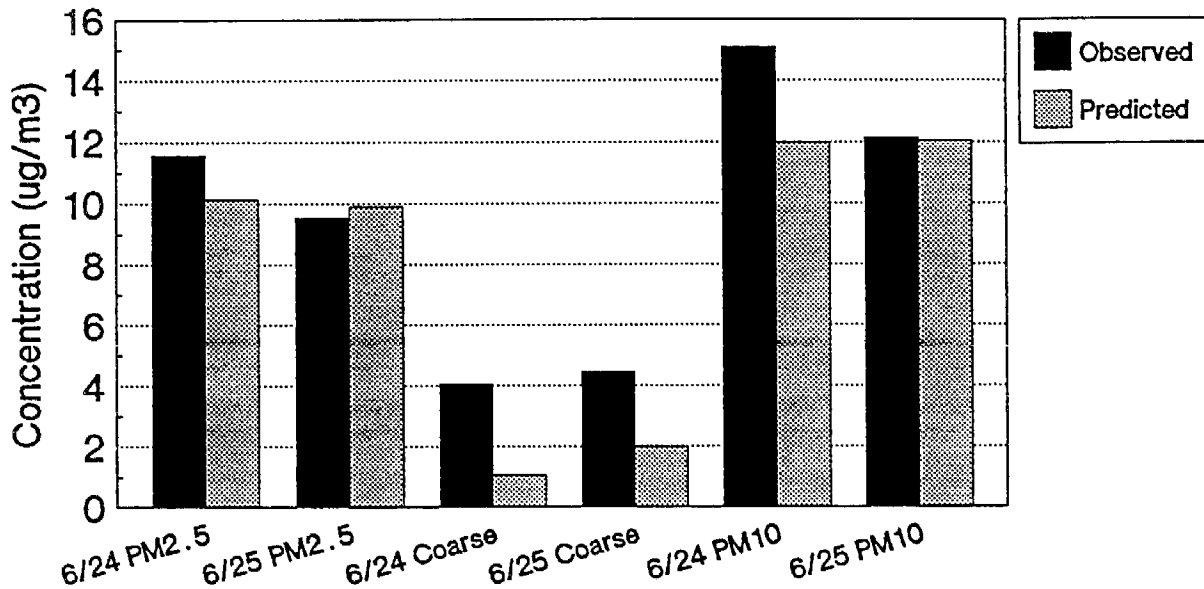


Figure 5-46. Predicted and observed mean and maximum 24-hr average nitrate on June 24-25, 1987.

Maximum Ammonium
 24-hr Average at the Highest SCAQS Station
 June 24-25, 1987



Average Ammonium
 24-hr Average - Mean at the SCAQS Stations
 June 24-25, 1987

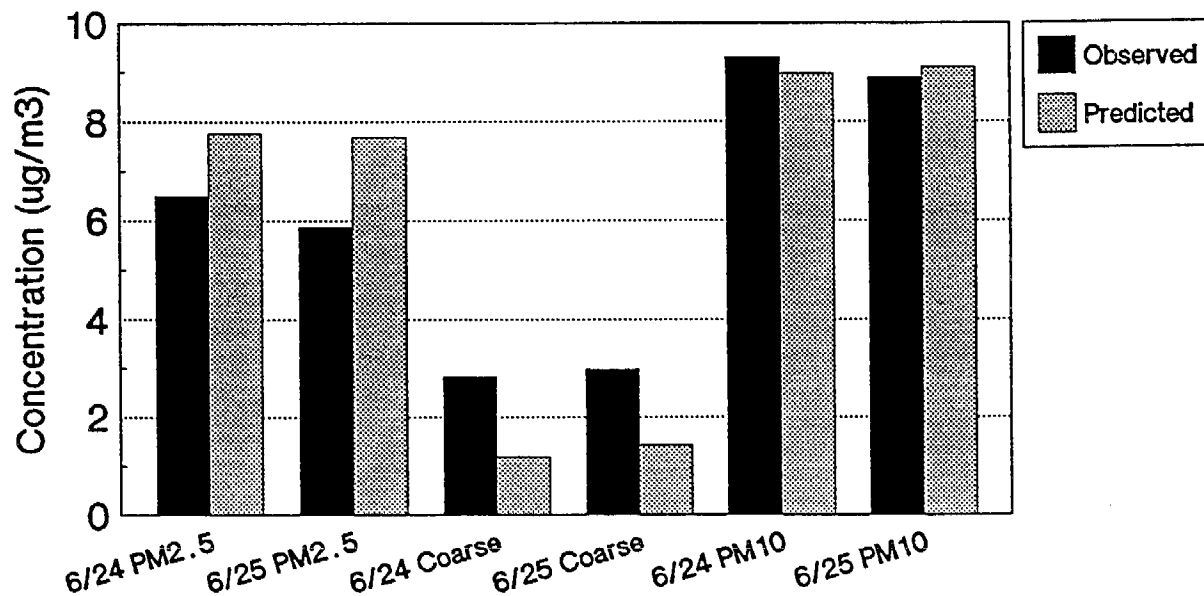
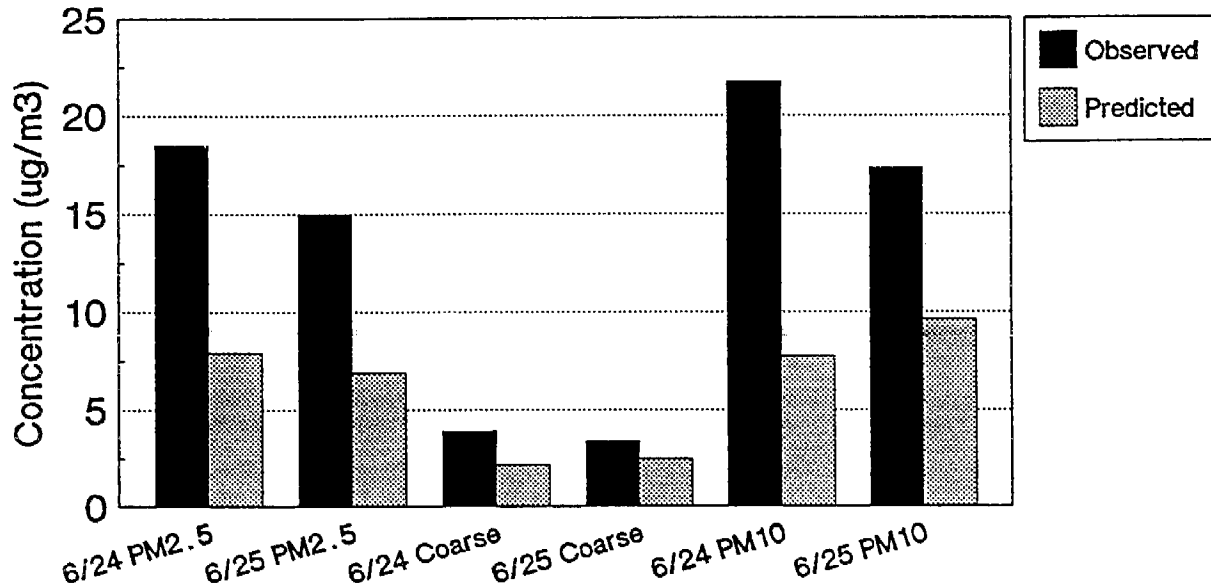


Figure 5-47. Predicted and observed mean and maximum 24-hr average ammonium on June 24-25, 1987.

Maximum Sulfate
24-hr Average at the Highest SCAQS Station
June 24-25, 1987



Average Sulfate
24-hr Average - Mean at the SCAQS Stations
June 24-25, 1987

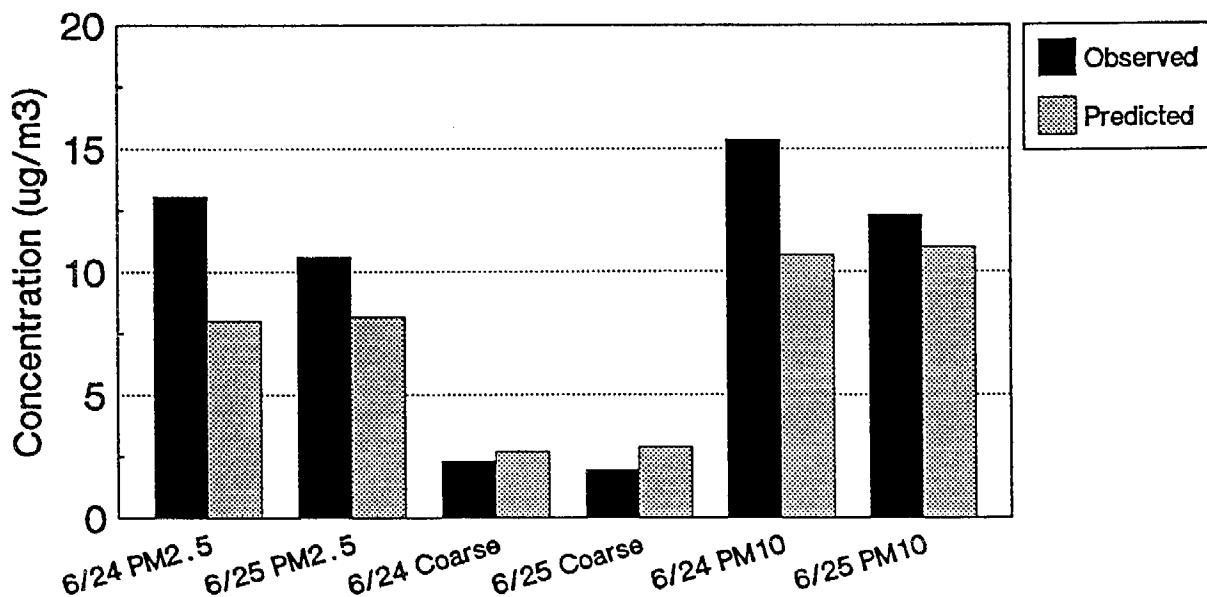
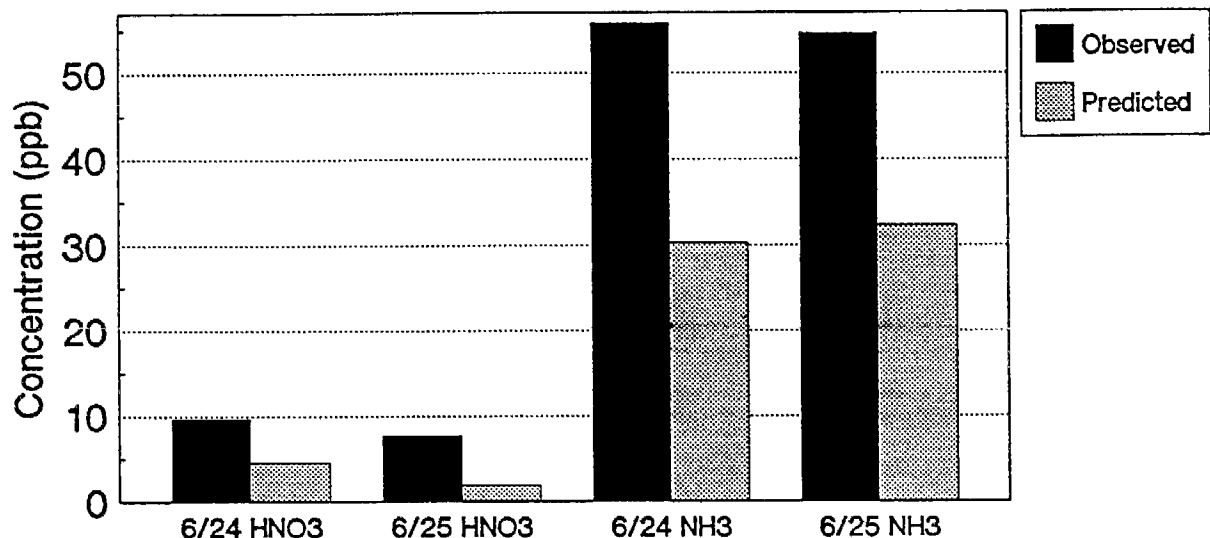


Figure 5-48. Predicted and observed mean and maximum 24-hr average sulfate on June 24-25, 1987.

Maximum Nitric Acid and Ammonia
24-hr Average at the Highest SCAQS Station
June 24-25, 1987



Average Nitric Acid and Ammonia
24-hr Average at the Highest SCAQS Station
June 24-25, 1987

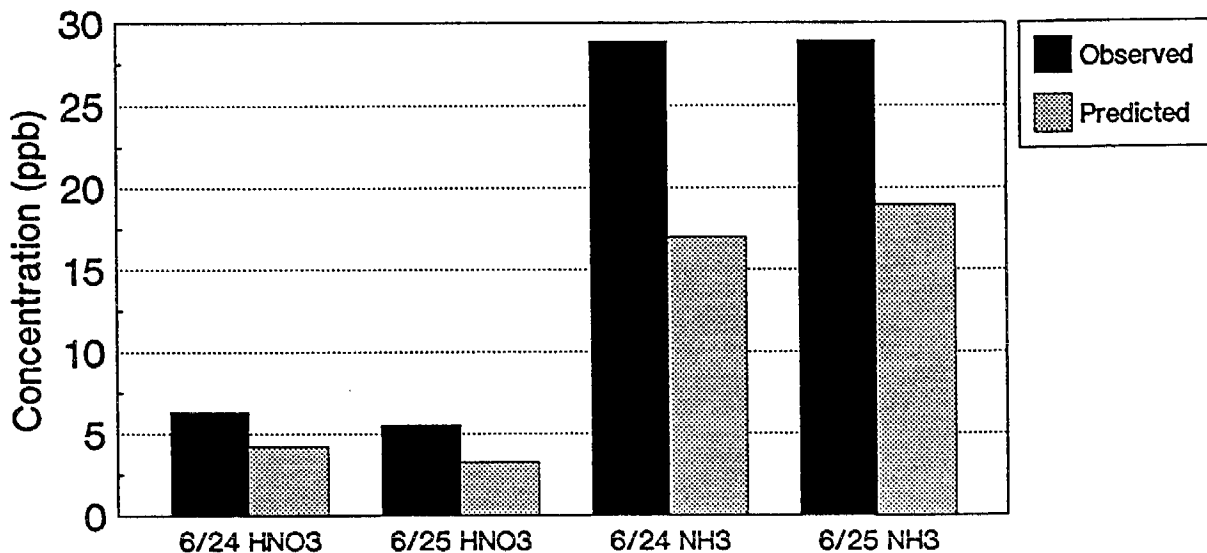
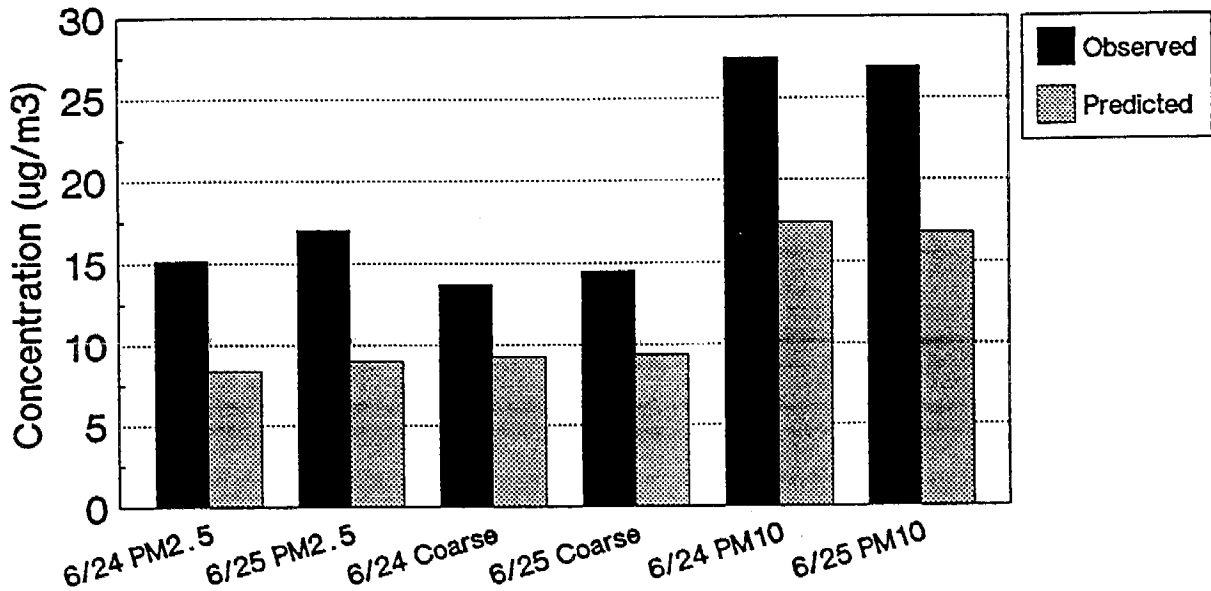


Figure 5-49. Predicted and observed mean and maximum 24-hr average nitric acid and ammonia on June 24-25, 1987.

Maximum Organic PM
24-hr Average at the Highest SCAQS Station
June 24-25, 1987



Average Organic PM
24-hr Average - Mean at the SCAQS Stations
June 24-25, 1987

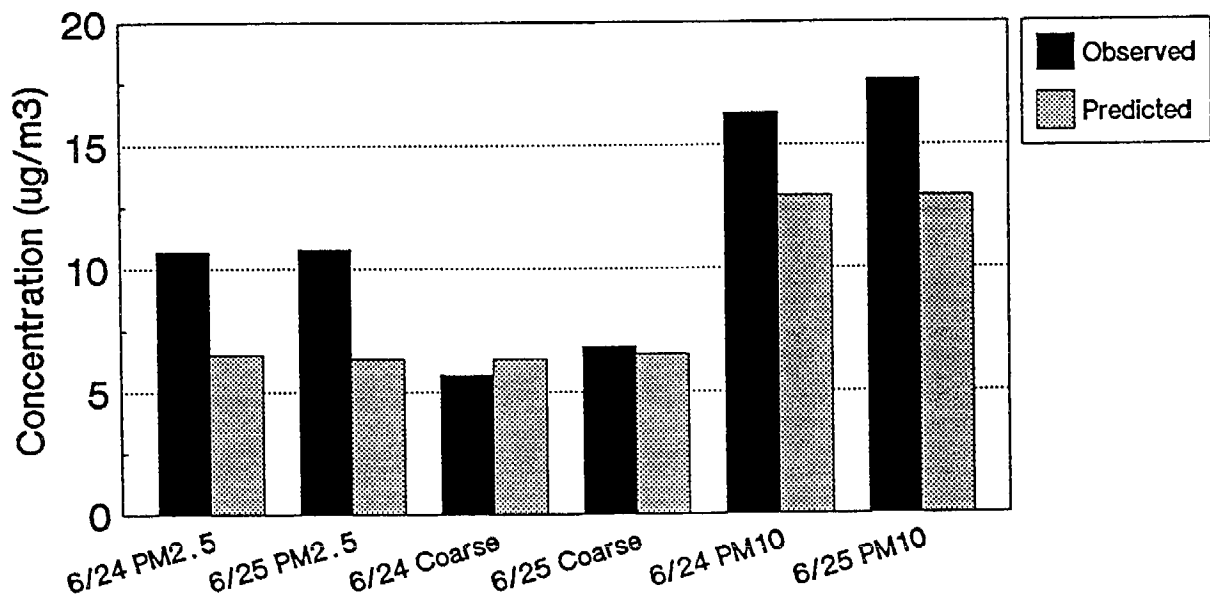
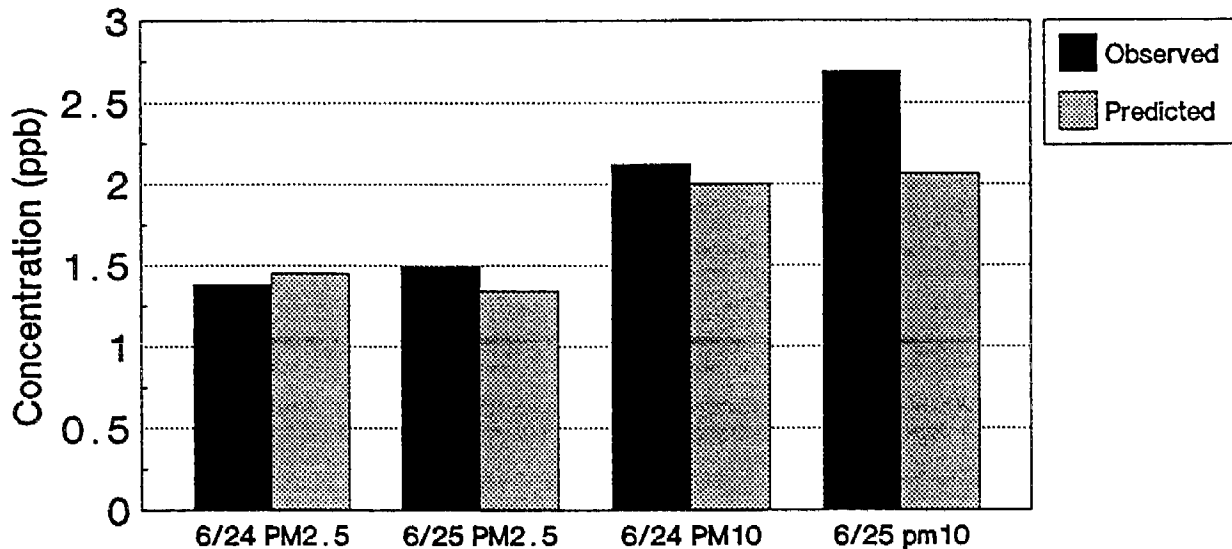


Figure 5-50. Predicted and observed mean and maximum 24-hr average organic PM on June 24-25, 1987.

Average Elemental Carbon
24-hr Average at the Highest SCAQS Station
June 24-25, 1987



UAM-AERO Run 23

Maximum Elemental Carbon
24-hr Average at the Highest SCAQS Station
June 24-25, 1987

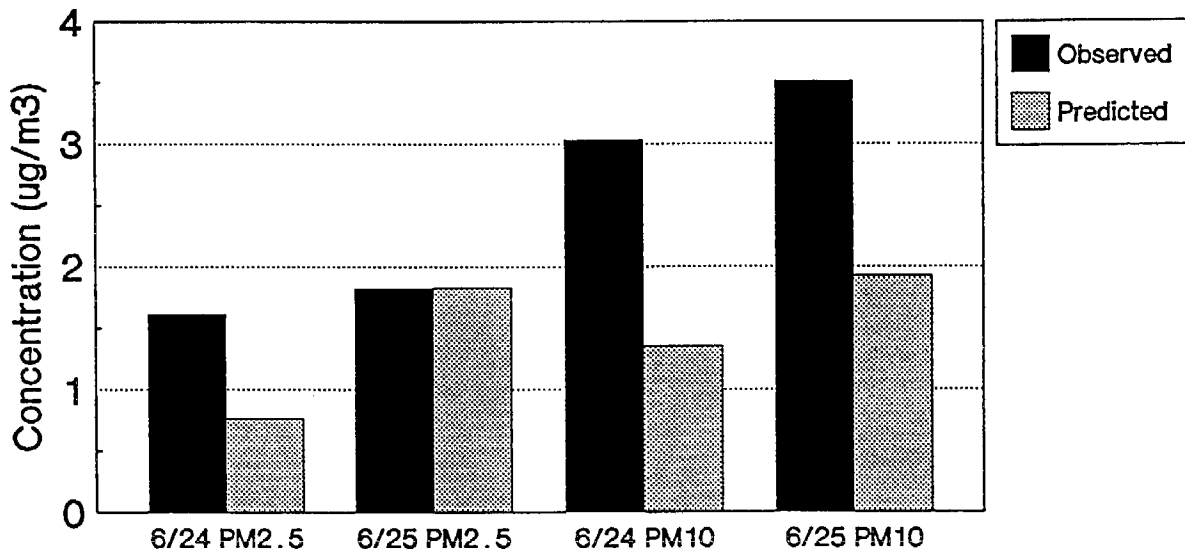
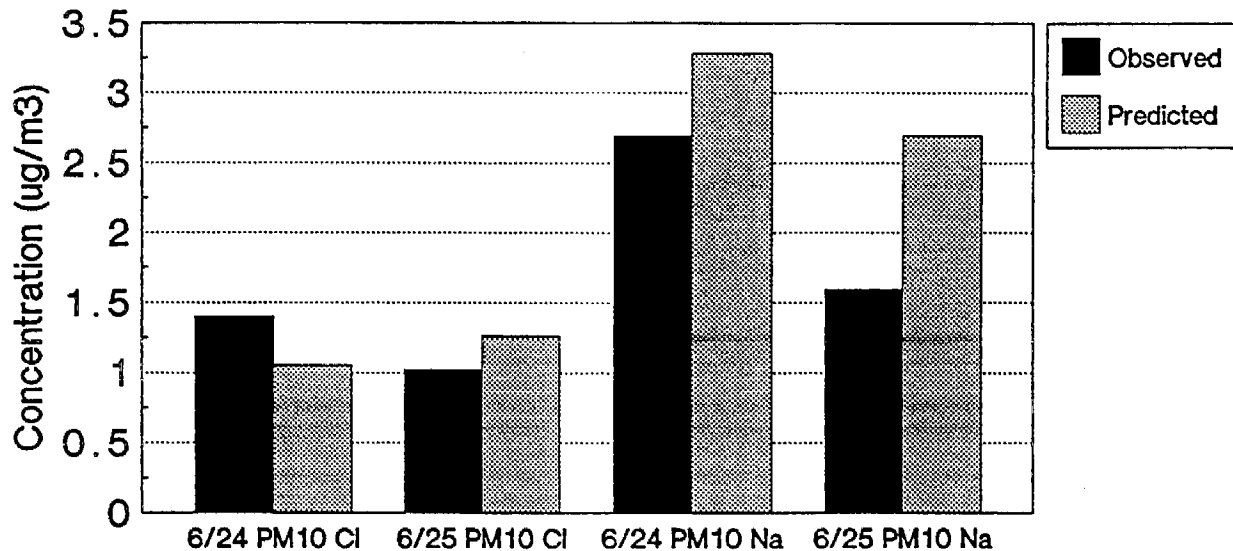


Figure 5-51. Predicted and observed mean and maximum 24-hr average elemental carbon on June 24-25, 1987.

Maximum Sodium and Chloride
24-hr Average at the Highest SCAQS Station
June 24-25, 1987



Average Sodium and Chloride
24-hr Average - Mean at the SCAQS Stations
June 24-25, 1987

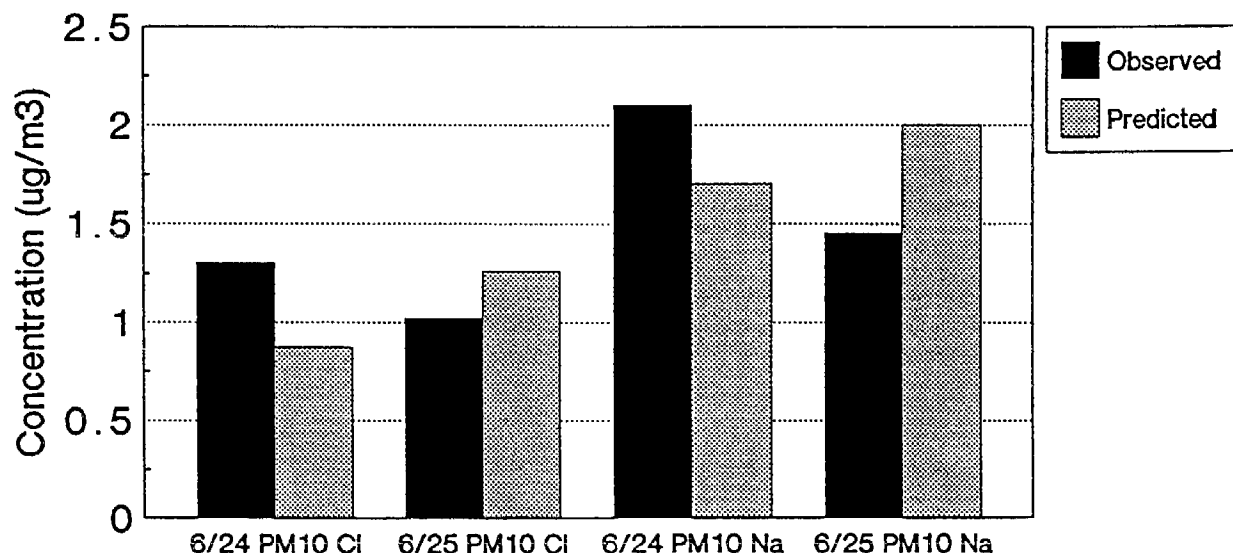


Figure 5-52. Predicted and observed mean and maximum 24-hr average sodium and chloride on June 24-25, 1987.

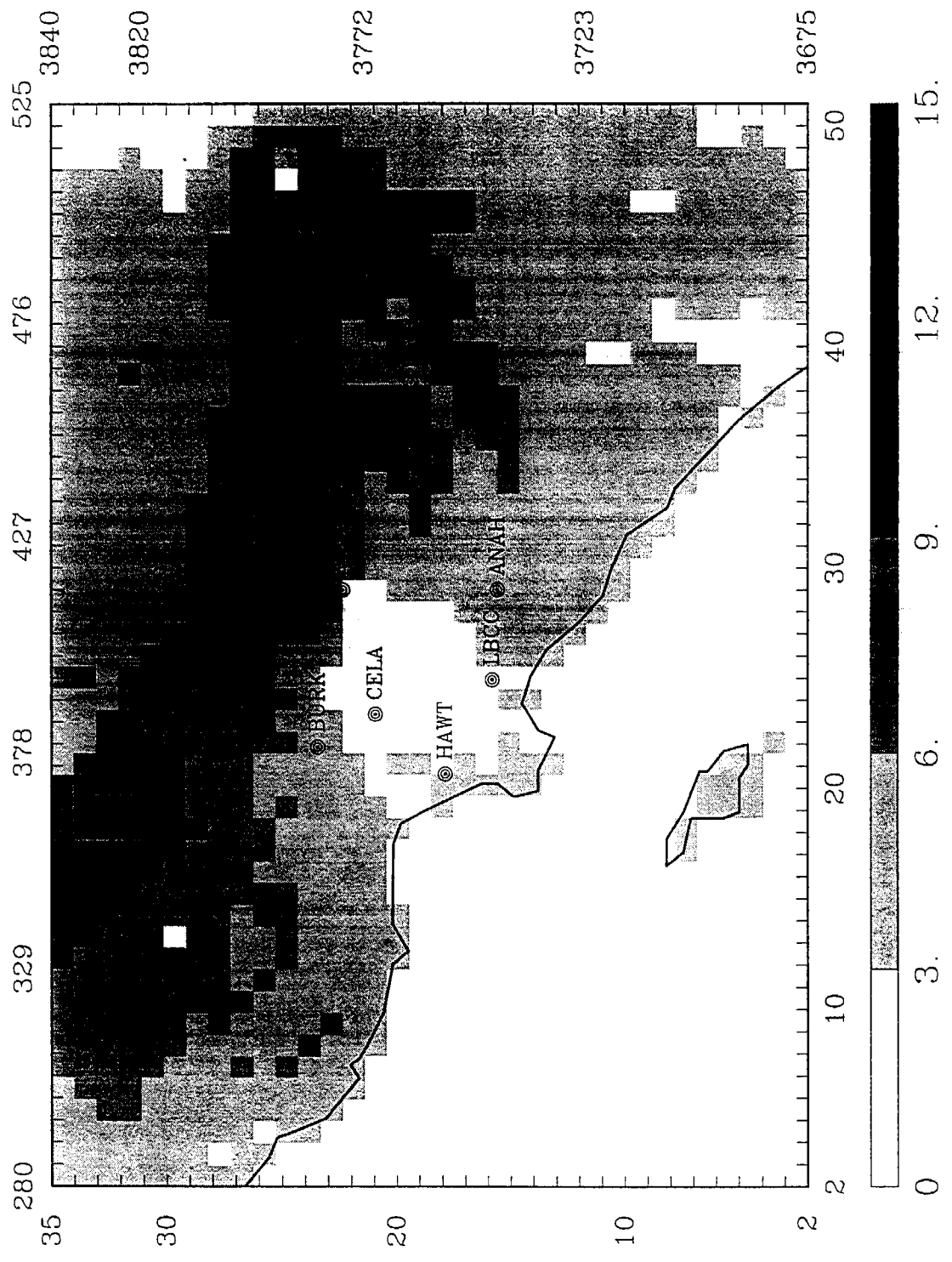


Figure 5-53. Estimated ozone deposition in moles/hectare-day on June 25, 1987 in the SoCAB.

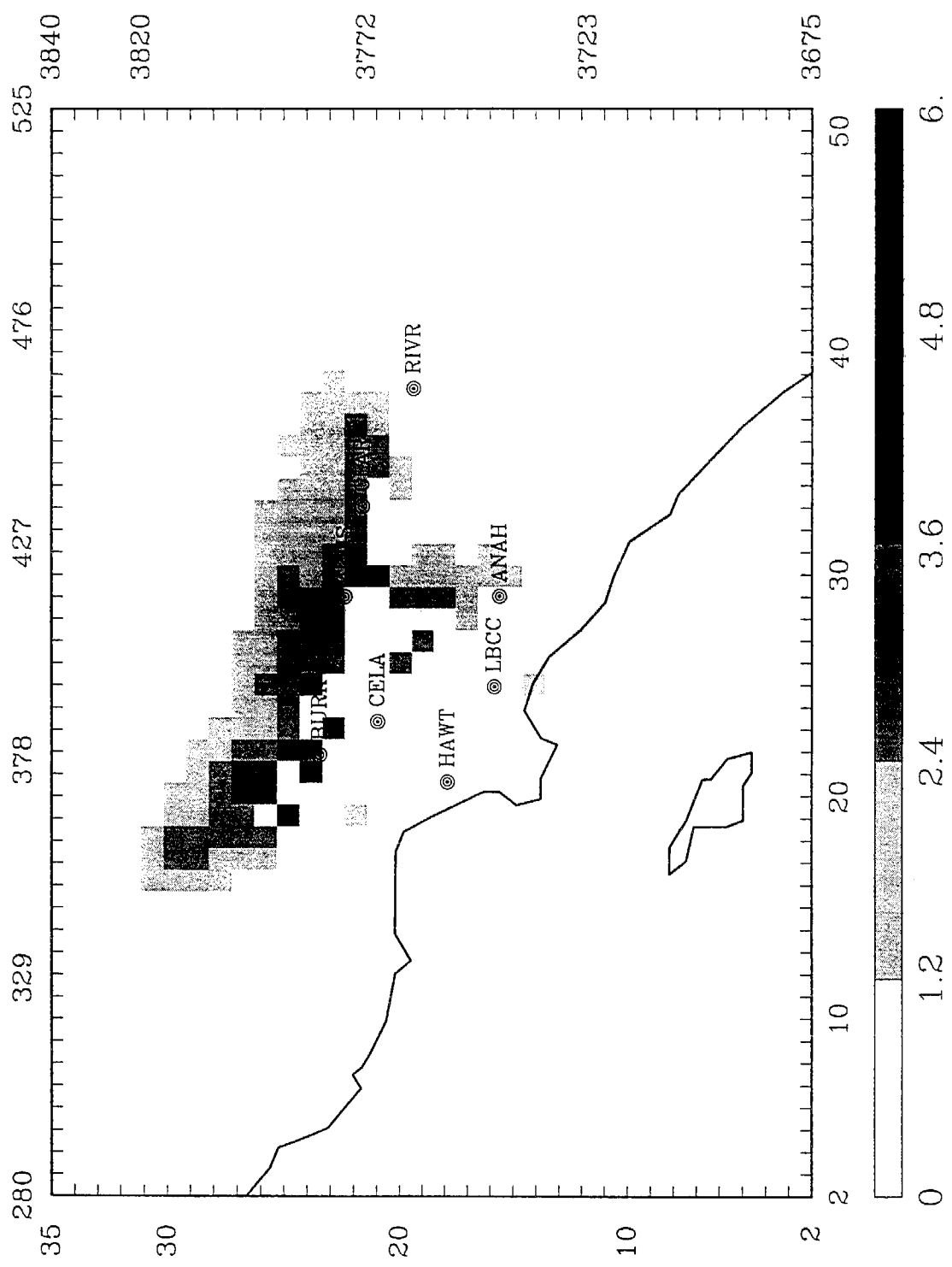


Figure 5-54. Estimated nitrogen dioxide deposition in moles/hectare-day on June 25, 1987 in the SoCAB.

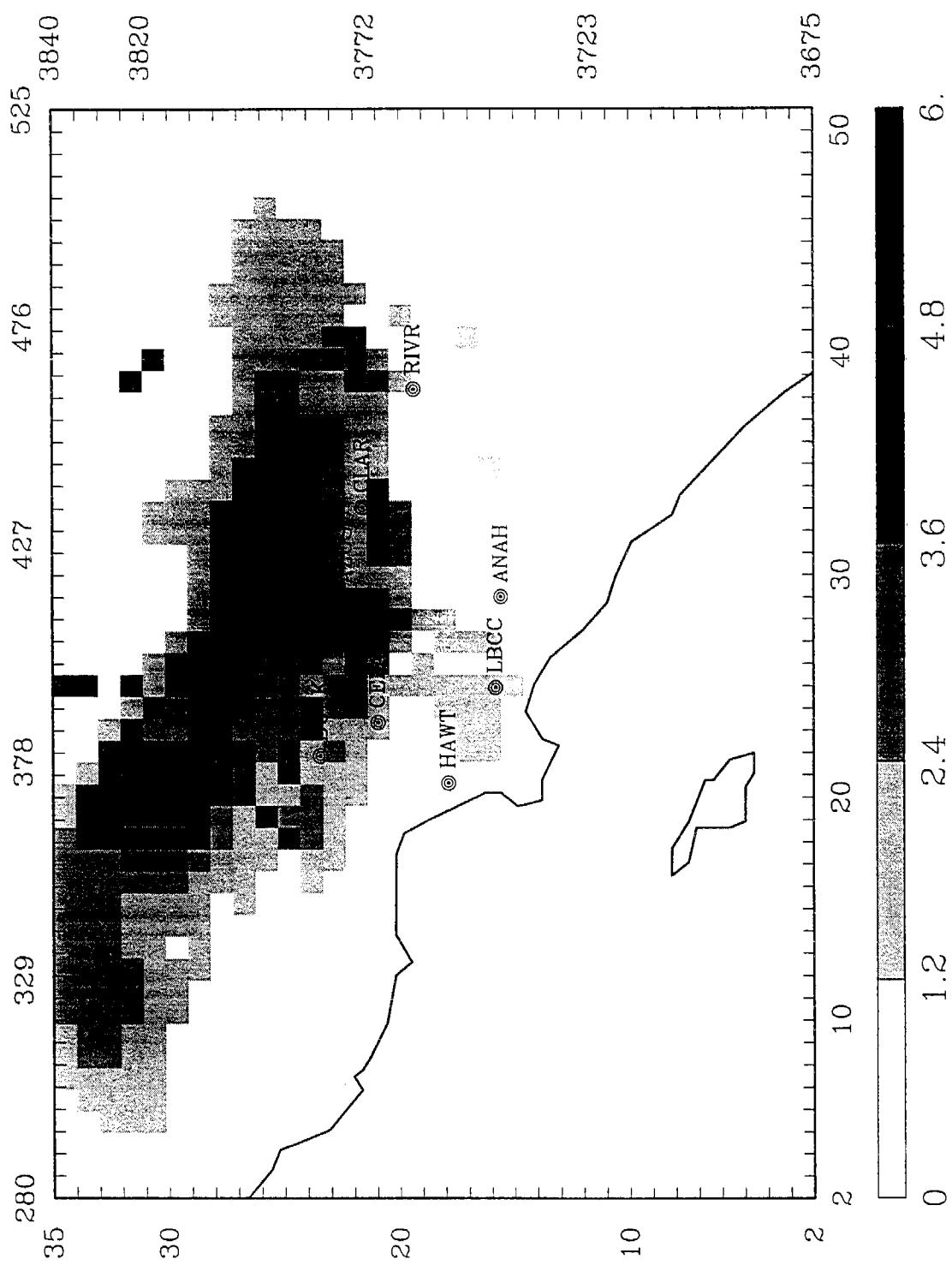


Figure 5-55. Estimated nitric acid deposition in moles/hectare-day on June 25, 1987 in the SoCAB.

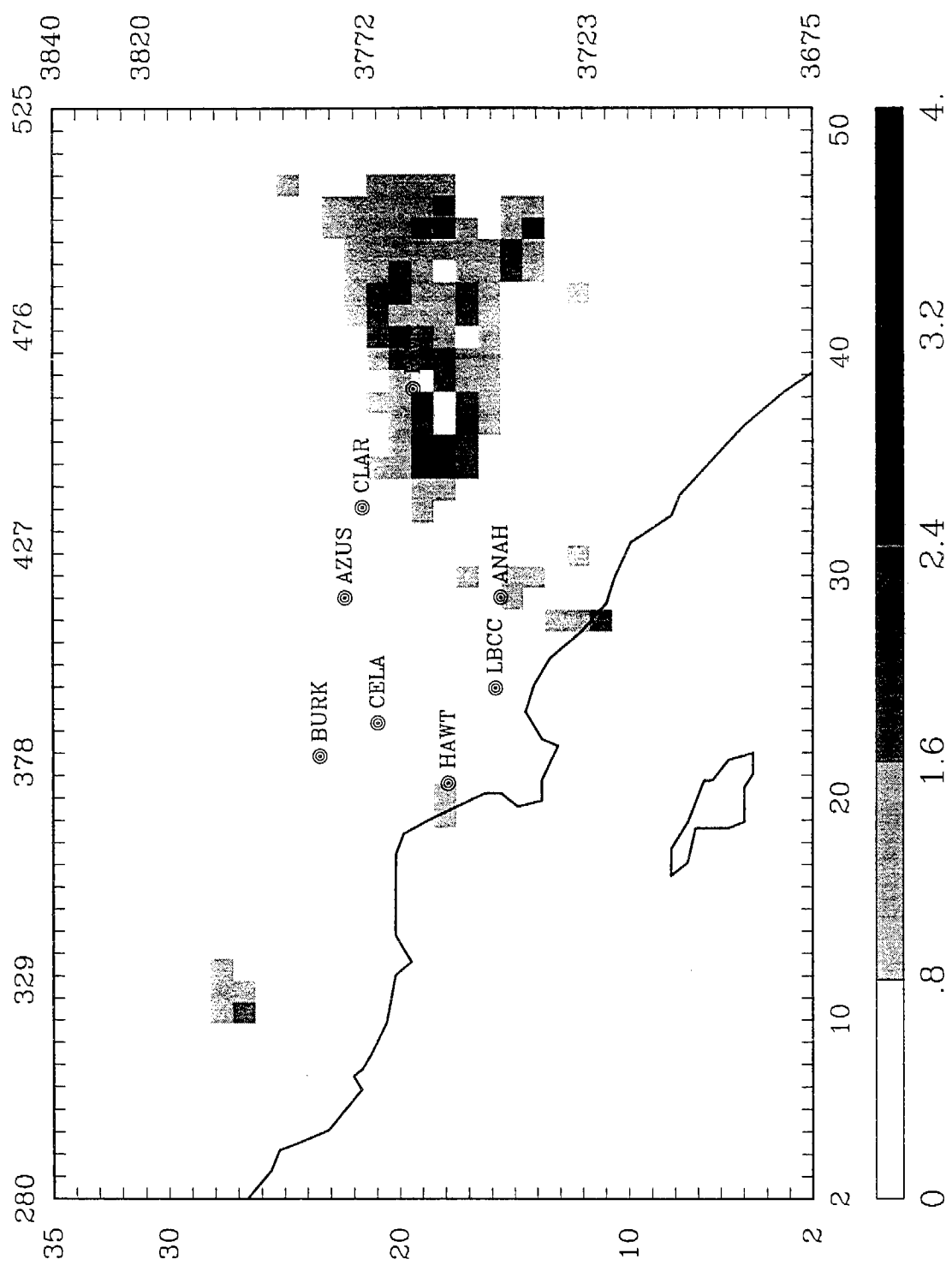


Figure 5-56. Estimated ammonia deposition in moles/hectare-day on June 25, 1987 in the SoCAB.

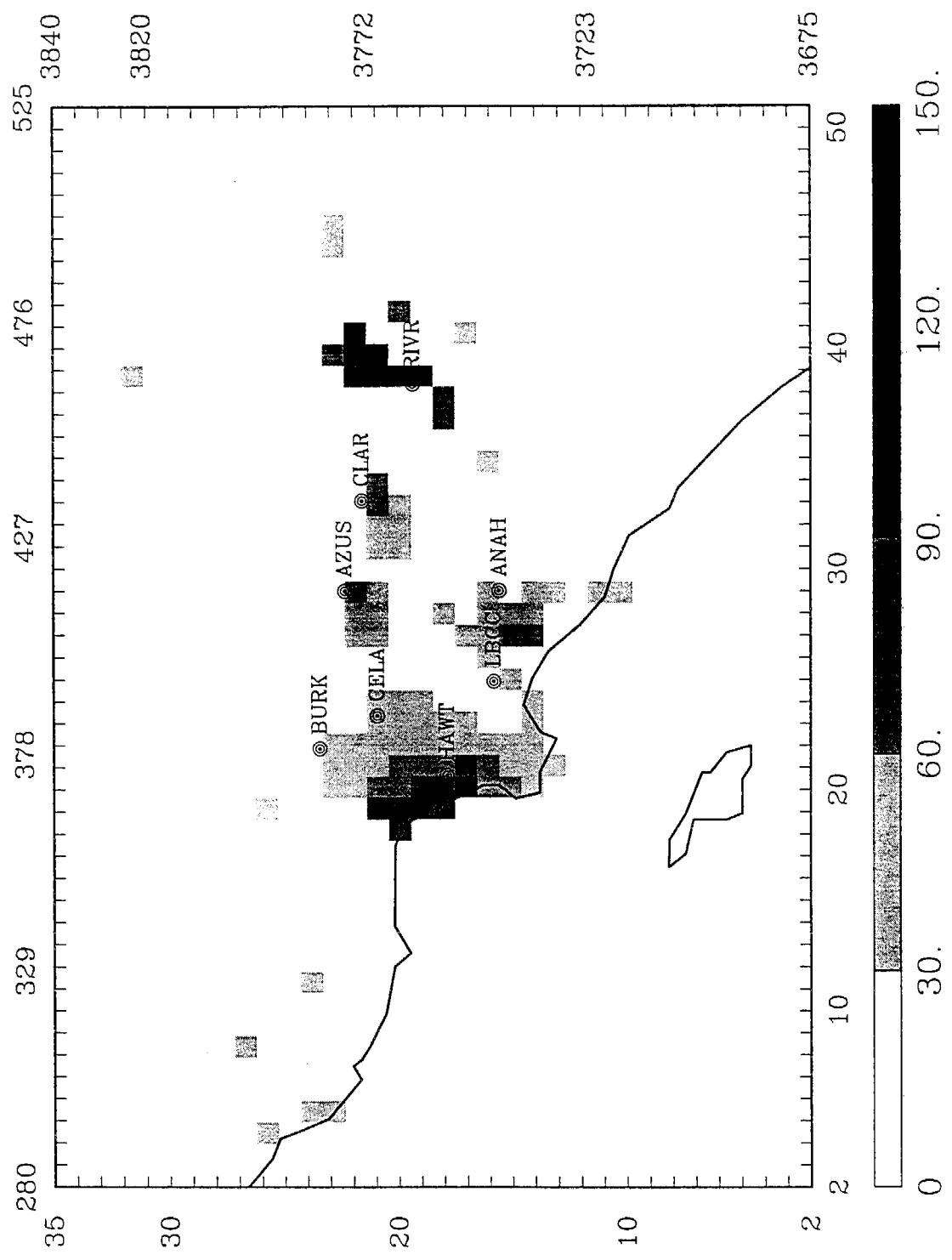


Figure 5-57. Estimated PM₁₀ nitrate deposition in grams/hectare-day on June 25, 1987 in the SoCAB.

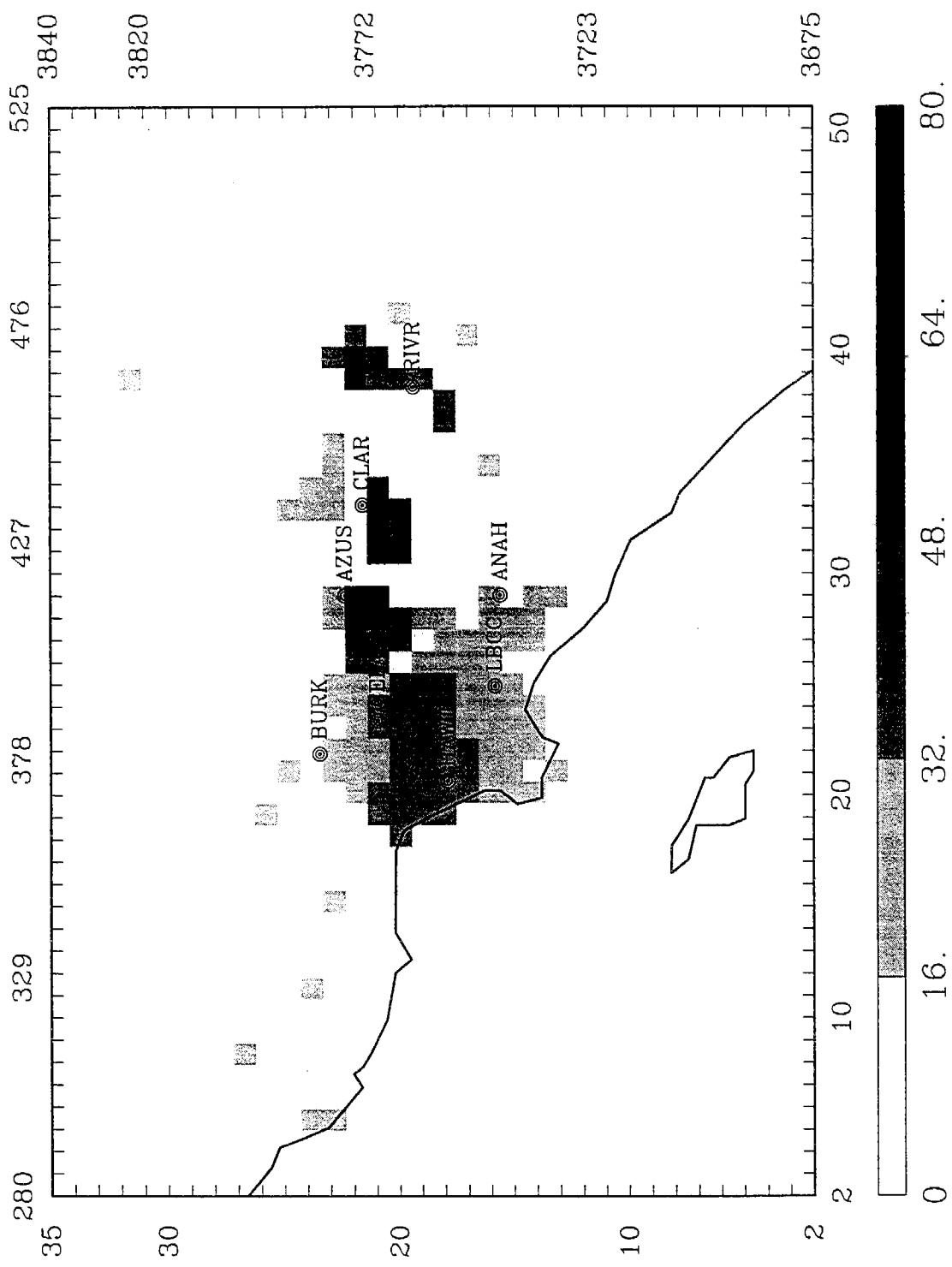


Figure 5-58. Estimated PM_{10} sulfate deposition in grams/hectare-day on June 25, 1987 in the SoCAB.

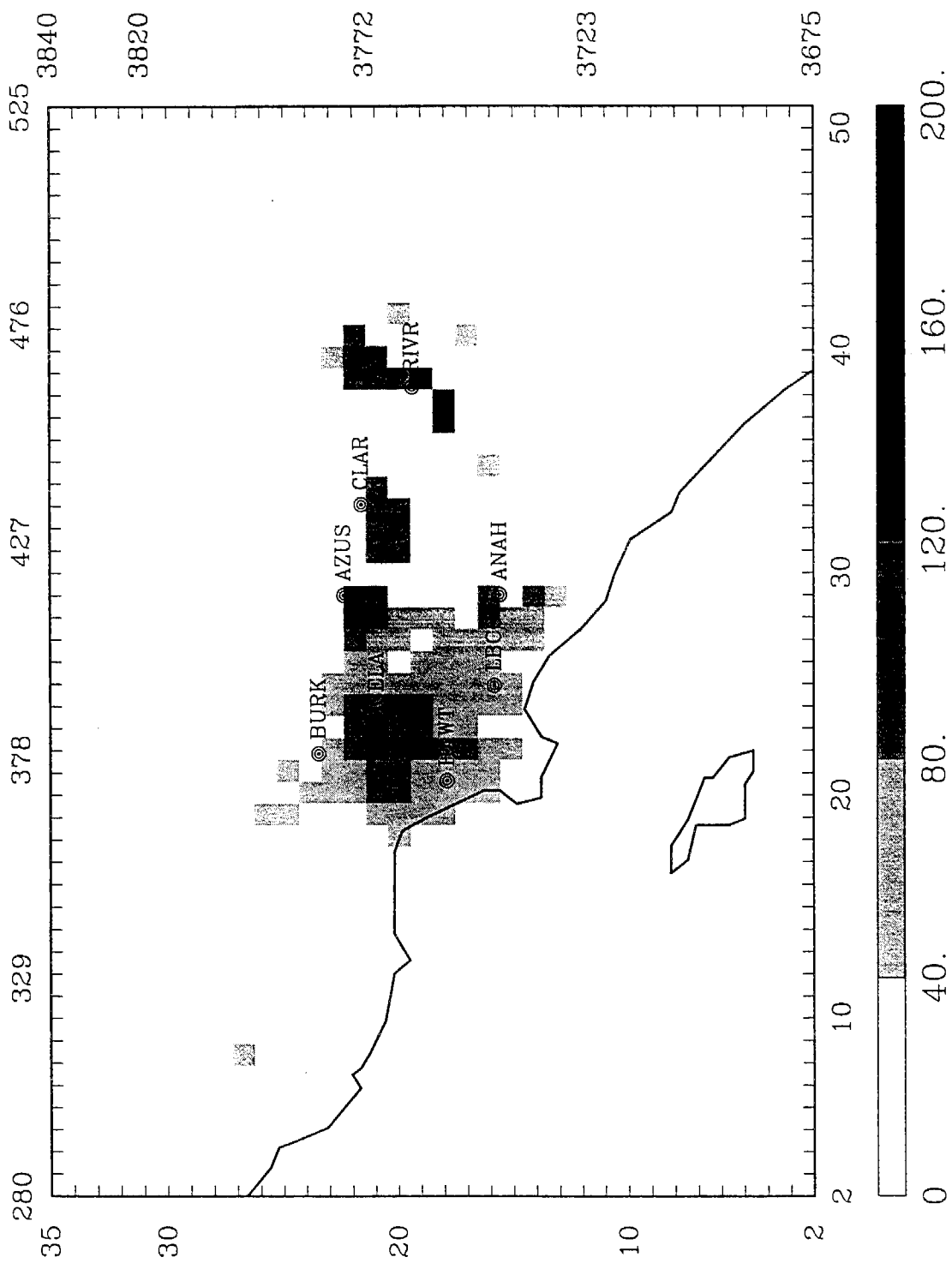


Figure 5-59. Estimated PM₁₀ organic material deposition in grams/hectare-day on June 25, 1987 in the SoCAB.

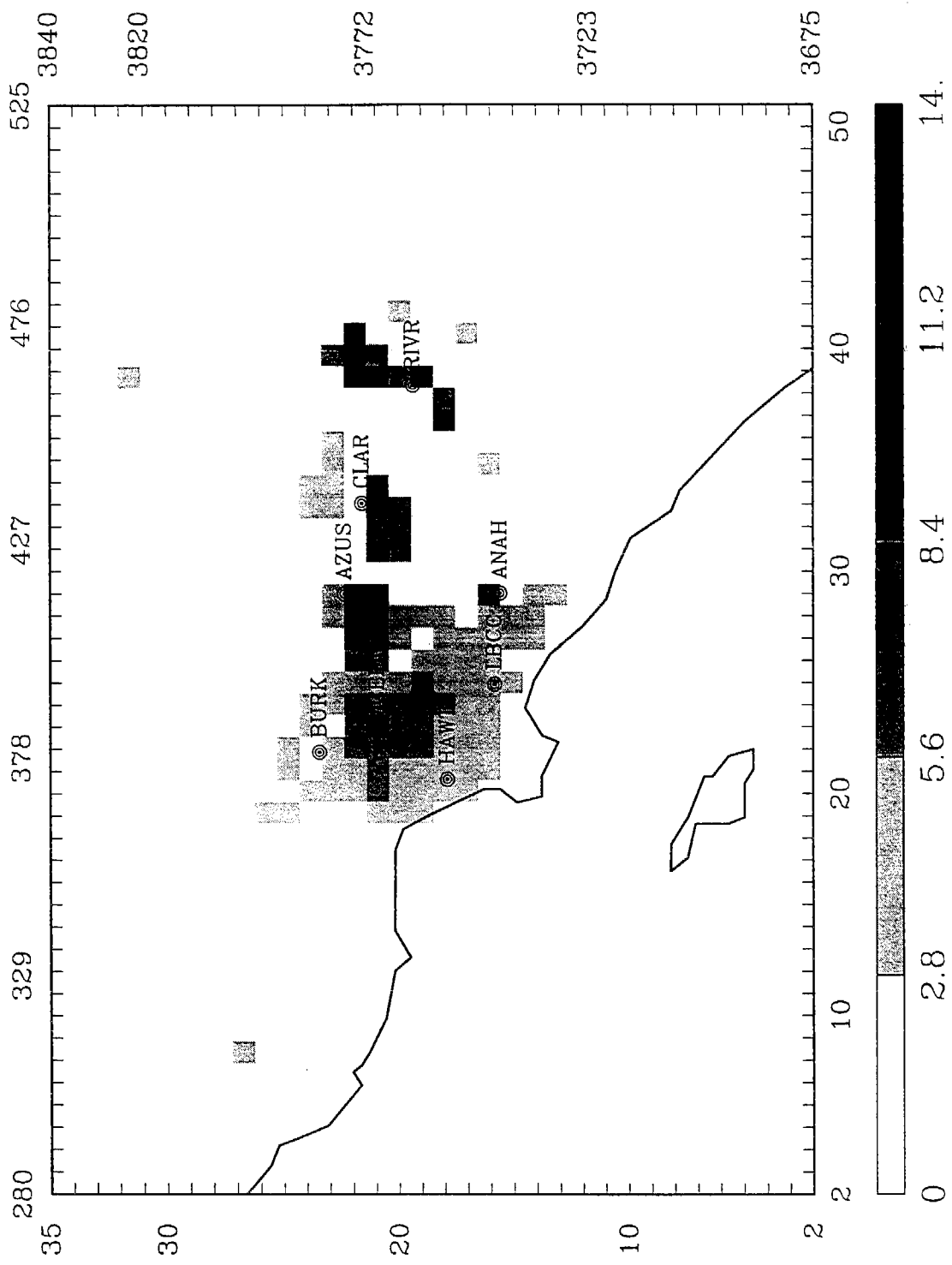


Figure 5-60. Estimated PM₁₀ elemental carbon deposition in grams/hectare-day on June 25, 1987 in the SoCAB.

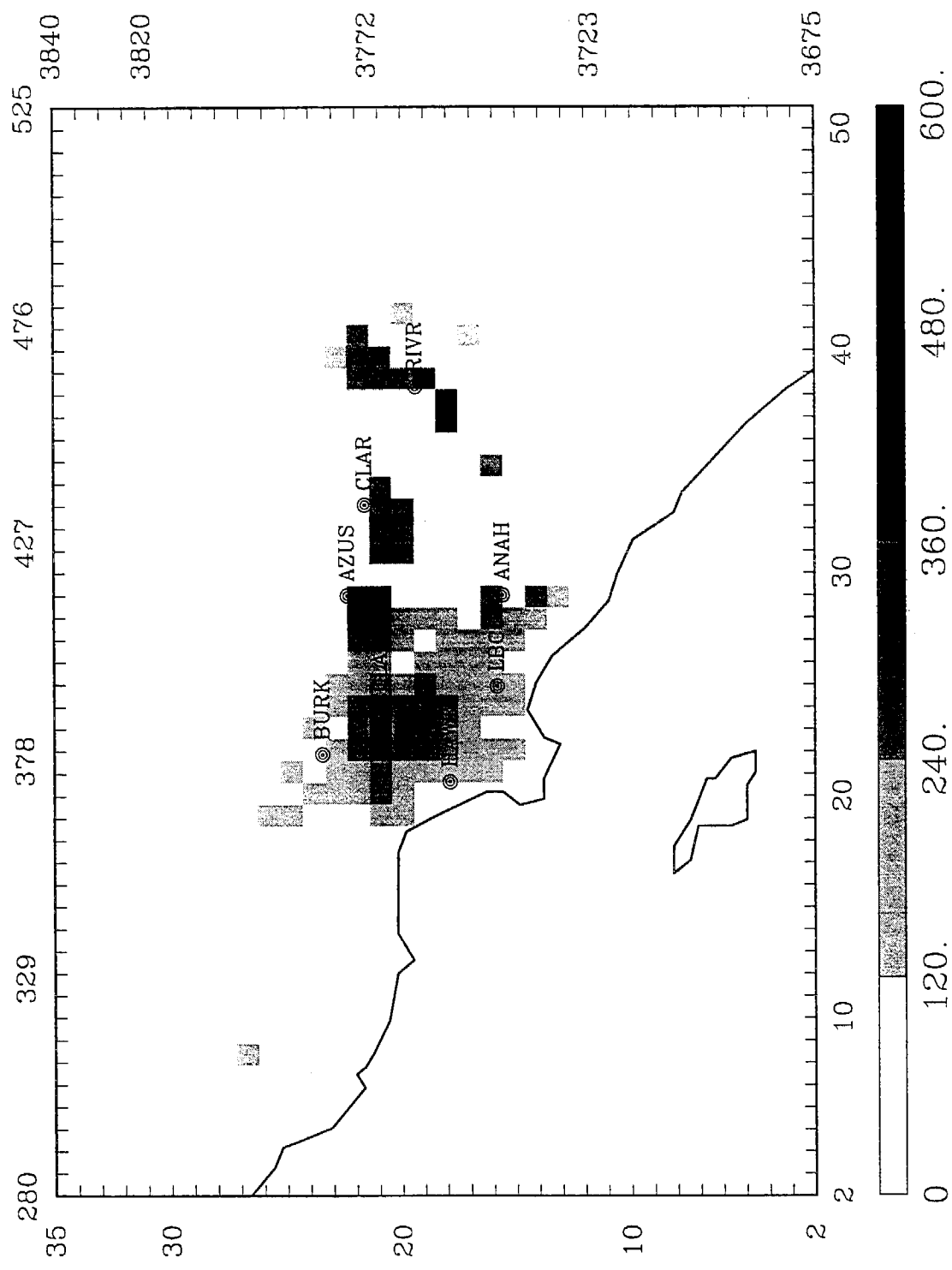


Figure 5-61. Estimated crustal PM₁₀ deposition in grams/hectare-day on June 25, 1987 in the SoCAB.

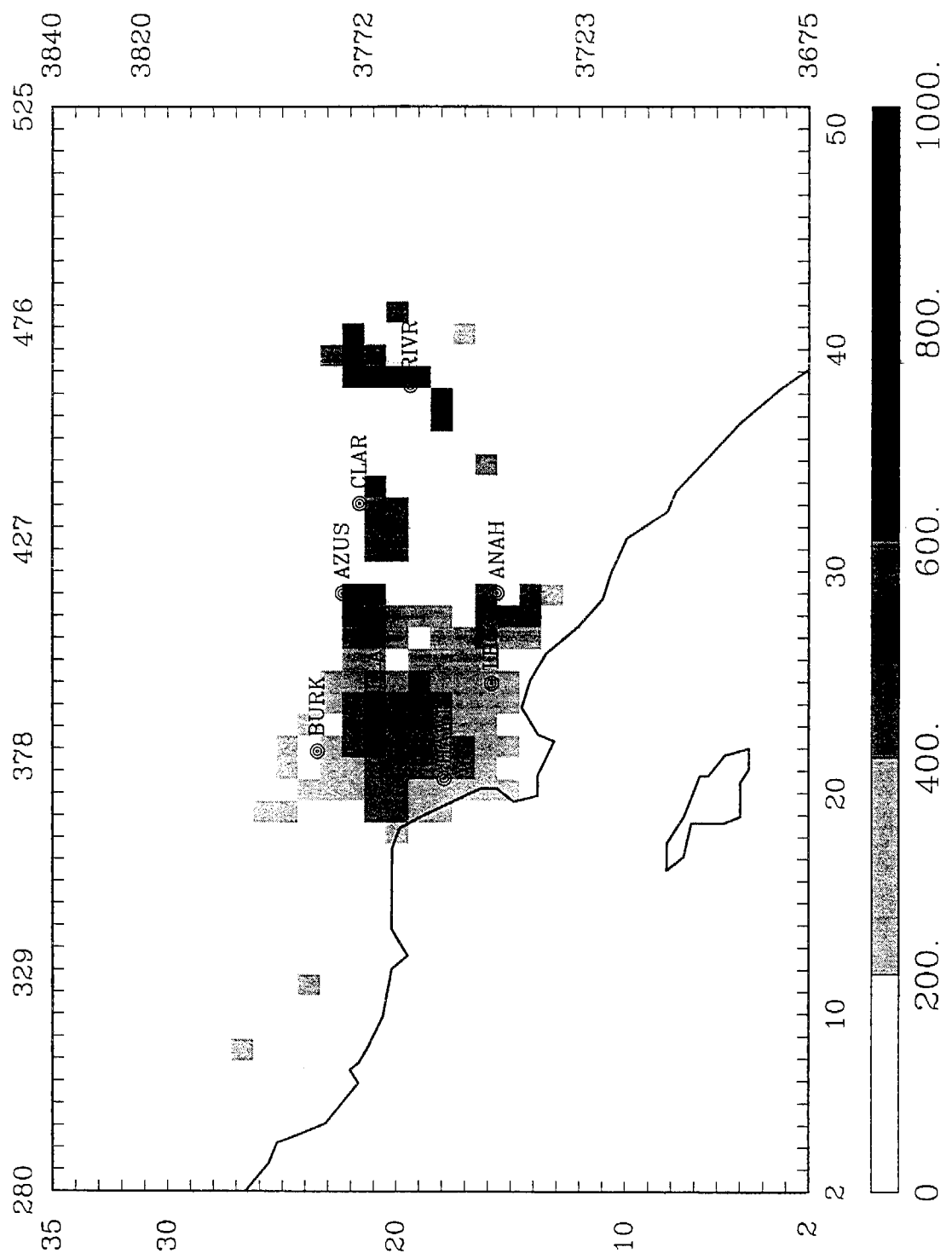


Figure 5-62. Estimated PM_{10} mass deposition in grams/hectare-day on June 25, 1987 in the SoCAB.

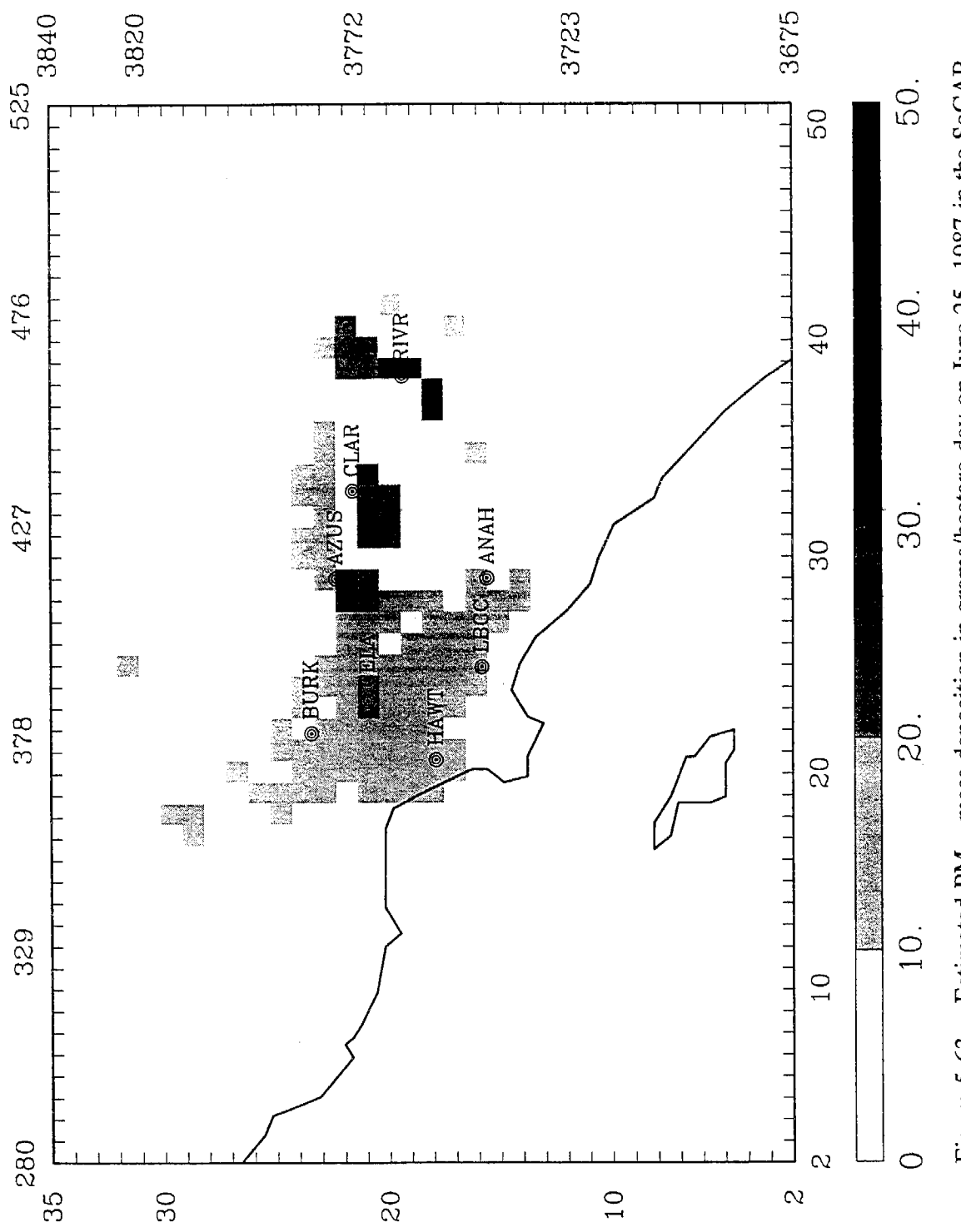


Figure 5-63. Estimated $\text{PM}_{2.5}$ mass deposition in grams/hectare-day on June 25, 1987 in the SoCAB.

6. SIMULATION OF A FALL EPISODE

6.1 EPISODE SELECTION

Historically, the highest ambient PM concentrations in Southern California occur in fall under conditions with moist stagnant air. The SCAQS study did not capture a truly classic fall PM episode, nevertheless, we felt it was important to test the model for fall conditions using the most suitable SCAQS episode. The SCAQMD staff reviewed conditions for the November 11-13, 1987 and December 10-11, 1987 fall episodes (SCAQMD, 1991a). Both episodes included complex meteorology involving transitions from offshore to onshore flow. The November episode was complicated by rain on November 13. The NO₂ and PM₁₀ concentrations were substantially higher during the December episode. The SCAQMD staff selected the December 10-11, 1987 episode and set up the wind and mixing height meteorological fields for model testing in this study. Their reasons for selecting the December episode were primarily that it had higher ambient NO₂ and PM concentrations than the November episode.

As with the summer simulations, the model simulations were initiated 24 hours before the beginning of the SCAQS episode in order to allow sufficient time for the calculations to be driven by emissions rather than initial concentrations. The model was applied using the same modeling domain and grid resolution used in the summer simulations (i.e., 51 x 36 grid squares with 5 km grid resolution). The vertical structure extended from the surface to 1000 meters, with two layers below the mixing height and 3 layers above the mixing height.

6.2 METEOROLOGICAL AND AIR QUALITY CONDITIONS

Meteorological conditions for the December 9-11, 1987 period were characterized by a complicated high-pressure system and a transition from an offshore to onshore wind flow pattern. The high pressure caused a strong low-temperature inversion which trapped pollutants in a shallow surface layer. Mixing heights reached 500 to 600 m at mid-day in the central area of the basin. On December 9 and 10, when the high-pressure system was strengthening in the Great Basin and Four Corners areas, the winds were northerly and northeasterly except for westerly winds below 300 m during a short weak sea breeze period. On December 11, the surface pressure pattern shifted significantly allowing more consistent onshore (westerly and southwesterly) flow at the surface. The flow on December 11 was still northerly aloft and at the surface in the inland portion of the basin. The net effect of the situation was a fairly complicated transition from offshore to onshore during the episode.

Hourly 3-dimensional wind fields and mixing height fields were developed using a combination of prognostic (for December 9) and diagnostic (for December 10 and 11) procedures for the episode by the SCAQMD staff for use in the study. These were the same meteorological fields used for the SCAQMD's 1991 episodic PM₁₀ modeling for the SoCAB (SCAQMD 1991b). The modeled surface layer winds for hours 9 and 15 on the three days are

illustrated in **Figures 6-1 through 6-3**. They show offshore winds in the morning and onshore winds in the afternoon. The modeled nighttime winds were northerly. Three-dimensional hourly temperature and water vapor concentration fields were also developed from the observed data using diagnostic procedures. Two-dimensional fog fields, which classify conditions as clear, hazy, or foggy, were developed from the surface observations.

Air quality conditions were adverse during the episode. **Table 6-1** shows the maximum concentrations observed during the period. The maximum 1-hr NO₂ concentrations reached 210 and 230 ppb at Anaheim and Burbank on December 10 and 11, respectively. The maximum 1-hr NO concentrations exceeded 700 ppb at Lynnwood on both days. The ozone levels were fairly low, with peak 1-hr concentrations of 60 to 80 ppb. The 4-hr average PM₁₀ sulfate, PM₁₀ nitrate, and PM₁₀ mass reached 17, 117, and 191 $\mu\text{g}/\text{m}^3$, respectively, on December 11 with the highest sulfate occurring in the coastal area at Long Beach and the highest nitrate and mass occurring in the central area at the Burbank station. The highest 4-hr average nitric acid was 20 ppb at Burbank. High ammonia concentrations (4-hr average > 50 ppb) were observed at Hawthorne and Riverside on December 10 and 11, respectively. The ambient concentration were generally higher on December 11 than December 10, so there is evidence of a pollution buildup during the three-day episode. It is worth noting that this is not a classic fall episode with the highest PM concentrations near Riverside; because of the counteracting effects of the offshore winds, the highest PM₁₀ levels occurred at Anaheim on December 10 (145 $\mu\text{g}/\text{m}^3$ 4-hr average and 105 $\mu\text{g}/\text{m}^3$ 24-hr average) and at Burbank on December 11 (191 $\mu\text{g}/\text{m}^3$ 4-hr average and 132 $\mu\text{g}/\text{m}^3$ 24-hr average).

PM, nitric acid, ammonia, and NMOC ambient data were not available for December 8 or 9. Initial concentrations for hour 0 on December 9 were obtained by spatial interpolation of observed NO, NO₂, ozone, SO₂, and CO data for that hour; monthly average PM₁₀ values; and 50 percent of the observed NMOC values at hour 6 December 10. Dummy stations with background air quality conditions (see below) were used near the boundaries of the domain and in the less populated portions of the domain to establish plausible initial concentration fields. The PM size and chemical composition were estimated based on the annual average SoCAB PM data reported by Solomon et al. (1988). The detailed size/composition splits of the initial and boundary PM concentrations were the same as used in the summer simulations.

The boundary concentrations and initial concentrations above the mixing height are shown in **Table 6-2**. The NO, NO₂, ozone, CO, and NMOC concentrations were the values used by the SCAQMD in their PM₁₀ modeling studies. On some portions of the boundaries (e.g., the over water portion in Ventura County), the inflowing ozone concentrations were based on the observed hourly data from coastal stations. The assumed NMOC boundary concentration was 80 ppbC, of which 68 ppbC was reactive. The background NMOC concentration is slightly higher than the value used for the summer simulations but is still consistent with the NMOC data obtained from San Nicolas Island during the SCAQS (Lurmann and Main, 1992; Roberts et al., 1991). The background H₂O₂ concentration used for the fall simulations was 0.1 ppb, which is significantly lower than the 3 ppb used for the summer simulations. A background ambient PM₁₀ level of 15 $\mu\text{g}/\text{m}^3$ was used for the simulations. The assumed background PM₁₀ concentration is lower than the annual average PM₁₀ (21 $\mu\text{g}/\text{m}^3$)

observed on San Nicolas Island (Solomon et al., 1988), however, this value is used from the surface up to 1000 meters.

6.3 EMISSIONS

The modeling emissions inventory for the fall episode was provided by the SCAQMD and included average fall day area source emissions, day-specific on-road motor vehicle emissions, and major point source emissions. Emissions of biogenic hydrocarbons were assumed to be negligible because of the cool fall temperatures and the likelihood that the vegetation was dormant in December. The fall emissions were adjusted in the same manner as the summer emissions. The on-road motor vehicle exhaust hydrocarbon (but not carbonyls) were quadrupled, which approximately doubled the ROG emissions. The primary PM emissions from all sources were reduced by 50 percent.

The adjusted fall emissions inventory for the SoCAB is summarized in Table 6-3. The total emissions of NO_x, ROG, CO, SO₂, and PM₁₀ are 1218, 2290, 9390, 121, and 534 tons per day, respectively. These totals are for December 10. In addition, the inventory included 220 tons per day of ammonia emissions and 75 ton per day of sea salt emissions, as described in Section 5.2. The fall emission estimates provided by SCAQMD are very similar to the summer estimates; the notable differences are 10 percent lower ROG and 3 percent higher CO emissions in the fall estimates. The inventory does not indicate emissions of crustal PM from windblown dust, agricultural tillage, and unpaved road dust sources are lower in the fall as would be expected because of the higher soil moisture content in the fall. The overall size distribution and chemical composition of the PM emissions are also the same in the fall and summer emissions inventory.

6.4 MODEL RESULTS

6.4.1 Spatial Patterns

The spatial patterns of predicted 24-hr average pollutant concentrations on December 10 and 11 are shown in Figures 6-4 through 6-33. The predicted pattern of NO₂ and PM₁₀ mass concentrations show relatively high concentrations in the central and coastal areas, and low concentrations north of Azusa and east of Riverside. A band of high concentrations extends from Burbank in the San Fernando Valley through Orange County, with the highest concentrations occurring southeast of Anaheim on both days. The crustal, OM, and EC PM show the same spatial pattern as PM mass. The area of high nitrate is primarily southeast of Anaheim. The area of high ammonium is southwest of Anaheim and south of Long Beach. The predicted sulfate pattern shows a plume of high sulfate extending south from the Long Beach area. The area with high levels (> 3 ppb) of nitric acid is offshore, south of Anaheim. High ammonia levels (> 100 ppb) are predicted near large agricultural sources and coastal sewage treatment plants. The sewage treatment plant ammonia emissions are probably overestimated (SCAQMD, 1996), causing exaggerated coastal hot spots. Sodium levels are

low everywhere onshore and highest over the water. The highest predicted concentrations in the domain are substantially higher on December 11 than December 10, although the predictions at the SCAQS stations are similar on both days.

An important feature of the predicted spatial pattern is that the center of the pollution cloud is mostly south of the SCAQS measurement network. The SCAQS measurement network design was not optimized for northerly flow conditions. There were no enhanced measurement stations southwest of Long Beach or Anaheim, which makes it difficult to assess the fidelity of the predicted spatial pattern. The routine data available at Costa Mesa indicate relatively high NO₂ levels existed near the coast in Orange County. The ozone data at El Toro in southern Orange County show typical fall/winter levels (30 to 40 ppb daily 1-hr maxima). As discussed below, the model underpredicted the concentrations of most species at the SCAQS stations on December 11 and it is likely that the wind fields used in the model transported the pollutants too far south. The observed data are more consistent with there being less transport (or more stagnation) or a transport pattern where the December 11 emissions were added to the pollutant cloud created on December 9-10 and carried over the SCAQS station network on December 11.

6.4.2 Predicted Aerosol-Size Distribution

The predicted aerosol-size distributions at the six SCAQS stations operated in the fall are shown in **Figures 6-34 through 6-39**. The relative size distribution of the principal chemical components predicted for Anaheim on December 10 is shown in **Table 6-4**. The relative chemical composition of each size section predicted for Anaheim on December 10 is shown in **Table 6-5**. The size distributions are quite similar for all sites; they show mass concentrations increasing with particle size up to 10 μm . About half of the mass is predicted to be in the fine (0-2.5 μm) size sections, and approximately 20 and 30 percent of the mass is predicted to be in particles with diameters between 2.5-5 μm and 5-10 μm , respectively.

The predicted PM size distribution is dominated by the size distribution of crustal material in this episode. Crustal material is the most abundant chemical component in all but the smallest two size sections. Crustal material is predicted to account for 35 to 50 percent of the fine mass and 66 to 74 percent of the coarse mass (2.5-10 μm). Organic material is predicted to be distributed across all sections and it is estimated to account for about 20 percent of mass in each size sections. The predicted size distribution for organic material is evenly split between fine and coarse particles on a mass basis. Ammonium and nitrate mostly occur on smaller particles. Nitrate is the most abundant chemical constituent in the smallest two or three size sections, accounting for 30 to 40 percent of the mass in those size sections. The size distribution of ammonium is similar to that for nitrate, with 80 percent of the ammonium in the fine mode. Elemental carbon and sulfate are estimated to account for 5 and 3 percent of the mass of particles in each of the size sections smaller than 2.5 μm in diameter. The majority of EC and sulfate (like nitrate and ammonium) are predicted to exist in particles with diameters less than 2.5 μm .

The observed data for the fall generally indicate PM_{2.5} mass concentrations were only slightly lower (5 to 25 percent) than PM₁₀ mass concentrations. The model significantly overestimates the amount of coarse PM relative to fine PM, and it appears that the model significantly overestimates the amount of crustal material present in the fall aerosol. Thus, even with the 50 percent PM emissions reduction used in the simulation, the model simulation still includes too much dirt, which dominates the predicted size distributions.

6.5 MODEL PERFORMANCE

The predicted concentrations are compared to observed data in **Figures 6-40 through 6-50**, and in **Tables 6-6 through 6-9**. The evaluation focuses on the mean bias and error at the stations with concentrations above minimum threshold values (1 $\mu\text{g}/\text{m}^3$ for PM components, 10 ppb for NO and NO₂, and 60 ppb for ozone) and the accuracy of the modeled concentrations at the monitoring stations with the highest observed concentration on each day. Tables 6-6 and 6-7 show the model performance statistics for 24-hr average concentrations. Tables 6-8 and 6-9 list the model results for short-term (1-hr to 6-hr) concentrations. Tables 6-7 and 6-9 show the maximum concentrations predicted anywhere in the domain as well as the maximum predicted at the highest station (paired in space). In addition, station plots of the 24-hr aerosol, nitric acid, and ammonia concentrations are shown in Appendix B.

6.5.1 Ozone and Nitrogen Dioxide

The graphical display of the model's ozone performance in the simulation (Figure 6-40) shows the model predicts daytime ozone levels that are usually comparable to the observed data. The observed ozone only reached 30 to 60 ppb at most stations during the episode. The model underestimated the peak 1-hr ozone levels of 60 and 80 ppb at Pasadena on December 10 and 11. The highest estimated 1-hr ozone concentrations were 90 and 122 ppb on December 10 and 11, and these were located offshore. The model performance statistics are not particularly informative for ozone because there were very few observations above the 60 ppb threshold for statistical consideration.

The nitrogen dioxide predictions, shown in Figure 6-41, illustrate cases with both good and poor performance. As with the summer NO₂ predictions, the temporal correlation of the predicted and observed NO₂ is poor at many stations. The hourly predictions track the fall NO₂ observations slightly better than those for the summer, perhaps because the NO₂ concentrations are substantially higher. On average, the model predicts 68 and 66 ppb when the observed means of the 1-hr NO₂ concentrations exceeding 10 ppb were 71 and 80 ppb on December 10 and 11. For the 24-hr average means, the model predicted 35 and 43 when 45 and 50 ppb were observed at the NO₂ monitoring stations. The mean bias and error in 1-hr average NO₂ values were +11 and -1 percent and ± 51 and ± 45 percent on December 10 and 11, respectively. The daily maximum 1-hr NO₂ levels (210-230 ppb) were underpredicted by 50 percent at Anaheim and Burbank, however, elsewhere in the domain concentrations higher

than the observed maximum were predicted (up to 320 ppb). This level of performance for NO₂ is similar to that found in most other UAM simulations of the SoCAB.

6.5.2 Nitrate

The model predicted mean 24-hr average PM_{2.5} nitrate of 21 and 16 $\mu\text{g}/\text{m}^3$, which was lower than the 26 and 36 $\mu\text{g}/\text{m}^3$ observed on December 10 and 11, respectively. The predicted mean PM₁₀ nitrate levels at the SCAQS stations were 26 and 20 $\mu\text{g}/\text{m}^3$, which was also lower than the observed levels of 29 and 41 $\mu\text{g}/\text{m}^3$ on these days. On a percentage basis, the model underpredicted the mean 24-hr average PM₁₀ nitrate by 9 and 49 percent on December 10 and 11, respectively, at the SCAQS stations. The modeled error in 24-hr PM₁₀ nitrate was ± 18 on December 10 and ± 49 on December 11. These results show reasonable nitrate performance on the December 10 and unreasonably low nitrate levels on December 11. This pattern is evident in the predictions for the maximum 24-hr nitrate, where the model predicted 26 $\mu\text{g}/\text{m}^3$ PM_{2.5} nitrate at Anaheim on December 10 where 42 $\mu\text{g}/\text{m}^3$ was observed and 15 $\mu\text{g}/\text{m}^3$ at Los Angeles on December 11 when 43 $\mu\text{g}/\text{m}^3$ was observed. However, the maximum PM_{2.5} nitrate levels predicted in the domain (47 and 76 $\mu\text{g}/\text{m}^3$) were significantly higher than the observed, especially on December 11. The maximum 24-hr PM₁₀ nitrate levels are underestimated by comparable amounts (32 and 64 percent on December 10 and 11). The maximum 24-hr average PM₁₀ nitrate concentrations predicted in the modeling domain were 62 and 101 $\mu\text{g}/\text{m}^3$ on December 10 and 11, respectively. Clearly, the model predicted high nitrate concentrations for the episode, however, they were probably displaced too far to the south or southeast.

Comparison of the short-term nitrate predictions with observations show larger biases and error, especially on December 10, than those for the 24-hr average predictions. The mean errors are ± 13 and $\pm 21 \mu\text{g}/\text{m}^3$ in short-term PM₁₀ nitrate (or ± 65 and ± 46 percent error). The model does not tract the short-term dynamics of nitrate well in this episode.

6.5.3 Ammonium

The model predictions of the mean 24-hr PM_{2.5} ammonium were 7.2 and 5.6 $\mu\text{g}/\text{m}^3$ when 6.3 and 8 $\mu\text{g}/\text{m}^3$ were observed on December 10 and 11, respectively. For PM₁₀, the model predicted 8.6 and 6.9 $\mu\text{g}/\text{m}^3$ when 7.5 and 13 $\mu\text{g}/\text{m}^3$ of PM₁₀ ammonium were observed. The mean bias and error in PM_{2.5} ammonium were +25 to ± 34 percent on December 10, and -27 and ± 27 percent on December 11, which is reasonably good performance considering the uncertainties in ammonia emissions. The PM₁₀ results are less accurate than the PM_{2.5} results for ammonium on average.

The model's predictions for maximum 24-hr average ammonium are lower than the observations. The model predicted 8.9 and 8.7 $\mu\text{g}/\text{m}^3$ for PM_{2.5} ammonium at Anaheim when 10.8 and 11.3 $\mu\text{g}/\text{m}^3$ were observed on December 10 and 11, respectively. The model predicted maximum 24-hr values of 11.2 and 6.9 $\mu\text{g}/\text{m}^3$ for PM₁₀ ammonium at Anaheim and Los Angeles when 13.6 and 14.8 $\mu\text{g}/\text{m}^3$ were observed. Thus, as was the case for other

aerosol components in this simulation, the concentrations are more accurately predicted on December 10 than December 11.

6.5.4 Nitric Acid and Ammonia

The model estimates for nitric acid and ammonia are shown in Figures 6-46 and 6-47. They show that the model underestimates nitric acid concentrations and overestimates ammonia concentrations. For example, the 24-hr average nitric acid concentrations were 1 and 0.8 ppb at Burbank when 3.7 and 7.5 ppb were observed on December 10 and 11, respectively. The average 24-hr average ammonia concentrations were 32 ppb, compared to observed levels of 15 to 17 ppb. The maximum 24-hr ammonia concentrations predicted were 52 and 23 ppb on December 10 and 11, which are both higher and lower than the observed maximum values of 29 and 27 ppb. The maximum 24-hr average ammonia concentrations predicted in the domain were much higher than any of the observations (.360 ppb). The maximum 4-hr average ammonia concentrations (51 ppb at Burbank and 52 ppb at Riverside) were reproduced reasonably well (66 ppb at Burbank and 50 ppb at Riverside).

These two biases are of course related through the aerosol chemistry. In this fall simulation, the total nitrate was underestimated and the total ammonia was overestimated. The simulated system was more ammonia-rich and nitrate-lean in the western and central areas than most simulations because of the northeasterly winds. The nitric acid predictions are particularly low because the ammonia-rich conditions favor ammonium nitrate aerosol rather than nitric acid. The ammonia levels are high because there is insufficient nitric acid to produce additional ammonium nitrate aerosol. Hence, too much of the total ammonia and too little of the nitric acid remained in the gas phase.

6.5.5 Sulfate

The predicted sulfate levels were higher than the observed data on December 10 and lower than the observed levels on December 11. On December 10, 2.6 and 4.2 $\mu\text{g}/\text{m}^3$ of $\text{PM}_{2.5}$ and PM_{10} sulfate were estimated when 2.2 and 2.7 $\mu\text{g}/\text{m}^3$ were observed on average. On December 11, the $\text{PM}_{2.5}$ and PM_{10} sulfate concentrations were estimated as 3.3 and 5.6 $\mu\text{g}/\text{m}^3$ when 4.8 and 6.9 $\mu\text{g}/\text{m}^3$ were observed on average. Likewise, the maximum 24-hr sulfate was overestimated on December 10 and underestimated on December 11. The model estimated 3.7 and 5.8 $\mu\text{g}/\text{m}^3$ of $\text{PM}_{2.5}$ and PM_{10} sulfate concentrations when 3.3 and 3.9 $\mu\text{g}/\text{m}^3$ were observed at the highest SCAQS station. Elsewhere in the domain, the model predicted maximum 24-hr average PM_{10} sulfate levels of 19 and 40 $\mu\text{g}/\text{m}^3$ on December 10 and 11, respectively.

Several factors may be responsible for the underestimation of sulfate on December 11. Most probably, the bias in the transport pattern, which pushed the polluted cloud too far south on December 10 (rather than southwestern or westerly which might have allowed it to buildup and be brought back into the SCAQS monitoring network area) was responsible for the underprediction on December 11. In addition, sulfate production may have been enhanced

during foggy conditions on the night of December 10, and the model's empirical fog module may have underestimated the aqueous-phase conversion of SO₂ to sulfate.

6.5.6 Organic Material

The organic PM estimated by the model is a combination of primary and secondary organic material. The restricted sunlight in December limits the amount of photochemical activity and, therefore, the amount of secondary organic material formed. The mean 24-hr average PM_{2.5} OM concentrations were 19 and 17 µg/m³ at the SCAQS stations where 27 and 28 µg/m³ were observed. The mean 24-hr average PM₁₀ OM concentrations were in reasonable agreement with the data; 37 predicted versus 33 µg/m³ observed on December 10, and 39 predicted versus 40 µg/m³ observed on December 11. The errors in the 24-hr average PM₁₀ OM predictions were ±19 and ±17 percent on December 10 and 11.

The maximum 24-hr average predicted PM_{2.5} OM concentrations were 21 and 27 µg/m³ on December 10 and 11, which were below the maximum observed levels of 33 and 39 µg/m³. The maximum 24-hr average predicted PM₁₀ OM levels were 41 and 53, which were in reasonable agreement with the observed levels of 45 and 52 µg/m³ at Long Beach and Los Angeles. Thus, the model underestimates fine OM, overestimates coarse OM, and provides reasonably accurate PM₁₀ OM on average.

6.5.7 Elemental Carbon

The elemental carbon concentrations were consistently underestimated in the December simulation. The mean observed levels were 8 to 10 µg/m³, which is substantial higher than in the summer episode. The mean and maximum PM_{2.5} EC concentrations were underestimated by 50 percent. The mean and maximum PM₁₀ EC concentrations were underestimated by 40 percent. The maximum predicted EC in the domain was slightly higher than the highest observed values. Overall, the performance for EC was better prior to the 50 percent PM emissions reduction.

6.5.8 PM Mass

The estimated mean PM_{2.5} mass concentration was 91 µg/m³ on December 10 when 76 µg/m³ was observed. On December 11, the mean PM_{2.5} mass was 80 µg/m³ in the model while 92 µg/m³ was observed. The mean error in PM_{2.5} mass predictions were ±28 and ±21 percent on December 10 and 11, respectively. The maximum 24-hr average PM_{2.5} concentrations were 118 and 113 µg/m³ when 97 and 132 µg/m³ were observed on December 10 and 11. Clearly, there are a number of compensating errors which make the PM_{2.5} mass predictions appear more accurate than the results for the PM_{2.5} components would suggest. In particular, overestimation of the amount of crustal material in PM_{2.5} compensates for the underestimation of the PM_{2.5} nitrate, sulfate, OM, and EC.

The estimated PM₁₀ mass concentrations are considerably higher than the observed data. On average, the model predicted 182 and 191 $\mu\text{g}/\text{m}^3$ of PM₁₀ mass on December 10 and 11, when 76 and 100 $\mu\text{g}/\text{m}^3$ were observed. The mean bias in the PM₁₀ mass concentrations was +147 and +89 percent on December 10 and 11, and the mean error was ± 147 to ± 89 percent, indicating all observed PM₁₀ concentrations were overestimated. The model predicted 24-hr maximum PM₁₀ concentrations of 241 and 244 $\mu\text{g}/\text{m}^3$ at Anaheim and Los Angeles when 105 and 132 $\mu\text{g}/\text{m}^3$ were observed. The maximum 24-hr PM₁₀ mass predicted in the domain were 336 and 439 on December 10 and 11, respectively. Examination of the biases in the modeled components of PM₁₀ shows that PM₁₀ is overestimated because the crustal component is seriously overestimated at all SCAQS stations. Recall the emission estimates have the same amount of crustal PM in the summer and fall inventories. The comparison of the summer and fall model predictions with the data suggest that the lack of seasonal adjustment of crustal emission is a serious omission in the emissions inventory.

Overall, the PM_{2.5} mass estimates for this episode are much closer to the data than the PM₁₀ mass estimates, and the results for December 10 are more accurate and reliable than those for December 11 because of the difficulties in characterizing the transport fields associated with the flow reversal.

6.6 DEPOSITION

The UAM-AERO model predicts the amount of material deposited by each species each hour in each grid square. Comparable deposition data are not available for direct comparison with the model estimates. **Figures 6-51 through 6-60** show the predicted spatial pattern of deposition on the third day of the fall simulation for ozone, NO₂, nitric acid, ammonia, PM₁₀ nitrate, PM₁₀ ammonium, PM₁₀ sulfate, PM₁₀ OM, crustal PM₁₀, and PM₁₀ mass. The spatial deposition patterns are quite similar to the 24-hr ambient concentration spatial patterns. This similarity is expected because the dry deposition loss rate is a linear function of surface layer concentrations in the model.

The average amount of material deposited within the domain on December 10-11 is shown in **Table 6-10**. For gaseous species, the results indicate formaldehyde has the highest deposition rate on a mole basis, followed by ozone, acetaldehyde, ammonia, hydrochloric acid, nitrogen dioxide, nitric acid, PAN, formic acid, higher (C3+) aldehydes, sulfur dioxide, and acetic acid. For PM, the results indicate PM_{2.5} species deposit substantially less than PM₁₀ species as expected. The relative ranking of PM₁₀ component deposition is: crustal, material, water, organic material, nitrate, ammonium, sulfate, sodium, EC, and chloride on a mass basis.

Table 6-1. Observed maximum short-term (1 to 6-hr) pollutant concentrations ($\mu\text{g}/\text{m}^3$) on December 10-11, 1987.

Species	Day	Location	Maximum Observed Concentration ^a
PM ₁₀ NO ₃	Dec 10	Burbank	68
PM ₁₀ NO ₃	Dec 11	Burbank	117
PM ₁₀ NH ₄	Dec 10	Anaheim	19
PM ₁₀ NH ₄	Dec 11	Burbank	34
PM ₁₀ SO ₄	Dec 10	Anaheim	5.4
PM ₁₀ SO ₄	Dec 11	Long Beach	17
PM ₁₀ EC	Dec 10	Hawthorne	19
PM ₁₀ EC	Dec 11	Los Angeles	20
PM ₁₀ OM	Dec 10	Long Beach	63
PM ₁₀ OM	Dec 11	Burbank	65
PM _{2.5} Mass	Dec 10	Anaheim	137
PM _{2.5} Mass	Dec 11	Burbank	180
PM ₁₀ Mass	Dec 10	Anaheim	145
PM ₁₀ Mass	Dec 11	Burbank	191
HNO ₃ (ppb)	Dec 10	Burbank	16
HNO ₃ (ppb)	Dec 11	Burbank	20
NH ₃ (ppb)	Dec 10	Hawthorne	51
NH ₃ (ppb)	Dec 11	Riverside	52
Ozone (ppb)	Dec 10	Pasadena	60
Ozone (ppb)	Dec 11	Pasadena	80
NO ₂ (ppb)	Dec 10	Anaheim	210
NO ₂ (ppb)	Dec 11	Burbank	230
NO (ppb)	Dec 10	Lynnwood	770
NO (ppb)	Dec 11	Lynnwood	740

^a Ozone, NO₂, and NO concentrations are 1-hr maxima. All other species are 4- to 6-hr maximum.

Table 6-2. Boundary conditions used for the December 9-11, 1987 simulations.

Species	Concentration (ppm)	Species	Concentration ($\mu\text{g}/\text{m}^3$)
NO	0.001	PM _{2.5} Mass	11.25
NO ₂	0.002	PM _{2.5-10} Mass	3.75
O ₃	Station Readings	PM _{2.5} NO ₃	1.688
HONO	0.00006	PM _{2.5-10} NO ₃	0.5623
HNO ₃	0.0001	PM _{2.5} NH ₄	0.8977
HNO ₄	0.00001	PM _{2.5-10} NH ₄	0.266
H ₂ O ₂	0.0001	PM _{2.5} SO ₄	1.2
CO	0.2	PM _{2.5-10} SO ₄	0.2999
ALK1	4.62E-03	PM _{2.5} EC	0.1383
ALK2	2.55E-03	PM _{2.5-10} EC	2.07E-02
OLE1	3.52E-04	PM _{2.5} OC	3.038
OLE2	3.02E-04	PM _{2.5-10} OC	1.012
OLE3	1.42E-08	PM _{2.5} NA	0.2243
ARO1	3.38E-04	PM _{2.5-10} NA	0.1826
ARO2	8.89E-04	PM _{2.5} CL	0.2626
ETHE	6.00E-04	PM _{2.5-10} CL	0.2624
HCHO	3.80E-03	PM _{2.5} OTR	3.673
CCHO	3.05E-03	PM _{2.5-10} OTR	1.122
RCHO	6.67E-04	PM _{2.5} H ⁺	1.50E-04
MEK	5.00E-04	PM _{2.5-10} H ⁺	7.83E-07
MGLY	1.00E-05	PM _{2.5-10} H ₂ O	3.00E-02
PAN	1.00E-04	PM _{2.5} H ₂ O	0.12
PPN	1.00E-05		
AFG2	1.00E-05		
CRES	1.00E-05		
SO ₂	1.00E-04		
Formic Acid	1.00E-04		
Acetic Acid	1.00E-04		
HCL	1.00E-05		
NH ₃	1.00E-04		

Table 6-3. 1987 Fall emissions for the SoCAB.

Species	Emissions (tons per day)
THC	3467.
ROG	2290.
CO	9390.
NOx	1216.
SOx	121.
PART	1131.
NO	1134.
NO2	76.6
HONO	6.1
ALK1	746.
ALK2	505.
ETHE	185.
OLE1	160.
OLE2	65.9
OLE3	2.9
ARO1	292.
ARO2	227.
HCHO	13.1
CCHO	8.8
RCHO	1.4
MEK	33.8
NH3	220.
PM _{2.5} SO ₄	6.3
PM _{2.5} EC	12.8
PM _{2.5} OM	43.3
PM _{2.5} OTR	97.9
PM _{2.5} Na	2.9
PM _{2.5} Cl	4.6
PM _{2.5-10} SO ₄	3.6
PM _{2.5-10} EC	4.3
PM _{2.5-10} OM	74.7
PM _{2.5-10} OTR	291.
PM _{2.5-10} Na	26.1
PM _{2.5-10} Cl	41.4

Table 6-4. Relative size distribution of each aerosol chemical component at Anaheim on December 10, 1987.

Chemical Constituent	Percent of Component Mass in Section 1	Percent of Component Mass in Section 2	Percent of Component Mass in Section 3	Percent of Component Mass in Section 4	Percent of Component Mass in Section 5	Percent of Component Mass in Section 6	Percent of Component Mass in Section 7	Percent of Component Mass in Section 8	Component Mass ($\mu\text{g}/\text{m}^3$) in Sections 1-8
	$0 < D_p < 0.08 : \text{m}$	$0.08 < D_p < 0.16 : \text{m}$	$0.16 < D_p < 0.31 : \text{m}$	$0.31 < D_p < 0.62 : \text{m}$	$0.62 < D_p < 1.2 : \text{m}$	$1.2 < D_p < 2.5 : \text{m}$	$2.5 < D_p < 5 : \text{m}$	$5 < D_p < 10 : \text{m}$	$0 < D_p < 10 : \text{m}$
Crustal Material	1	2	4	6	9	14	25	38	134
Organic Material	2	4	8	10	12	15	21	28	49
Elemental Carbon	3	7	13	16	17	16	14	13	8
Nitrate	5	12	17	17	16	14	12	9	32
Ammonium	5	11	16	17	16	14	12	9	11
Sulfate	2	6	11	14	15	16	17	18	6
Mass	2	5	8	10	11	14	21	30	240

a 24-hr average concentrations.

Table 6-5. Relative chemical composition of each aerosol size section at Anaheim on December 10, 1987.

Chemical Constituent	Percent of Mass in Section 1	Percent of Mass in Section 2	Percent of Mass in Section 3	Percent of Mass in Section 4	Percent of Mass in Section 5	Percent of Mass in Section 6	Percent of Mass in Section 7	Percent of Mass in Section 8
	$0 < D_p < 0.08 : \text{m}$	$0.08 < D_p < 0.16 : \text{m}$	$0.16 < D_p < 0.31 : \text{m}$	$0.31 < D_p < 0.62 : \text{m}$	$0.62 < D_p < 1.2 : \text{m}$	$1.2 < D_p < 2.5 : \text{m}$	$2.5 < D_p < 5 : \text{m}$	$5 < D_p < 10 : \text{m}$
Crustal Material	24	26	31	37	44	55	66	73
Organic Material	19	19	21	22	22	21	20	20
Elemental Carbon	5	5	6	6	5	3	2	1
Nitrate	37	35	29	24	19	13	7	3
Ammonium	12	11	10	8	7	5	3	1
Sulfate	3	3	3	3	3	3	2	1
Mass ($\mu\text{g}/\text{m}^3$)	4.3	11.2	18.1	22.9	26.9	34.7	51.3	71.2

a 24-hr average concentrations.

Table 6-6. UAM-AERO model performance on mean 24-hr average concentrations ($\mu\text{g}/\text{m}^3$) on December 10-11, 1987.

Page 1 of 2

Species	Day	Mean Observed	Mean Predicted	Mean Normalized Bias (%)	Mean Bias	Mean Normalized Error (%)	Mean Error
PM _{2.5} NO3	344	25.7	21.3	-12	-4.4	20	5.9
PM _{2.5} NO3	345	34.9	16.1	-51	-18.8	51	18.8
PM ₁₀ NO3	344	29.6	25.8	-9	-3.8	18	5.7
PM ₁₀ NO3	345	40.7	19.9	-49	-20.8	49	20.8
PM _{2.5} NH4	344	6.3	7.2	25	0.9	34	1.7
PM _{2.5} NH4	345	8	5.6	-27	-2.3	27	2.4
PM ₁₀ NH4	344	7.5	8.6	25	1.1	32	2.1
PM ₁₀ NH4	345	12.8	6.9	-45	-5.9	45	5.9
PM _{2.5} SO4	344	2.2	2.6	23	0.4	29	0.5
PM _{2.5} SO4	345	4.8	3.3	-30	-1.5	30	1.5
PM ₁₀ SO4	344	2.7	4.2	62	1.5	62	1.5
PM ₁₀ SO4	345	6.9	5.6	-17	-1.4	19	1.5
PM _{2.5} EC	344	7.9	4.0	-49	-3.8	49	3.8
PM _{2.5} EC	345	8	3.9	-52	-4.1	52	4.1
PM ₁₀ EC	344	9.5	5.5	-42	-4.0	42	4.0
PM ₁₀ EC	345	10.2	6.2	-39	-4.0	39	4.0
PM _{2.5} OM	344	26.7	18.7	-30	-8.1	30	8.1
PM _{2.5} OM	345	28.5	17.2	-40	-11.2	40	11.2
PM ₁₀ OM	344	33.3	36.8	11	3.5	19	6.2
PM ₁₀ OM	345	39.4	39.8	2	0.4	17	6.2
PM ₁₀ Na	344	0.6	0.4	21	-0.2	86	0.3
PM ₁₀ Na	345	0.5	0.3	-8	-0.1	47	0.2
PM _{2.5} Mass	344	76.3	90.6	20	14.3	28	20.5
PM _{2.5} Mass	345	91.7	80.4	-13	-11.3	21	18.3
PM ₁₀ Mass	344	75.6	182	147	106	147	107

Table 6-6. UAM-AERO model performance on mean 24-hr average concentrations ($\mu\text{g}/\text{m}^3$) on December 10-11, 1987.

Page 2 of 2

Species	Day	Mean Observed	Mean Predicted	Mean Normalized Bias (%)	Mean Bias	Mean Normalized Error (%)	Mean Error
PM ₁₀ Mass	345	99.8	191	89	90.7	89	90.7
HNO ₃ (ppb)	344	3.7	1.0	-73	-2.7	73	2.7
HNO ₃ (ppb)	345	7.5	0.8	-89	-6.7	89	6.7
NH ₃ (ppb)	344	16.8	32.5	98	15.8	98	15.8
NH ₃ (ppb)	345	15	32.4	195	17.4	199	18.5
Coarse NO ₃	344	4	4.4	20	0.5	32	0.9
Coarse NO ₃	345	5.3	3.6	-25	-1.7	41	2.0
Coarse NH ₄	344	2.2	1.7	-14	-0.5	25	0.7
Coarse NH ₄	345	4.4	1.4	-56	-3.0	56	3.0
Coarse SO ₄	344	-99	-99	-99	-99	-99	-99
Coarse SO ₄	345	1.6	1.9	38	0.3	55	0.7
Coarse EC	344	1.6	1.5	-3	-0.1	29	0.5
Coarse EC	345	1.6	1.7	10	0.1	23	0.3
Coarse OM	344	7.8	18.5	161	10.8	161	10.8
Coarse OM	345	8.2	20.4	158	12.2	158	12.2
Coarse Mass	344	5.6	112	2052	106	2052	106
Coarse Mass	345	7.4	103	1300	95.8	1300	95.8

Table 6-7. UAM-AERO model performance for maximum 24-hr average concentrations ($\mu\text{g}/\text{m}^3$) on December 10-11, 1987.

Page 1 of 2

Species	Day	Location	Maximum Observed	Maximum Predicted	Accuracy (%)	Maximum in Domain
PM _{2.5} NO ₃	344	Anaheim	42.0	25.8	-39	46.7
PM _{2.5} NO ₃	345	Los Angeles	43.1	14.8	-66	76.1
PM ₁₀ NO ₃	344	Anaheim	47.0	31.8	-32	61.9
PM ₁₀ NO ₃	345	Los Angeles	49.4	17.8	-64	101
PM _{2.5} NH ₄	344	Anaheim	10.8	8.9	-18	14.1
PM _{2.5} NH ₄	345	Anaheim	11.3	8.7	-23	23.7
PM ₁₀ NH ₄	344	Anaheim	13.6	11.2	-18	18.8
PM ₁₀ NH ₄	345	Los Angeles	14.8	6.9	-53	32.9
PM _{2.5} SO ₄	344	Anaheim	3.3	3.7	12	16.4
PM _{2.5} SO ₄	345	Hawthorne	7.5	4.1	-45	35.7
PM ₁₀ SO ₄	344	Anaheim	3.9	5.6	44	18.7
PM ₁₀ SO ₄	345	Hawthorne	10.1	5.8	-43	39.9
PM _{2.5} EC	344	Long Beach	9	4.6	-49	10.5
PM _{2.5} EC	345	Los Angeles	12.1	6.2	-49	13.5
PM ₁₀ EC	344	Long Beach	10.3	6.3	-39	12.8
PM ₁₀ EC	345	Los Angeles	13.3	8.2	-38	16.8
PM _{2.5} OM	344	Long Beach	33.2	20.6	-38	36.5
PM _{2.5} OM	345	Los Angeles	38.9	26.8	-31	38.5
PM ₁₀ OM	344	Long Beach	44.6	40.7	-9	70.9
PM ₁₀ OM	345	Los Angeles	51.8	53.2	3	80.4
PM ₁₀ Na	344	Hawthorne	1.3	0.7	-46	6.5
PM ₁₀ Na	345	Hawthorne	0.8	0.6	-25	7.4
PM _{2.5} Mass	344	Anaheim	97.4	118	21	162
PM _{2.5} Mass	345	Los Angeles	132	113	-14	217
PM ₁₀ Mass	344	Anaheim	105	241	130	336

Table 6-7. UAM-AERO model performance for maximum 24-hr average concentrations ($\mu\text{g}/\text{m}^3$) on December 10-11, 1987.

Page 2 of 2

Species	Day	Location	Maximum Observed	Maximum Predicted	Accuracy (%)	Maximum in Domain
PM ₁₀ Mass	345	Los Angeles	132	244	85	439
HNO ₃ (ppb)	344	Burbank	3.7	1.0	-73	8.9
HNO ₃ (ppb)	345	Burbank	7.5	0.8	-89	19.6
NH ₃ (ppb)	344	Riverside	29.5	52.4	78	367
NH ₃ (ppb)	345	Riverside	26.9	23.5	-13	359
Coarse NO ₃	344	Long Beach	5.7	5.2	-9	15.6
Coarse NO ₃	345	Anaheim	6.6	5.9	-11	27.5
Coarse NH ₄	344	Burbank	3.3	1.3	-61	4.7
Coarse NH ₄	345	Burbank	7.7	0.6	-92	9.2
Coarse SO ₄	344	Hawthorne	0.8	1.6	100	-99
Coarse SO ₄	345	Hawthorne	2.6	1.7	-35	4.3
Coarse EC	344	Anaheim	2	2.1	5	4.0
Coarse EC	345	Anaheim	2.3	2.3	0	4.5
Coarse OM	344	Anaheim	11.6	24.3	109	34.4
Coarse OM	345	Los Angeles	12.9	26.4	105	41.9
Coarse Mass	344	Anaheim	7.2	122	1,594	174.4
Coarse Mass	345	Long Beach	7.4	103	1,292	222

Table 6-8. UAM-AERO model performance for mean short-term (1 to 6-hr) average concentrations ($\mu\text{g}/\text{m}^3$) on December 10-11, 1987.

Page 1 of 2

Species	Day	Mean Observed	Mean Predicted	Mean Normalized Bias (%)	Mean Bias	Mean Normalized Error (%)	Mean Error
PM _{2.5} NO ₃	344	25.7	21.3	38	-4.3	83	12.2
PM _{2.5} NO ₃	345	33.5	15.6	-39	-17.8	48	18.9
PM ₁₀ NO ₃	344	29.6	25.8	24	-3.6	65	12.9
PM ₁₀ NO ₃	345	38.9	19.4	-37	-19.3	46	21.1
PM _{2.5} NH ₄	344	6.8	7.2	54	0.4	80	3.2
PM _{2.5} NH ₄	345	8.6	5.9	-12	-2.8	38	3.7
PM ₁₀ NH ₄	344	7.7	8.9	76	1.2	94	3.3
PM ₁₀ NH ₄	345	12.1	7.4	-22	-4.8	41	5.9
PM _{2.5} SO ₄	344	2.4	2.8	35	0.1	62	1.1
PM _{2.5} SO ₄	345	5.1	3.5	-21	-2.1	38	2.1
PM ₁₀ SO ₄	344	2.8	4.3	71	1.2	76	1.6
PM ₁₀ SO ₄	345	6.5	5.2	-4	-1.8	37	2.6
PM _{2.5} EC	344	7.9	4.0	-42	-3.8	45	4.0
PM _{2.5} EC	345	8.6	4.2	-46	-4.4	53	4.8
PM ₁₀ EC	344	9.5	5.5	-34	-4	43	4.5
PM ₁₀ EC	345	9.9	5.6	-39	-4.3	48	5.1
PM _{2.5} OM	344	26.7	18.7	-22	-8.1	38	10.5
PM _{2.5} OM	345	28.5	17.2	-21	-11.2	61	14.0
PM ₁₀ OM	344	33.3	36.8	20	3.4	48	14.6
PM ₁₀ OM	345	37.4	36.3	-3	-0.9	39	15.8
PM ₁₀ Na	344	1.3	0.5	-64	-0.5	64	0.8
PM ₁₀ Na	345	2.1	0.4	-82	-1.7	82	1.7
PM ₁₀ Cl	344	3.1	0.5	-85	-2.3	85	2.6
PM ₁₀ Cl	345	2.7	0.3	-86	-2.3	86	2.4

Table 6-8. UAM-AERO model performance for mean short-term (1 to 6-hr) average concentrations ($\mu\text{g}/\text{m}^3$) on December 10-11, 1987.

Page 2 of 2

Species	Day	Mean Observed	Mean Predicted	Mean Normalized Bias (%)	Mean Bias	Mean Normalized Error (%)	Mean Error
PM _{2.5} Mass	344	76.3	90.6	35	14	59	35.8
PM _{2.5} Mass	345	95.7	82.8	-3	-13.3	44	36.4
PM ₁₀ Mass	344	75.6	182	171	106.4	172	107
PM ₁₀ Mass	345	95.1	175	90	80.9	97	88.2
HNO ₃ (ppb)	344	5.2	2.0	-51	-3.2	52	3.2
HNO ₃ (ppb)	345	9.3	1.4	-78	-8	78	8.0
NH ₃ (ppb)	344	16.1	32.5	162	16.5	170	19.3
NH ₃ (ppb)	345	15	32.4	264	17.4	293	24.5
Ozone (ppb)	344	60	34.7	-42	-25.9	42	25.3
Ozone (ppb)	345	64.6	30.4	-52	-34.2	52	34.1
NO ₂ (ppb)	344	71.4	68.6	11	-2.9	51	31.4
NO ₂ (ppb)	345	79.8	65.8	-1	-14.1	46	33.0
NO (ppb)	344	177.6	105	-16	-73.1	74	106
NO (ppb)	345	189	130	-3	-60.2	80	118
CO (ppm)	344	4.7	2.9	-16	-1.8	62	2.6
CO (ppm)	345	4.9	3.1	-10	-1.8	70	2.7

Table 6-9. UAM-AERO model performance for maximum short-term (1 to 6-hr) average concentrations ($\mu\text{g}/\text{m}^3$) on December 10-11, 1987.

Page 1 of 2

Species	Day	Location	Maximum Observed	Maximum Predicted	Accuracy (%)	Maximum in Domain
PM _{2.5} NO3	344	Burbank	63.4	39.9	-37	95.8
PM _{2.5} NO3	345	Burbank	102.4	17.1	-83	156
PM ₁₀ NO3	344	Burbank	67.7	43.7	-35	122
PM ₁₀ NO3	345	Burbank	117.2	18.6	-84	176
PM _{2.5} NH4	344	Riverside	14.2	10	-30	28.6
PM _{2.5} NH4	345	Burbank	19.1	5.6	-71	48.2
PM ₁₀ NH4	344	Anaheim	18.8	13.6	-28	36.9
PM ₁₀ NH4	345	Burbank	33.6	6.4	-81	55.1
PM _{2.5} SO4	344	Anaheim	4.5	5.3	18	45.6
PM _{2.5} SO4	345	Hawthorne	12.7	7.7	-39	71.4
PM ₁₀ SO4	344	Anaheim	5.4	8.3	54	52.1
PM ₁₀ SO4	345	Long Beach	17	10	-41	78.4
PM _{2.5} EC	344	Hawthorne	14.7	5.9	-60	15.9
PM _{2.5} EC	345	Los Angeles	19.4	14.7	-24	22.4
PM ₁₀ EC	344	Hawthorne	18.8	8.1	-57	18.1
PM ₁₀ EC	345	Los Angeles	19.9	19.5	-2	28.3
PM _{2.5} OM	344	Long Beach	50.7	30.1	-41	56.8
PM _{2.5} OM	345	Los Angeles	50.8	64	26	74.3
PM ₁₀ OM	344	Long Beach	63.5	59	-7	113
PM ₁₀ OM	345	Burbank	64.7	53.1	-18	153
PM ₁₀ Na	344	Hawthorne	1.9	1.4	-26	9.4
PM ₁₀ Na	345	Hawthorne	2.1	0.9	-57	13.4
PM ₁₀ Cl	344	Hawthorne	4.9	1.9	-61	13.1
PM ₁₀ Cl	345	Hawthorne	5.8	1.9	-67	17.3
PM _{2.5} Mass	344	Anaheim	137.2	181.3	32	225

Table 6-9. UAM-AERO model performance for maximum short-term (1 to 6-hr) average concentrations ($\mu\text{g}/\text{m}^3$) on December 10-11, 1987.

Page 2 of 2

Species	Day	Location	Maximum Observed	Maximum Predicted	Accuracy (%)	Maximum in Domain
PM _{2.5} Mass	345	Burbank	179.7	103.8	-42	347
PM ₁₀ Mass	344	Anaheim	145.4	389	168	509
PM ₁₀ Mass	345	Burbank	191	228	19	697
HNO ₃ (ppb)	344	Burbank	16.3	3.6	-78	28.3
HNO ₃ (ppb)	345	Burbank	19.8	2.4	-88	32.8
NH ₃ (ppb)	344	Hawthorne	51.2	66	29	534
NH ₃ (ppb)	345	Riverside	52.1	50.3	-3	762
Ozone (ppb)	344	Pasadena	60	40.8	-32	90
Ozone (ppb)	345	Pasadena	80	39.7	-50	122
NO ₂ (ppb)	344	Anaheim	210	166.7	-21	272
NO ₂ (ppb)	345	Burbank	230	114.5	-50	320
NO (ppb)	344	Lynnwood	770	340.9	-56	1015
NO (ppb)	345	Lynnwood	740	490.5	-34	1496
CO (ppm)	344	Lynnwood	22	6.8	-69	19.0
CO (ppm)	345	Lynnwood	22	7.6	-65	20.1

Table 6-10. Estimated domain-wide average pollutant deposition for December 10-11, 1987.

Species	Deposition Moles/hectare-day	Species	Deposition Grams/hectare-day
O ₃	0.776	HNO ₃	9.77
NO ₂	0.205	NH ₃	4.56
HNO ₃	0.155	NO ₃ PM _{2.5}	0.586
NH ₃	0.268	NO ₃ PM ₁₀	4.58
H ₂ O ₂	7.08E-02	NH ₄ PM _{2.5}	0.191
HCHO	0.860	NH ₄ PM ₁₀	1.21
CCHO	0.334	SO ₄ PM _{2.5}	0.809
RCHO	0.105	SO ₄ PM ₁₀	0.944
PAN	0.123	EC PM _{2.5}	0.481
PPN	3.47E-02	EC PM ₁₀	0.547
SO ₂	0.104	OM PM _{2.5}	0.317
FACD	0.116	OM PM ₁₀	5.99
AACD	0.101	OTR PM _{2.5}	0.569
HCL	0.267	OTR PM ₁₀	18.3
NO	2.13E-03	NA PM _{2.5}	0.240
HONO	6.20E-02	NA PM ₁₀	0.937
HNO ₄	1.36E-03	CL PM _{2.5}	0.187
XOOH	2.50E-02	CL PM ₁₀	0.500
RNO ₃	8.97E-02	H ₂ O PM _{2.5}	0.801
MGLY	1.80E-02	H ₂ O PM ₁₀	11.7
CRES	8.22E-03		

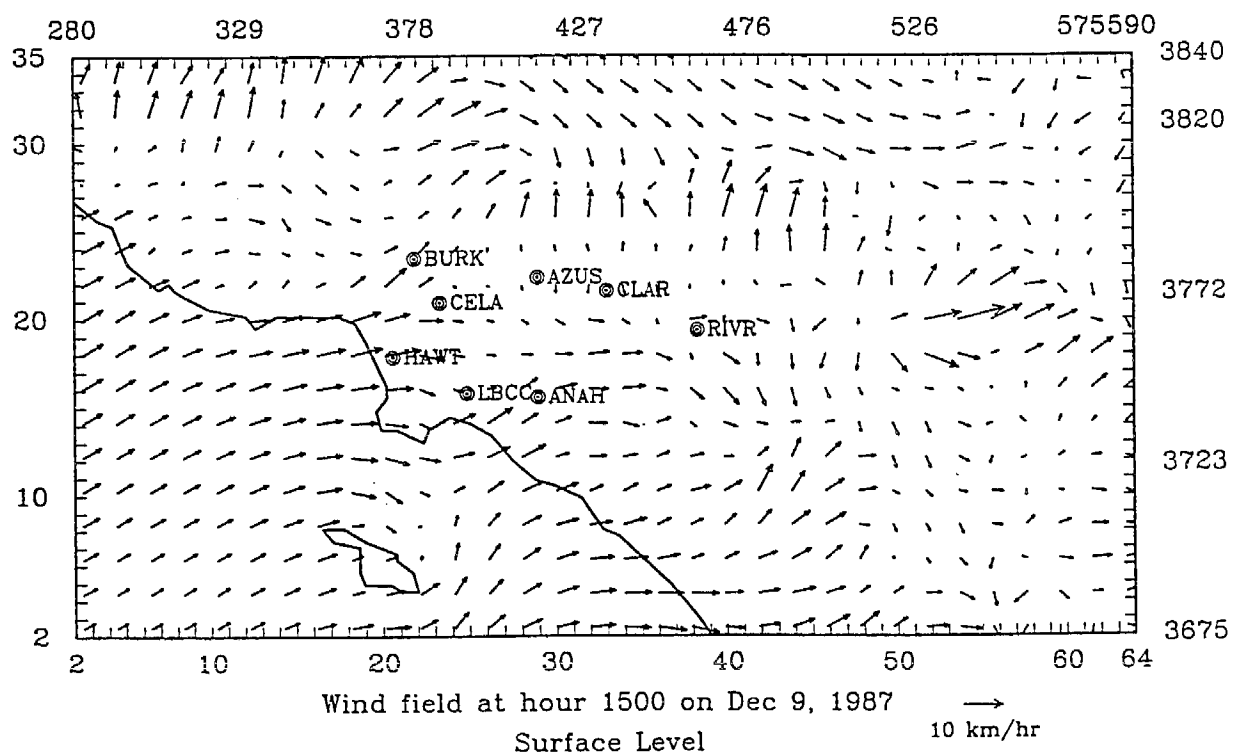
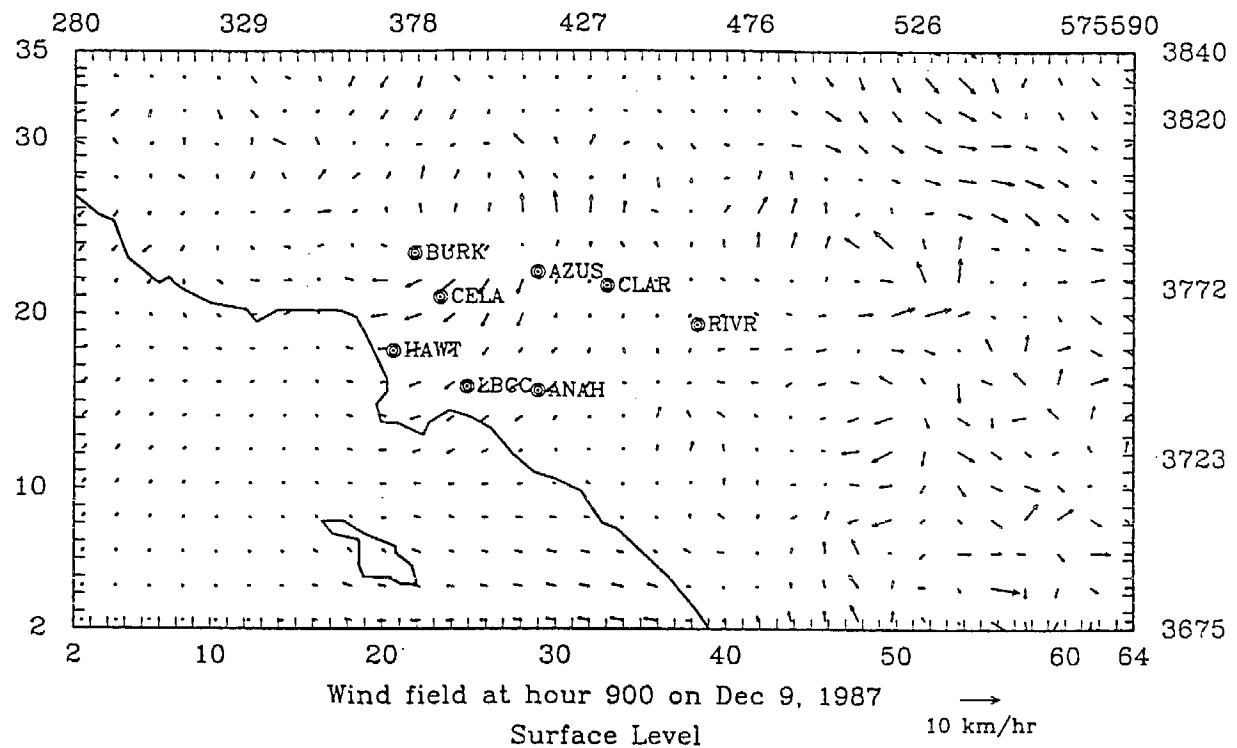


Figure 6-1. Surface layer wind field for hours 09 (top) and 15 (bottom) on December 9, 1987.

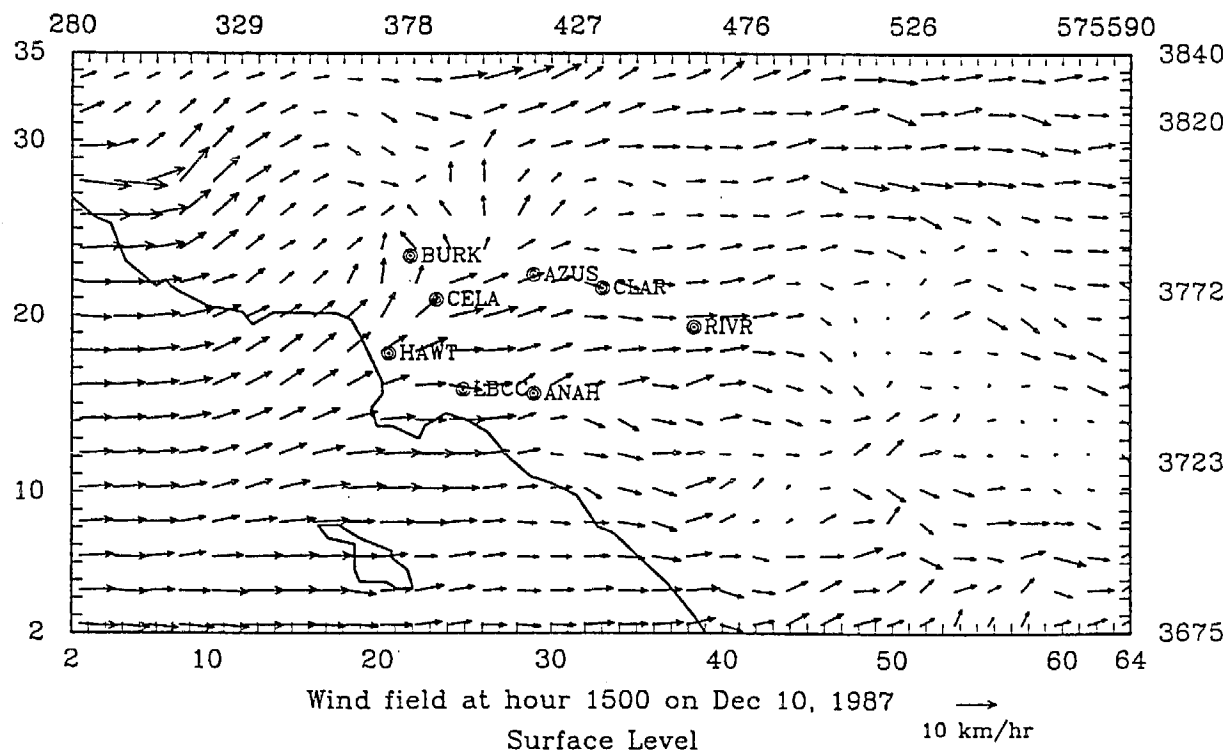
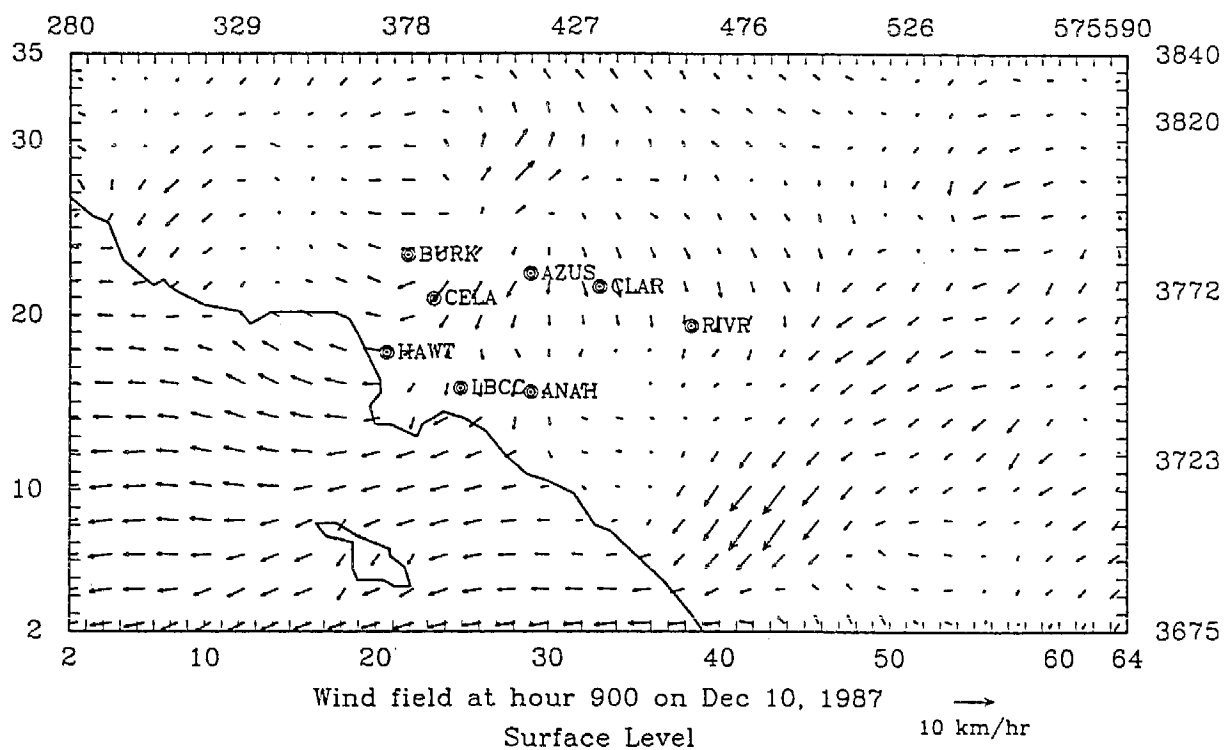


Figure 6-2. Surface layer wind field for hours 09 (top) and 15 (bottom) on December 10, 1987.

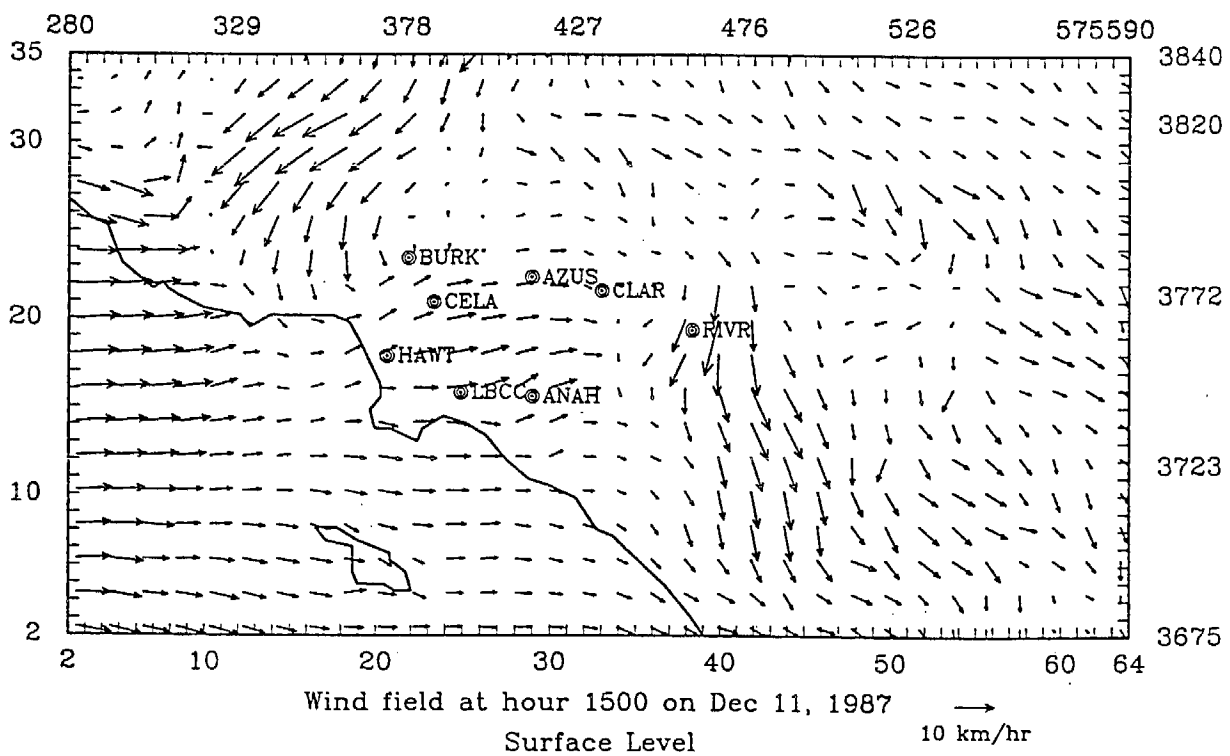
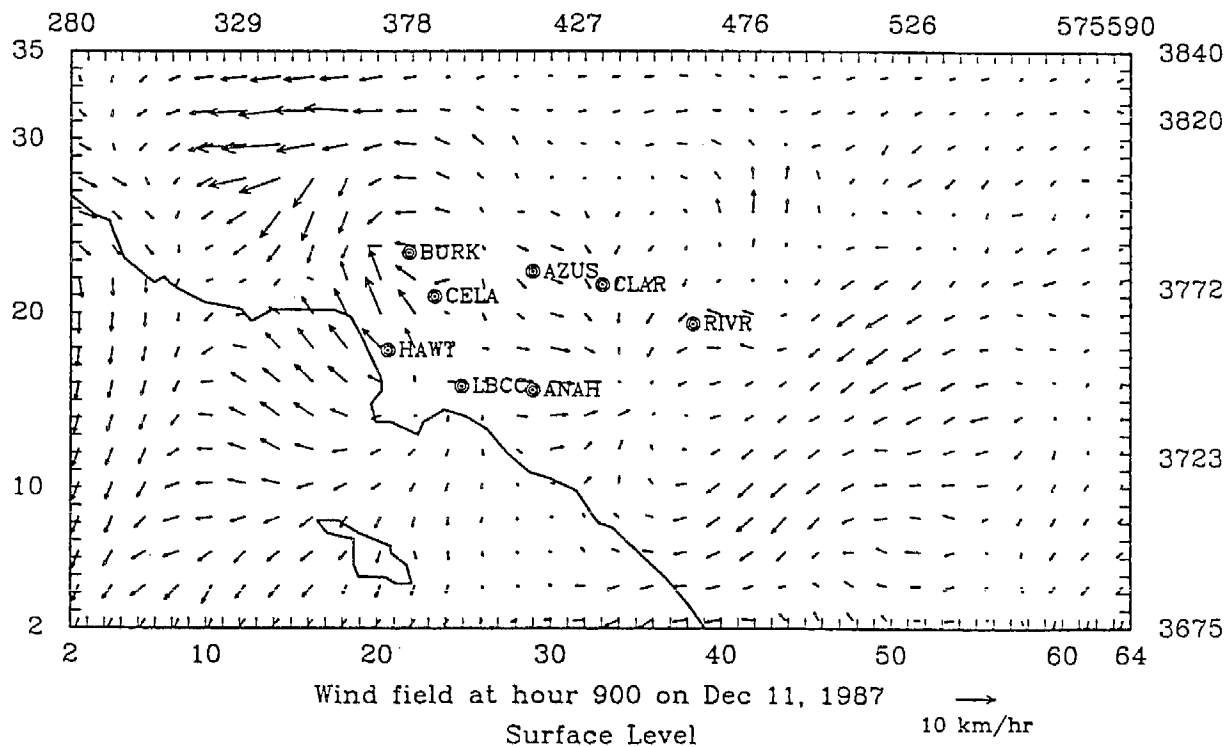


Figure 6-3. Surface layer wind field for hours 09 (top) and 15 (bottom) on December 11, 1987.

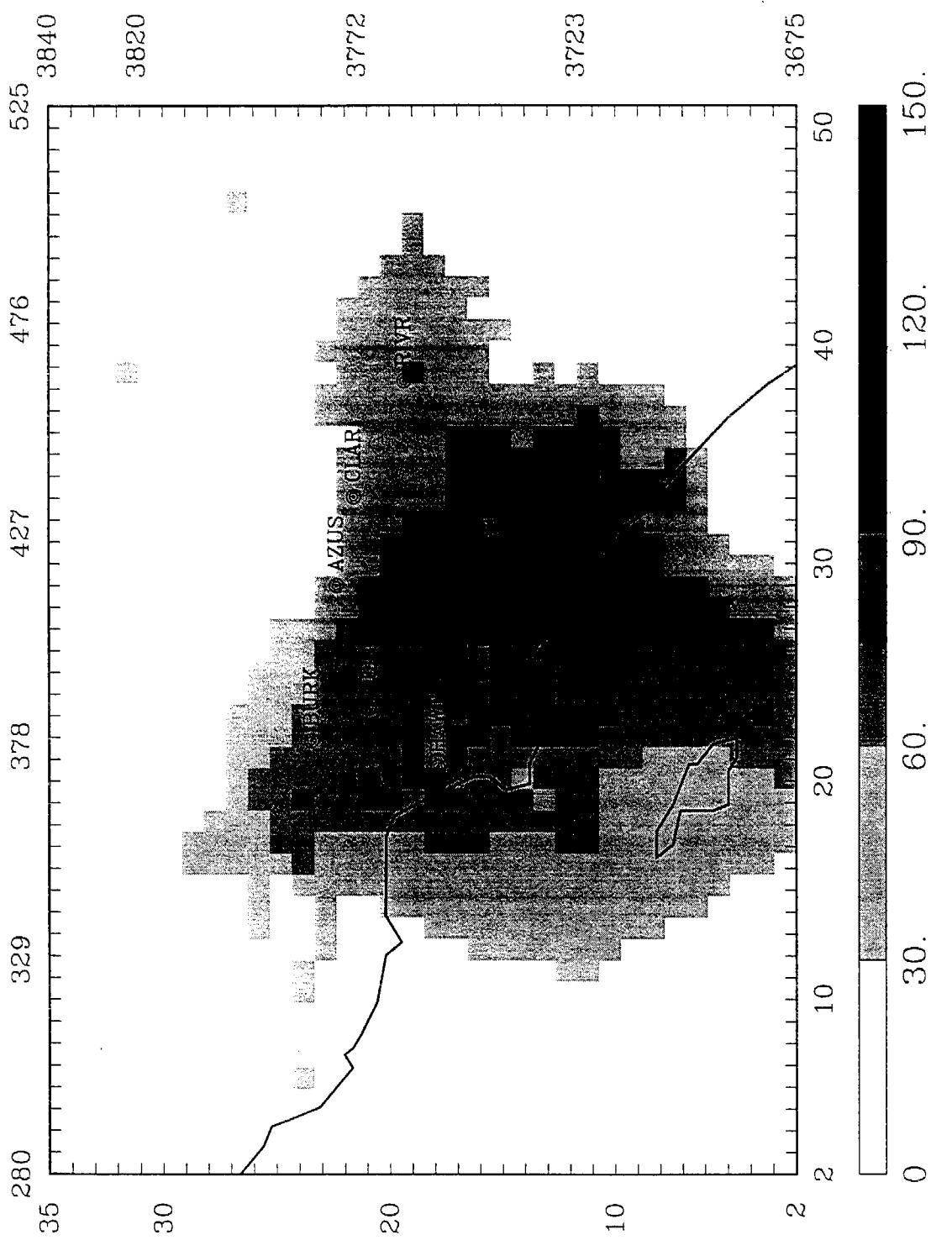


Figure 6-4. Predicted 24-hr average NO_2 concentration on December 10, 1987.

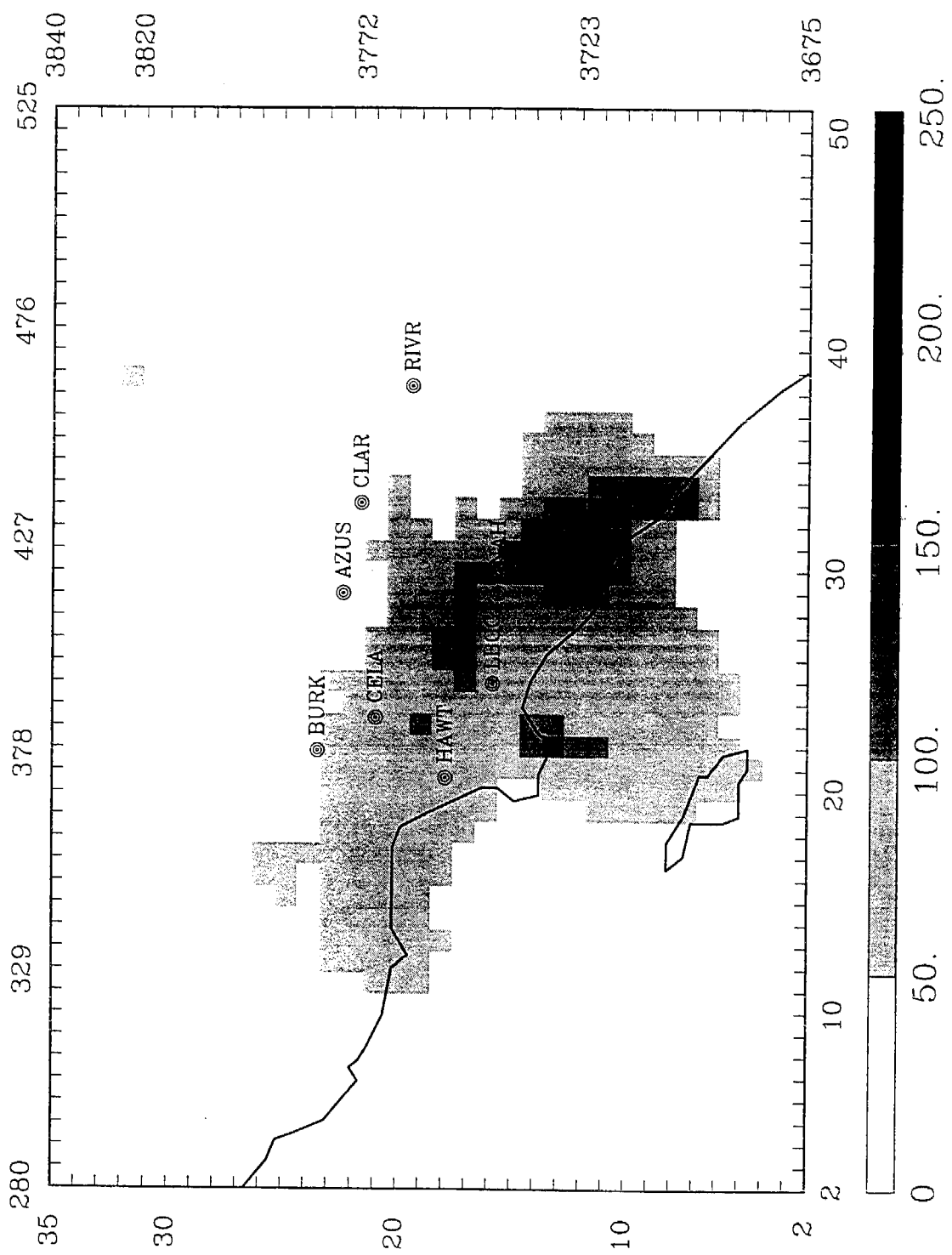


Figure 6-5. Predicted 24-hr average NO_2 concentration on December 11, 1987.

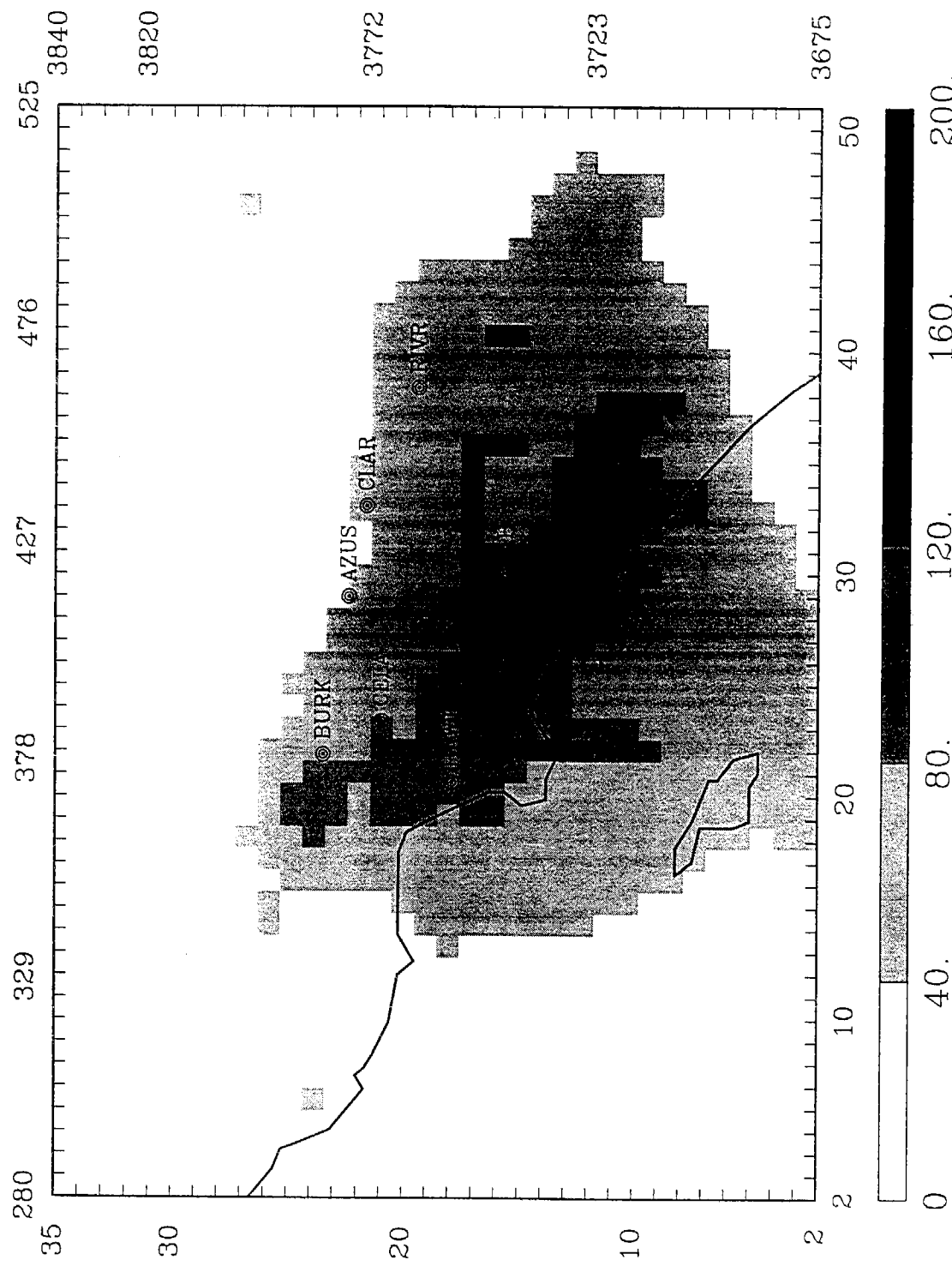


Figure 6-6. Predicted 24-hr average $\text{PM}_{2.5}$ mass concentration on December 10, 1987.

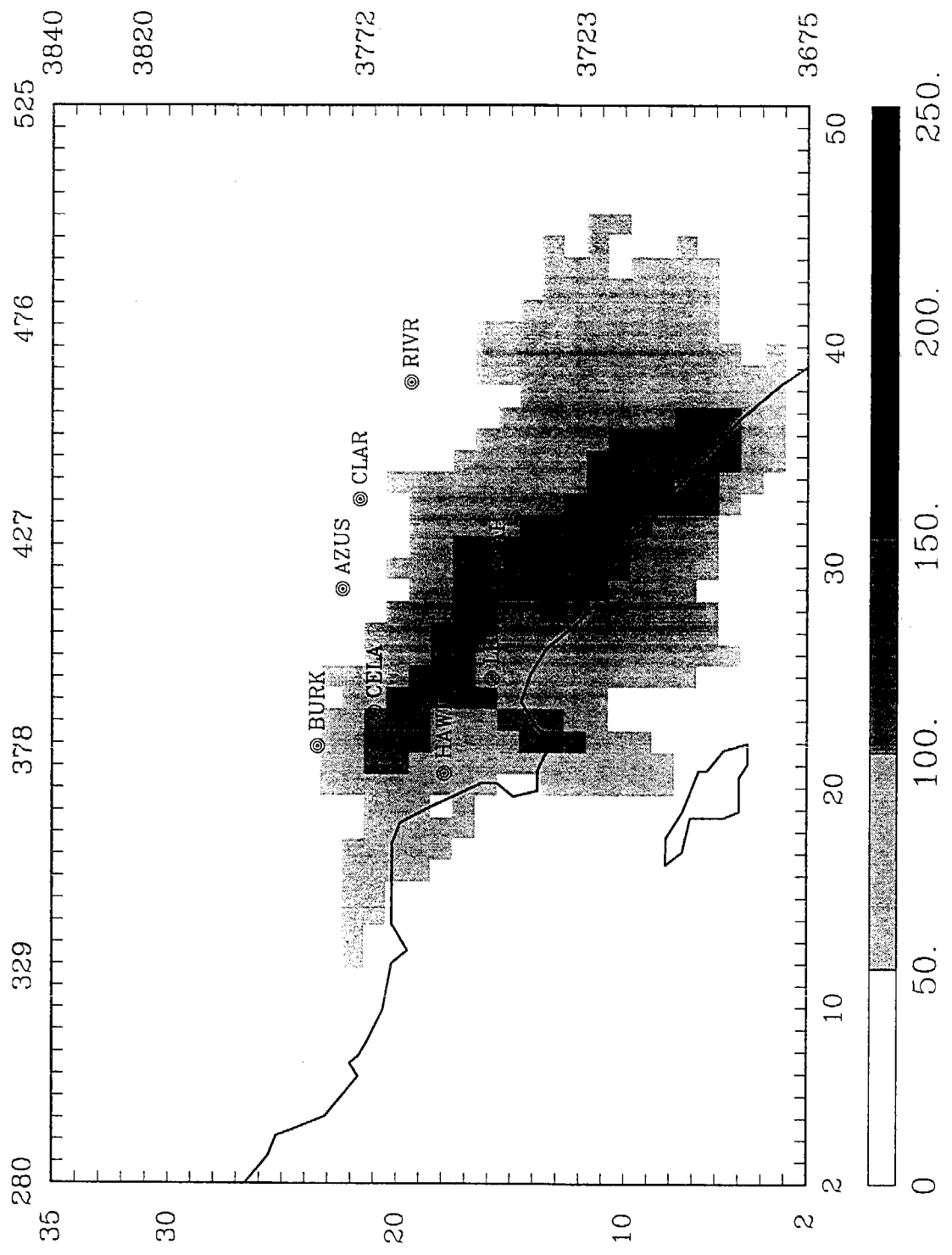


Figure 6-7. Predicted 24-hr average $\text{PM}_{2.5}$ mass concentration on December 11, 1987.

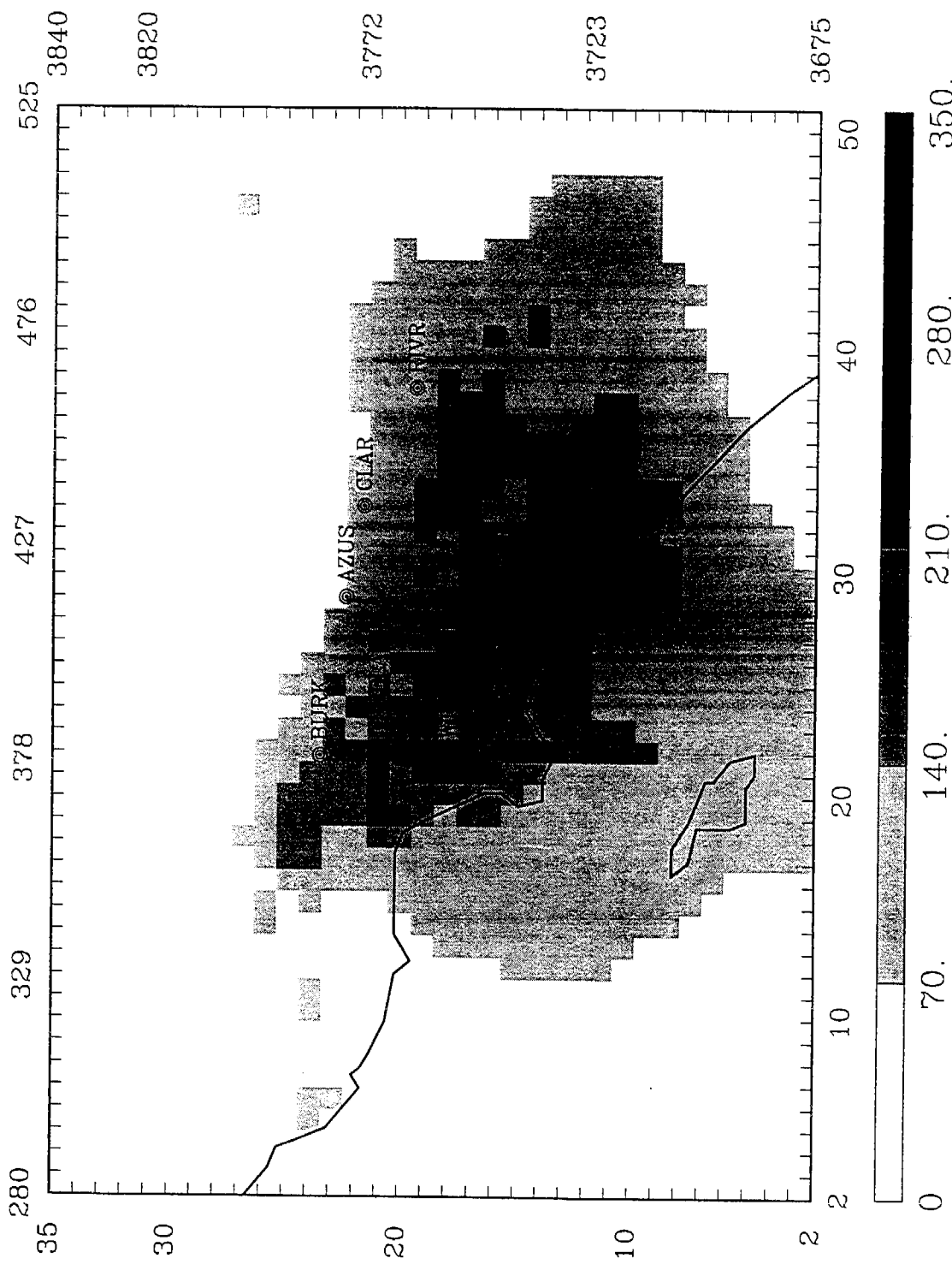


Figure 6-8. Predicted 24-hr average PM_{10} mass concentration on December 10, 1987.

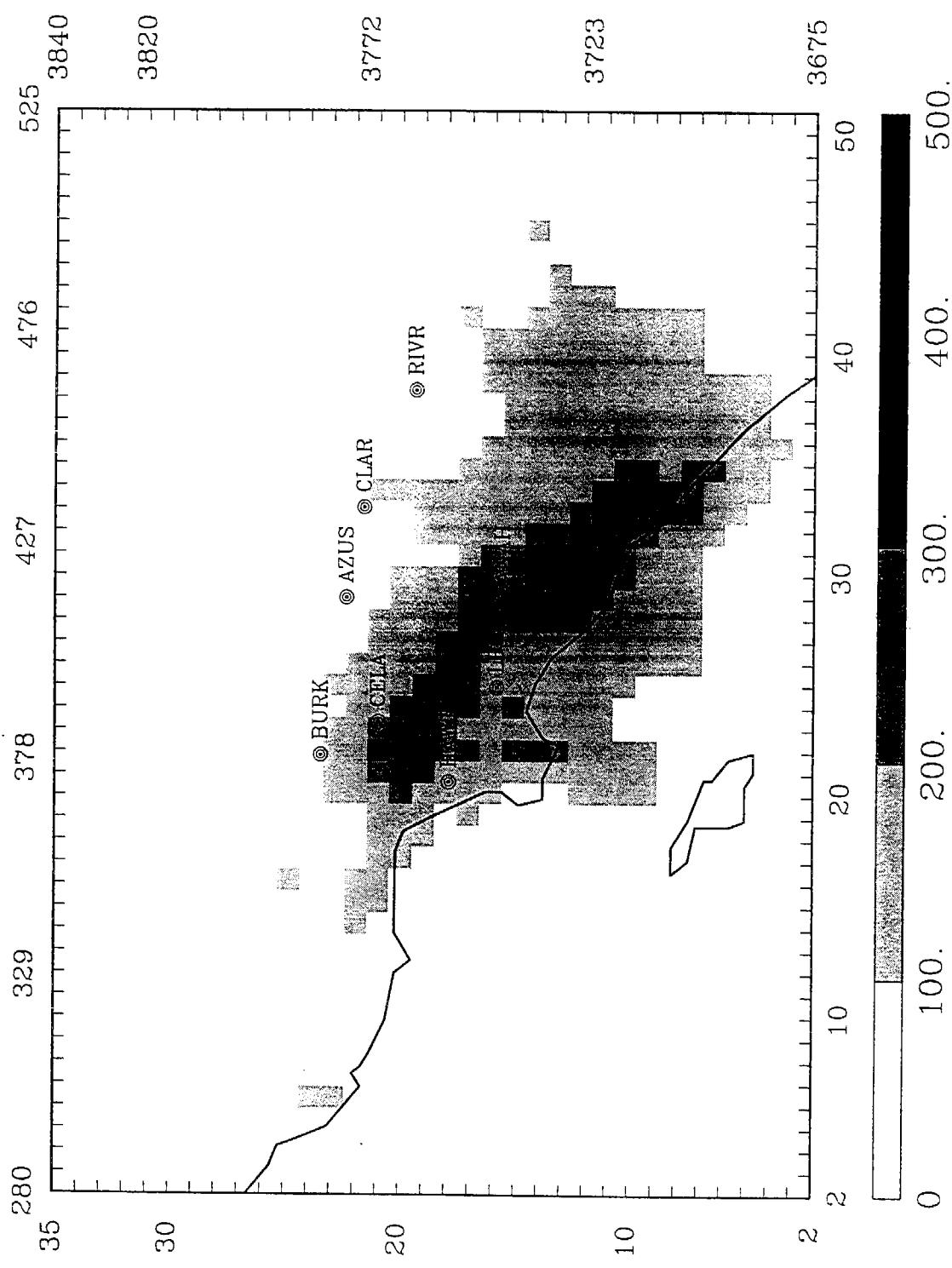


Figure 6-9. Predicted 24-hr average PM_{10} mass concentration on December 11, 1987.

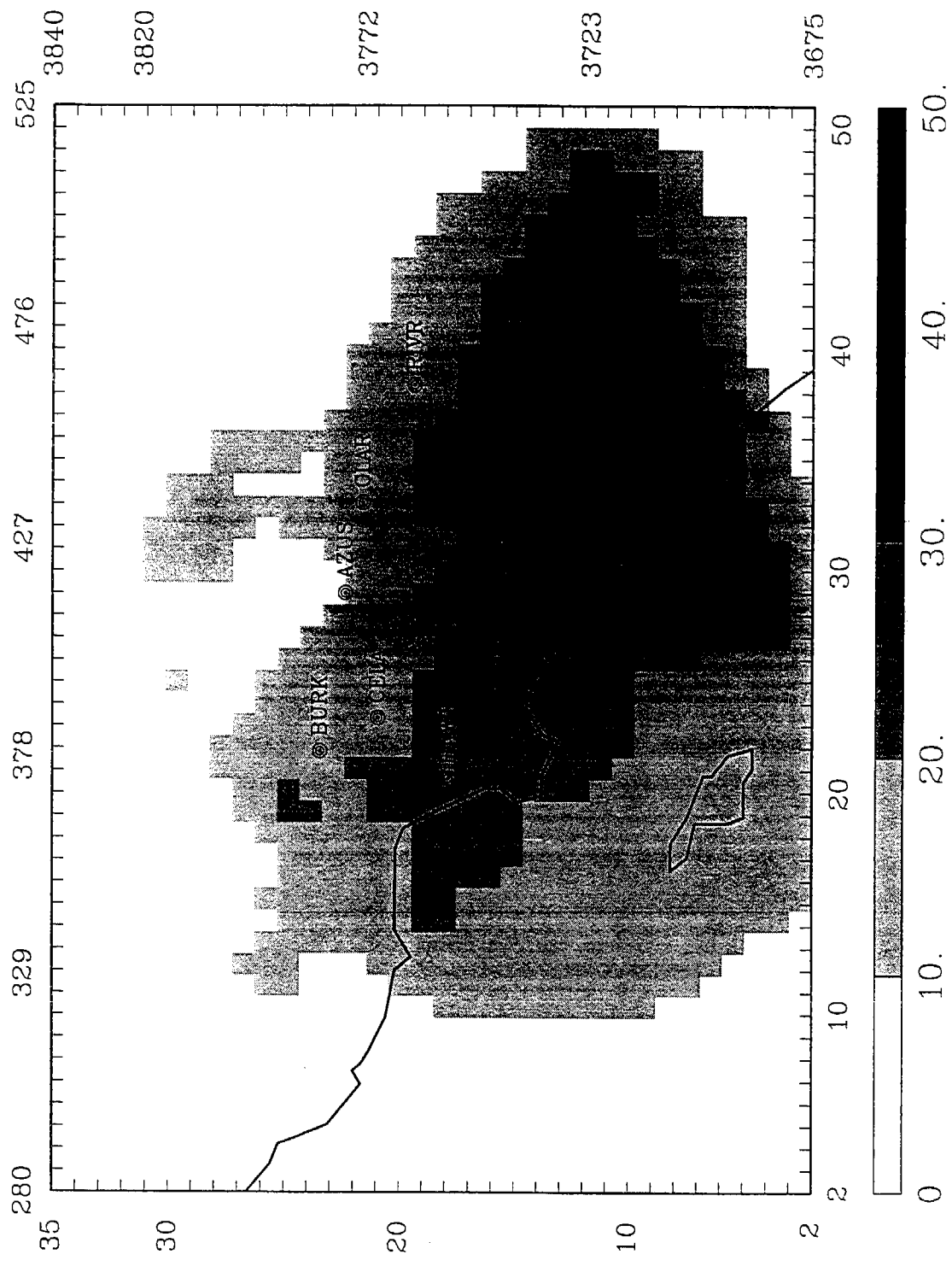


Figure 6-10. Predicted 24-hr average $\text{PM}_{2.5}$ NO_3 concentration on December 10, 1987.

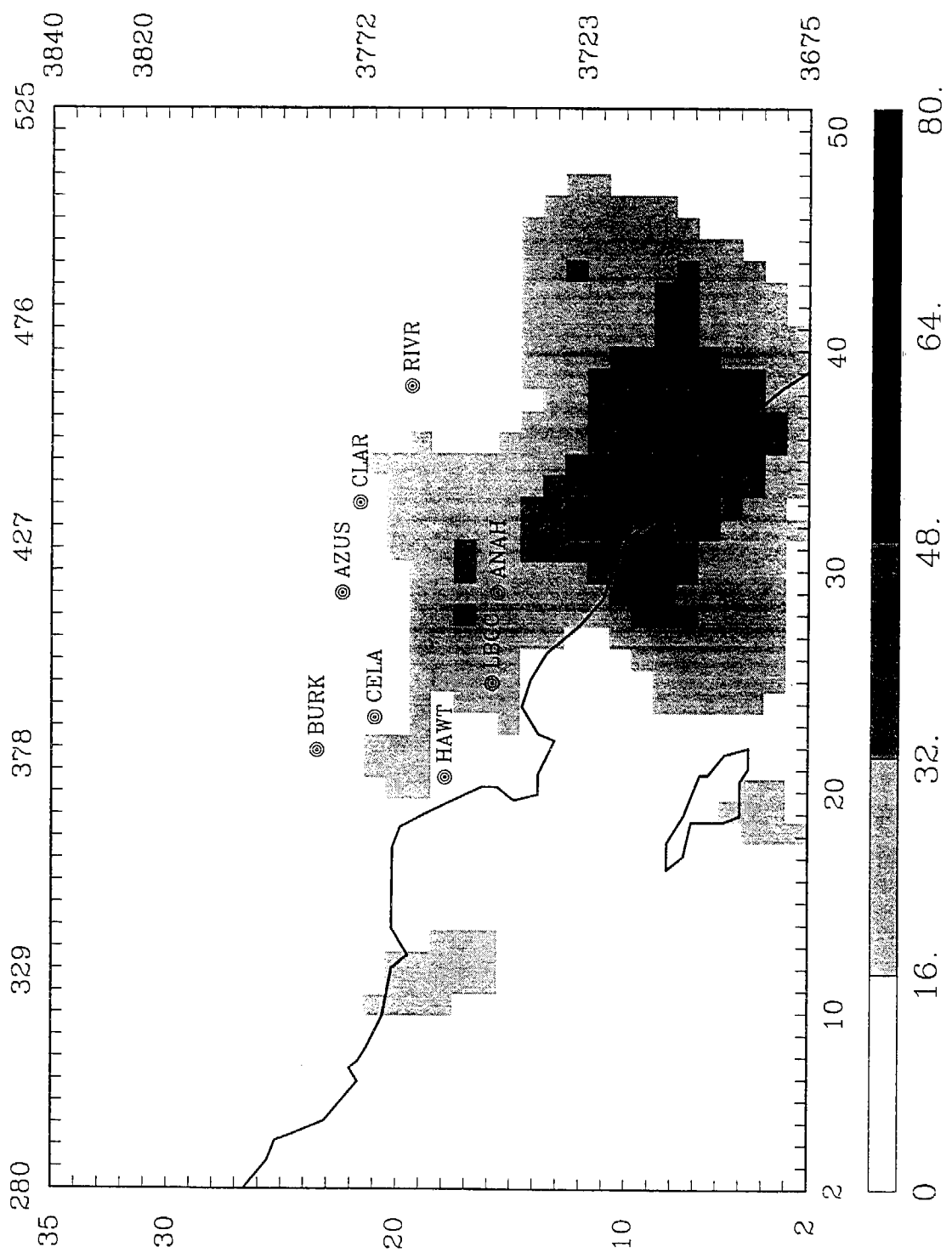


Figure 6-11. Predicted 24-hr average $\text{PM}_{2.5}$ NO_3 concentration on December 11, 1987.

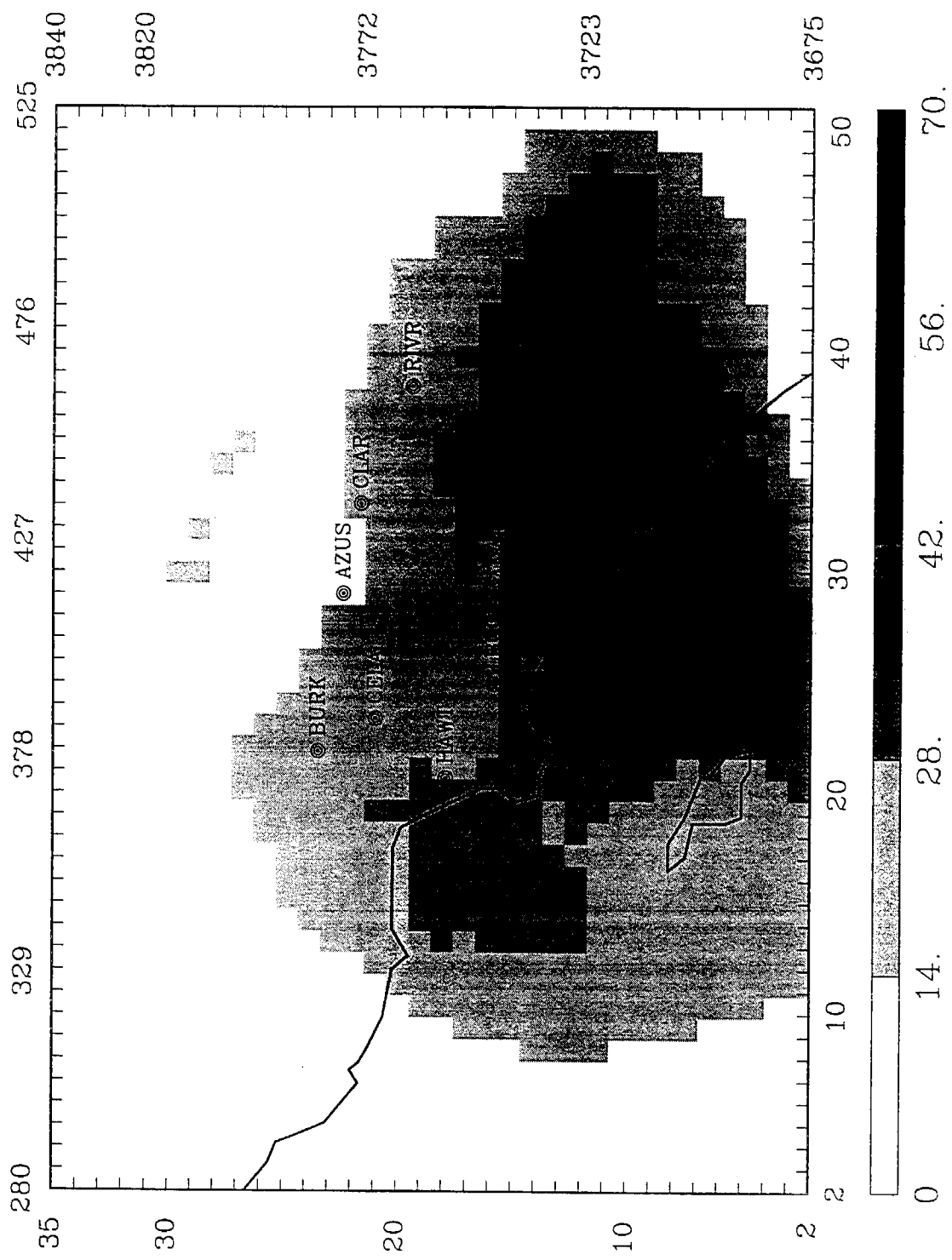


Figure 6-12. Predicted 24-hr average $\text{PM}_{10} \text{NO}_3$ concentration on December 10, 1987.

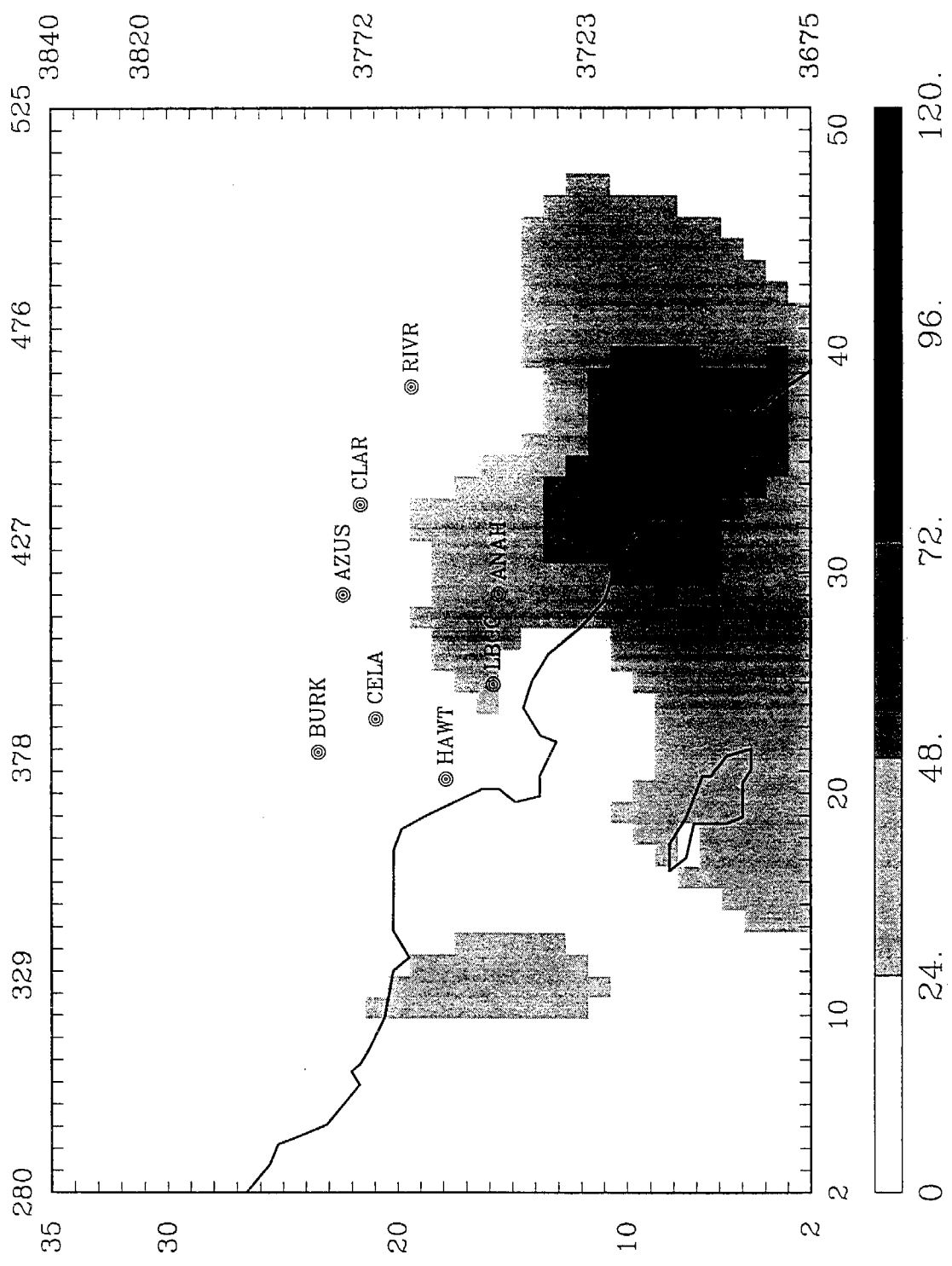


Figure 6-13. Predicted 24-hr average PM_{10} NO_3 concentration on December 11, 1987.

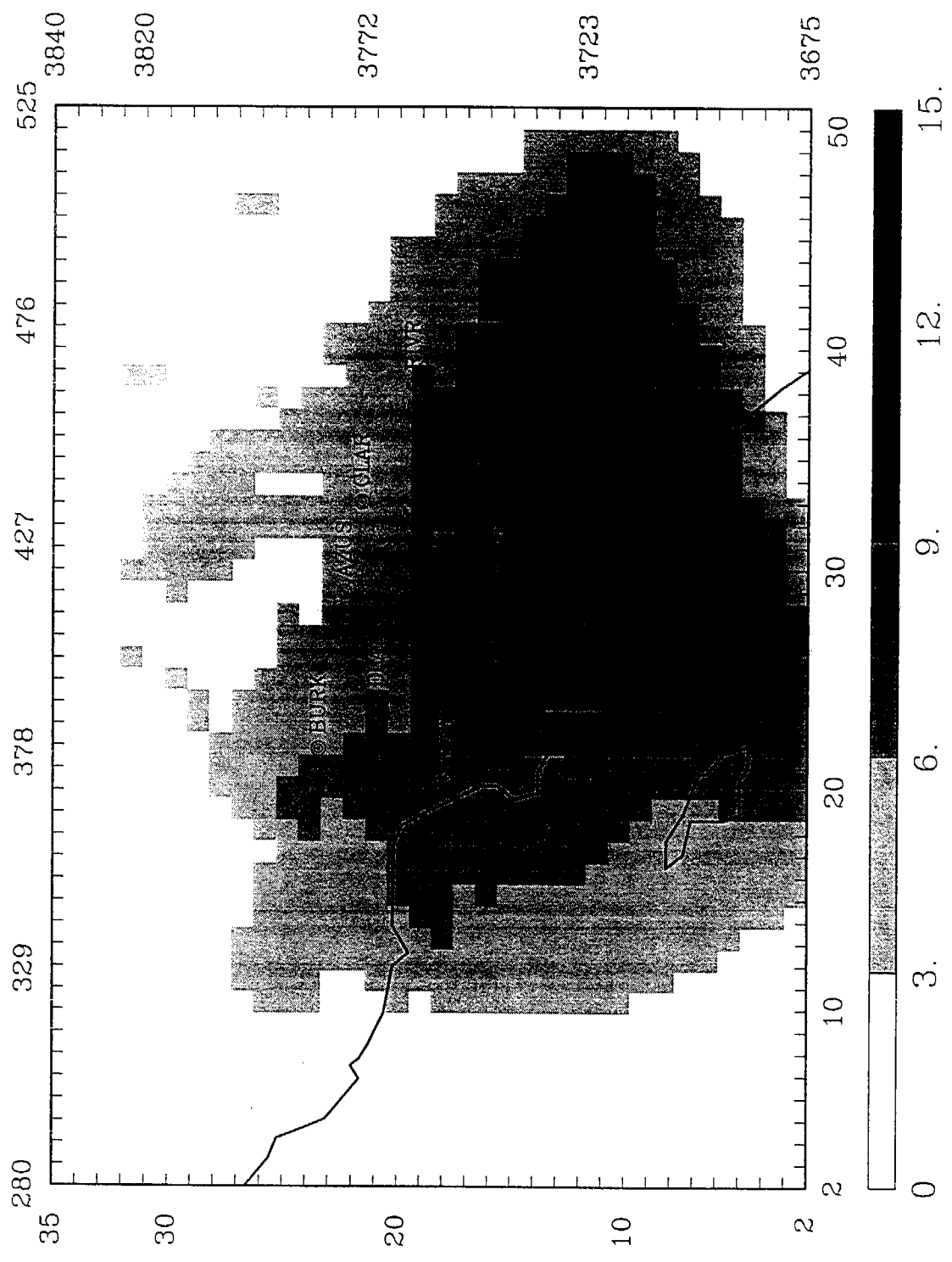


Figure 6-14. Predicted 24-hr average $\text{PM}_{2.5}$ NH_4 concentration on December 10, 1987.

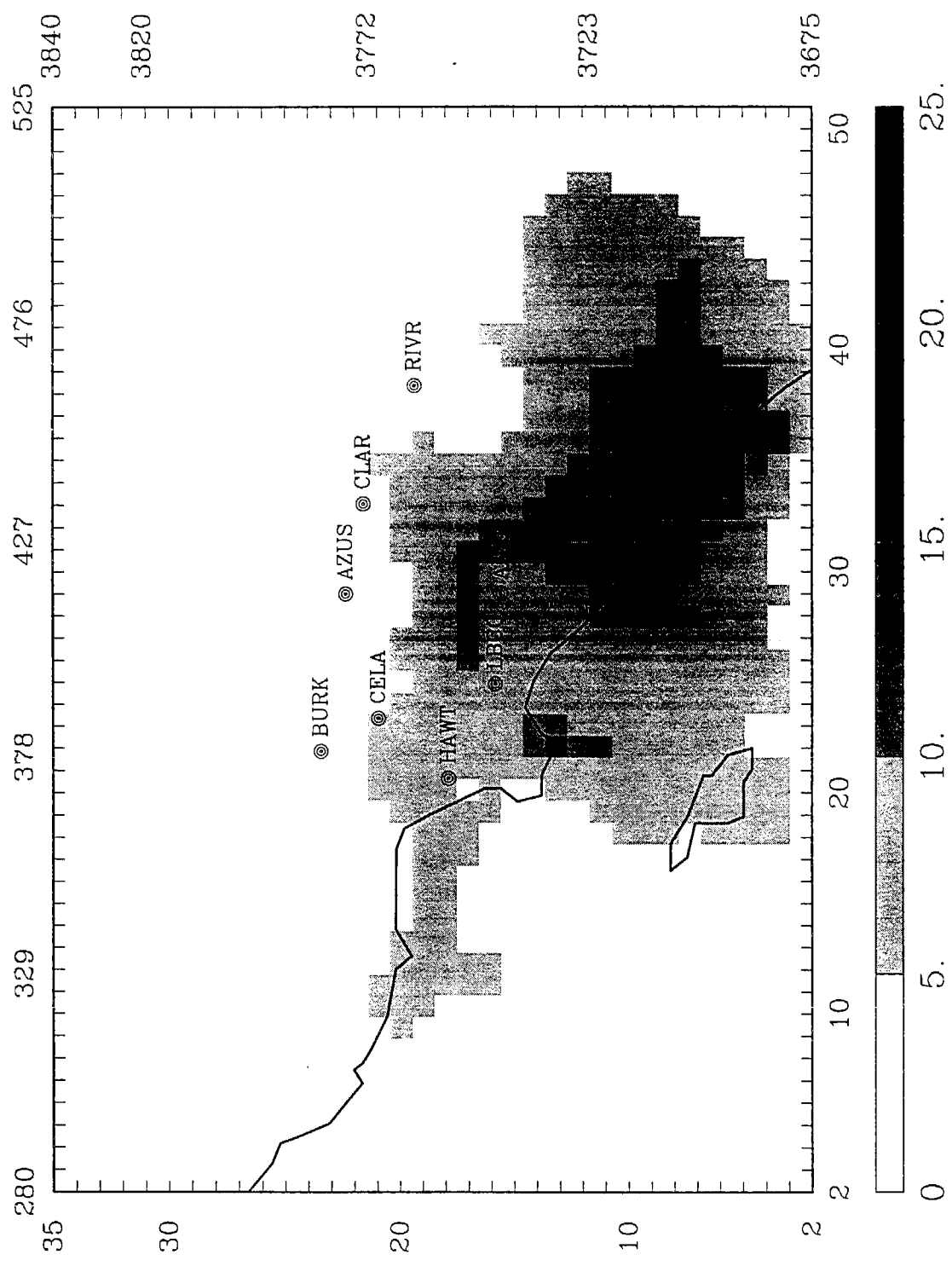


Figure 6-15. Predicted 24-hr average $\text{PM}_{2.5}$ NH_4 concentration on December 11, 1987.

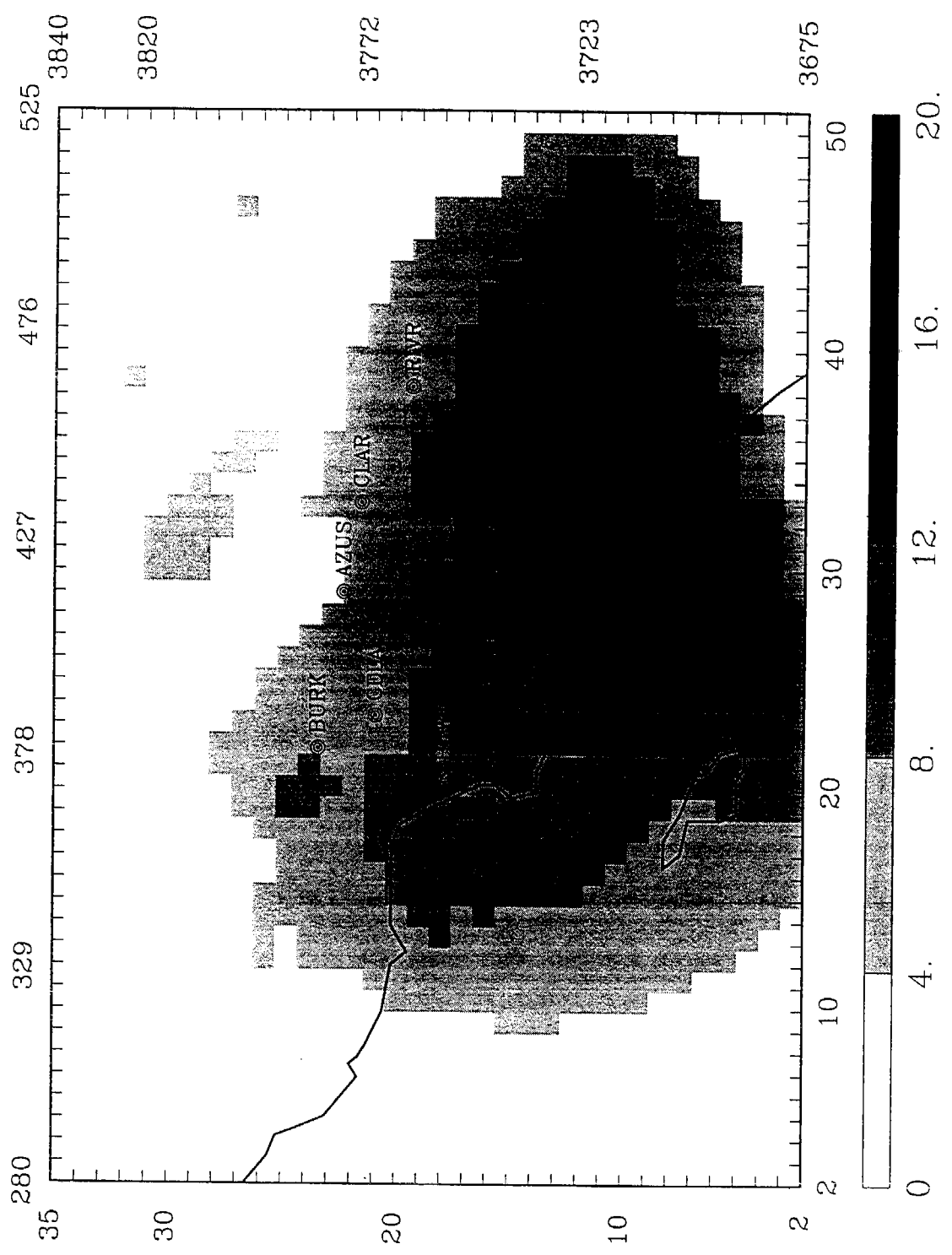


Figure 6-16. Predicted 24-hr average PM_{10} NH_4 concentration on December 10, 1987.

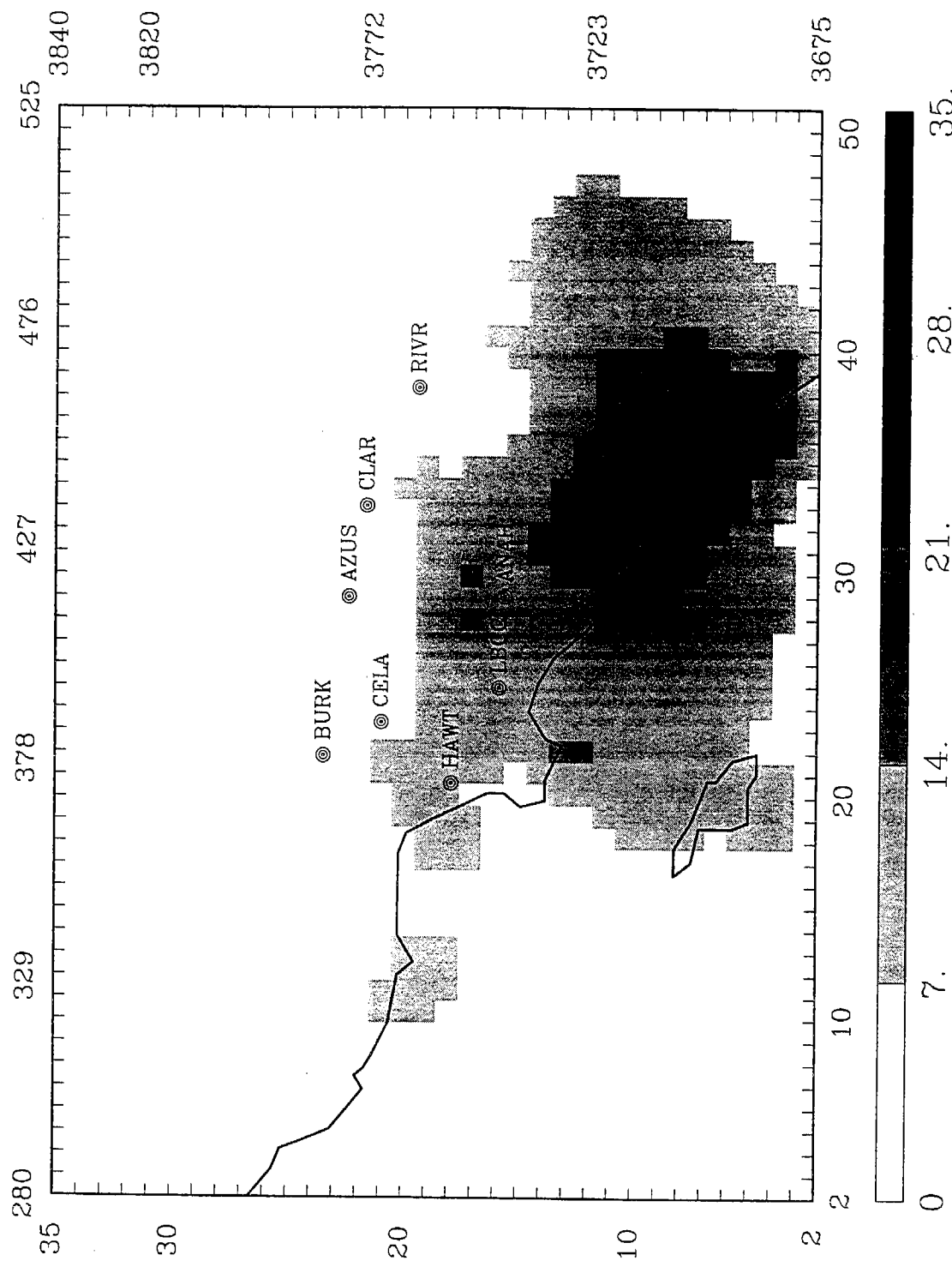


Figure 6-17. Predicted 24-hr average PM_{10} NH_4 concentration on December 11, 1987.

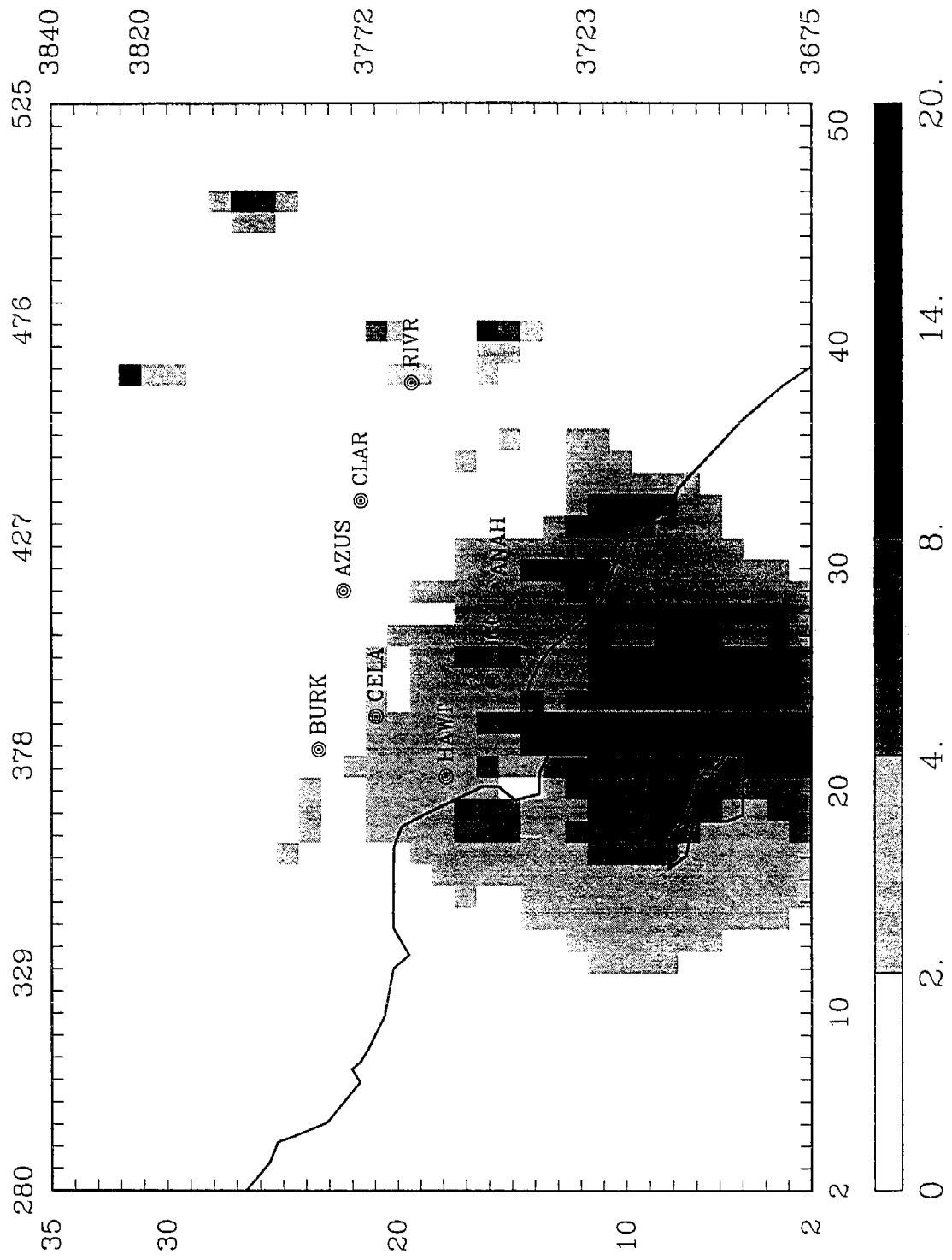


Figure 6-18. Predicted 24-hr average $\text{PM}_{2.5}$ concentration on December 10, 1987.

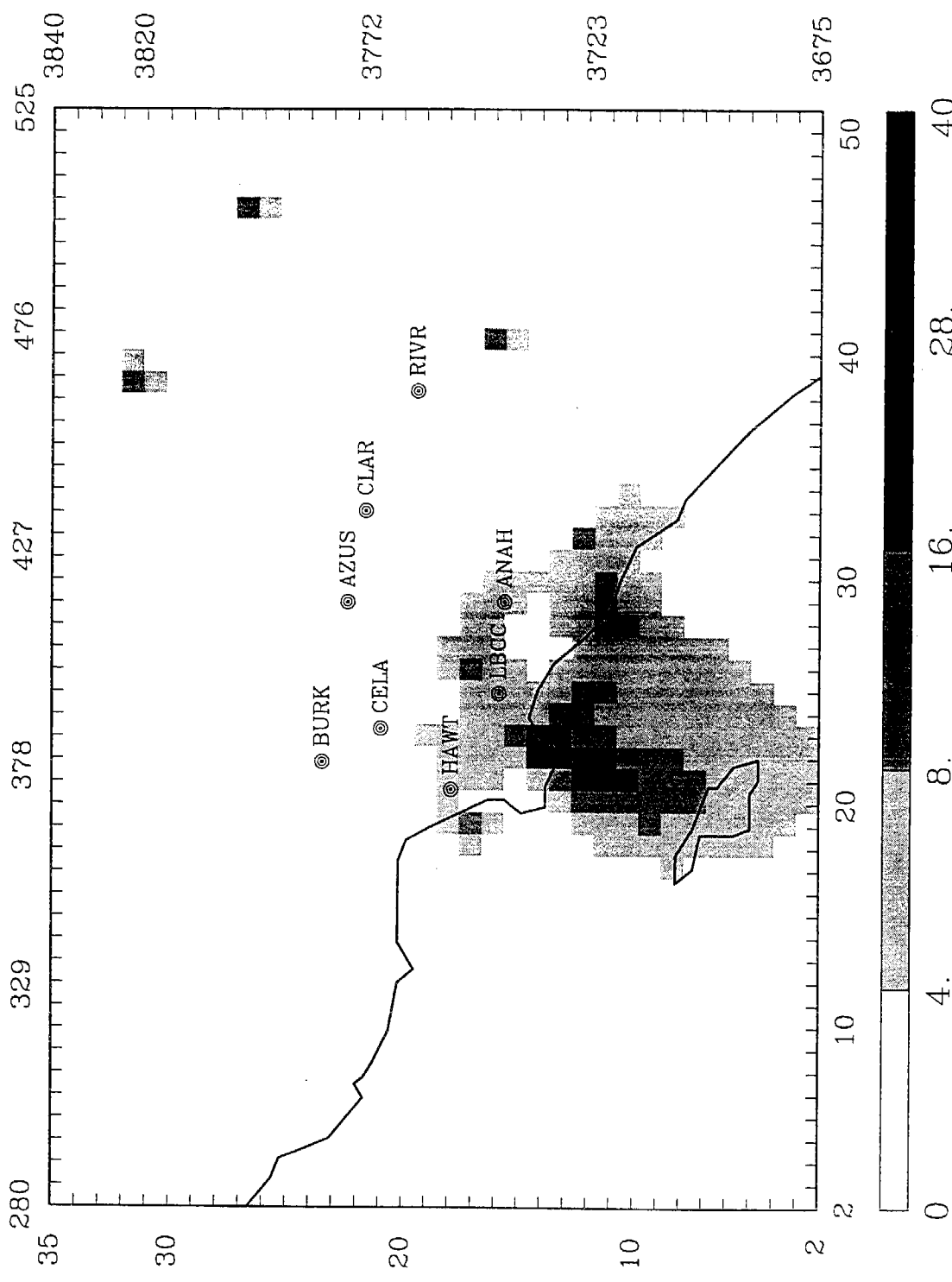


Figure 6-19. Predicted 24-hr average $\text{PM}_{2.5}$ SO_4 concentration on December 11, 1987.

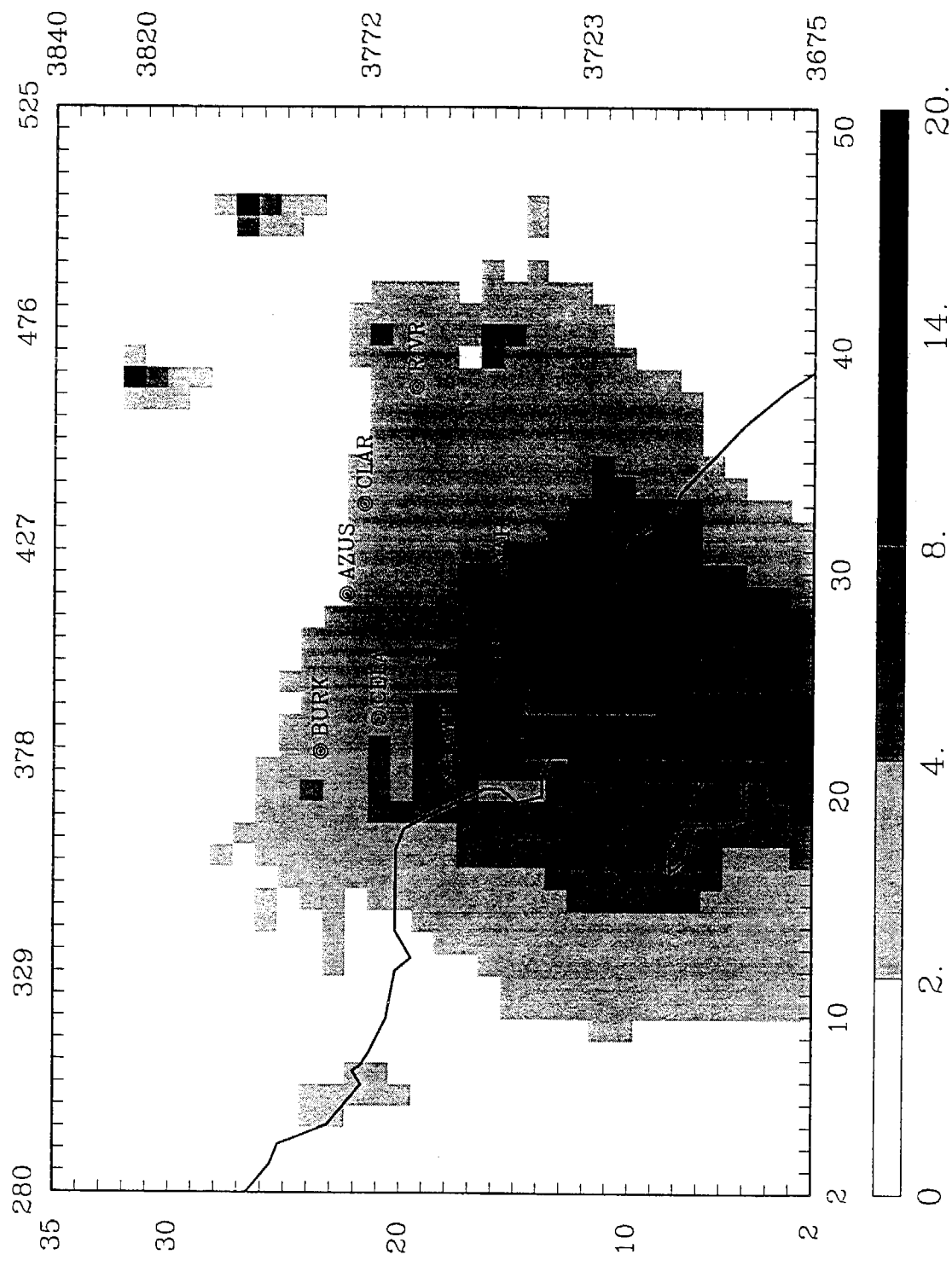


Figure 6-20. Predicted 24-hr average PM_{10} SO_4 concentration on December 10, 1987.

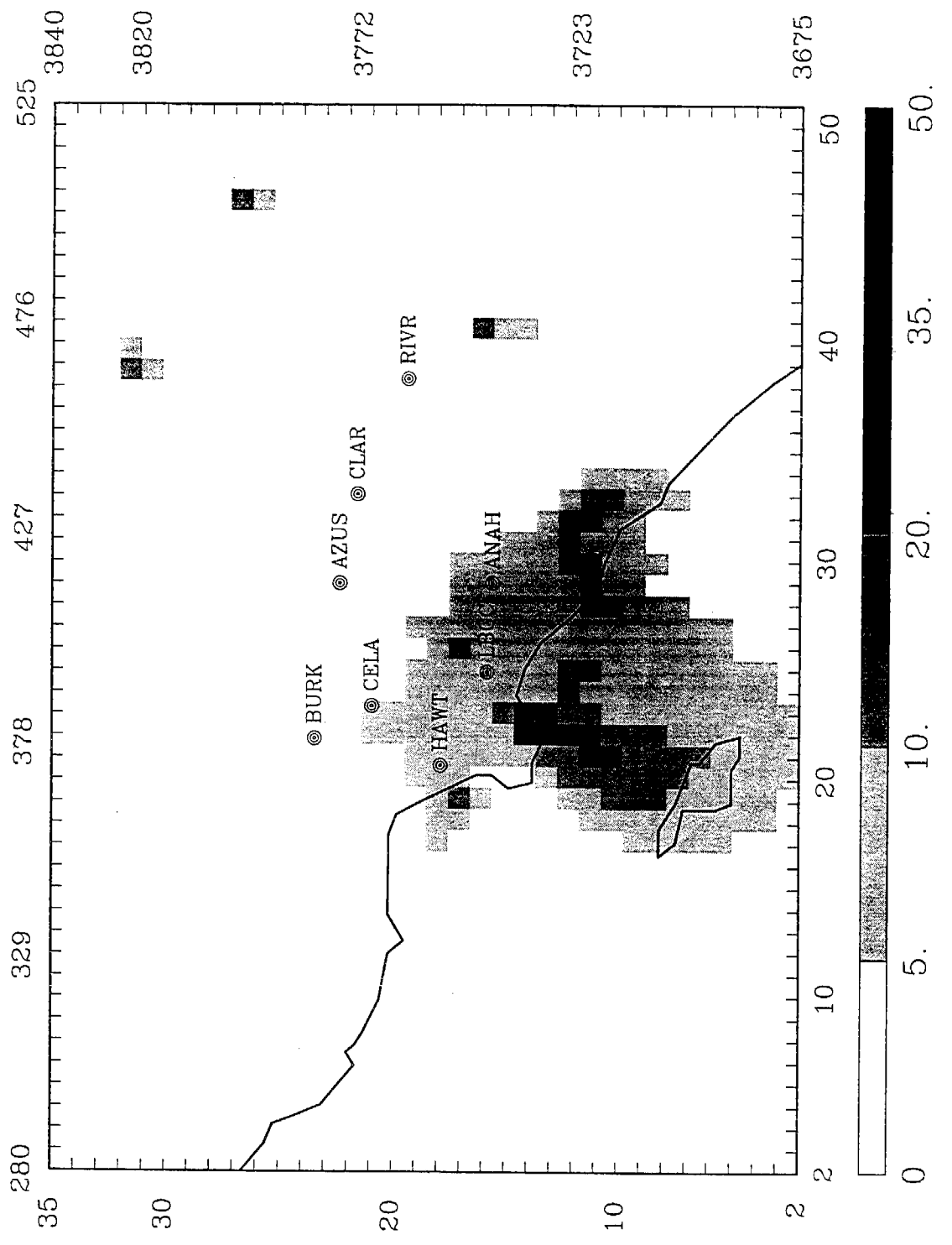


Figure 6-21. Predicted 24-hr average PM_{10} SO_4 concentration on December 11, 1987.

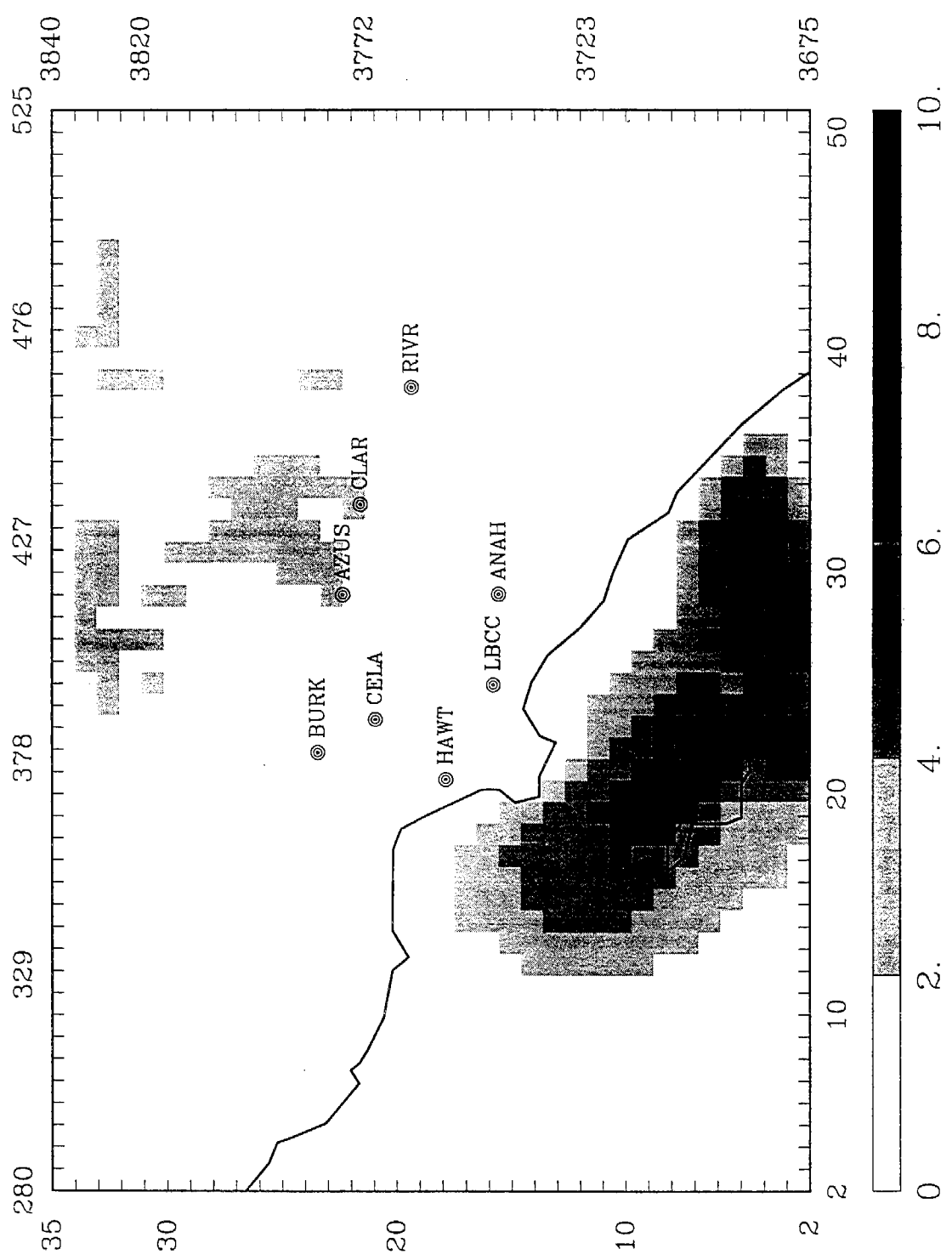


Figure 6-22. Predicted 24-hr average HNO_3 concentration on December 10, 1987.

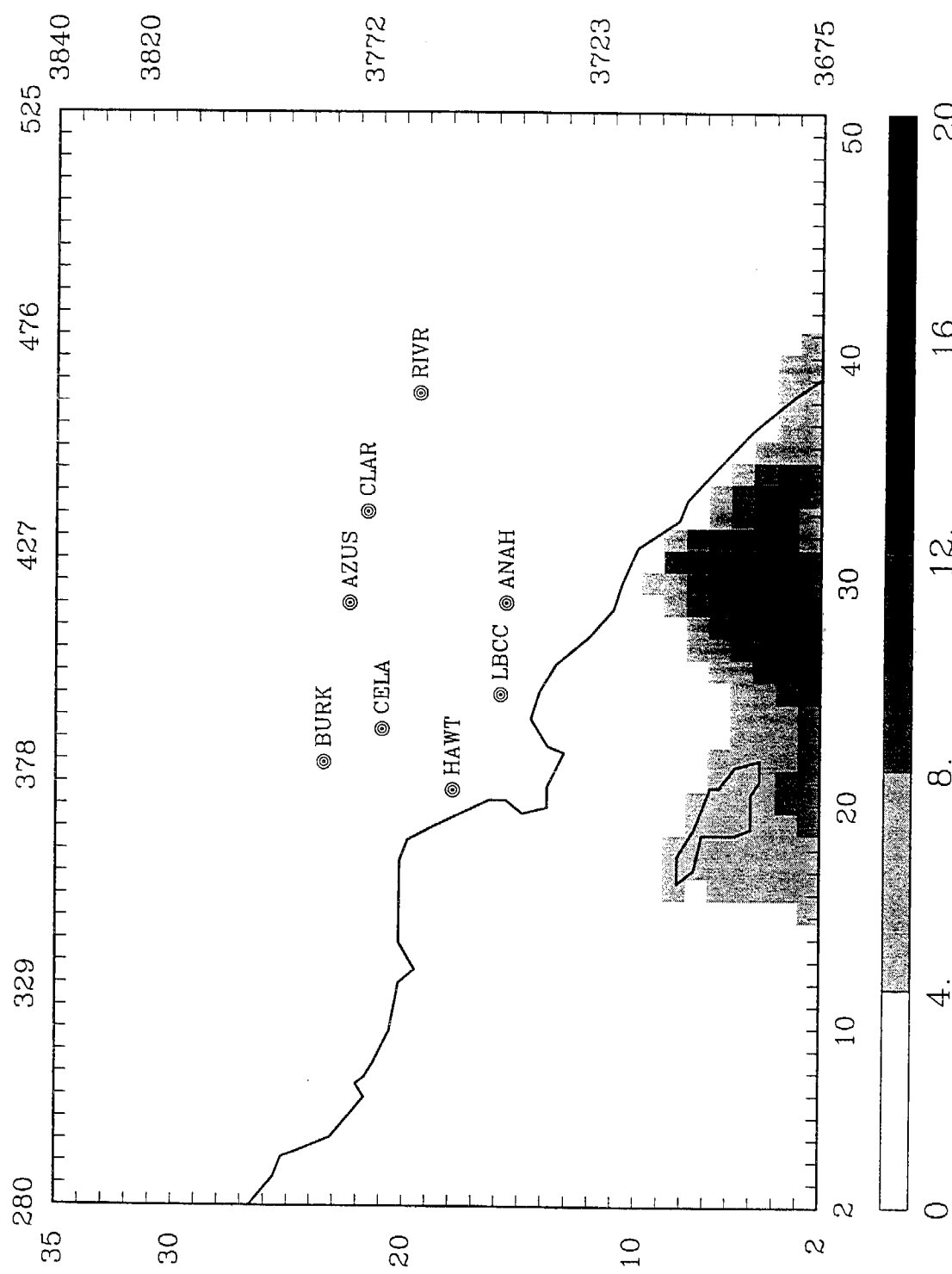


Figure 6-23. Predicted 24-hr average HNO_3 concentration on December 11, 1987.

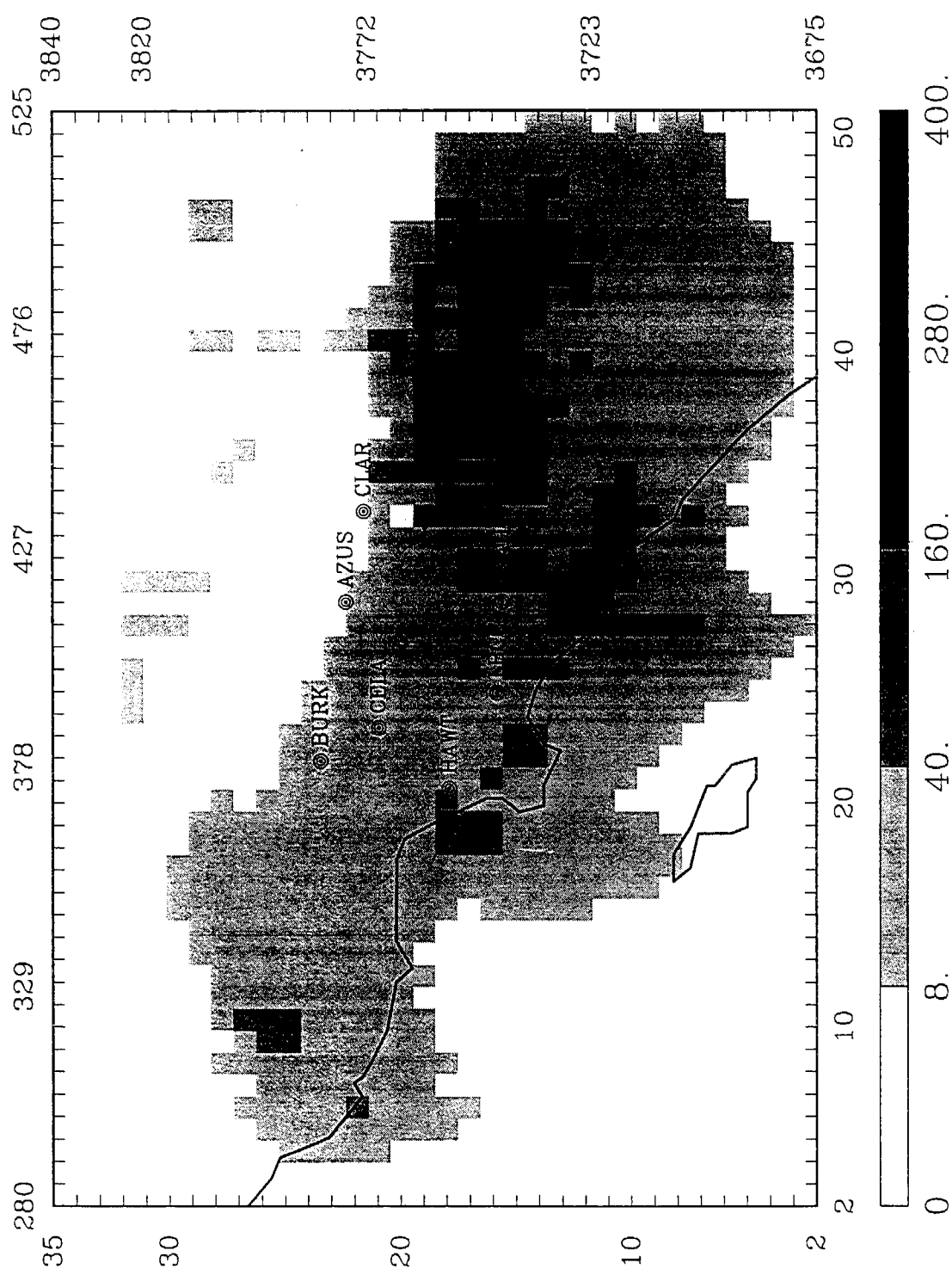


Figure 6-24. Predicted 24-hr average NH₃ concentration on December 10, 1987.

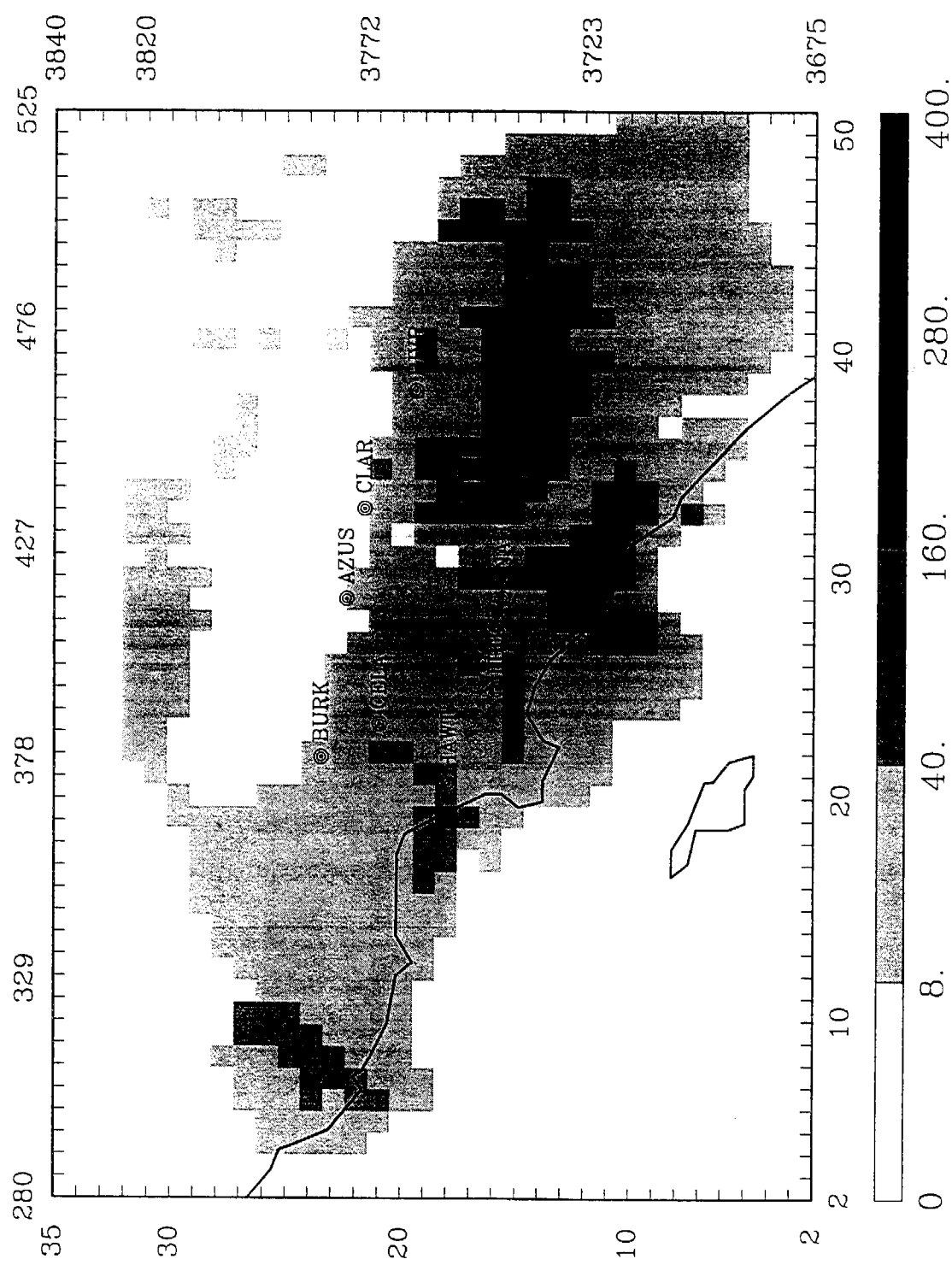


Figure 6-25. Predicted 24-hr average NH₃ concentration on December 11, 1987.

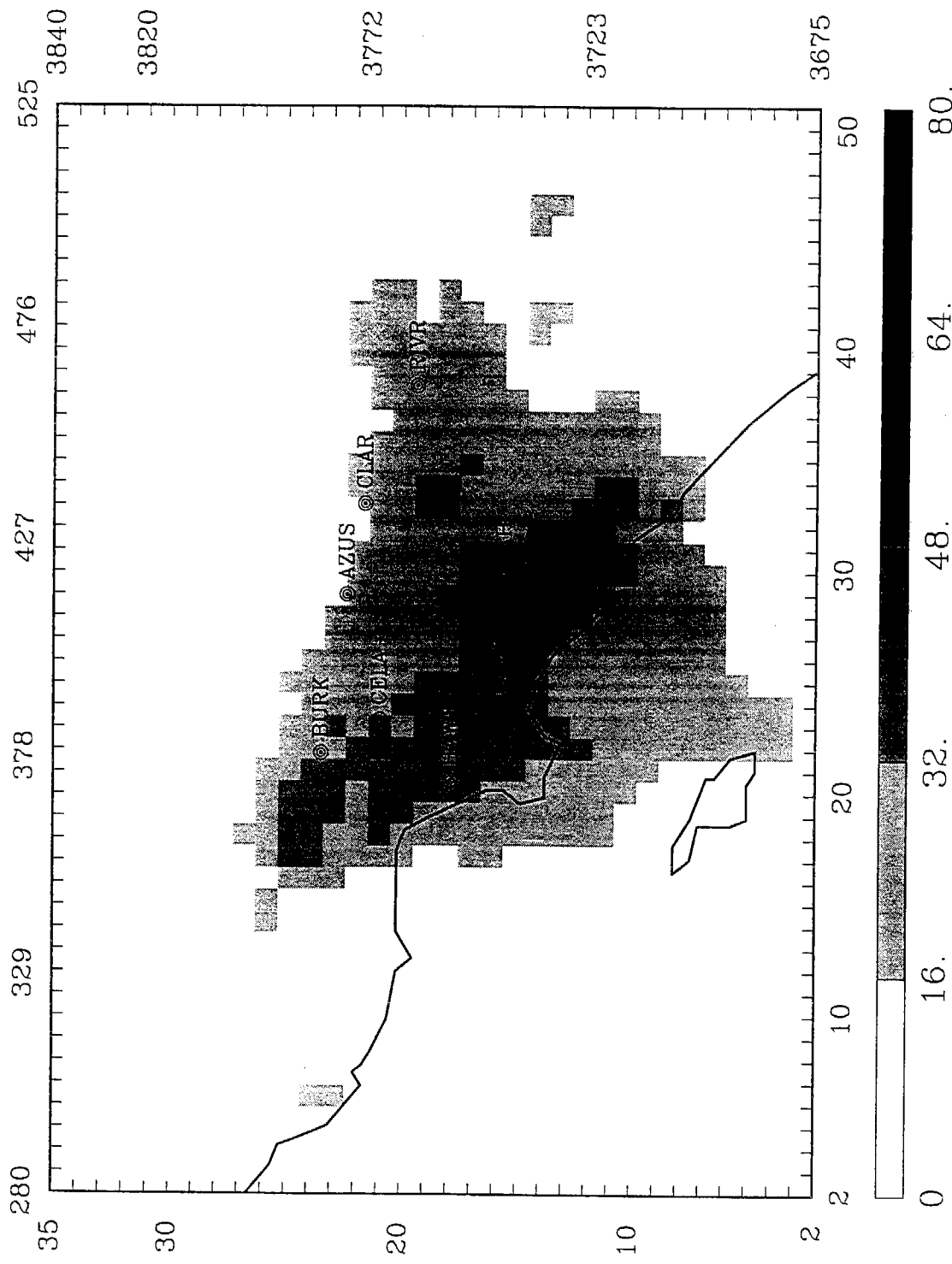


Figure 6-26 Predicted 24-hr average PM_{10} OM concentration on December 10, 1987.

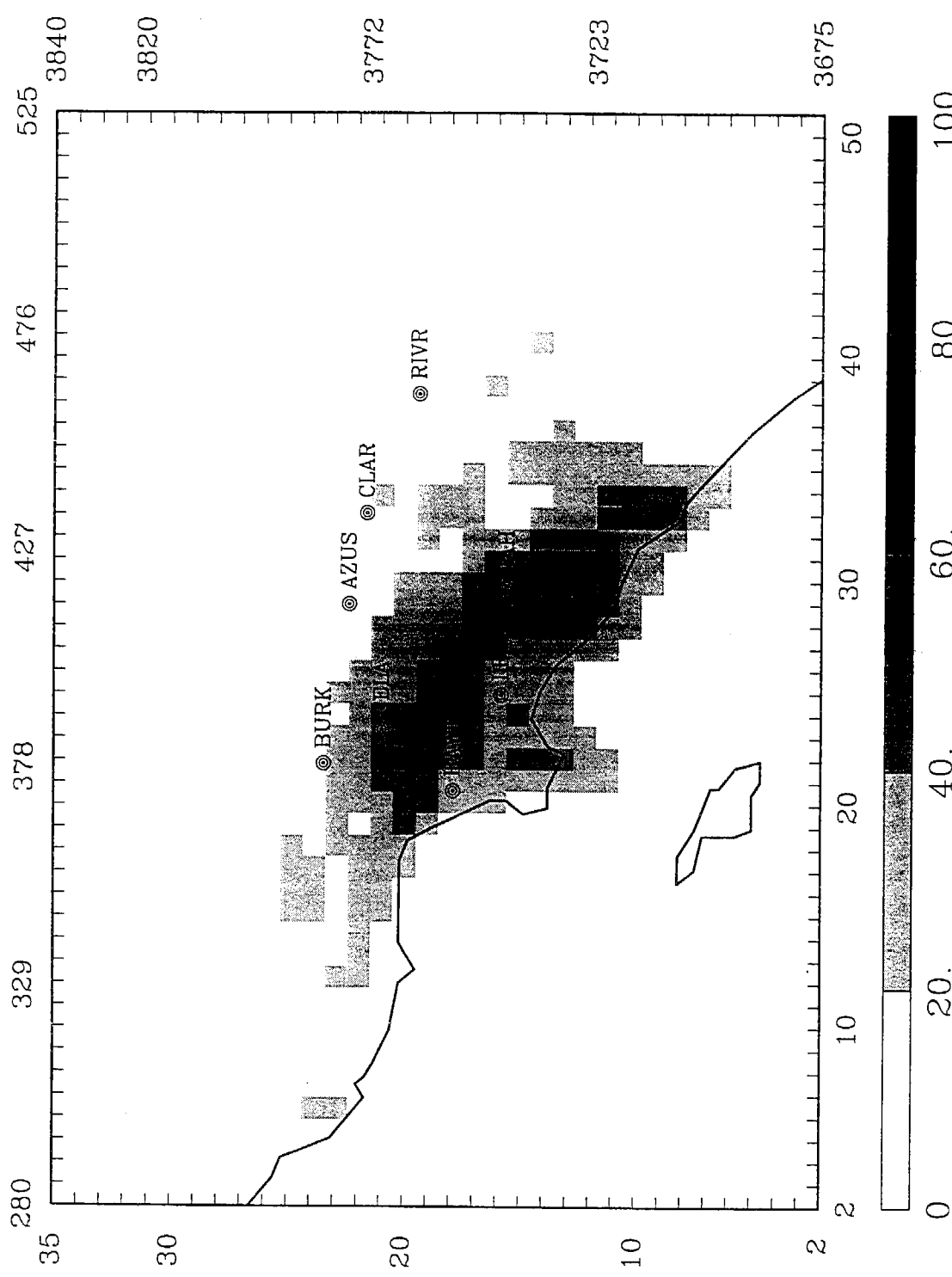


Figure 6-27. Predicted 24-hr average PM_{10} OM concentration on December 11, 1987.

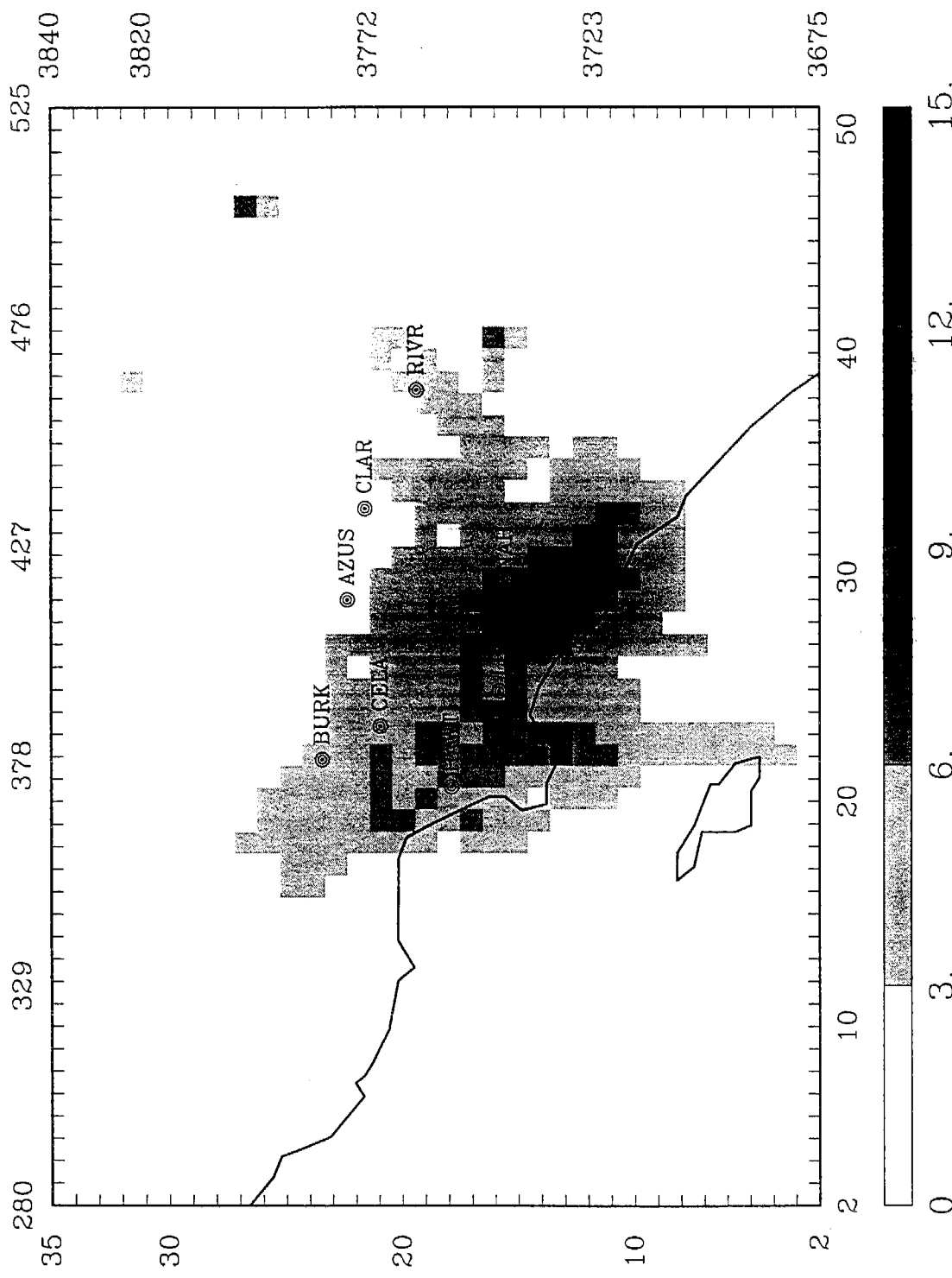


Figure 6-28. Predicted 24-hr average PM_{10} EC concentration on December 10, 1987.

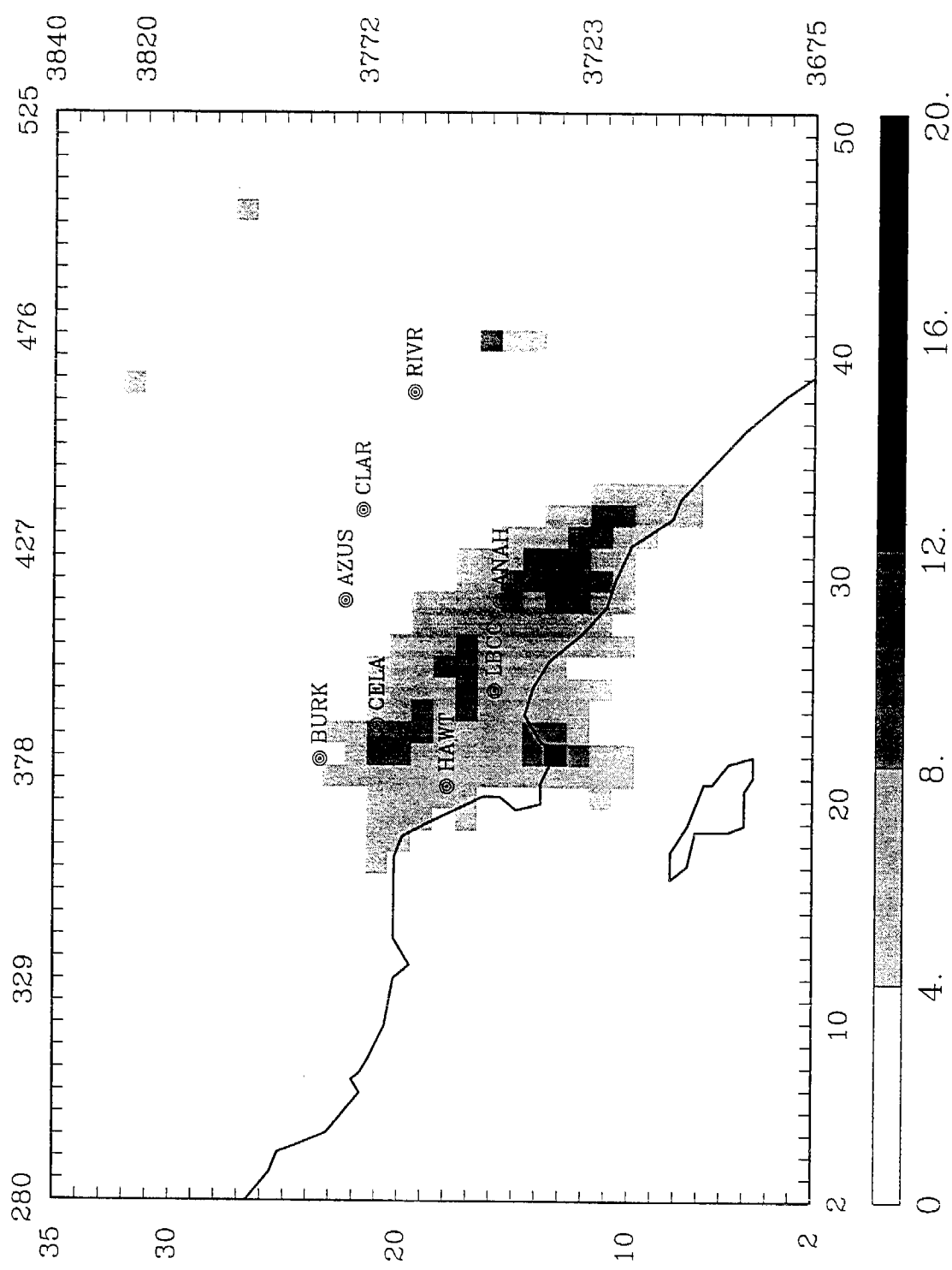


Figure 6-29. Predicted 24-hr average PM_{10} EC concentration on December 11, 1987.

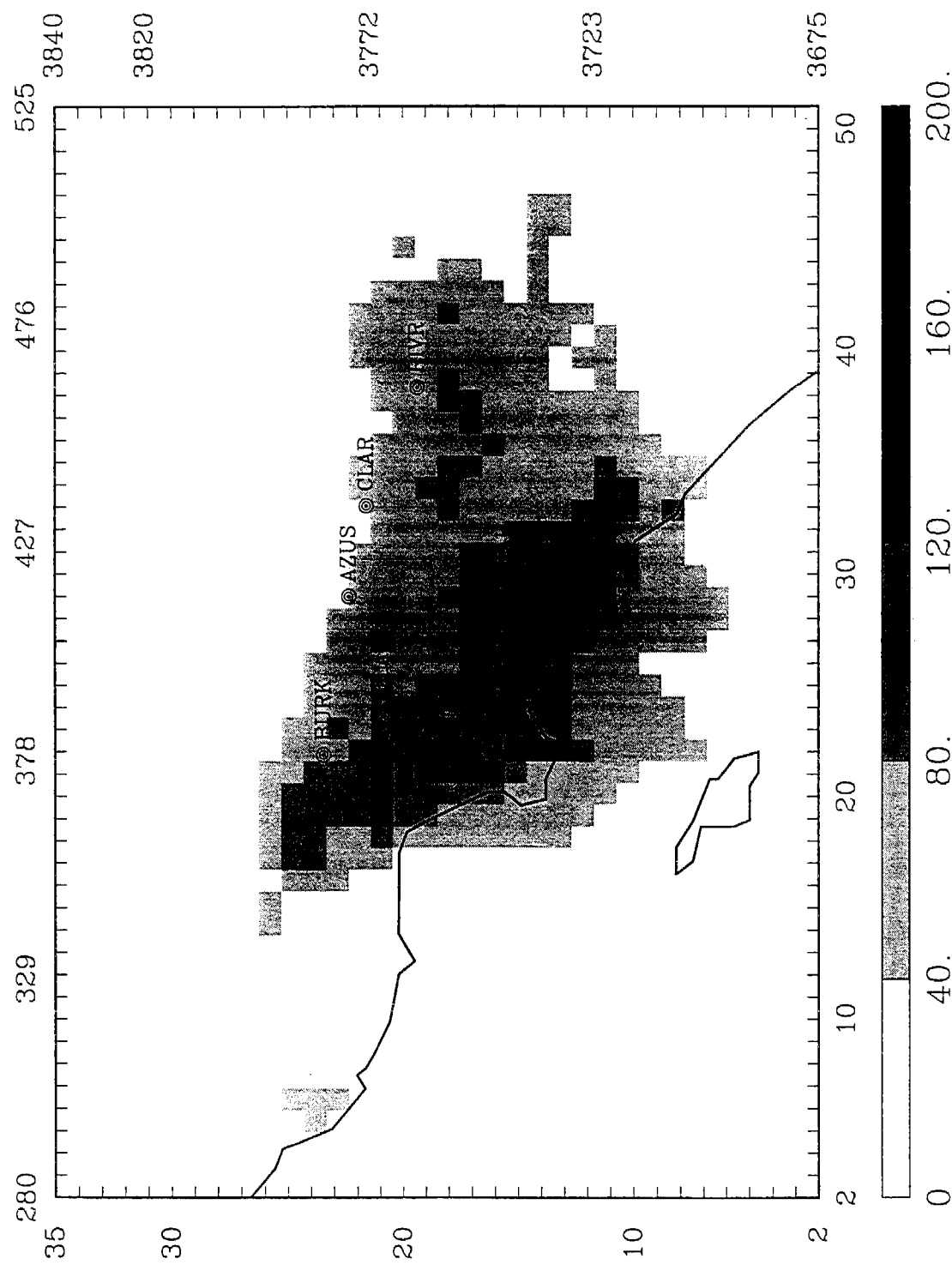


Figure 6-30. Predicted 24-hr average crustal PM₁₀ concentration on December 10, 1987.

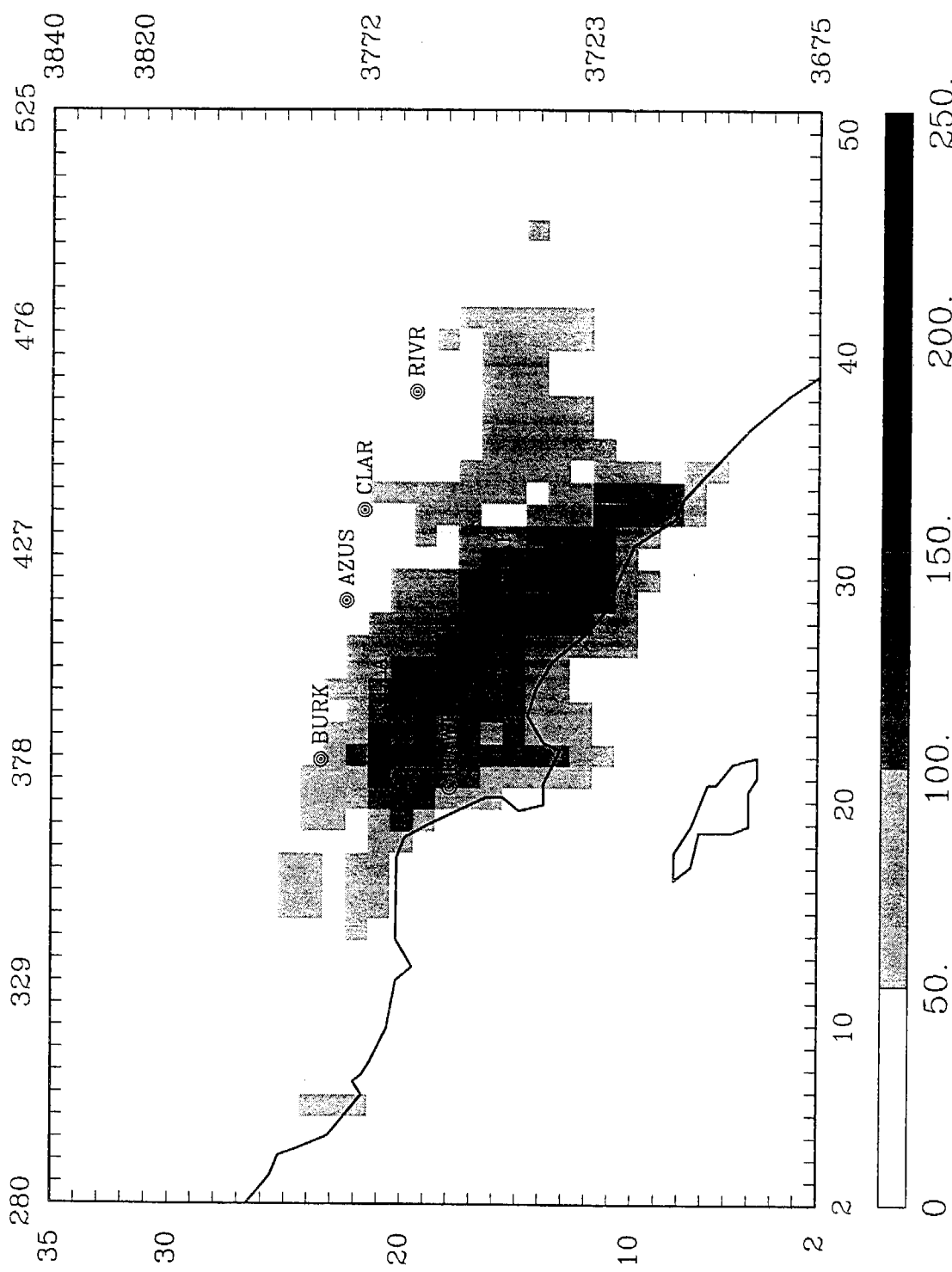


Figure 6-31. Predicted 24-hr average crustal PM₁₀ concentration on December 11, 1987.

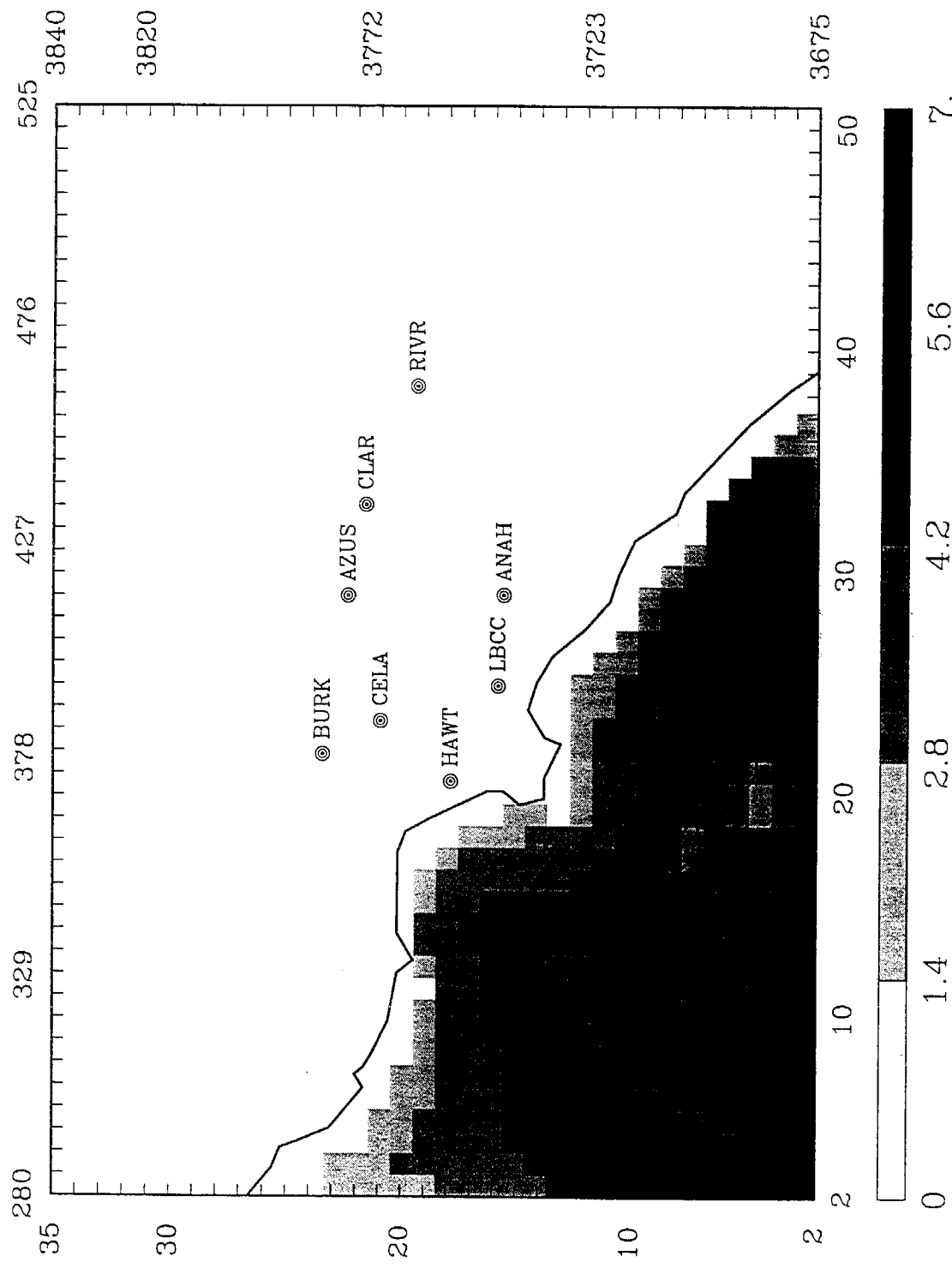


Figure 6-32. Predicted 24-hr average PM_{10} Na concentration on December 10, 1987.

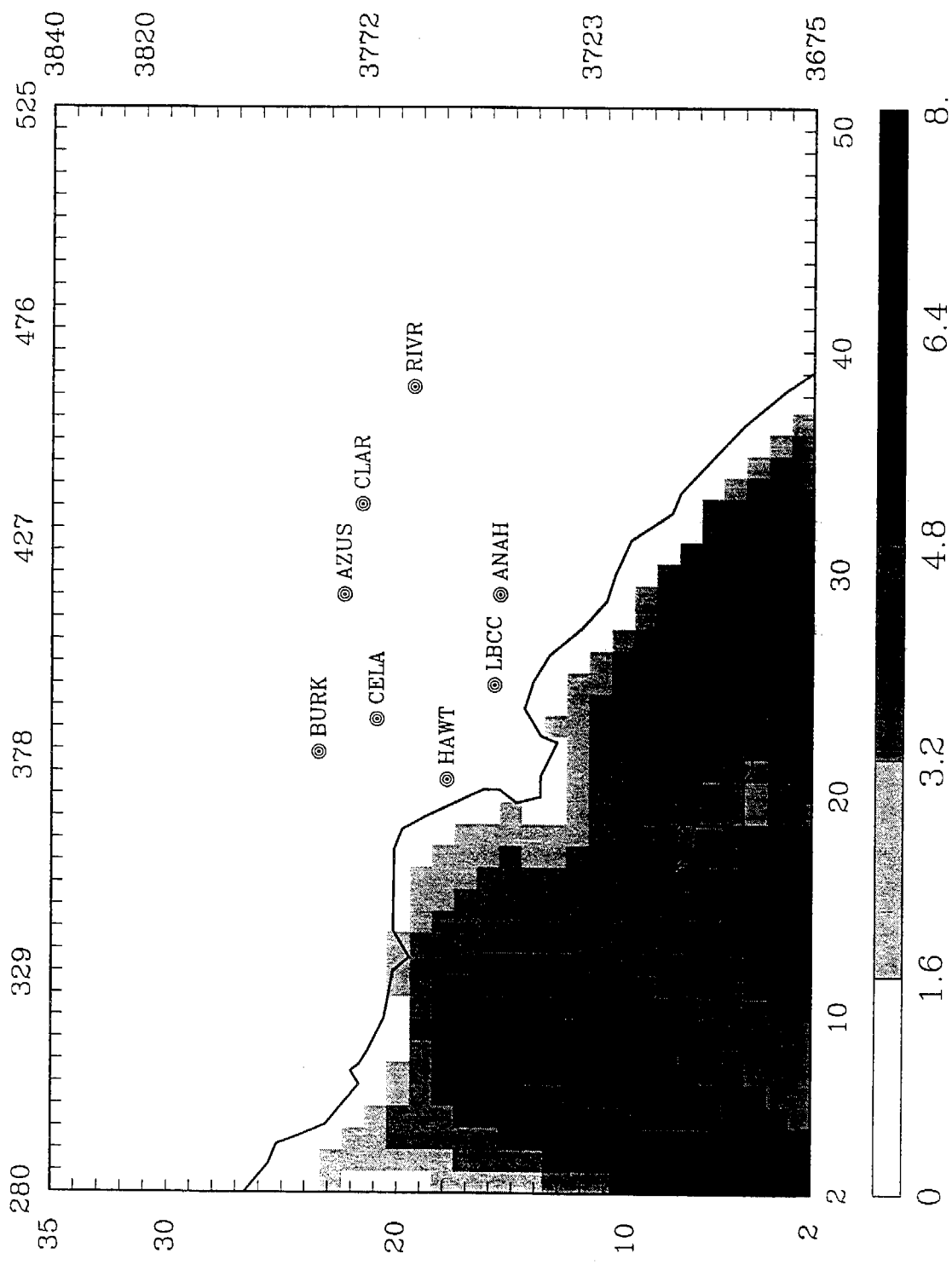
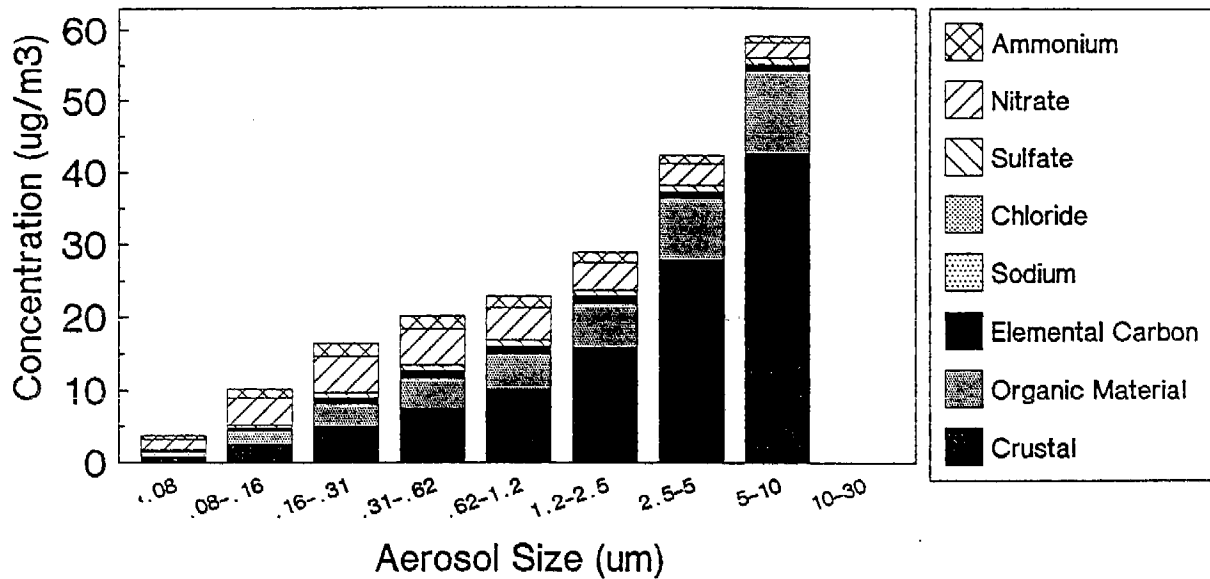


Figure 6-33. Predicted 24-hr average PM_{10} Na concentration on December 11, 1987.

Long Beach December 10, 1987



Long Beach December 11, 1987

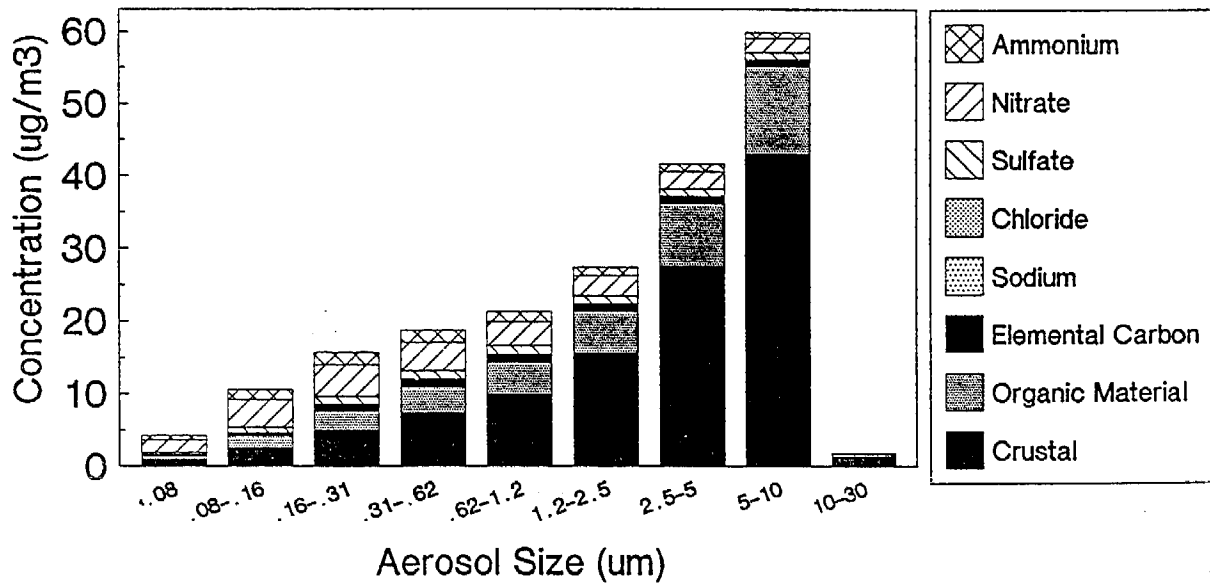
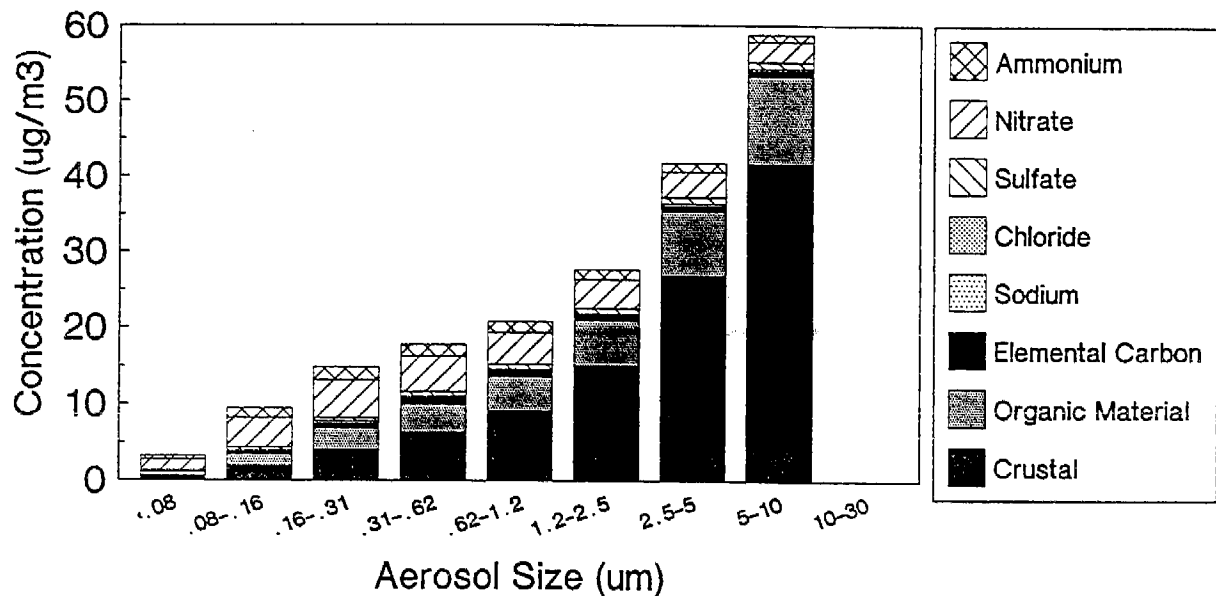


Figure 6-34. Predicted aerosol-size distribution at Long Beach on December 10-11, 1987.

Hawthorne December 10, 1987



Hawthorne December 11, 1987

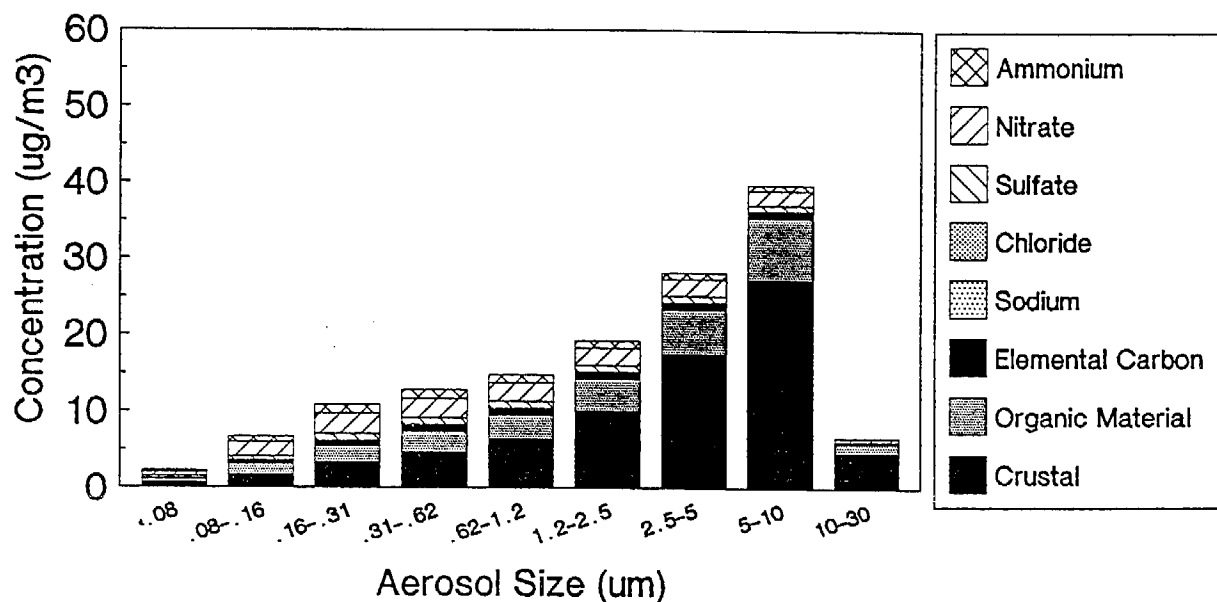
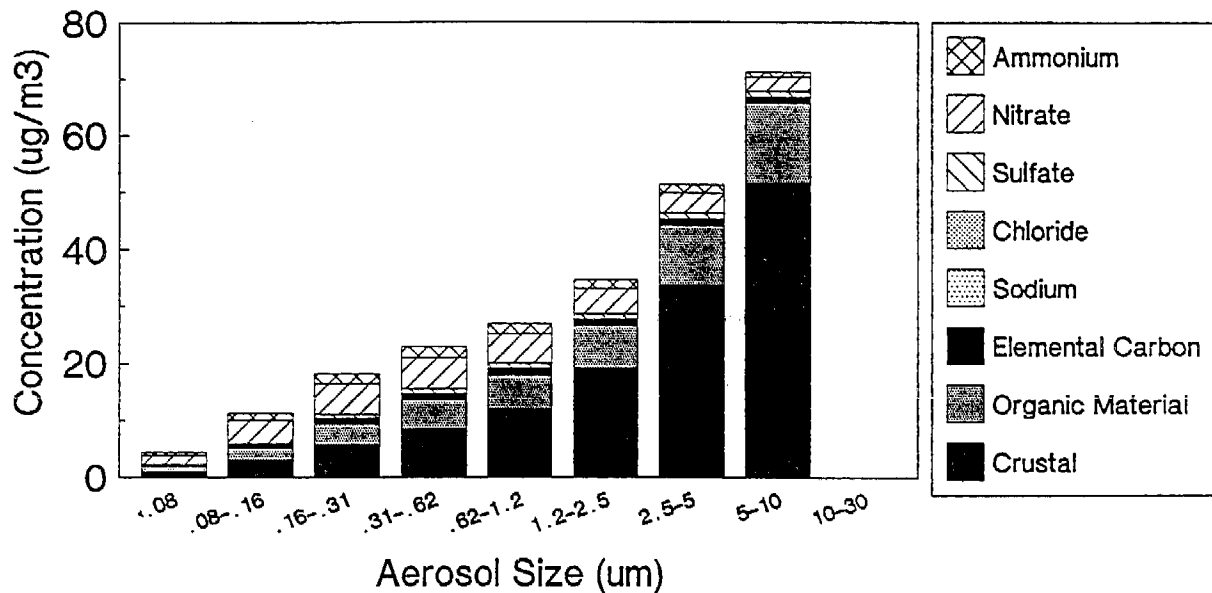


Figure 6-35. Predicted aerosol-size distribution at Hawthorne on December 10-11, 1987.

Anaheim December 10, 1987



Anaheim December 11, 1987

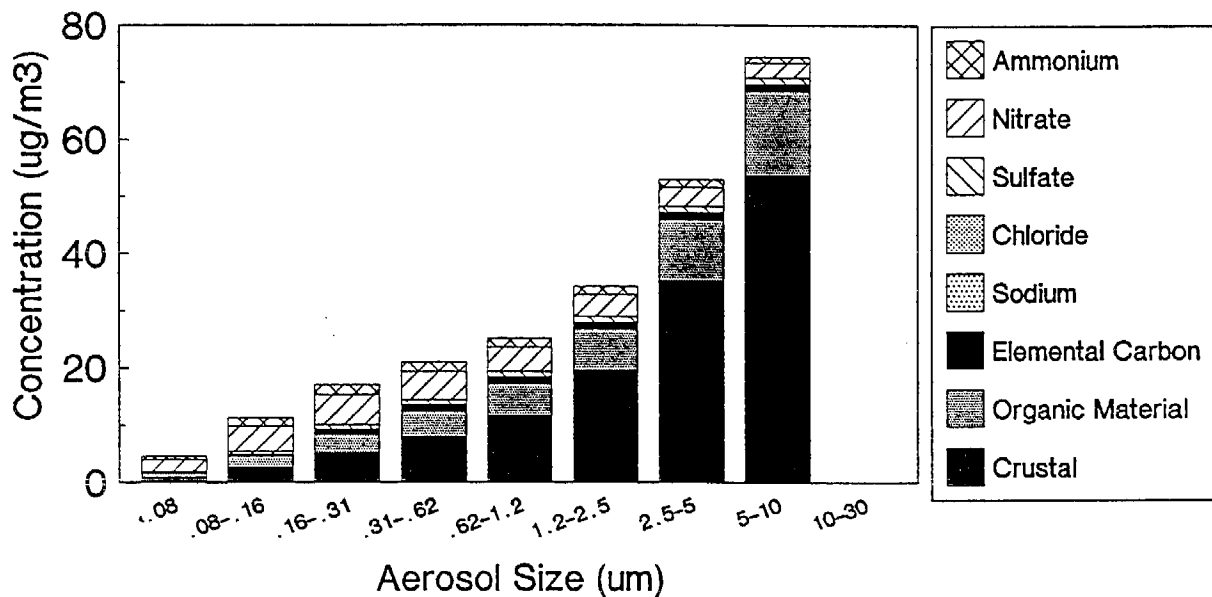


Figure 6-36. Predicted aerosol-size distribution at Anaheim on December 10-11, 1987.

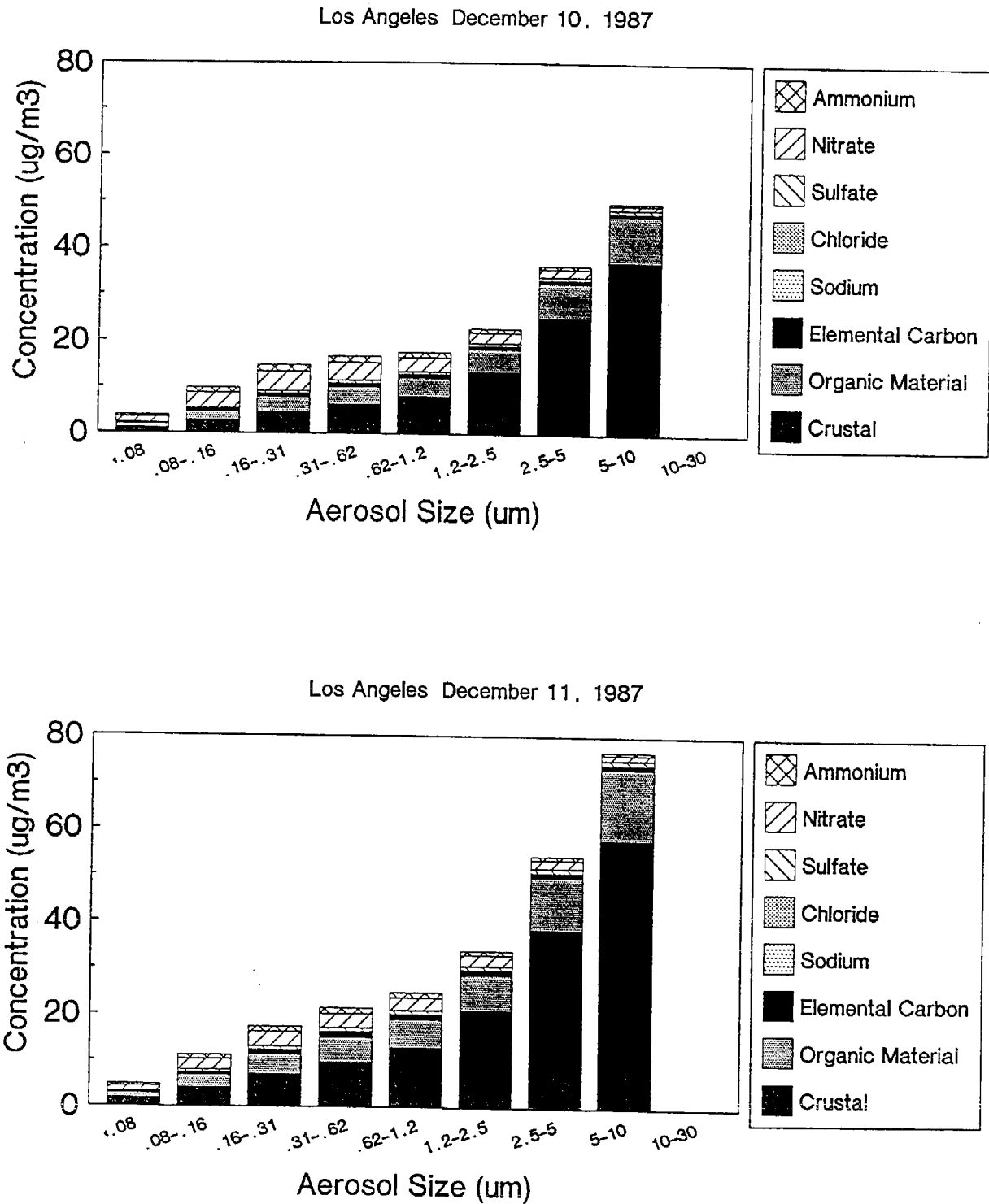
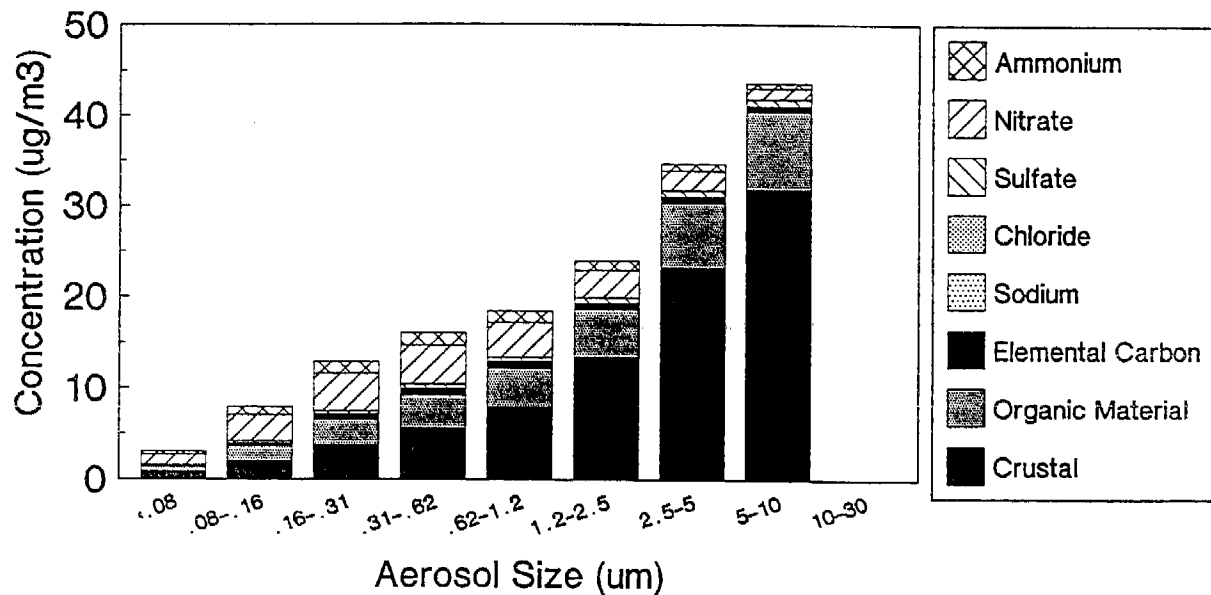


Figure 6-37. Predicted aerosol-size distribution at Los Angeles on December 10-11, 1987.

Burbank December 10, 1987



Burbank December 11, 1987

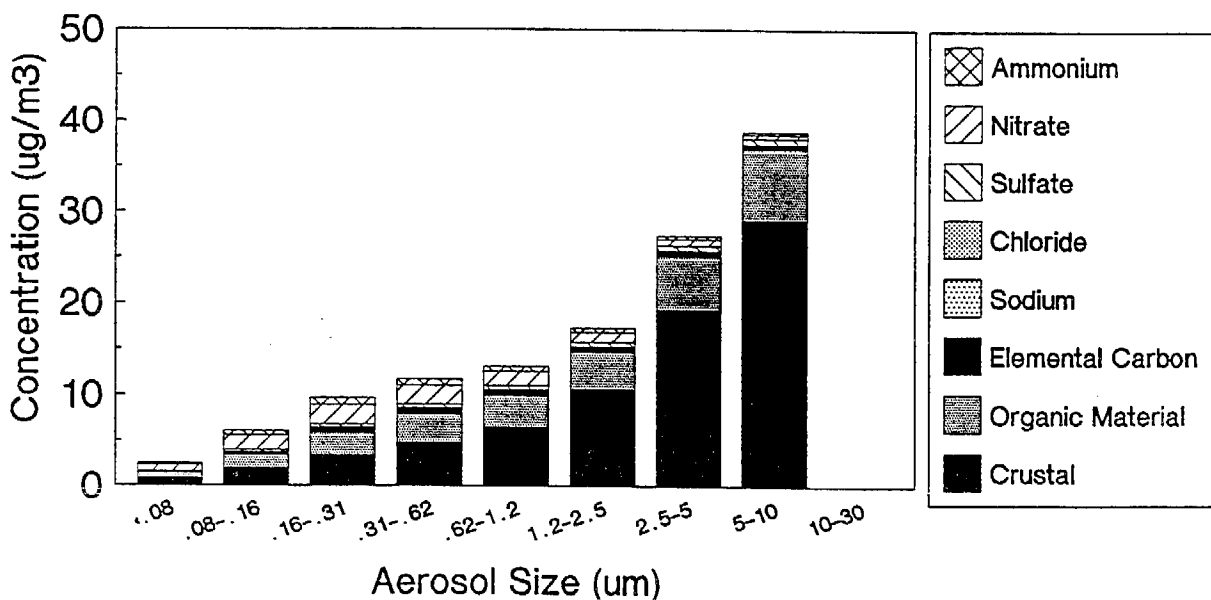
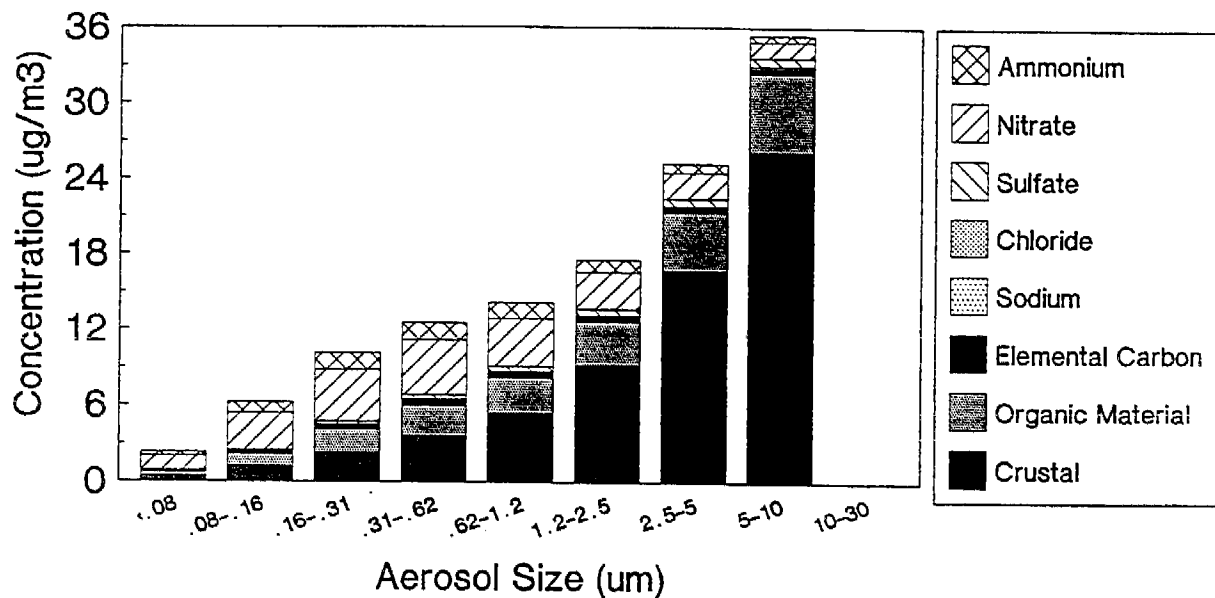


Figure 6-38. Predicted aerosol-size distribution at Burbank on December 10-11, 1987.

Riverside December 10, 1987



Riverside December 11, 1987

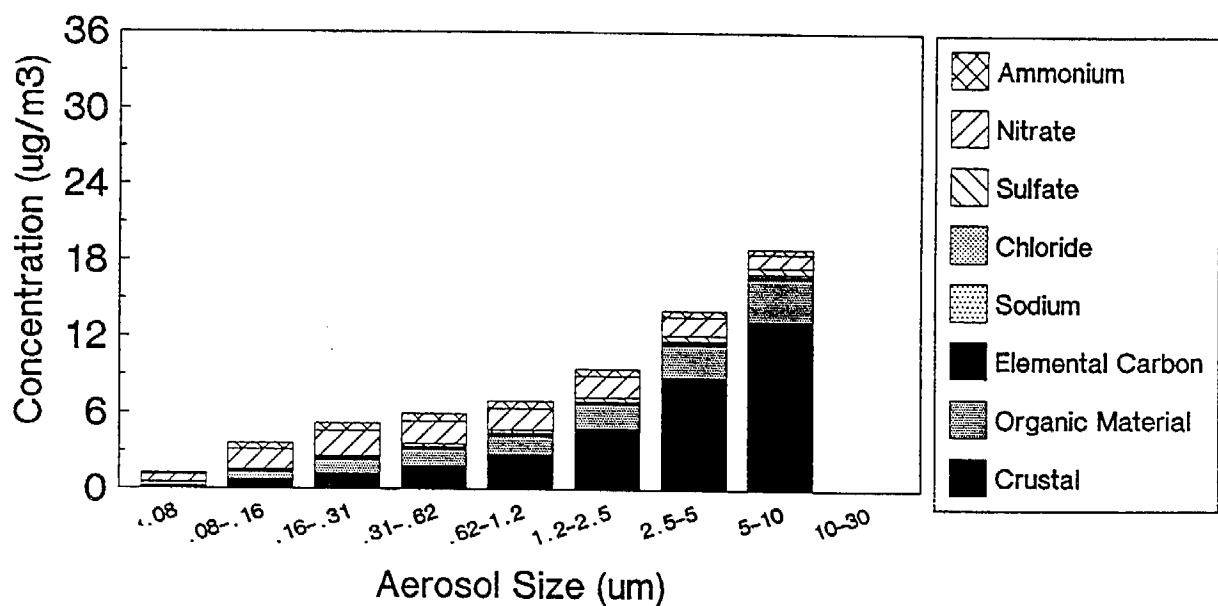


Figure 6-39. Predicted aerosol-size distribution at Riverside on December 10-11, 1987.

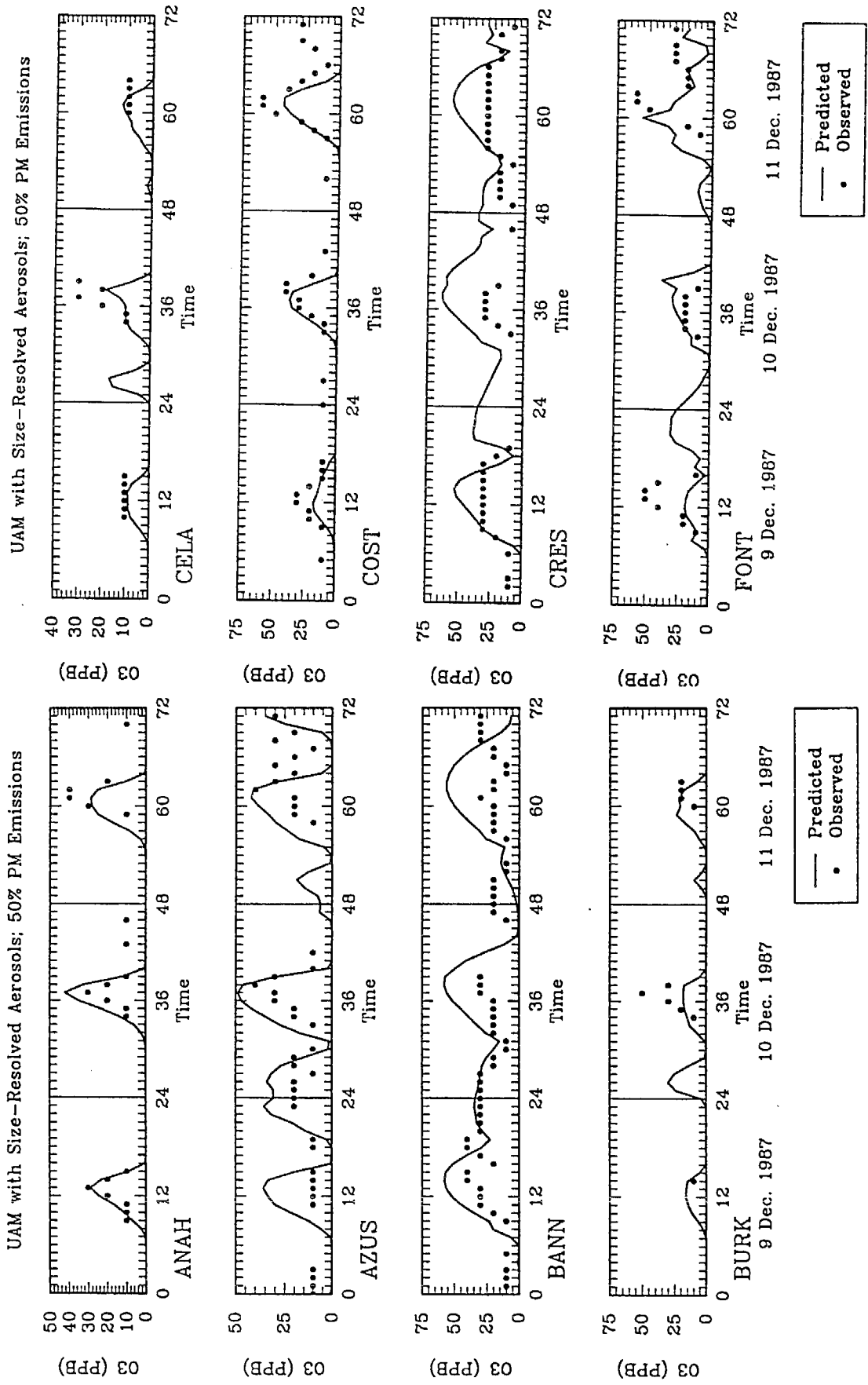


Figure 6-40. Predicted (—) and observed (•) 1-hr ozone concentrations on December 9-11, 1987.

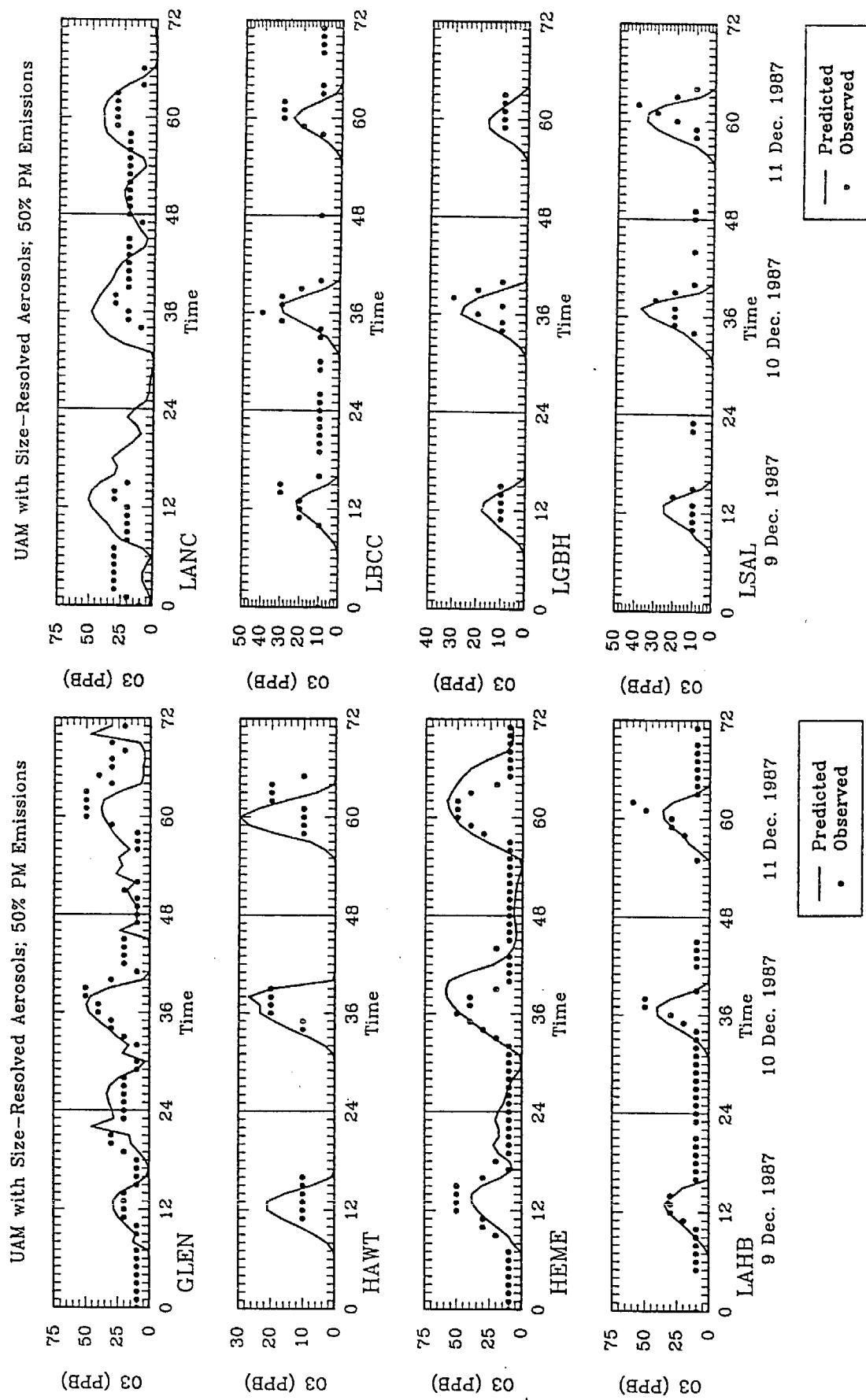


Figure 6-40. Predicted (—) and observed (•) 1-hr ozone concentrations on December 9-11, 1987.

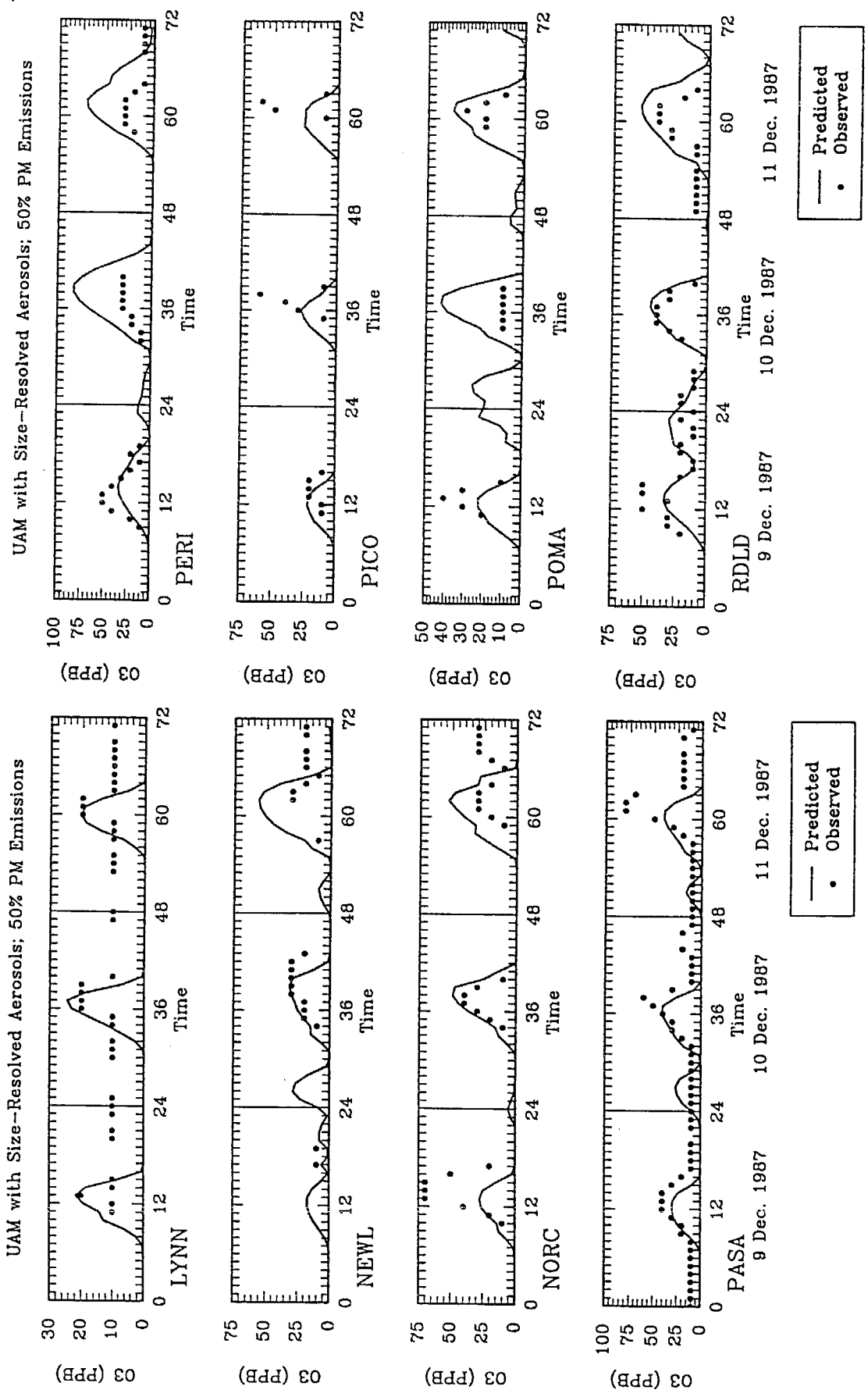


Figure 6-40. Predicted (—) and observed (•) 1-hr ozone concentrations on December 9-11, 1987.

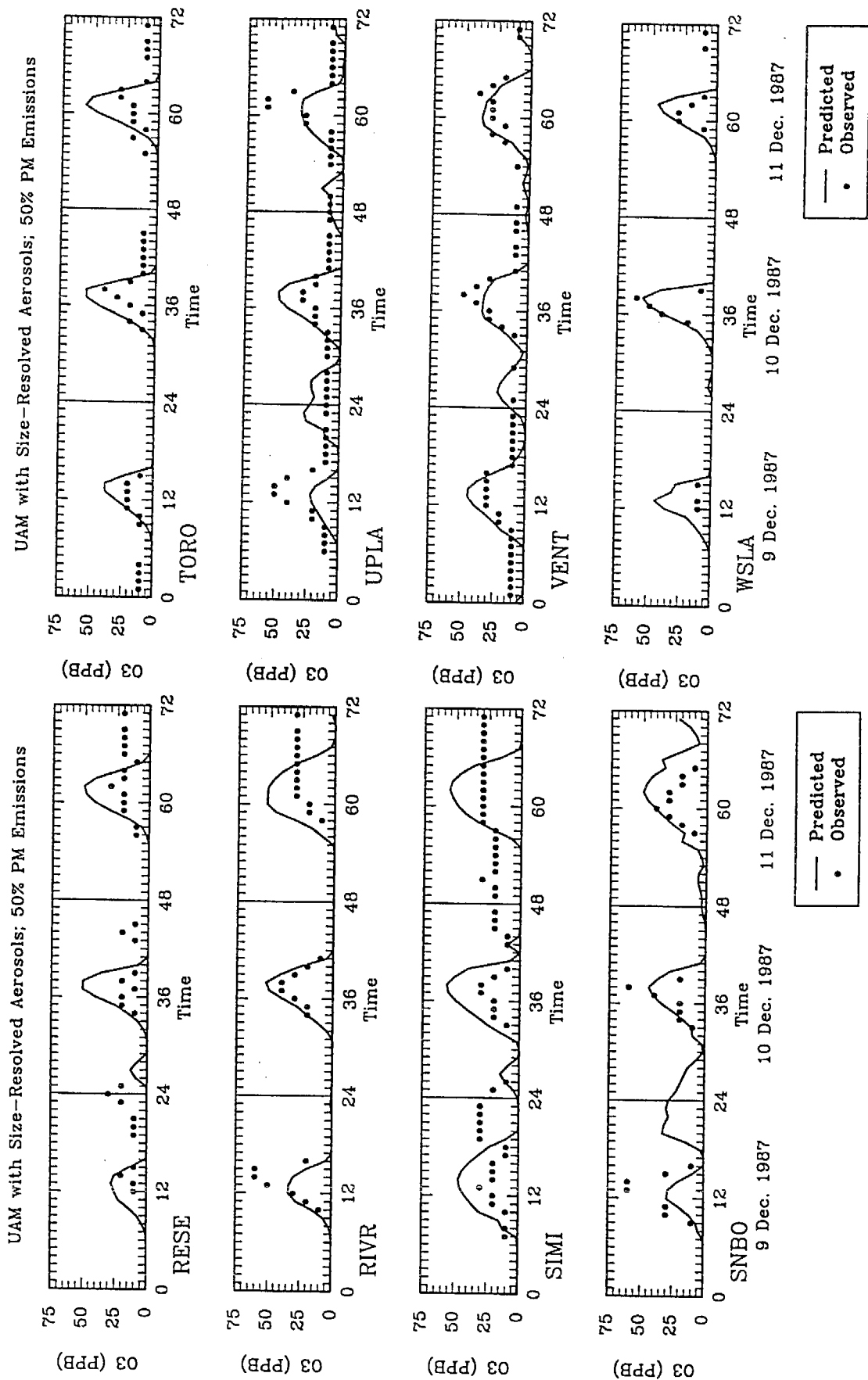


Figure 6-40. Predicted (—) and observed (•) 1-hr ozone concentrations on December 9-11, 1987.

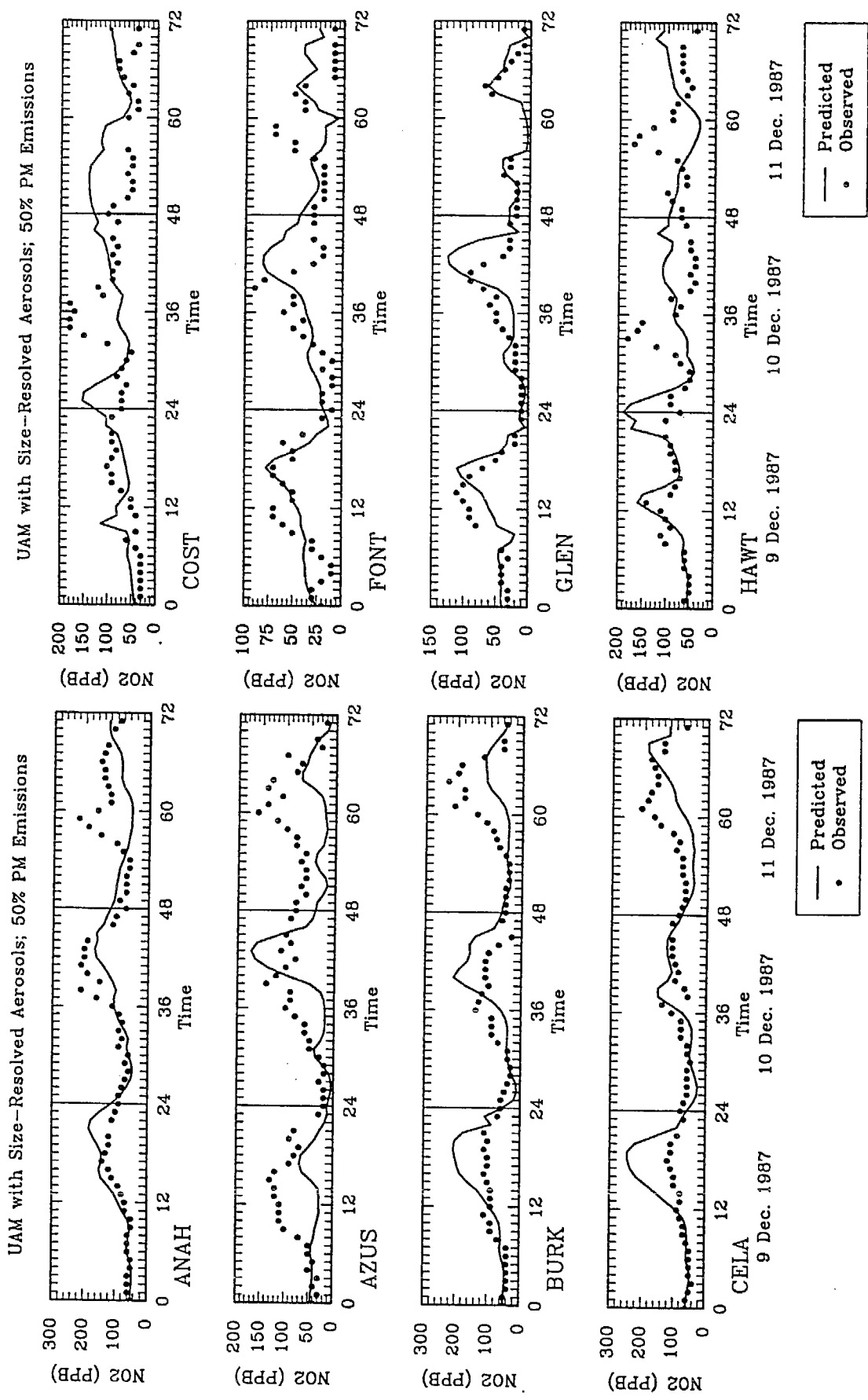


Figure 6-41. Predicted (—) and observed (•) 1-hr nitrogen dioxide concentrations on December 9-11, 1987.
Page 1 of 3

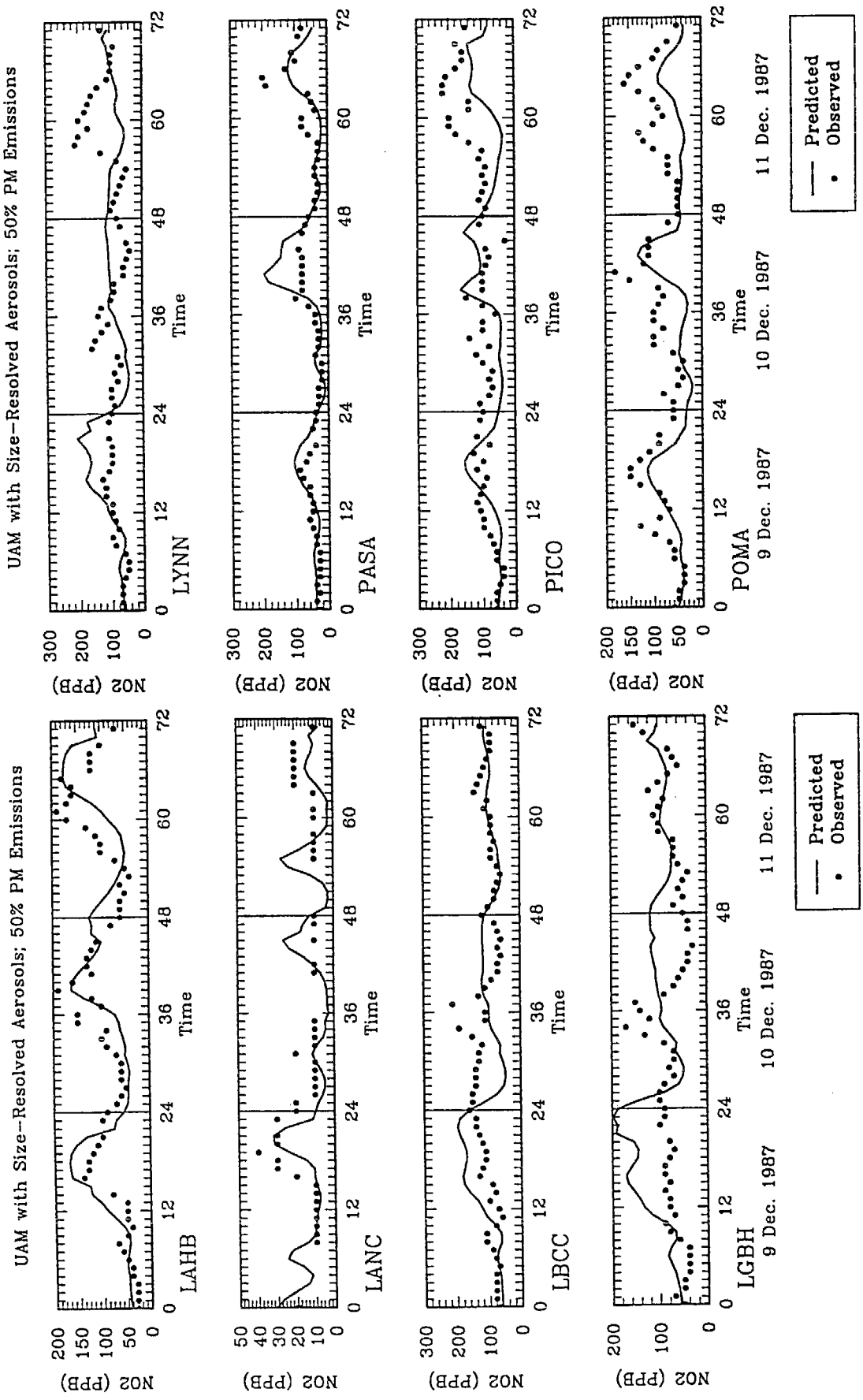


Figure 6-41. Predicted (—) and observed (•) 1-hr nitrogen dioxide concentrations on December 9-11, 1987.

Page 2 of 3

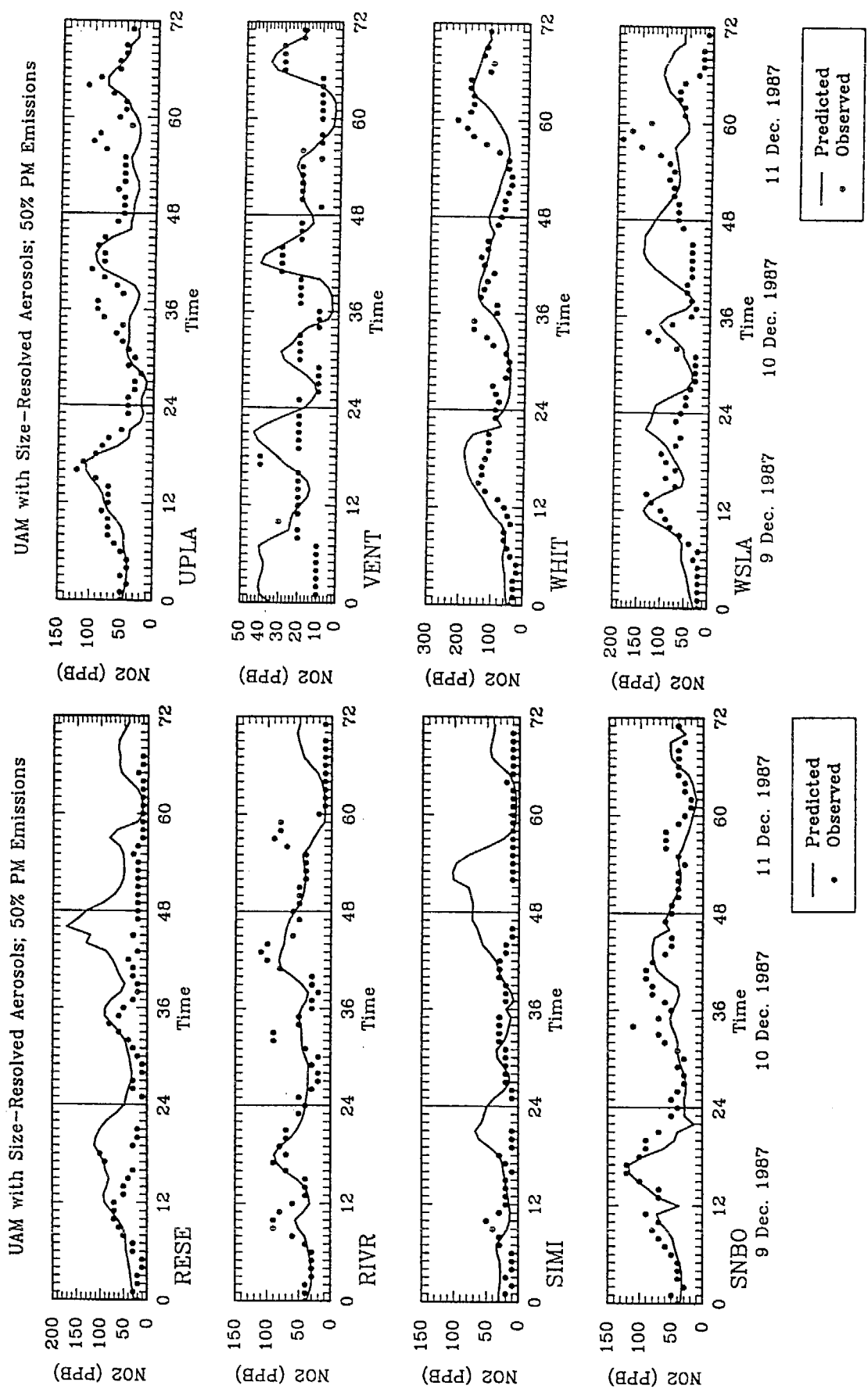
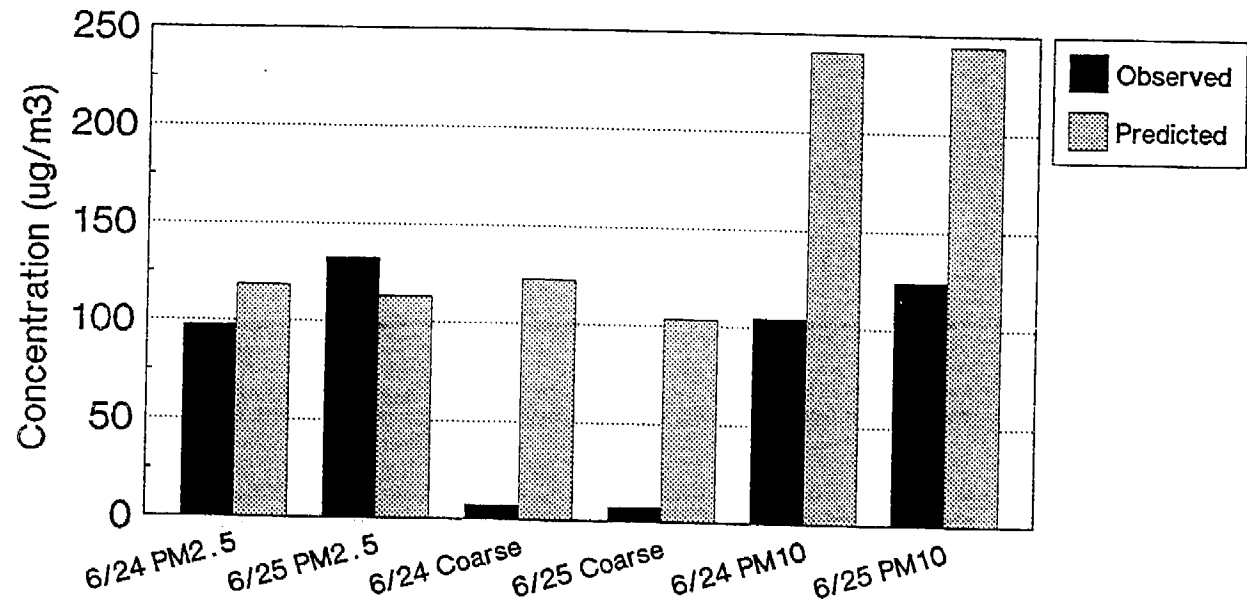


Figure 6-41. Predicted (—) and observed (•) 1-hr nitrogen dioxide concentrations on December 9-11, 1987.
Page 3 of 3

Maximum PM Mass
 24-hr Average at the Highest SCAQS Station
 December 10-11, 1987



Average PM Mass
 24-hr Average - Mean at the SCAQS Stations
 December 10-11, 1987

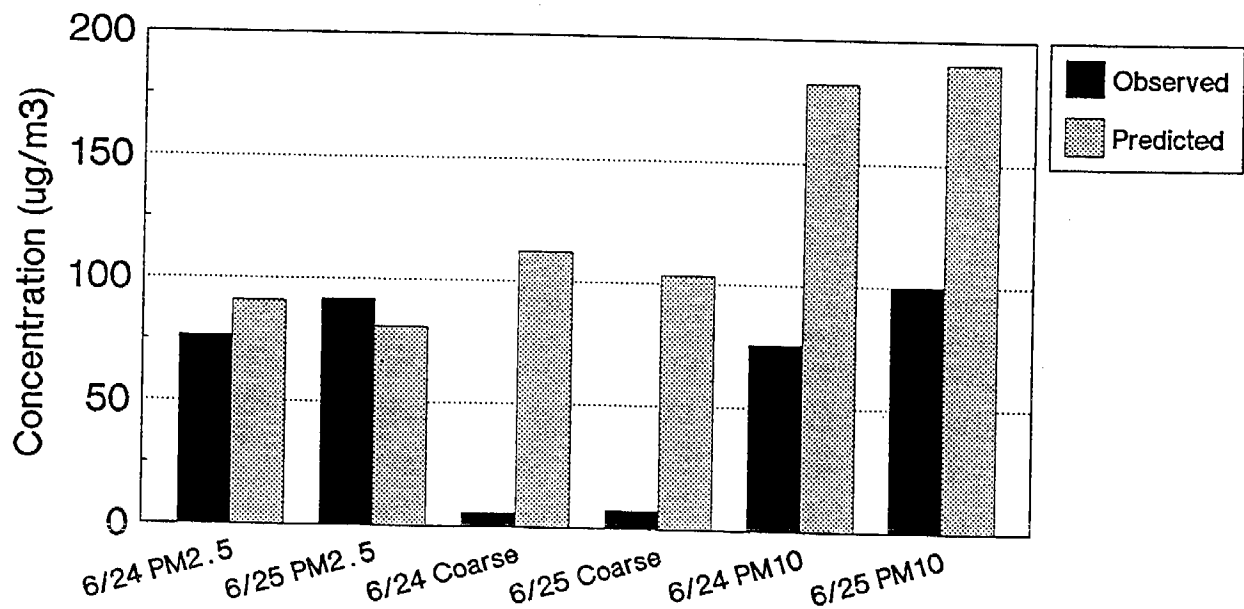
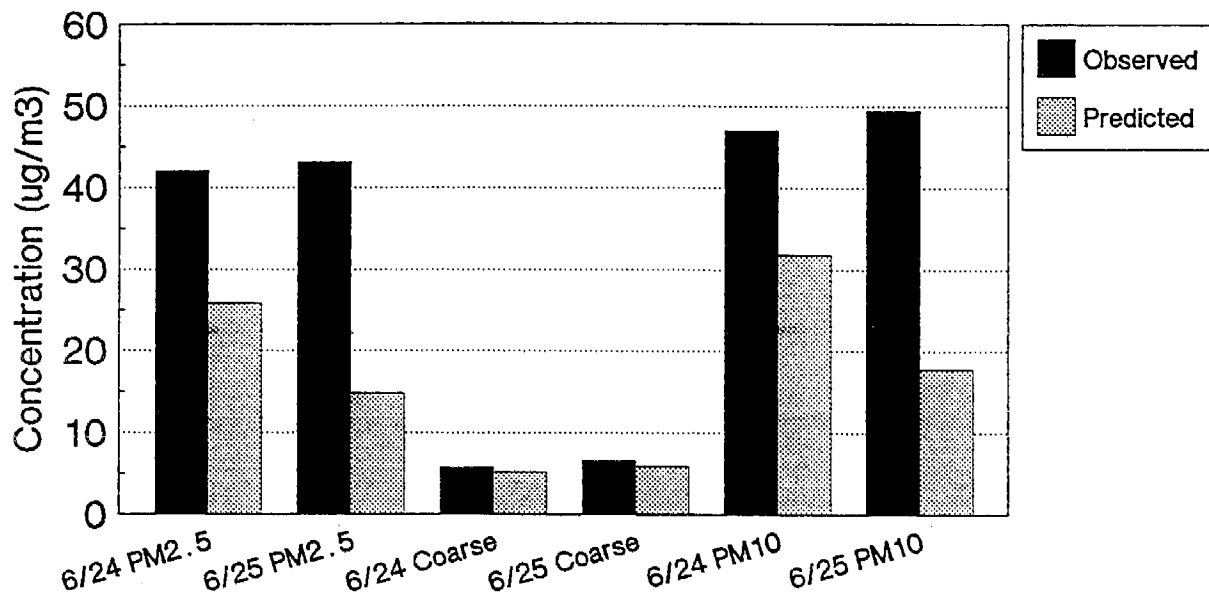


Figure 6-42. Predicted and observed mean and maximum 24-hr average PM mass on December 10-11, 1987.

Maximum Nitrate
 24-hr Average at the Highest SCAQS Station
 December 10-11, 1987



Average Nitrate
 24-hr Average - Mean at the SCAQS Stations
 December 10-11, 1987

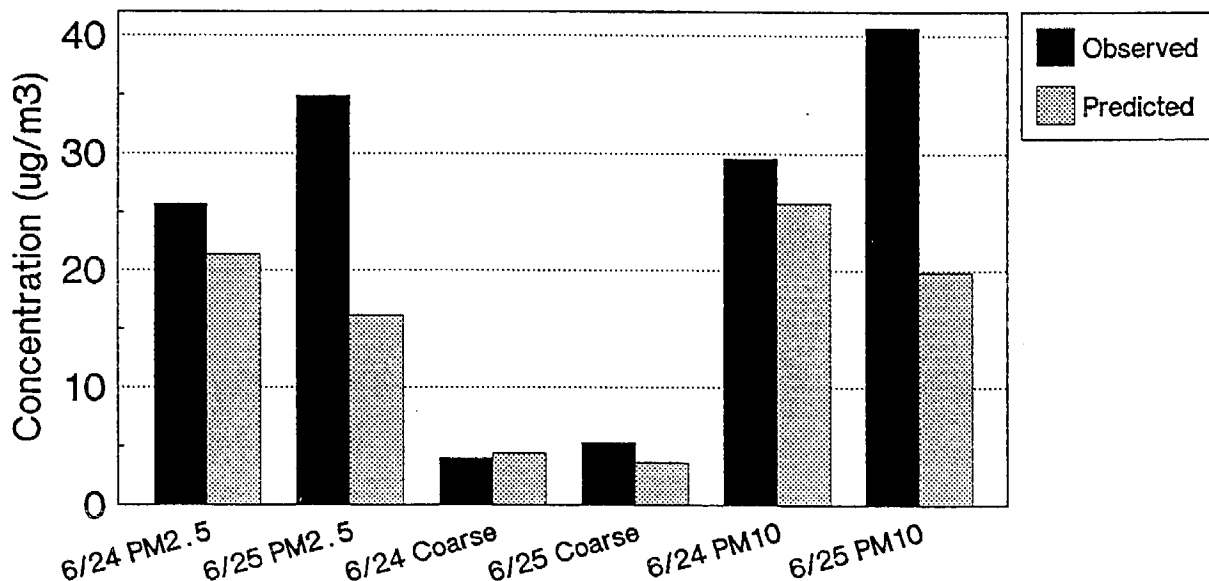
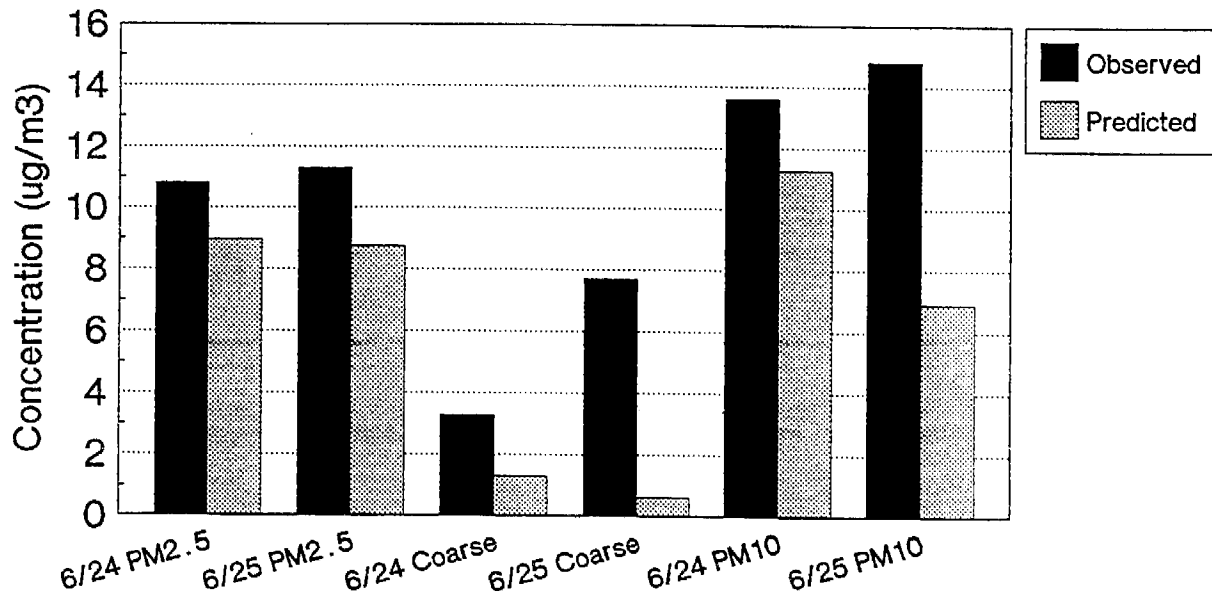


Figure 6-43. Predicted and observed mean and maximum 24-hr average nitrate on December 10-11, 1987.

Maximum Ammonium
 24-hr Average at the Highest SCAQS Station
 December 10-11, 1987



Average Ammonium
 24-hr Average – Mean at the SCAQS Stations
 December 10-11, 1987

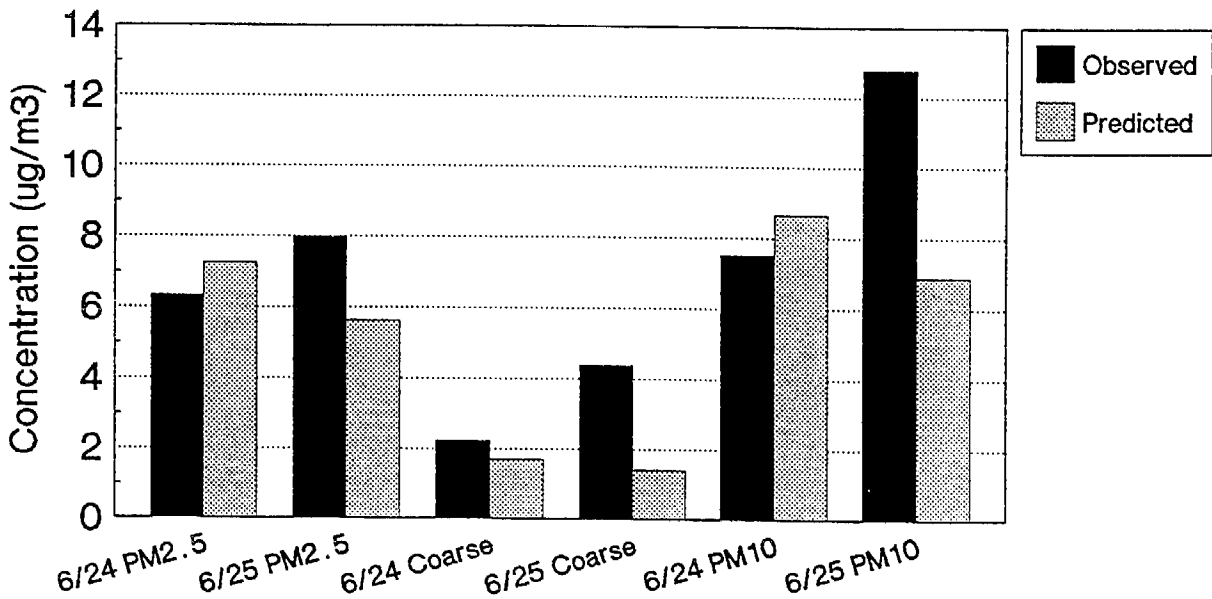
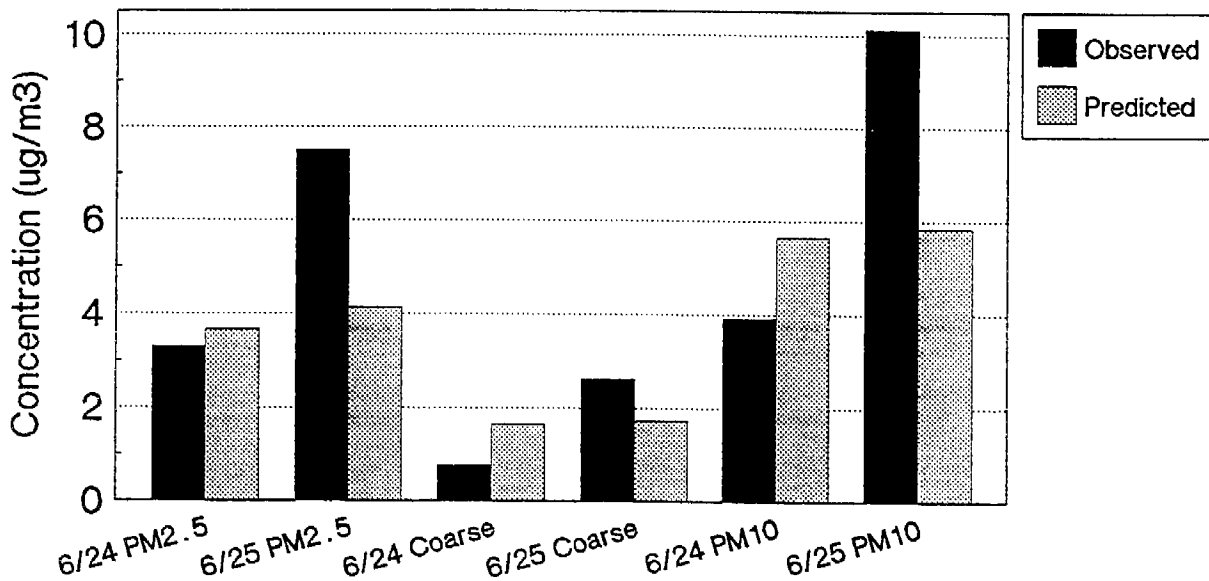


Figure 6-44. Predicted and observed mean and maximum 24-hr average ammonium on December 10-11, 1987.

Maximum Sulfate
 24-hr Average at the Highest SCAQS Station
 December 10-11, 1987



Average Sulfate
 24-hr Average – Mean at the SCAQS Stations
 December 10-11, 1987

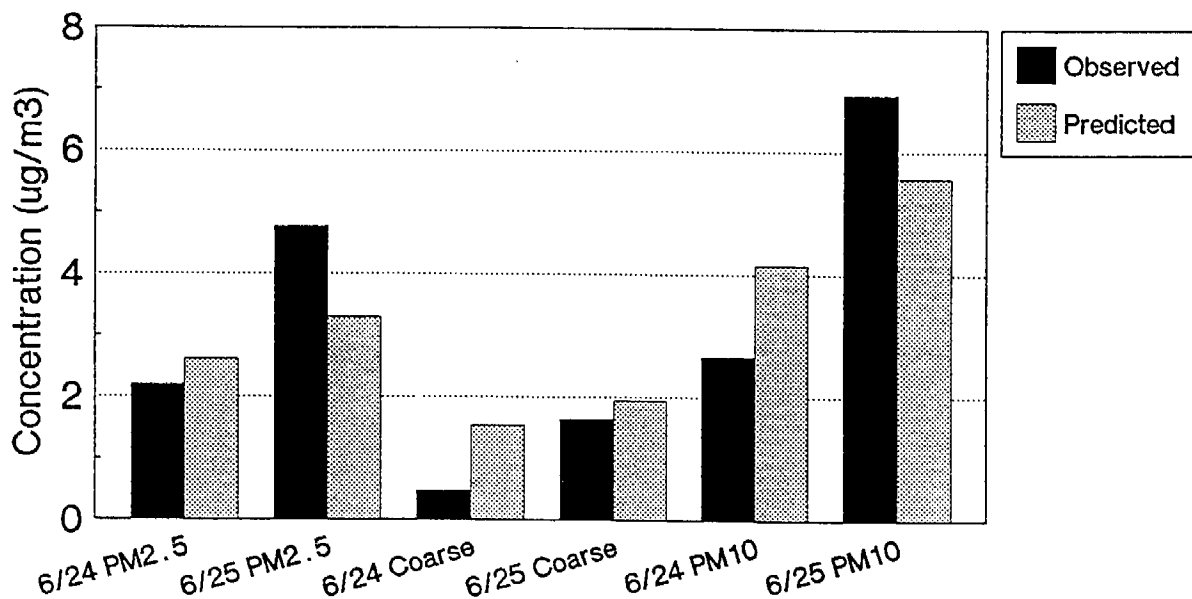
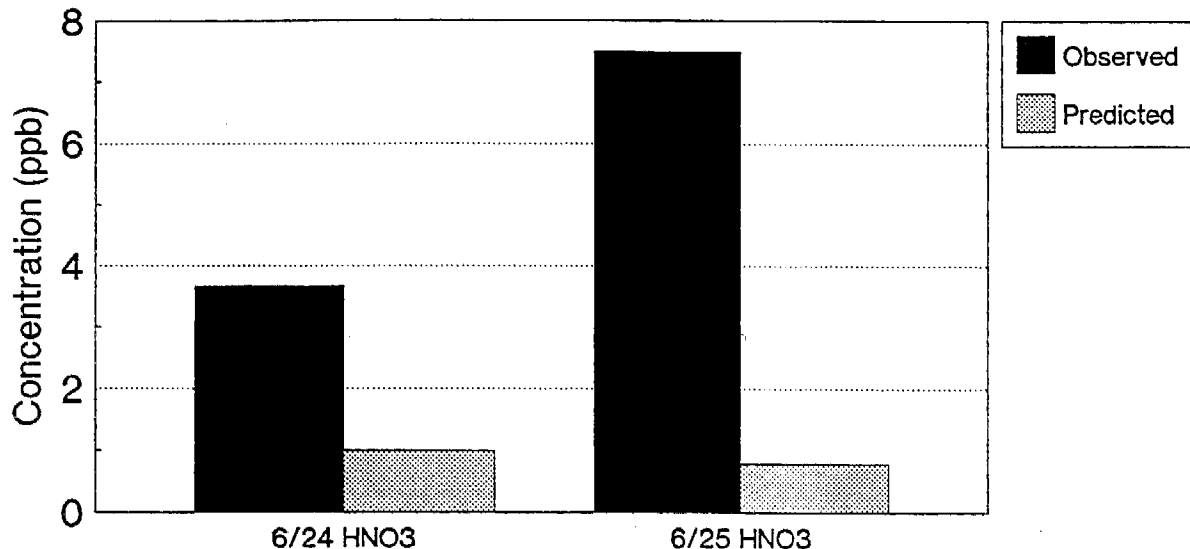


Figure 6-45. Predicted and observed mean and maximum 24-hr average sulfate on December 10-11, 1987.

Maximum Nitric Acid
24-hr Average at the Highest SCAQS Station
December 10-11, 1987



Average Nitric Acid
24-hr Average at the Highest SCAQS Station
December 10-11, 1987

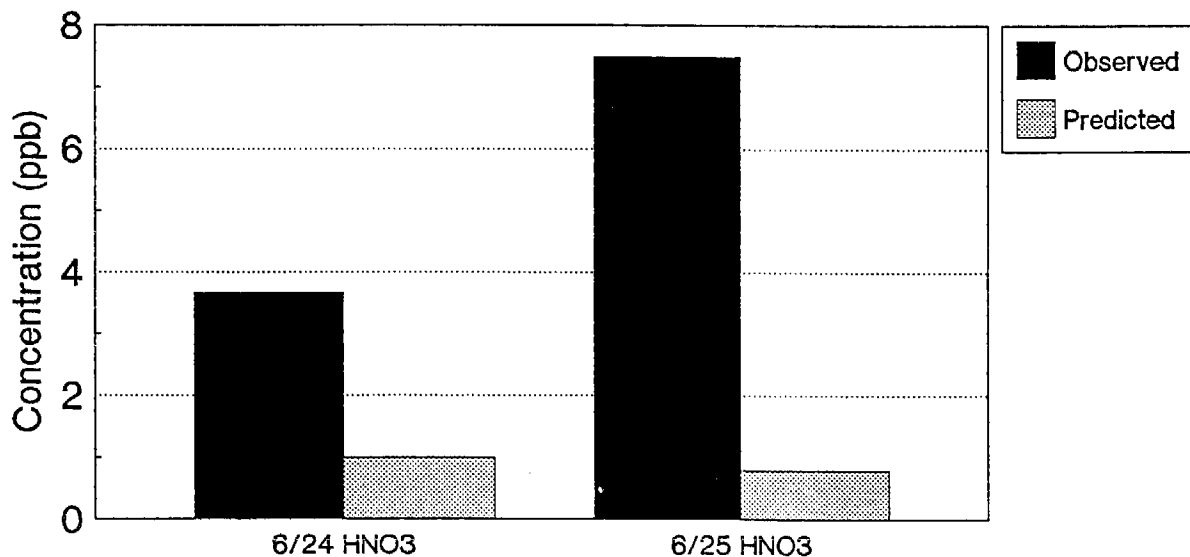
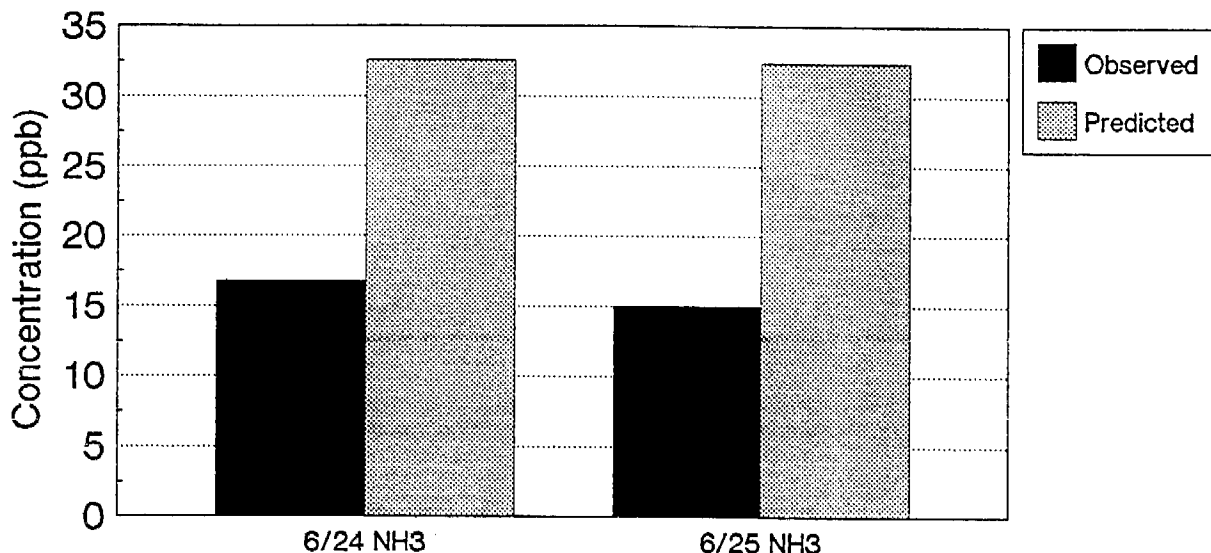


Figure 6-46. Predicted and observed mean and maximum 24-hr average nitric acid on December 10-11, 1987.

Average Ammonia
24-hr Average at the Highest SCAQS Station
December 10-11, 1987



Maximum Ammonia
24-hr Average at the Highest SCAQS Station
December 10-11, 1987

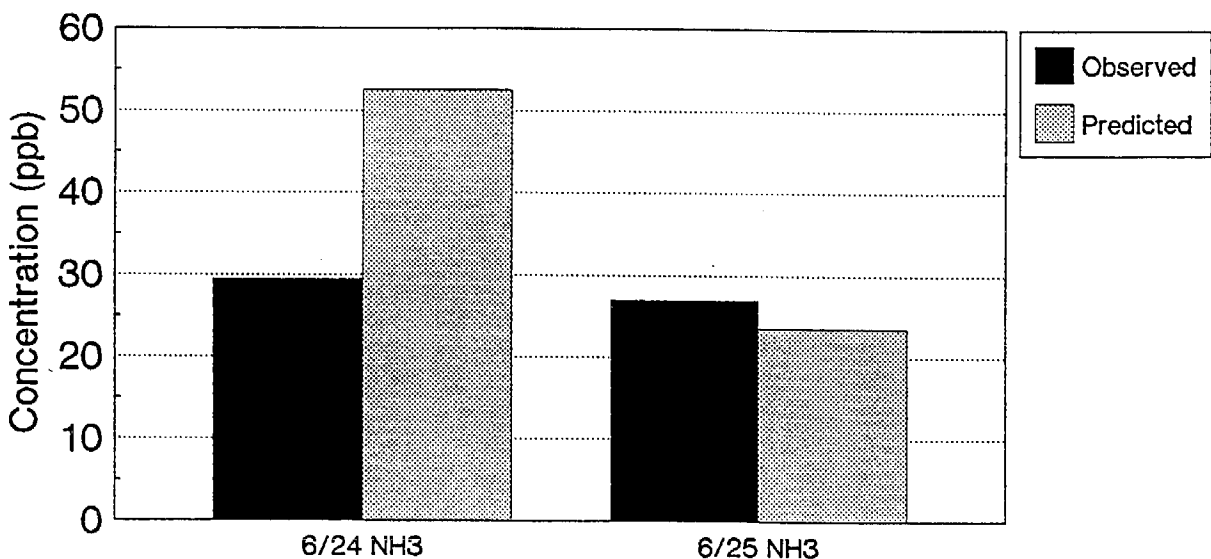
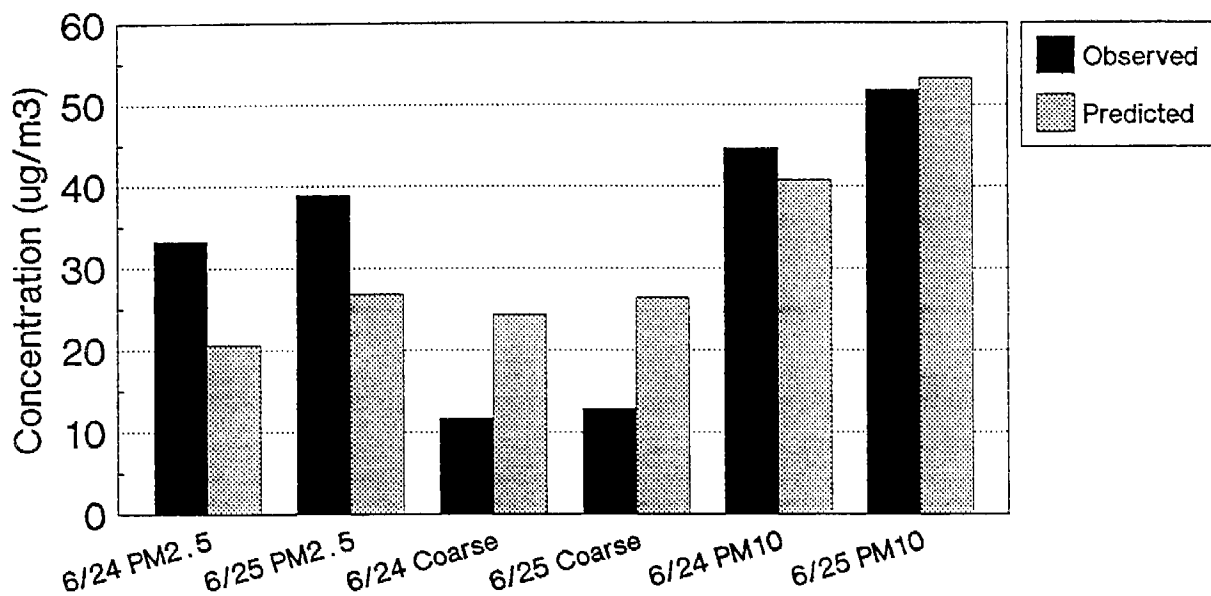


Figure 6-47. Predicted and observed mean and maximum 24-hr average ammonia on December 10-11, 1987.

Maximum Organic PM
 24-hr Average at the Highest SCAQS Station
 December 10-11, 1987



Average Organic PM
 24-hr Average – Mean at the SCAQS Stations
 December 10-11, 1987

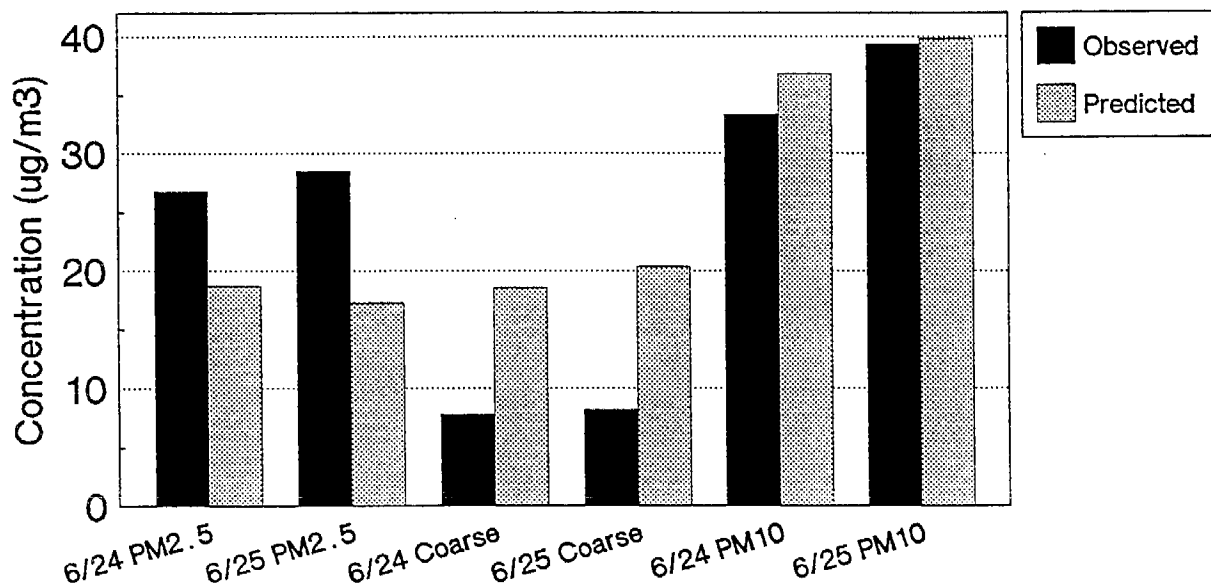
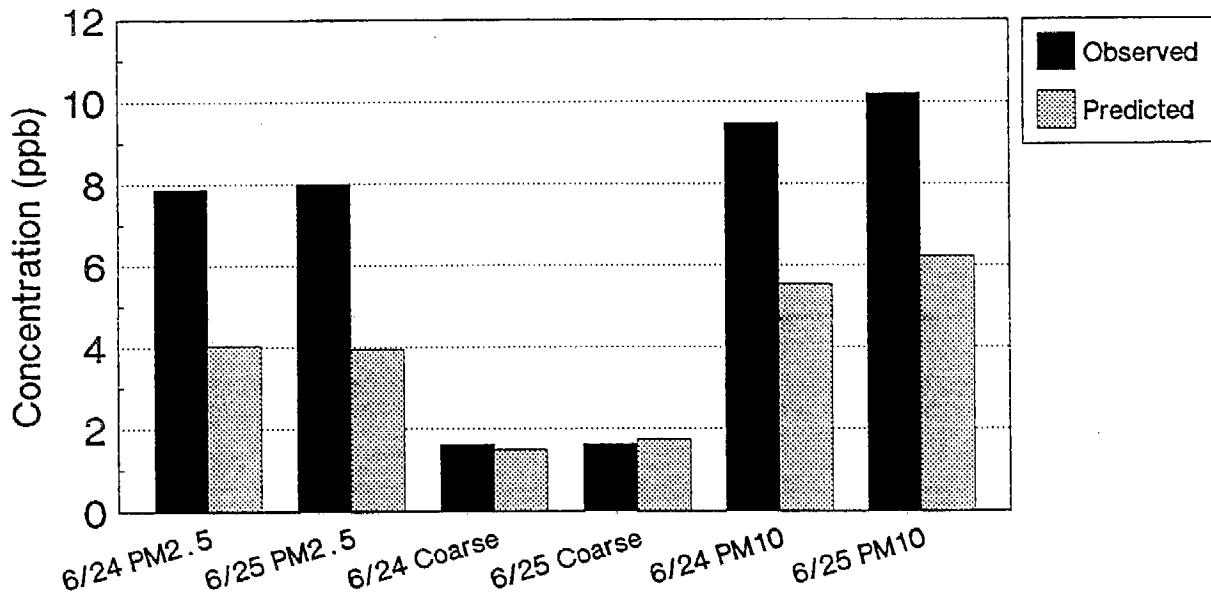


Figure 6-48. Predicted and observed mean and maximum 24-hr average organic PM on December 10-11, 1987.

Average Elemental Carbon
24-hr Average at the Highest SCAQS Station
December 10-11, 1987



Maximum Elemental Carbon
24-hr Average at the Highest SCAQS Station
December 10-11, 1987

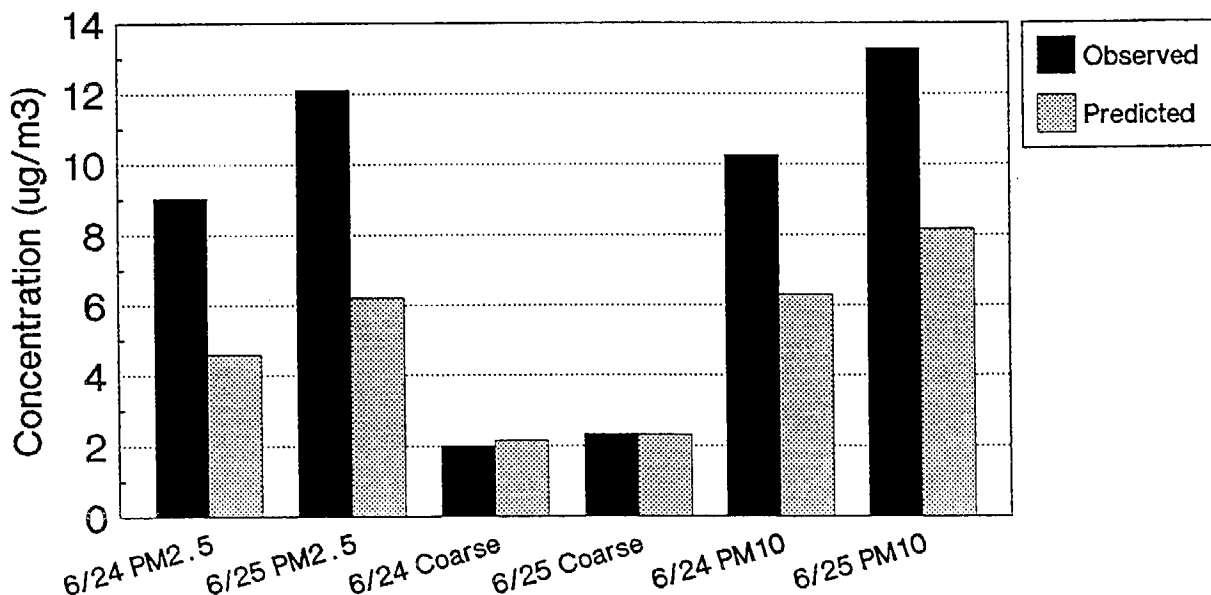
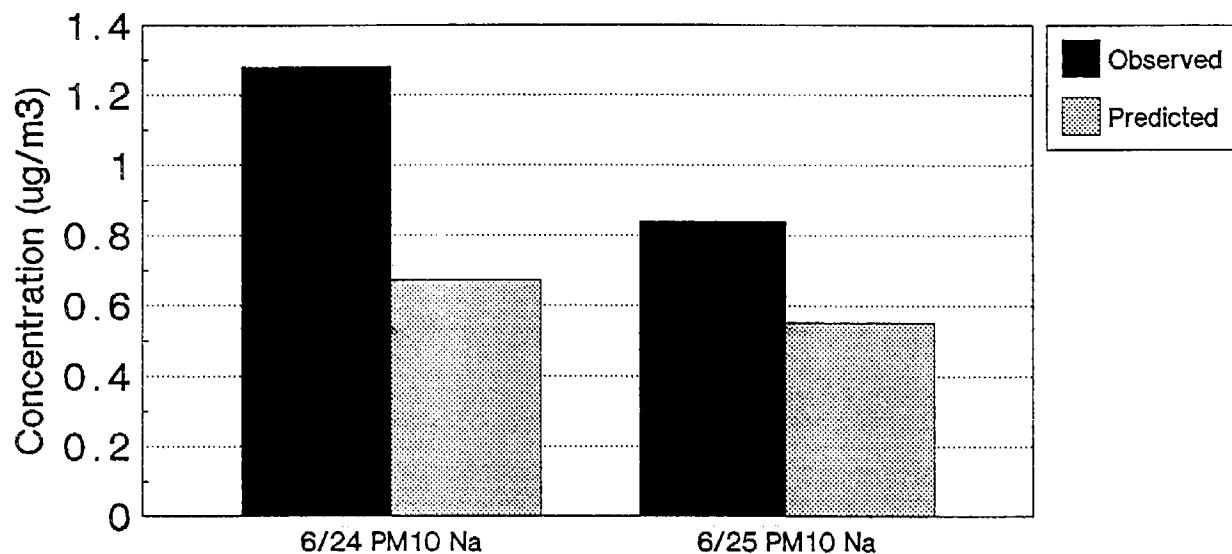


Figure 6-49. Predicted and observed mean and maximum 24-hr average elemental carbon on December 10-11, 1987.

Maximum Sodium
24-hr Average at the Highest SCAQS Station
December 10-11, 1987



Average Sodium
24-hr Average – Mean at the SCAQS Stations
December 10-11, 1987

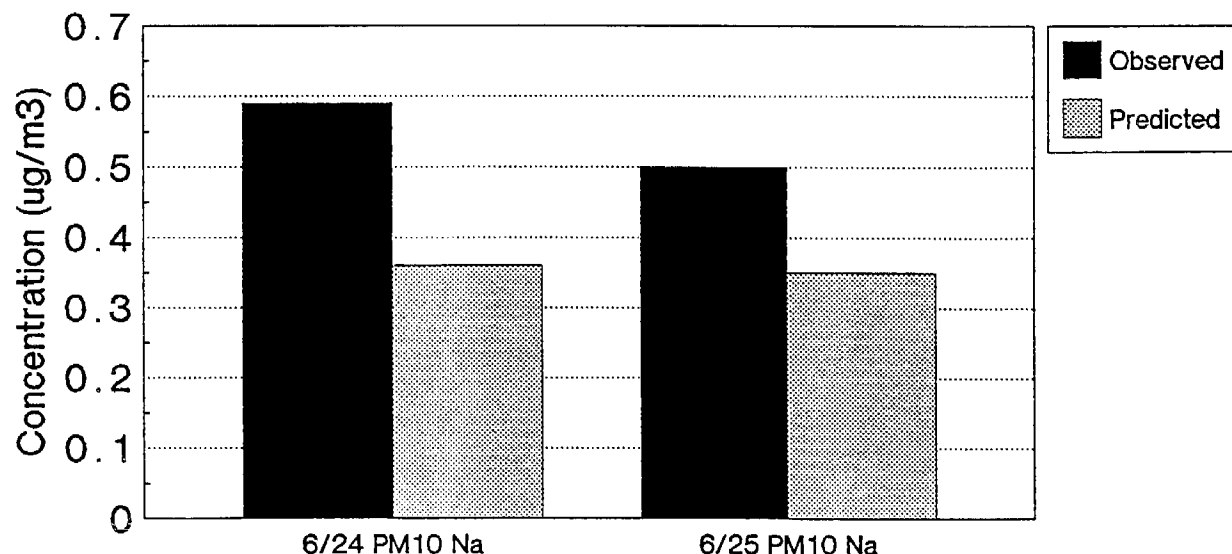


Figure 6-50. Predicted and observed mean and maximum 24-hr average sodium on December 10-11, 1987.

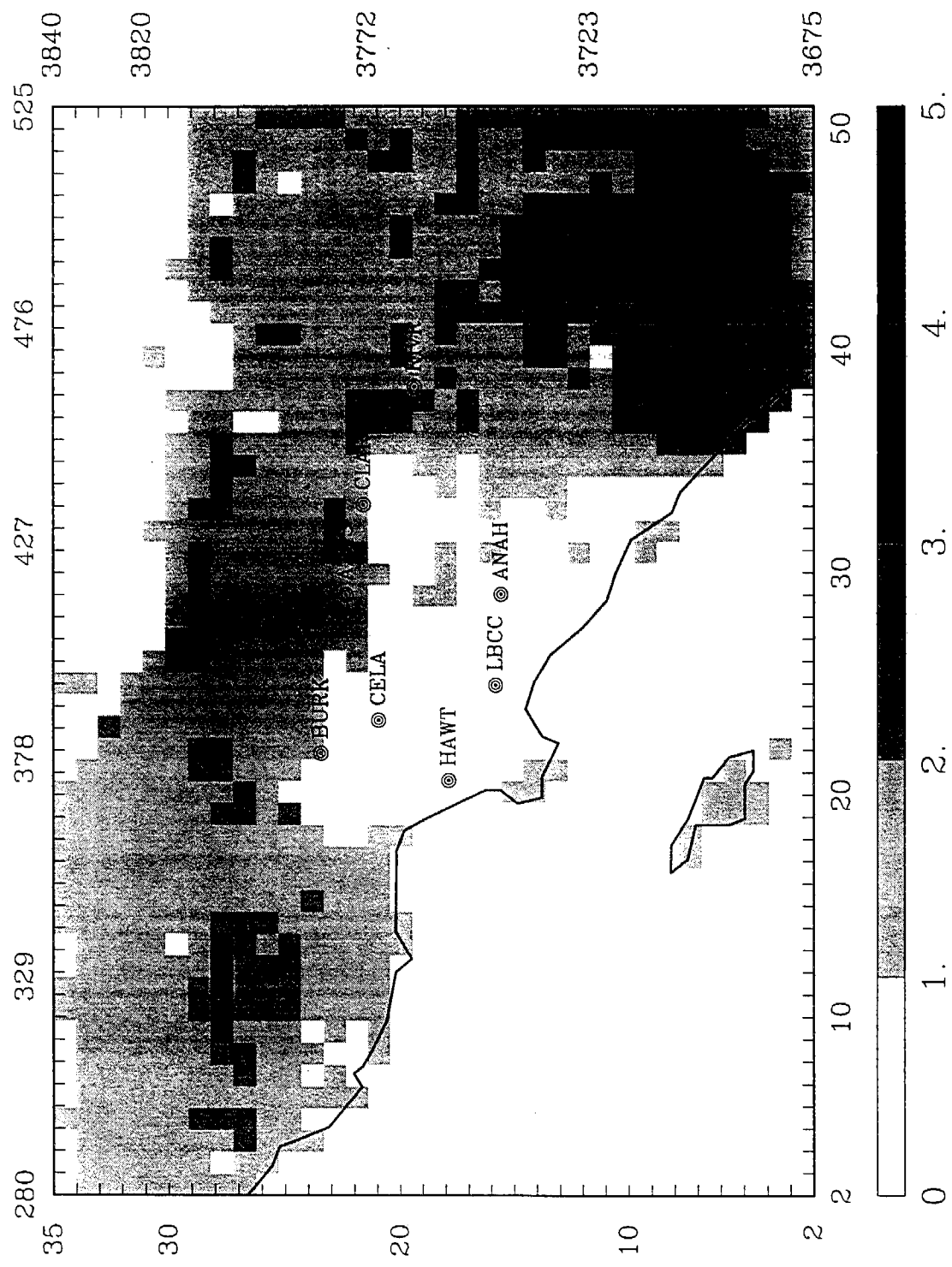


Figure 6-51. Predicted spatial pattern of ozone deposition in moles/hectare-day on December 11, 1987.

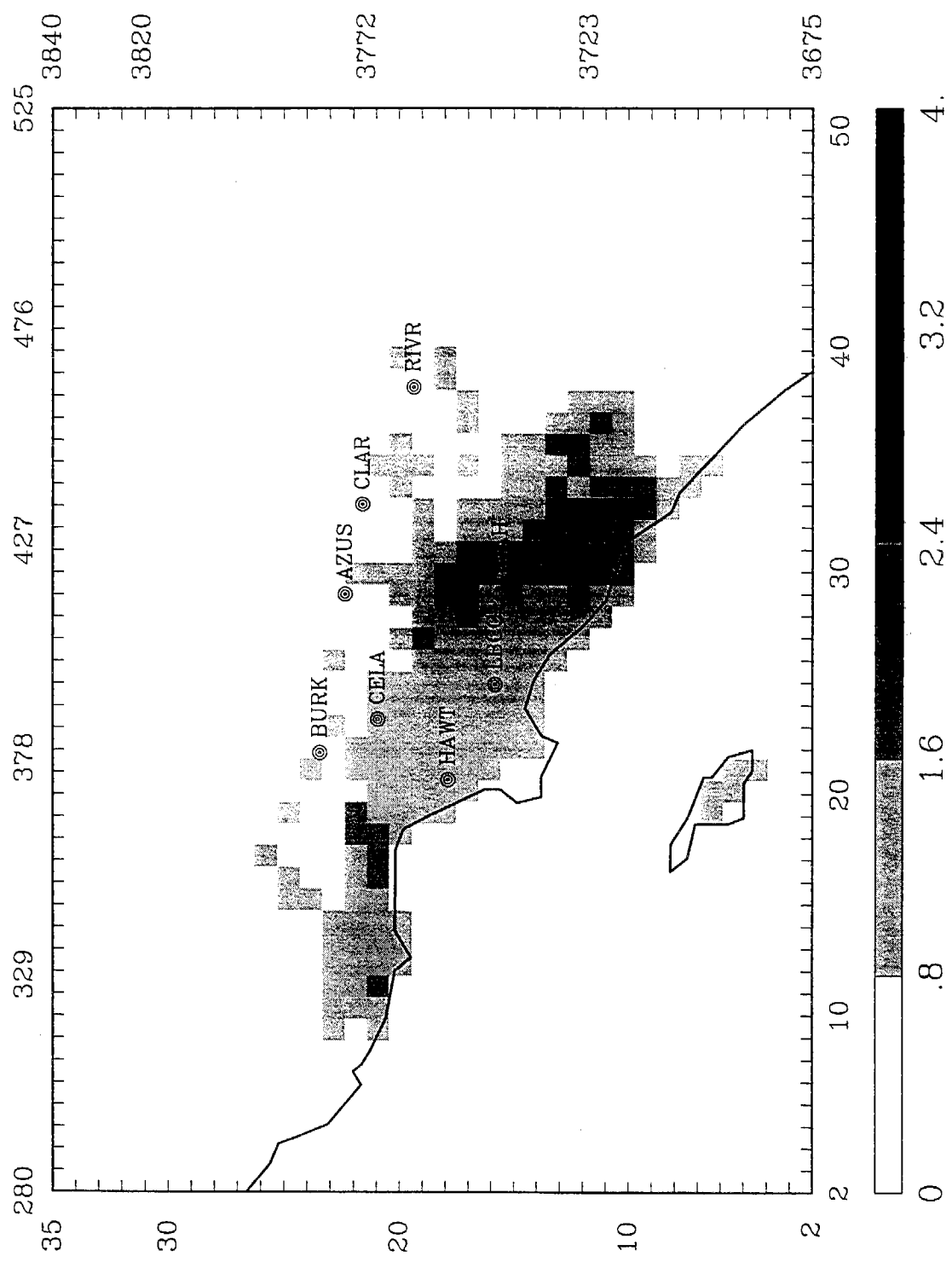
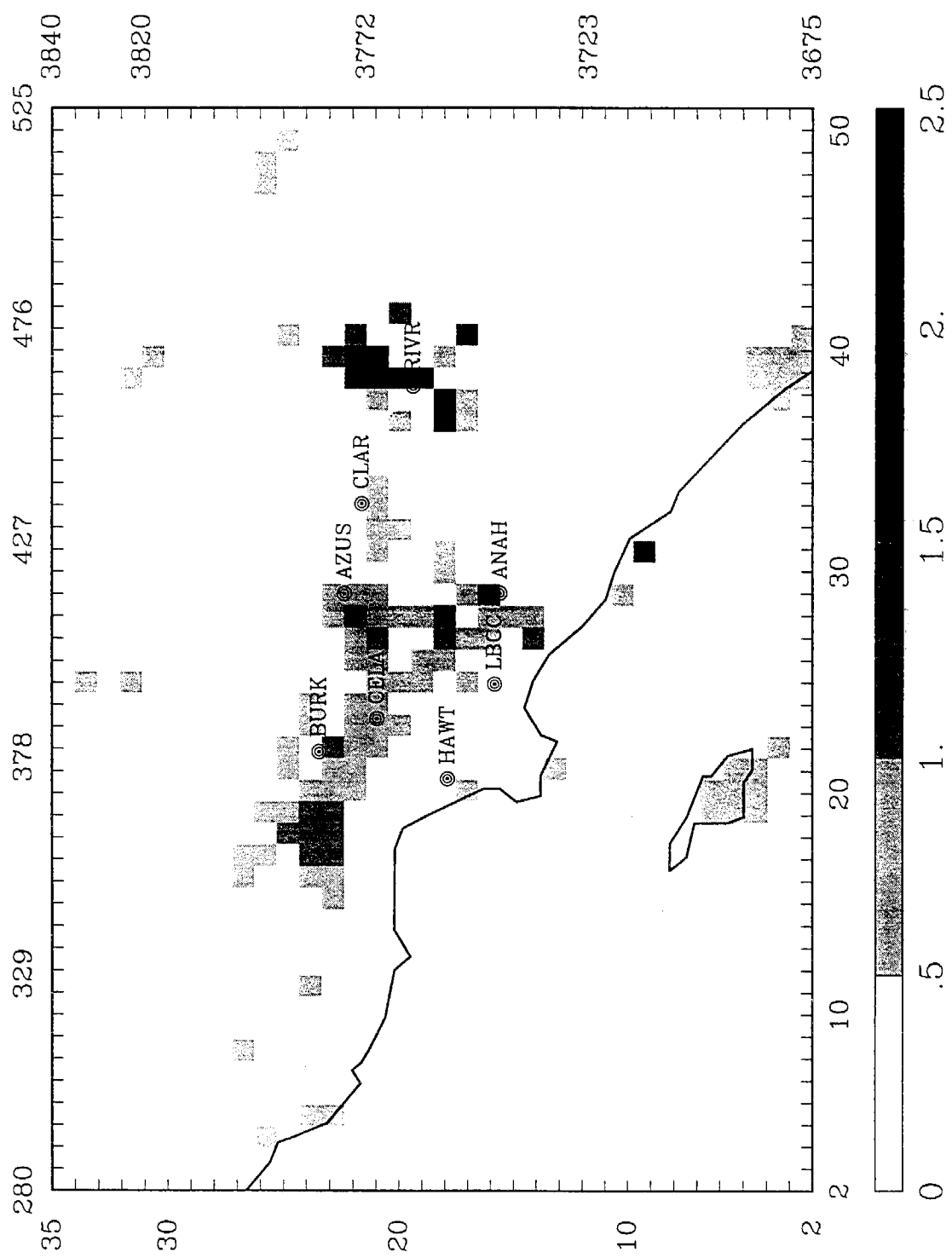


Figure 6-52. Predicted spatial pattern of NO_2 deposition in moles/hectare-day on December 11, 1987.



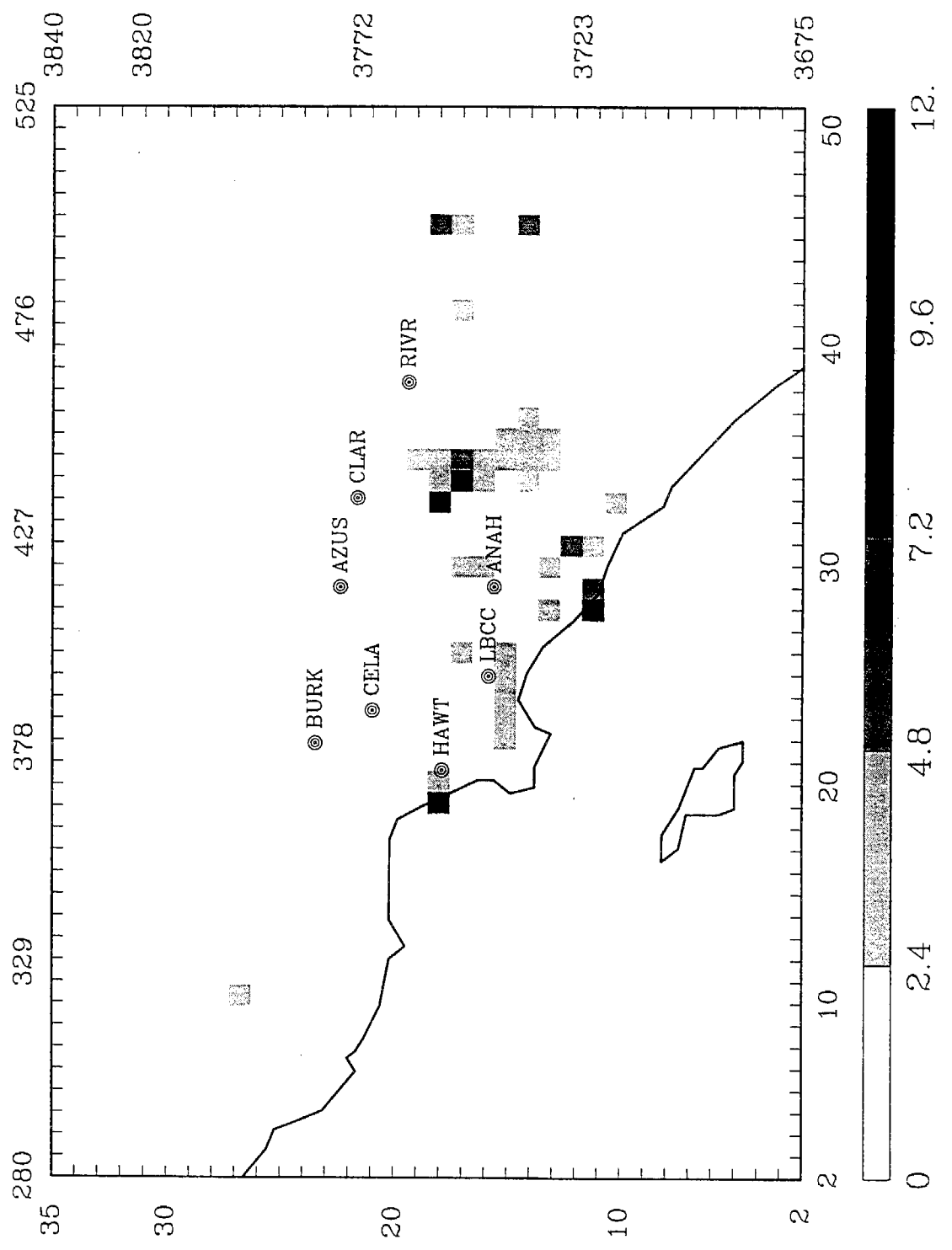


Figure 6-54. Predicted spatial pattern of ammonia deposition in moles/hectare-day on December 11, 1987.

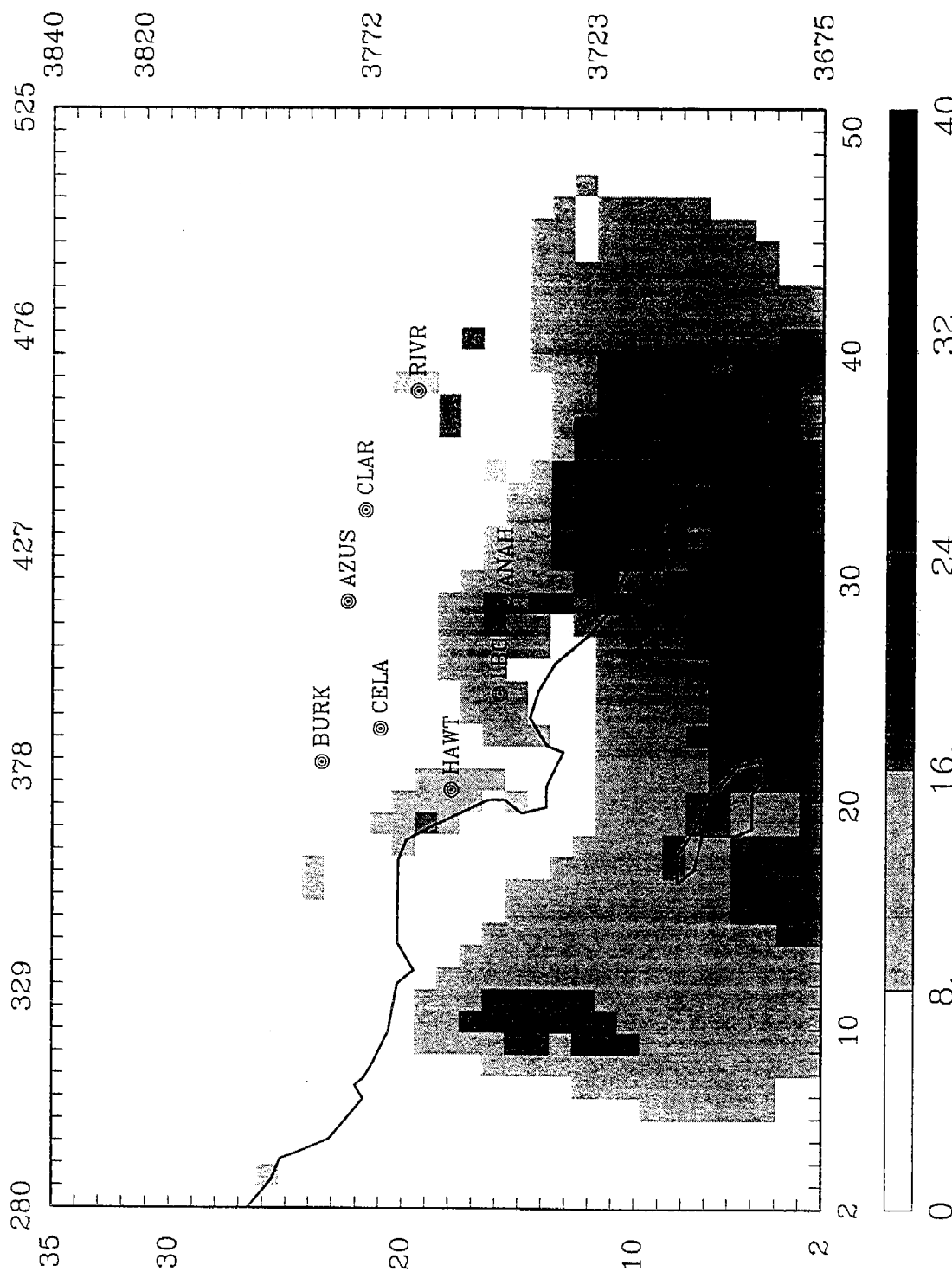


Figure 6-55. Predicted spatial pattern of PM_{10} nitrate deposition in grams/hectare-day on December 11, 1987.

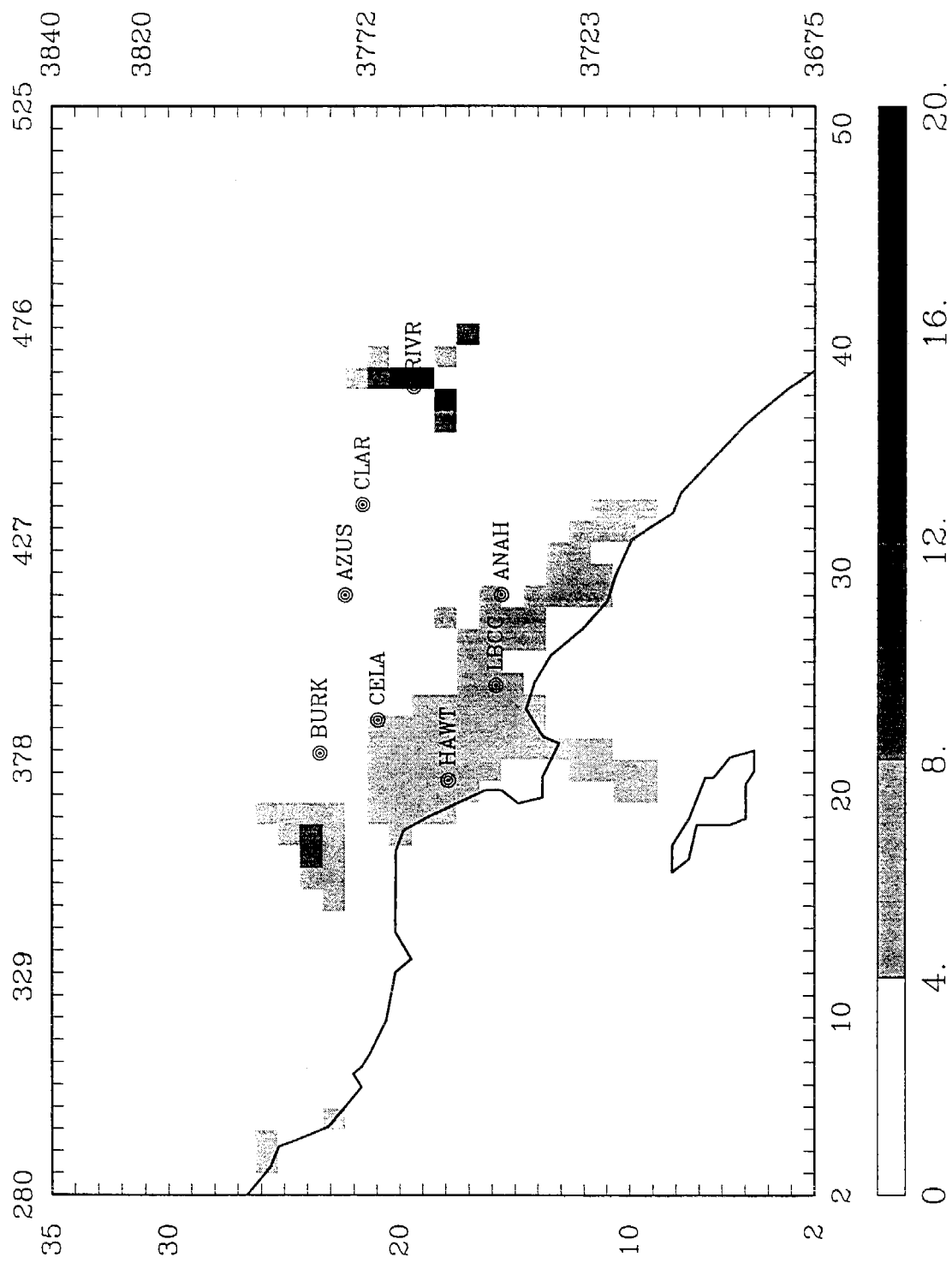


Figure 6-56. Predicted spatial pattern of PM_{10} ammonium deposition in grams/hectare-day on December 11, 1987.

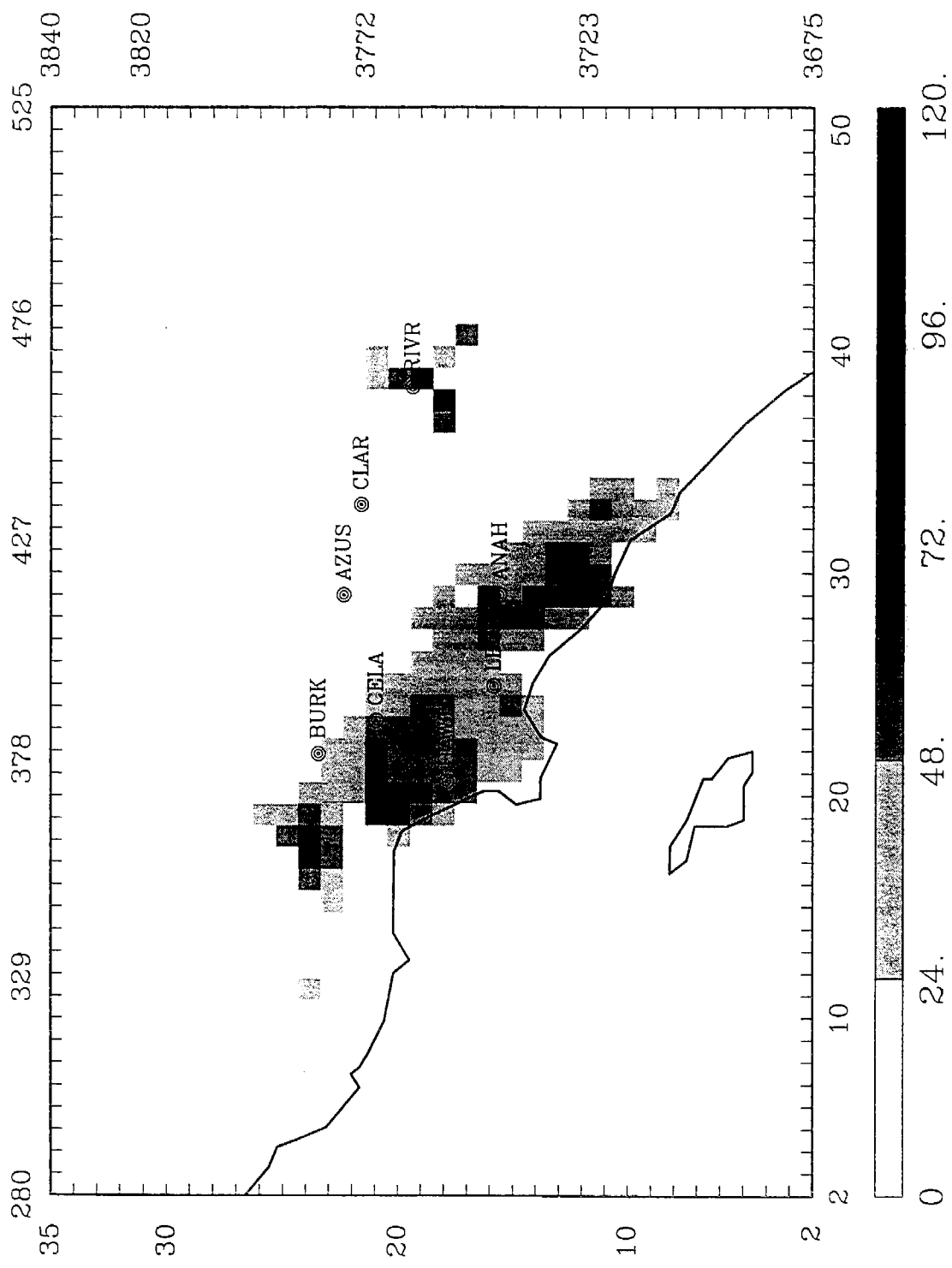


Figure 6-57. Predicted spatial pattern of PM_{10} sulfate deposition in grams/hectare-day on December 11, 1987.

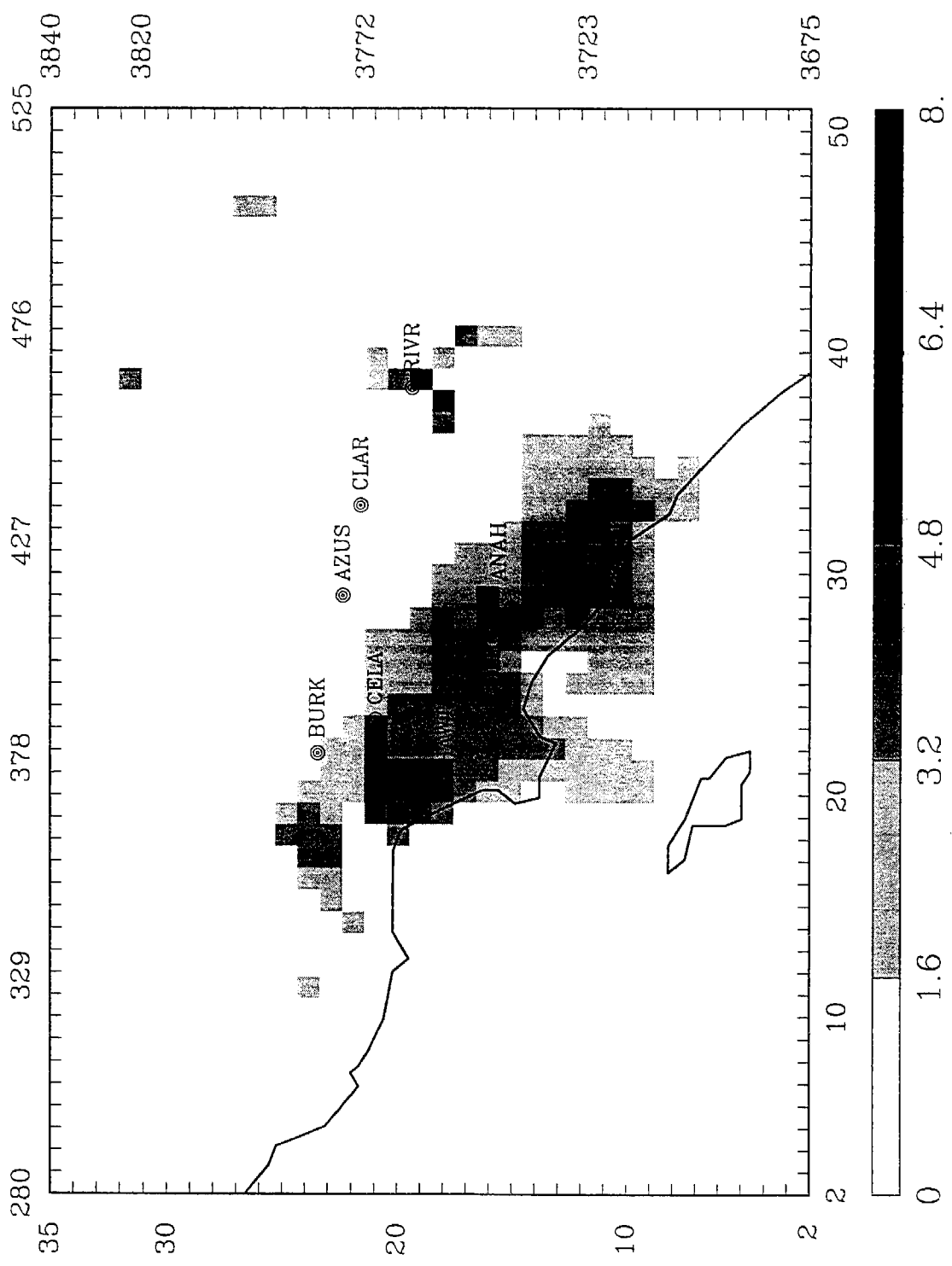


Figure 6-58. Predicted spatial pattern of PM_{10} OM deposition in grams/hectare-day on December 11, 1987.

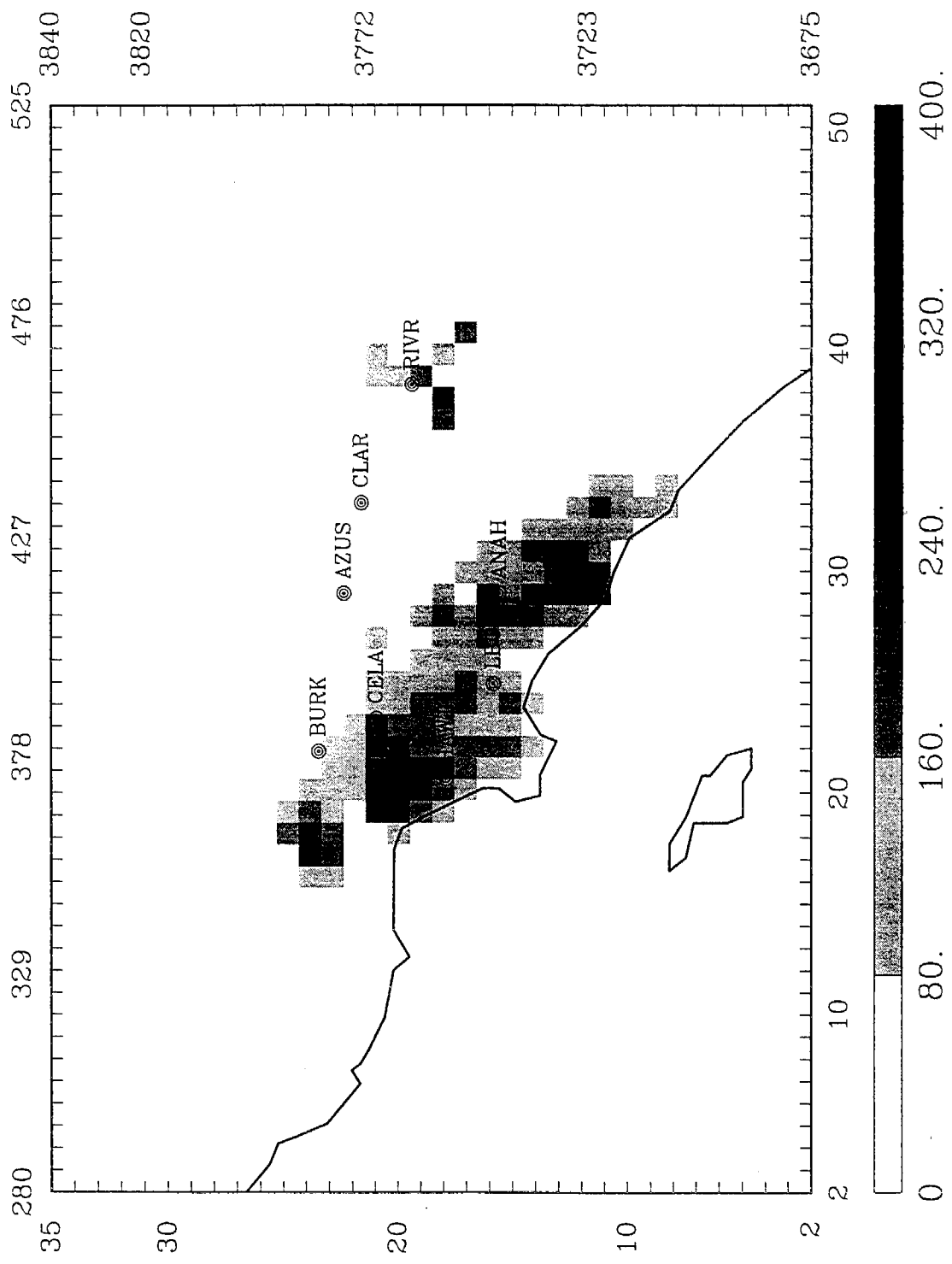


Figure 6-59. Predicted spatial pattern of crustal PM_{10} deposition in grams/hectare-day on December 11, 1987.

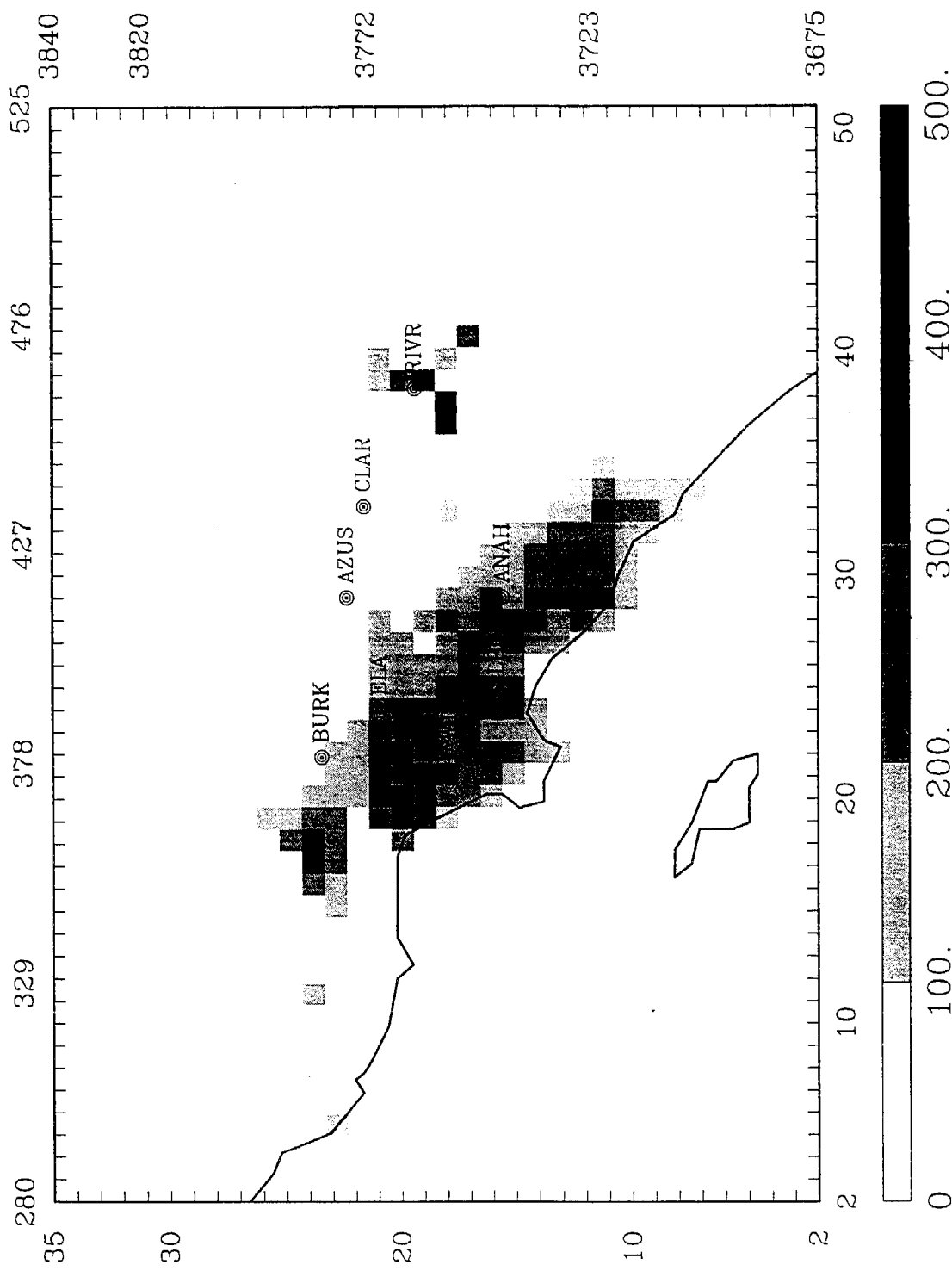


Figure 6-60. Predicted spatial pattern of PM₁₀ mass deposition in grams/hectare-day on December 11, 1987.

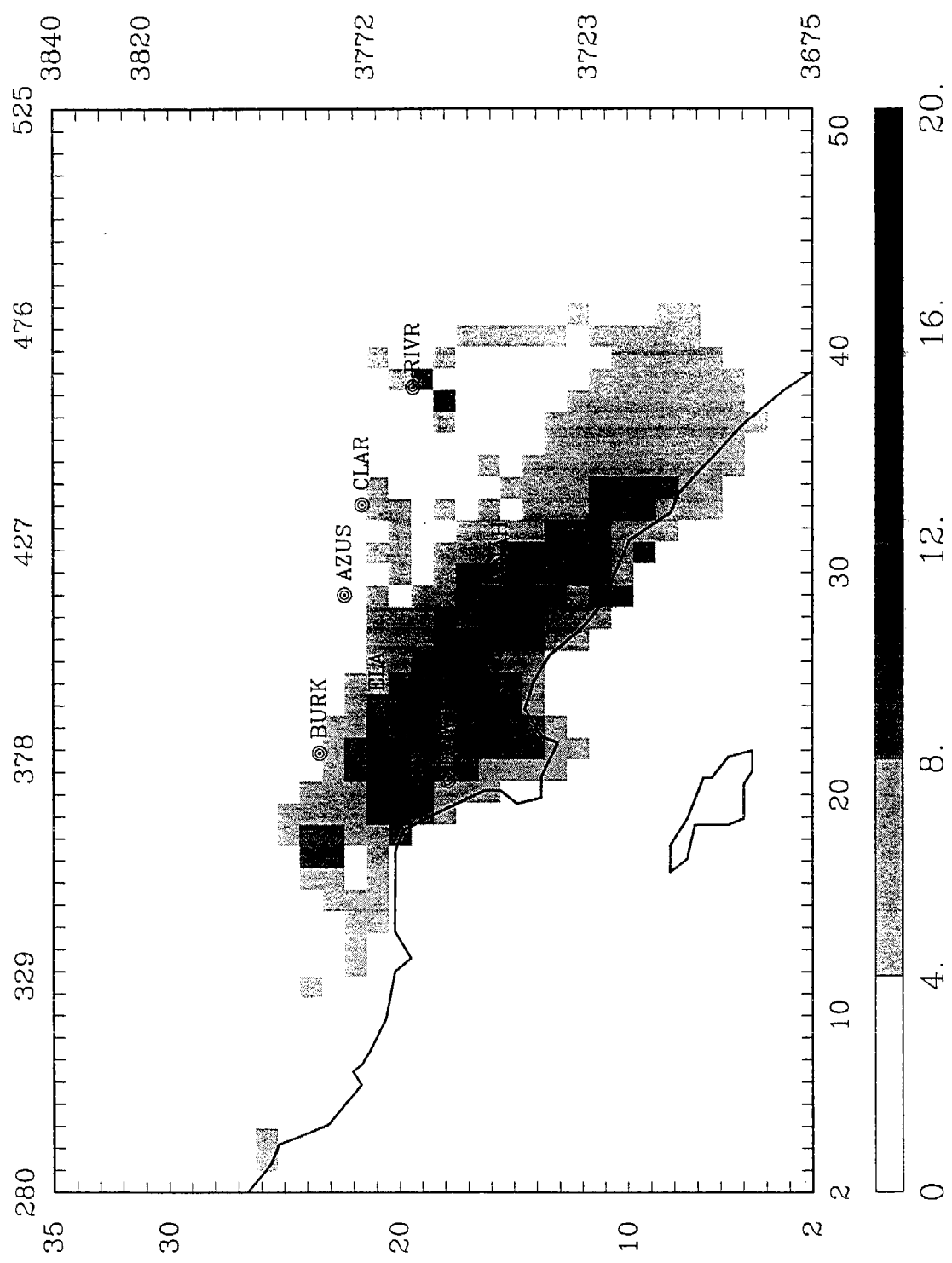


Figure 6-61. Predicted spatial pattern of $\text{PM}_{2.5}$ mass deposition in grams/hectare-day on December 11, 1987.